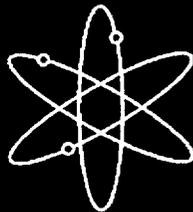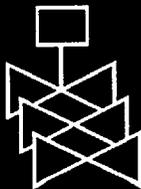# Hanford Tank Waste Remediation System Pretreatment Chemistry and Technology

Center for Nuclear Waste Regulatory Analyses

U.S. Nuclear Regulatory Commission
Office of Nuclear Material Safety and Safeguards
Washington, DC 20555-0001

AVAILABILITY OF REFERENCE MATERIALS
IN NRC PUBLICATIONS

Hanford Tank Waste Remediation System Pretreatment Chemistry and Technology

Prepared by
R. T. Pabalan, V. Jain, R. F. Vance,
S. Ioannidis, D. A. Pickett, C. S. Brazel,
J. T. Persyn, E. J. Taylor, M. E. Inman

Center for Nuclear Waste Regulatory Analyses
Southwest Research Institute
6220 Culebra Road
San Antonio, TX 78238-5166

A. Murray, NRC Project Manager

ABSTRACT

The U.S. Department of Energy (DOE) will remediate the high-level radioactive wastes (HLWs) stored in 177 aging underground storage tanks at the Hanford, Washington site. The retrieved wastes will be separated into a HLW stream containing most of the radionuclides and a low-activity waste (LAW) stream containing the bulk of the nonradioactive chemicals and the soluble components of the tank waste. Both waste streams will be vitrified. Pretreatment of the LAW stream is required to remove cesium-137, strontium-90, technetium-99, and transuranic elements.

This report provides information useful to U.S. Nuclear Regulatory Commission staff for understanding the technical bases of the pretreatment technologies proposed by DOE privatization contractors and for identifying potential hazards associated with those technologies. A review of publicly available information on the chemistry and technology of unit operations proposed by BNFL Inc. and by Lockheed Martin Advanced Environmental Systems is presented. These unit operations are sludge washing, ion exchange, electrochemical methods, organic destruction, and precipitation/filtration. The physicochemical bases of the unit operations and published experimental studies involving alkaline tank wastes are discussed. The proposed pretreatment technology is discussed in the context of its application to Hanford wastes, including operational and safety considerations.

CONTENTS

CONTENTS (cont'd)

CONTENTS (cont'd)

CONTENTS (cont'd)

CONTENTS (cont'd)

Appendices

Figures

Figures (cont'd)

Tables

Tables (cont'd)

Tables (cont'd)

Tables (cont'd)

EXECUTIVE SUMMARY[1]

The U.S. Department of Energy (DOE) is legally bound to remediate the 204,000 m³ (54 million gal.) of high-level radioactive wastes stored in 177 aging underground storage tanks at the Hanford site. Under the Tank Waste Remediation System (TWRS) program, the current plan for remediating these wastes consists of waste retrieval, pretreatment, immobilization, and disposal. Because of the expected high cost of high-level waste vitrification and geologic disposal, the retrieved wastes will be chemically separated to form a high-level waste stream, which will contain most of the radionuclides, and a low-activity waste stream, which will contain the bulk of the nonradioactive chemicals and the soluble components of the tank waste. The high-level waste stream will be vitrified and the product stored until it can be transferred to a licensed high-level waste geologic repository. The low-activity waste stream will be solidified in a glass form also, but will be stored at an onsite retrievable disposal facility. The radionuclide concentrations in the immobilized low-activity waste are required to meet the Nuclear Regulatory Commission (NRC) Class C limits. To meet these limits, pretreatment of the low-activity waste stream is required to remove cesium-137, strontium-90, technetium-99, and transuranic elements from the waste feed. Removal of nonradioactive elements that could significantly increase the volume of immobilized low-activity waste, such as sodium, or deleteriously affect vitrification of the wastes, such as sulfur, may also be necessary.

Information on the chemistry of pretreatment processes proposed by the DOE privatization contractors for Hanford tank wastes is needed to understand the technical bases of the proposed technologies and help identify potential hazards associated with those technologies. The objective of this report is to provide NRC staff information on the chemical aspects of the waste pretreatment technologies that had been proposed by BNFL Inc. and Lockheed Martin Advanced Environmental Systems (LMAES). Although LMAES is no longer a privatization contractor, some of the pretreatment technologies that it had proposed could be viable alternatives to those proposed by BNFL Inc. Therefore, the LMAES technologies are also discussed in this report. It should be noted that the material presented in this report is based on the pretreatment methods proposed by BNFL Inc. and LMAES at the 3 percent design stage. Therefore, information regarding the BNFL Inc. pretreatment methods represents only a snapshot of the BNFL Inc. approach. Although the actual BNFL Inc. process flowsheet may change from what is presented in this report, the identified approaches, technologies, and methods will likely envelope the design and safety issues for the pretreatment of Hanford tank wastes.

An overview of the TWRS program is given in chapter 1. The DOE will provide tank waste to BNFL Inc. that includes three low-activity waste feed types and one high-level waste type. The wastes will be processed by BNFL Inc. in a sludge washing facility to remove from sludges those elements that increase high-level waste production. The wash liquids, following separations, will be treated to separate cesium-137, strontium-90, technetium-99, and transuranic elements and produce waste streams suitable for vitrification and disposal as immobilized low-activity waste. The separated radionuclides will be included in the high-level waste stream for immobilization. Chapter 1 provides an overview of the pretreatment processes proposed by BNFL Inc., which include (i) ion exchange to remove cesium-137 and technetium-99 and (ii) precipitation/filtration to remove strontium-90 and transuranics. In addition to (i)

---

[1]
The discussion presented in this report is based on information that was publicly available as of January 15, 2000. Subsequent to completion of this report, the DOE has terminated its privatization contract with BNFL Inc. The DOE issued a request for proposals for design and construction of a Hanford waste treatment facility in August 2000, and plans to select a replacement contractor by January 15, 2001 (http:\\www.hanford.gov\press\2000\orp\062900.orp.html).

and (ii), BNFL Inc. is developing an ion-exchange process to remove sulfate from low-activity waste. Also summarized in chapter 1 are the pretreatment processes that had been proposed by LMAES, which include (i) ion exchange, aided by electrochemical elution, to remove cesium-137; (ii) ozonation/filtration to destroy organic compounds and remove strontium-90 and transuranic elements; and (iii) electroreduction to separate technetium-99. LMAES had also proposed to evaluate unit operations for removal of cobalt-60, europium-154, and europium-155. The overview of BNFL Inc. and LMAES pretreatment processes is supplemented in chapter 1 by a discussion of high-level waste pretreatment experiences at the West Valley Demonstration Project (West Valley, New York), and at the Defense Waste Processing Facility (Savannah River Site, Aiken, South Carolina), and by additional discussion of the safety issues that could be important in the processing of Hanford tank wastes, such as hydrogen gas generation, exothermic reactions, high-heat generation, radiolysis effects, and plugging of process lines.

The unit operations proposed by BNFL Inc. and LMAES are discussed in chapters 2 through 6. These unit operations are sludge washing (chapter 2), ion exchange (chapter 3), electrochemical methods (chapter 4), organic destruction (chapter 5), and precipitation/filtration (chapter 6). In each chapter, the physicochemical bases of the unit operation are presented, and published experimental studies involving alkaline tank wastes are reviewed. In addition, the proposed pretreatment technology is discussed in the context of its application to Hanford wastes, including operational and safety considerations. At the end of each chapter, a brief evaluation is presented of the discussed technologies as they apply to the planned BNFL Inc. process.

Sludge washing, discussed in chapter 2, is a major pretreatment process planned for the sludge content of Hanford tank wastes. The washing process can reduce substantially the amount of high-level waste glass by separating the soluble, nonradioactive components (e.g., aluminum hydroxides and sodium) from the radioactively contaminated solids. Chapter 2 reviews the chemistry of processes and experimental studies relevant to dilute alkaline and caustic washing of Hanford tank sludge. The chemical mechanisms responsible for sludge dissolution, particularly aluminum, chromium, phosphorus, and iron, are discussed, and the sludge washing operations at West Valley Demonstration Project and Defense Waste Processing Facility are briefly reviewed. BNFL Inc. has proposed to wash the tank waste solids with an equivalent volume of water up to four times to reduce the concentration of sodium to less than 60 g of sodium per kilogram of dry solids. Published data on sludge washing indicate the BNFL Inc. target sodium concentration is achievable by repetitive water washes of the alkaline sludge. The removal of sodium will significantly reduce the amount of glass necessary to solidify the low-activity waste. In relative terms, the removal of other elements from the waste would have only a small impact on the volume of the final glass waste form. Consistent with this assessment, BNFL Inc. has proposed no wash steps to selectively remove other metals, such as aluminum, chromium, phosphorus, or iron.

Ion exchange is a mature technology that has been used extensively in the nuclear industry. In the TWRS, the ion-exchange process has the goal of removing enough of the radionuclides from the low-activity waste feed so that the resulting immobilized low-activity waste will meet the NRC Class C limits. BNFL Inc. plans to remove cesium-137 and technetium-99 from the low-activity waste using ion exchange, whereas LMAES had proposed to use ion exchange to remove cesium-137 from the low-activity waste. Chapter 3 reviews several aspects of ion exchange, including theory, models, and important operating parameters (pH, temperature, competing ions). Ion-exchange materials that have been used in radionuclide removal from alkaline wastes, such as crystalline silicotitanate, resorcinol-formaldehyde, superligands, and zeolites, are covered in chapter 3, including the chemical, thermal, and radiation stability of those materials. The application of ion exchange to Hanford tank wastes is also discussed, as

well as safety and ion-exchange material management considerations. Based on published experimental data reviewed in chapter 3, the ion-exchange resin, SuperLig®-644, that BNFL Inc. plans to use to remove cesium-137 is believed appropriately selective for the cesium ion in an alkaline solution, even in the presence of high concentrations of the major competing ion, sodium. However, the effectiveness of SuperLig®-644 in removing cesium-137 from aqueous solutions containing organic complexants is uncertain because no published data were found on the performance of SuperLig®-644 in solutions with significant amounts of organic material. The crystalline silicotitanate that BNFL Inc. had planned to use for a low-activity waste-only facility—an option that is no longer being considered—would have performed its intended function well. BNFL Inc. plans to use SuperLig®-639 to remove technetium-99 from the low-activity waste stream. No definitive statements regarding the suitability of SuperLig®-639 for its intended use can be made at this time because no performance data are available in the published literature.

In chapter 4, the electrochemical methods proposed by LMAES—electrochemical ion exchange and electroreduction—are discussed. LMAES had proposed to use electrochemical ion exchange to enhance elution of the loaded resorcinol-formaldehyde resin, subsequent to the use of that resin for removing cesium-137 from low-activity waste by conventional ion exchange. LMAES had planned to remove technetium-99 using an electroreduction process—technetium-99 would be electrolytically plated onto a cathode and subsequently recovered by dissolution in a nitric acid solution. Chapter 4 reviews the physicochemical basis of electrochemical ion exchange and electroreduction, the important operating parameters and safety considerations in their application, and published experimental studies that used those techniques to separate radionuclides from alkaline wastes. The review indicates that insufficient information is available to make an accurate assessment of the viability of electrochemical ion exchange or electroreduction for the treatment of Hanford waste streams. This assessment is consistent with the DOE finding that the technologies proposed by LMAES had significant technical risk. BNFL Inc. does not plan to use electrochemical methods in pretreating Hanford waste feeds.

LMAES had proposed to destroy organic materials in one of the Hanford low-activity waste feeds by oxidation with ozone prior to removal of strontium-90 and transuranic elements by precipitation and filtration. Ozonation was expected to improve the efficiency of the precipitation/filtration step by oxidizing organic complexants that bind and keep in solution strontium-90 and transuranics. Chapter 5 provides background information on the chemistry of ozone and its interaction with different organic types and specific organic complexants that may be present in the Hanford low-activity waste feed. Operational considerations, such as pH, temperature, ozone flowrate, and reactor design, in the application of ozonation to waste pretreatment are discussed, as well as safety aspects in the use of ozonation. The other organic destruction processes considered by LMAES—electrochemical oxidation and thermal destruction—are also briefly discussed. BNFL Inc. proposed no organic material destruction operation. Should an organic destruction step be needed, published data suggest that ozonation would be a logical choice to evaluate because it is better developed for this application than either electrochemical oxidation or thermal destruction. However, further tests would be needed to verify the applicability of ozonation on actual Hanford waste feeds and to obtain data for scaling up to an industrial size reactor.

In the proposed BNFL Inc. pretreatment flowsheet, a Hanford low-activity waste feed that contains high amounts of organic complexants will be subjected to a pretreatment process that involves strontium precipitation and ferric floc coprecipitation to remove strontium-90 and transuranic elements. Chapter 6 discusses the different mechanisms that could play a role in the BNFL Inc. process, including solid solution formation, coagulation, adsorption, displacement, and isotope dilution. Published test results on

strontium and transuranic element removal from Hanford wastes or similar wastes are reviewed. The BNFL Inc. process encompasses a number of chemical and physical mechanisms. Although published studies suggest these mechanisms can be effective for removing trace metals from solution, they could be highly waste-specific. Thus, to assure that the BNFL Inc. pretreatment process will meet contract and regulatory requirements, experimental testing using samples of actual low-activity waste feeds should precede finalizing the system design.

ACKNOWLEDGMENTS

QUALITY OF DATA, ANALYSES, AND CODE DEVELOPMENT

This report was prepared in accordance with the quality assurance requirements described in the CNWRA Quality Assurance Manual. Proprietary information included in a version of this report submitted to the NRC have been deleted.

DATA: This report contains no CNWRA-generated laboratory or field data. Sources of data are referenced within the report. Data from these sources are used freely, and these sources should be consulted for determining the level of quality for those data.

ANALYSES AND CODES: In this report, no computer software was used for analysis.

1 INTRODUCTION[1]

During the past few years, the primary mission at the U.S. Department of Energy (DOE) Hanford site has changed from producing plutonium for national defense to waste management and restoration, including treatment and disposal of the 204,000 m³ (54 million gal.) of high-level radioactive wastes. These wastes, generated during past plutonium production and other operations, are stored in 177 aging underground storage tanks onsite. Of these tanks, 149 are single-shell tanks constructed between 1944 and 1964, and 28 are double-shell tanks constructed between 1968 and 1986. All the single-shell tanks have exceeded their 20-yr design lives, and 67 of the single-shell tanks are known or are suspected to have leaked 4,000 m³ (1 million gal.) of high-level waste into the ground (U.S. Department of Energy, 1998a). None of the double-shell tanks are known to have leaked, but a number of them will reach the end of their design lives prior to waste retrieval and treatment (U.S. Department of Energy, 1998a).

The DOE is legally bound to remediate the waste tanks under the Hanford Federal Facilities Agreement and Consent Order of 1989 (Ecology, 1994), also known as the Tri-Party Agreement. To manage the maintenance and cleanup of the tank wastes, the Tank Waste Remediation System (TWRS) program was established at Hanford by the DOE in 1991.

The current plan for remediating the Hanford tank wastes consists of waste retrieval, pretreatment, immobilization, and disposal. The high-level waste is proposed to be immobilized in a borosilicate glass matrix; the resulting glass canisters will then be disposed in a geologic repository. The low-activity waste resulting from the pretreatment activities also is proposed to be immobilized in a borosilicate glass matrix and stored at an onsite retrievable disposal facility.

Because of the expected high cost of high-level waste vitrification and geologic disposal, pretreatment processes will be implemented to reduce the volume of borosilicate glass produced in disposing the tank wastes. The TWRS privatization Contract Specification 2 limits the radionuclide concentration of the immobilized low-activity waste form to less than the Nuclear Regulatory Commission (NRC) Class C limits as defined in Title 10 of the Code of Federal Regulations Part 61 (Code of Federal Regulations, 1997) and as described in an NRC branch technical position on concentration averaging and encapsulation (Nuclear Regulatory Commission, 1995). Contract Specification 2 also specifies that the average concentrations of cesium-137, strontium-190, and technetium-90 in the immobilized low-activity waste shall be less than 3 Ci/m³, less than 20 Ci/m³, and less than 0.3 Ci/m³, respectively, and the transuranic element content of the immobilized low-activity waste must be less than 100 nCi/g. Furthermore, Contract Specification 7 specifies maximum values of radionuclide concentrations in the waste feed. These values are listed in table 1-1 and in appendix table A-2. Concentrations of these radionuclides, without pretreatment, in the low-activity waste feed would result in excessively high radionuclide concentrations in the immobilized low-activity waste. Therefore, pretreatment of the low-activity waste includes process steps to remove cesium-137, strontium-90, technetium-99, and transuranic elements, as well as entrained solids, from the waste feed. Note that the immobilized low-activity waste should not only meet the radionuclide content specification, but also the glass composition requirements. High-sodium concentration could result in low-durability glass not suitable for disposal, whereas low-

---

[1]The discussion presented in this report is based on information that was publicly available as of January 15, 2000. Subsequent to completion of this report, the DOE terminated its privatization contract with BNFL Inc. The DOE issued a request for proposals for design and construction of a Hanford waste treatment facility in August 2000, and plans to select a replacement contractor by January 15, 2001 (http://www.hanford.gov/press/2000/orp/062900.orp.html).

Introduction

Table 1-1. Concentration limits* for the A, B, and C low-activity waste feed envelopes (U.S. Department of Energy, 1996a,b). Values are given for 3 M and 10 M sodium, the contract-specified limits of sodium concentration.[†] Shading highlights the differences among the three envelopes.

Chemical Analyte	Envelope A		Envelope B		Envelope C	
	3 M Na	10 M Na	3 M Na	10 M Na	3 M Na	10 M Na
Al	7.50E−01	2.50E+00	7.50E−01	2.50E+00	7.50E−01	2.50E+00
Ba	3.00E−04	1.00E−03	3.00E−04	1.00E−03	3.00E−04	1.00E−03
Ca	1.20E−01	4.00E−01	1.20E−01	4.00E−01	1.20E−01	4.00E−01
Cd	1.20E−02	4.00E−02	1.20E−02	4.00E−02	1.20E−02	4.00E−02
Cl	1.11E−01	3.70E−01	2.67E−01	8.90E−01	1.11E−01	3.70E−01
Cr	2.07E−02	6.90E−02	6.00E−02	2.00E−01	2.07E−02	6.90E−02
F	2.73E−01	9.10E−01	6.00E−01	2.00E+00	2.73E−01	9.10E−01
Fe	3.00E−02	1.00E−01	3.00E−02	1.00E−01	3.00E−02	1.00E−01
Hg	4.20E−05	1.40E−04	4.20E−05	1.40E−04	4.20E−05	1.40E−04
K	5.40E−01	1.80E+00	5.40E−01	1.80E+00	5.40E−01	1.80E+00
La	2.49E−04	8.30E−04	2.49E−04	8.30E−04	2.49E−04	8.30E−04
Ni	9.00E−03	3.00E−02	9.00E−03	3.00E−02	9.00E−03	3.00E−02
NO$_2$	1.14E+00	3.80E+00	1.14E+00	3.80E+00	1.14E+00	3.80E+00
NO$_3$	2.40E+00	8.00E+00	2.40E+00	8.00E+00	2.40E+00	8.00E+00
Pb	2.04E−03	6.80E−03	2.04E−03	6.80E−03	2.04E−03	6.80E−03
PO$_4$	1.14E−01	3.80E−01	3.90E−01	1.30E+00	1.14E−01	3.80E−01
SO$_4$	3.00E−02	1.00E−01	2.10E−01	7.00E−01	6.00E−02	2.00E−01
TIC	9.00E−01	3.00E+00	9.00E−01	3.00E+00	9.00E−01	3.00E+00
TOC	1.50E+00	5.00E+00	1.50E+00	5.00E+00	1.50E+00	5.00E+00
U	3.60E−03	1.20E−02	3.60E−03	1.20E−02	3.60E−03	1.20E−02
TRU	1.44E+06	4.80E+06	1.44E+06	4.80E+06	9.00E+06	3.00E+07
Cs-137	1.29E+10	4.30E+10	6.0E+10	2.00E+11	1.29E+10	4.30E+10
Sr-90	1.32E+08	4.40E+08	1.32E+08	4.40E+08	2.40E+09	8.00E+09
Tc-99	2.13E+07	7.10E+07	2.13E+07	7.10E+07	2.13E+07	7.10E+07

*Units of moles per liter except for radionuclides (Becquerels per liter).
[†]The contract also specifies that the insoluble solids fraction will not exceed 2 weight percent (dry basis) of the waste transferred. Trace quantities of radionuclides, chemicals, and other impurities may be present in the waste feed.

sodium concentration in the glass could significantly increase the volume of immobilized low-activity waste.

Pretreatment strategies include using processes and equipment to separate and remove waste components to minimize treated waste volumes and produce waste fractions compatible with final waste forms and their disposal criteria. The currently envisioned pretreatment strategy proposes to

- Use washing and selective leaching to remove elements from sludges expected to drive high-level waste production

- Remove radionuclides from the aqueous waste fractions to produce streams suitable for disposal as immobilized low-activity waste

For cesium-137, the NRC established a Class C low-level waste limit of 4,600 Ci/m^3. A maximum of 2.0 × 10^{10} Bq of cesium-137 per mole of sodium could be present in envelope B wastes. Assuming a 10-M concentration for sodium, the maximum concentration for cesium-137 could be as much as 5,400 Ci/m^3. Even if no volume reduction results from the combined pretreatment and vitrification operations, the NRC limit for cesium-137 would be exceeded. Clearly, the amount of cesium-137 in the waste must be reduced. Cesium-137 can be removed from aqueous wastes by ion exchange.

For strontium-90, the NRC established a Class C low-level waste limit of 7,000 Ci/m^3. Envelope C waste has a higher concentration of strontium-90 than either A or B, with a maximum 8.0 × 10^8 Bq of strontium-90 per mole of sodium (see table A-2). Assuming a 10-M concentration for sodium, the maximum concentration for strontium-90 would be about 216 Ci/m^3. If the waste volume is reduced by a factor of 32.4 from the combined pretreatment and vitrification operations, then the NRC limit for strontium-90 in Class C waste could be exceeded. If such a volume reduction is anticipated, one can conclude that removal of strontium-90 from the low-activity waste would be necessary, for example, by precipitation and filtration.

For technetium-99 the NRC established a Class C low-level waste limit of 3 Ci/m^3. A maximum of 7.1 × 10^6 Bq of technetium-99 per mole of sodium could be present in envelope A, B, or C wastes. Assuming a 10-M concentration for sodium, the maximum concentration for technetium-99 could be as much as 1.9 Ci/m^3. If any concentration from volume reduction by a factor of about 1.6 occurs from the combined pretreatment and vitrification operations, then the NRC limit for technetium-99 in Class C waste would be exceeded. Clearly, the amount of technetium in the waste must be reduced. Technetium can be removed from aqueous wastes by ion exchange or electroreduction.

For transuranic elements that emit alpha particles and have a half-life of 5 yr or greater, the NRC established a Class C low-level waste limit of 100 nCi/g. Envelope C waste has a much higher concentration of transuranic elements than either A or B, nominally 3.0 × 10^6 Bq of transuranic elements per mole of sodium. Assuming a 10-M concentration for sodium, and a specific gravity of 1.3, the nominal concentration for transuranic elements would be about 624 nCi/g. Even if no volume reduction results from the combined pretreatment and vitrification operations, the NRC limit for transuranic elements would be exceeded. Clearly, the amount of transuranic elements in the envelope C waste must be reduced. Transuranic elements can be removed from aqueous wastes by precipitation and filtration.

Introduction

The amount of sulfates entering the melter should be limited to assure a high quality waste glass form. Sulfates tend to be water soluble and can be removed effectively by aqueous sludge washing operations. Removal by ion exchange is a possibility.

1.1 Objective of Report

Information on the chemistry of pretreatment processes proposed by DOE privatization contractors for Hanford tank wastes is needed to understand the technical bases of the proposed technologies and help identify potential hazards associated with those technologies. The objective of this report is to provide NRC staff information on the technical aspects of waste pretreatment technologies proposed by BNFL Inc. and Lockheed Martin Advanced Environmental Systems (LMAES). Although LMAES is no longer a privatization contractor, some of the pretreatment technologies that had been proposed by LMAES could be viable alternatives to those proposed by BNFL Inc. Therefore, the LMAES technologies are also discussed in this report. It should be noted that the material presented in this report is based on the pretreatment methods proposed by BNFL Inc. and LMAES at the 3 percent design stage. Therefore, information regarding the BNFL Inc. pretreatment methods represents only a snapshot of the BNFL Inc. approach. Although the actual BNFL Inc. process flowsheet may change from what is presented in this report, the identified approaches, technologies, and methods will likely envelope the design and safety issues for the pretreatment of Hanford tank wastes.

The unit operations proposed by BNFL Inc. and LMAES are discussed in chapters 2–6. Some chapters apply to one proposal, some apply to the other proposal, and some apply to both proposals. The unit operations discussed include "Sludge Washing," "Ion Exchange," "Electrochemical Methods," "Organic Destruction," and "Precipitation and Filtration." At the end of each of these sections, a brief evaluation of the discussed technologies is presented, as they apply to the planned BNFL Inc. process. Note that information considered proprietary was deleted from this report.

1.2 Overview of the Tank Waste Remediation System Program

The TWRS Environmental Impact Statement Record of Decision (U.S. Department of Energy, 1996d) states that the waste will be retrieved from the tanks, then chemically separated to form the high- and low-activity radioactive waste streams. The high-activity radioactive waste stream will contain most of the radionuclides. This waste stream will be vitrified, and the product stored until it can be transferred to a licensed high-level waste repository. The low-activity waste stream contains the bulk of the nonradioactive chemicals and is predominantly the soluble components of the tank waste. This waste stream will be solidified into a glass or other form that meets DOE contract specifications (U.S. Department of Energy, 1996a). Disposal of the immobilized low-activity waste form onsite in a manner that allows the waste to be retrievable for at least 50 yr has been proposed, although this time period has not been officially adopted. This overall strategy for the Hanford TWRS is shown in figure 1-1. The TWRS program is divided into Phase I (proof-of-concept phase) and Phase II (full-scale operations phase). Phase I consists of Phase IA, a 20-mo development period, and Phase IB, the design, construction, and operation periods for treating and immobilizing 6–13 percent of the tank waste by mass. In 1996, contracts were awarded to BNFL Inc. and to LMAES to proceed with Phase I (U.S. Department of Energy, 1996b,c). In the Phase IA deliverables submitted to the DOE in January 1998, BNFL Inc. and LMAES described the technologies they propose to treat and immobilize the Hanford tank wastes. The LMAES technical approach proposed a liquid-fed, high-temperature, ceramic

Hanford Tank Waste Remediation System
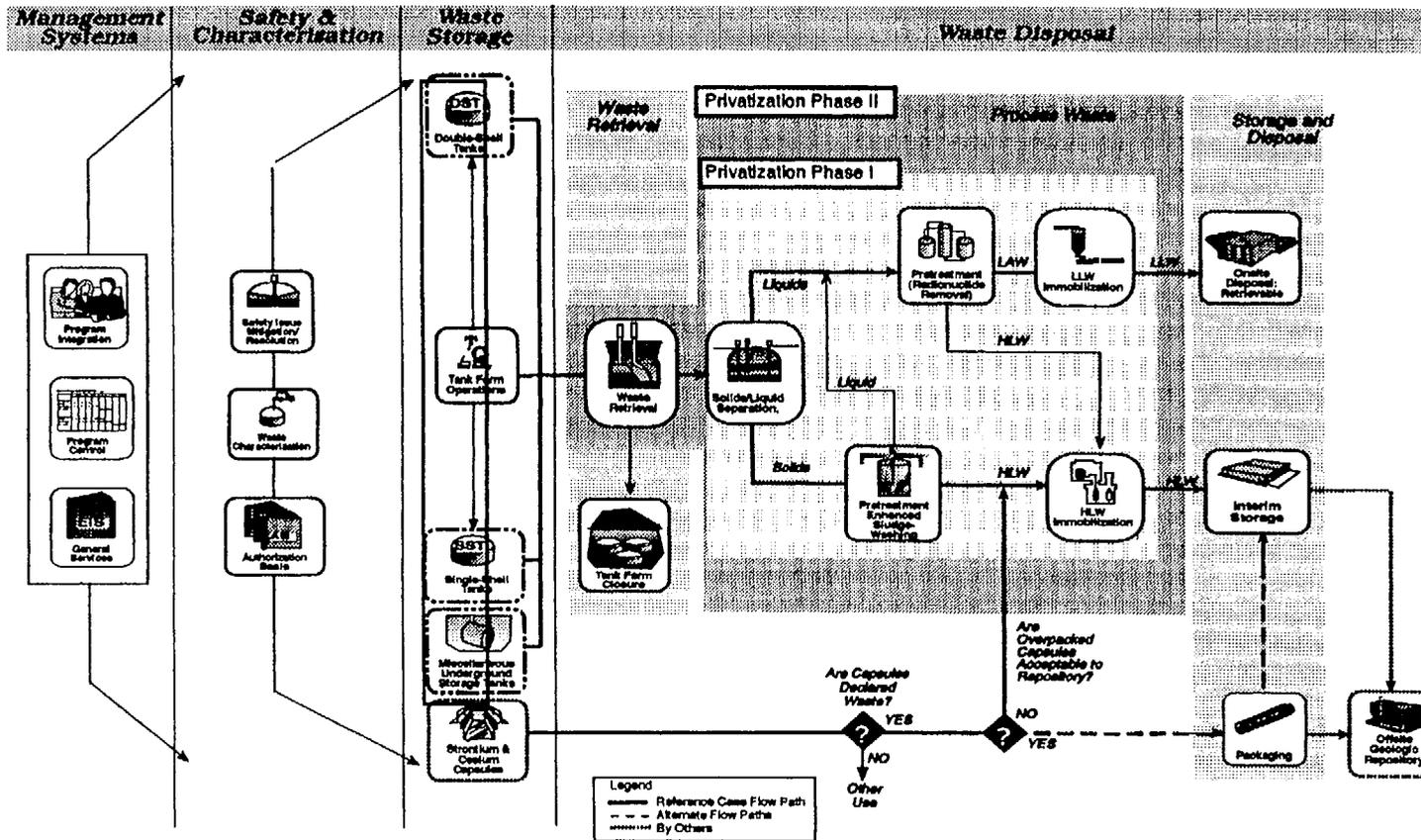
Figure 1-1. Hanford Tank Waste Remediation System strategy (U.S. Department of Energy, 1998b)

melter for low-activity waste immobilization; cold crucible melter for high-level waste immobilization; and ion exchange, ozonation, and electrochemical processing for radionuclide removal. The LMAES-proposed technologies and the previous applications of those technologies are shown in table 1-2. BNFL Inc. proposed mature technologies for treatment and vitrification of the wastes, including use of a liquid-fed, low-temperature, ceramic melter based on the same technology used for high-level waste vitrification at the West Valley Demonstration Project in New York and the Defense Waste Processing Facility at the Savannah River Site in South Carolina. The BNFL Inc.-proposed pretreatment technologies, including ion exchange, precipitation, and isotopic dilution, also have been applied at other facilities in the United Kingdom, Belgium, France, and Japan. Table 1-2 shows BNFL Inc. proposed technologies for key treatment functions and the previous applications of those technologies.

The DOE completed its review of the Phase IA deliverables received in January 1998 and entered into negotiations with BNFL Inc. and LMAES regarding each proposal to implement Phase IB. Based on evaluation of the proposals and negotiations with each contractor, DOE determined that the LMAES proposal was not viable because the technical approach had significant risk, and the business and financial approaches were not consistent with the goals of privatization (U.S. Department of Energy, 1998b). BNFL Inc. was judged viable, and DOE continued negotiations with BNFL Inc.

Based on these negotiations between BNFL Inc. and DOE, a number of changes were made to the TWRS program baseline. A 24-mo design phase was included under the negotiated plan for Phase IB, Part B-1, during which an improved basis for setting fixed prices will be achieved by reducing risks associated with facility design and regulatory requirements and which would provide time needed to obtain private financing and contractor equity commitments. Part B-2 of Phase IB comprises the construction and operations period. The facilities to be constructed will have a 30-yr design life rather than the original concept of a 5- to 9-yr demonstration facility. With a longer design life the plant would have the potential to treat waste for a longer period, to treat waste with a broader range of composition, and to treat more than half of the tank waste by mass and approximately 95 percent of the long-lived radionuclides if the plant is expanded with limited additional investment (U.S. Department of Energy, 1998a). Under Part B-2, BNFL Inc. will initiate waste pretreatment in 2005, high-level waste vitrification in 2006, and low-activity waste vitrification in 2007. The start of hot operations for each stage would occur during the same year or, in some cases, 1 yr later. Because of the sequencing of hot operations startup, low-activity waste liquids resulting from the BNFL Inc. waste separations process (i.e., pretreatment) would be transferred for approximately 2 yr to double-shell tanks maintained by the Hanford site management and integration contractor. Phase I will include immobilization operations from 2006 through 2016 when the facilities would be expanded for use in Phase II waste processing.

1.2.1 Waste Retrieval and Feed

The DOE will provide tank waste to BNFL Inc. that includes three low-activity waste feed types (i.e., envelope A, B, and C wastes). A fourth waste type (envelope D waste) would consist of the double-shell tank sludges, radionuclides separated from supernate, and solids separated from envelope A, B, and C wastes. The four waste types, with contract specifications described in appended tables A-1 through A-5, are representative of the range of Hanford tank wastes. Envelope A, B, and C wastes contain cesium and technetium at concentrations that make their removal necessary to ensure that the

Table 1-2. Treatment technologies proposed by BNFL Inc. and Lockheed Martin Advanced Environmental Systems (U.S. Department of Energy, 1998a)

Treatment Function	BNFL Inc.		Lockheed Martin Advanced Environmental Systems	
	Technology Proposed	Application History	Technology Proposed	Application History
Low–activity waste concentration	Evaporation	Evaporation of alkaline supernatant at Hanford since the 1950s, at Savannah River since the 1960s, and at West Valley during the 1990s	No evaporation proposed	Not applicable
Solid/Liquid separation	Ultrafiltration/ cross-flow filtration	Ultrafiltration/cross-flow filtration used at Enhanced Actinide Removal Plant at Sellafield, United Kingdom	Centrifuge, high shear rotary filter	Centrifuges used for gross separation at the Hanford AR Vault facility and in France for uranium processing. No known applications of high shear rotary filter in nuclear production industry.
Cesium removal	Elutable ion exchange SL-644	Elutable ion exchange used at the Hanford B Plant in 1970s. Non-elutable ion-exchange used at the Hanford B Plant in the 1970s and West Valley in the 1980–90s on chemically similar wastes.	Elutable ion exchange, electro-ion exchange, membrane ion exchange	Elutable ion exchangers used at the Hanford B Plant in 1970s. Electro-ion exchange in initial development stage for cesium removal. No known applications of membrane ion exchange used in nuclear waste processing.
Strontium/ Transuranic removal	Strontium-nitrate isotopic dilution	Used in the Hanford B Plant to enhance recovery of Sr-90 from retrieved Hanford tank wastes	Ozonation	Ozonation tested on radioactive laboratory-scale at Hanford for organic decomplexation

7

Introduction

Table 1-2. Treatment technologies proposed by BNFL Inc. and Lockheed Martin Advanced Environmental Systems (U.S. Department of Energy, 1998a) (cont'd)

| Treatment Function | BNFL Inc. | | Lockheed Martin Advanced Environmental Systems | |
	Technology Proposed	Application History	Technology Proposed	Application History
Strontium/ Transuranic removal	Iron-nitrate precipitation (Ferric floc precipitation)	Used at Enhanced Actinide Removal Plant for transuranic recovery from liquid wastes. Similar physical process at Hanford and Savannah River for the settling of transuranic in alkaline Plutonium-Uranium Extraction Facility wastes	High shear rotary filter or cross-flow filter	No known applications of high shear rotary filter in nuclear production industry
Technetium removal	Elutable ion exchange SL-639	30,000 gal. of Hanford tank waste treated in 1960. Continued research on use of anion exchange to recover technetium from Hanford wastes.	Electro-reduction for technetium recovery. Electrodialysis for technetium purification.	Technology tested on radioactive laboratory-scale only—results unclear
Cobalt and Europium removal	Not needed	Not applicable	Not identified	Limited studies for wastes similar to tank wastes, but unknown if relevant to LMAES technology
Low-activity waste vitrification	Liquid-fed ceramic melter–low temperature, 1,100 to 1,200 °C (2,012 to 2,182 °F)	Technology used for high-level waste vitrification at West Valley Demonstration Project and Defense Waste Processing Facility. Also demonstrated at Pamela Facility in Mol, Belgium; Radioactive Liquid-Fed Ceramic Melter at Hanford; and a demonstration melter in Tokai Reprocessing Plant, Japan. Some low-activity waste processing has been completed by Duratek at Savannah River, M-Area.	Liquid-Fed Ceramic Melter—high temperature, 1,250 to 1,350 °C (2,282 to 2,462 °F)	Transportable vitrification system with small-scale melter incorporating some design features of proposed melter has been tested at Oak Ridge National Laboratory. Some innovative features are undemonstrated.

Table 1-2. Treatment technologies proposed by BNFL Inc. and Lockheed Martin Advanced Environmental Systems (U.S. Department of Energy, 1998a) (cont'd)

Treatment Function	BNFL Inc.		Lockheed Martin Advanced Environmental Systems	
	Technology Proposed	Application History	Technology Proposed	Application History
Low-activity waste maintenance approach	Remote operations using manipulators	Used at West Valley Demonstration Project, Defense Waste Processing Facility, United Kingdom, and France	Contact maintenance	Not used in radioactive applications with highly volatile processes
High-level waste concentration	Cross-flow filter for supernatant separation	Cross-flow filtration used at Enhanced Actinide Removal Plant at Sellafield, United Kingdom	Centrifuge	Centrifuges used for gross separation at the Hanford AR Vault facility and in France for uranium processing
Feed preparation	Blending/ evaporation	Process similar to that used in the West Valley and Defense Waste Processing Facility Projects for feed concentration	Acidification/ blending	AVH Calciner used in the French R-7 and T-7 vitrification plants, with acidified feeds; some simulation work on Hanford-type wastes
High-level waste vitrification	Liquid-fed ceramic melter	Technology used for high-level waste vitrification at West Valley Demonstration Project and the Defense Waste Processing Facility. Also demonstrated at Pamela Facility in Mol, Belgium; Radioactive Liquid-Fed Ceramic Melter at Hanford; and a demonstration melter in Tokai Reprocessing Plant, Japan.	Cold crucible melter	70-percent scale melter tests performed with simulated high-level waste. Small-scale cold crucible melter used in low-activity waste vitrification in Russia.

9

low-activity waste glass specification can be met. Envelope B waste contains higher concentrations of cesium than envelope A and C wastes, as well as higher concentrations of chlorine, chromium, fluorine, phosphates, and sulfates, which may limit the waste loading in the glass. Envelope C waste contains organically complexed strontium and transuranic elements that will require removal. Envelope D waste contains a high-level waste slurry.

The DOE will order a minimum quantity of waste treatment services and additional treatment services if feed is available and BNF Inc. has the processing capability. During Phase IB/Part B–2, approximately 6–13 percent of the mass of Hanford site tank waste will be processed. BNFL Inc. will operate a double-shell tank (AP–106) as a waste feed receipt tank. From this tank, waste would be transferred by BNFL Inc. to the facility for treatment. A second tank (AP–108), which had been identified for use by a second contractor, would now be used by DOE for capacity management.

1.2.2 Waste Pretreatment

During Phase IB, sludge washing is to be completed by BNFL Inc. in the treatment facility rather than in existing double-shell tanks by the site management and integration contractor. The treatment facility is scheduled to begin operations in 2005. During Phase IB Part B–1 BNFL Inc. is to complete laboratory-scale and pilot-scale testing of solids/liquids separations and sludge washing. Solids in the high-level waste feed are to be transported as slurry by pipeline to the BNFL Inc. facility and batch washed in large tanks with solids to be separated using cross-flow filters. The washed solids are to be combined with cesium, strontium, transuranic elements, and technetium from envelope A, B, and C wastes, and with glass-forming chemicals to make the high-level waste feed. The wash liquids are to be sent to pretreatment for separation of radionuclides then returned to DOE for storage.

Once the low-activity waste facility is operational, the wash liquids, following separations, are to be routed to the low-activity waste treatment facility for processing. Low-activity waste is to be transferred to a feed receipt tank managed by BNFL Inc. and then transferred to smaller lag feed storage tanks in the treatment facility where the low-activity waste feed is to be evaporated or diluted as required for further processing. The feed then is to be pumped through a cross-flow filter to remove entrained solids. The entrained solids are to be washed and characterized by BNFL Inc. and, at DOE's option, either returned to DOE for storage, incorporated into the low-activity waste stream for immobilization, or included in the high-level waste stream for immobilization. BNFL Inc. is to use a cross-flow filtration system to separate suspended solids from low-activity waste feed streams. This separation is to reduce low-activity waste volume produced by in-tank sludge washing, eliminate the need for dedicated double-shell tanks for sludge washing, reduce the risk of not meeting feed specifications for certain waste streams, and provide sludge washing capability for additional waste beyond the current contract, enhance separations, and, thereby, reduce the high-level waste volume (U.S. Department of Energy, 1998b).

The waste to be processed during Phase I will also allow DOE to address safety issues associated with a number of the waste storage tanks. Six double-shell tanks that generate flammable gases will be treated during Phase I. One single-shell tank (C–106) requires periodic water additions to ensure temperature limits that might lead to tank failure are not exceeded. The waste in this tank will also be processed.

During Phase IB/Part B–1, BNFL Inc. is to complete laboratory-scale and pilot-scale testing of waste separations and ion-exchange systems. Under the negotiated approach, during Phase IB, BNFL Inc. is to

treat the liquid envelope A, B, or C wastes to separate cesium, strontium, technetium, and transuranic elements. Figure 1-2 provides a representation of the Phase IB low-activity waste and high-level waste treatment and immobilization services (U.S. Department of Energy, 1998b). Following solids/liquids separations to remove entrained solids, strontium nitrate and ferric floc are to be added to the envelope C wastes to precipitate the strontium and transuranic elements. The mixture is to be filtered again, and the strontium and transuranic solids are to be included in the high-level waste stream for immobilization. Following the second filtration step, the resulting liquids are to be pumped through an ion-exchange module to remove cesium. After cesium removal, the liquid is to be pumped to another ion-exchange module to remove technetium. Supernate pretreated during the first 2 yr of facility operations, prior to startup of low-activity waste vitrification, is to be concentrated in an evaporator and returned to DOE as pretreated low-activity waste for storage. The cesium, strontium, transuranic elements, and technetium removed from the waste feed are to be blended into the high-level waste stream for vitrification.

1.2.3 Waste Immobilization

The BNFL Inc. waste immobilization approach centers on using a liquid-fed ceramic melter based on technologies used for high-level waste vitrification at West Valley and Savannah River. The facility configuration is to include one pretreatment/high-level waste vitrification facility and one low-activity waste vitrification facility. The low-activity waste vitrification facility is to have a design capacity of 30 t/day (33 ton/day) of glass production, and the high-level waste facility is to have a design production capacity of 1 t/day (1.1 ton/day) of glass production. Assuming an operating efficiency of 60 percent, the effective average glass production rates would be 18 t/day (20 ton/day) for the low-activity waste facility and 600 kg/day (1,300 lb/day) for the high-level waste facility. Immobilized low-activity waste is to be poured into product containers and transferred to a storage area pending final transfer to DOE for disposal. BNFL Inc. is to immobilize the separated cesium, strontium, technetium, and transuranic elements, and is to have the option to vitrify the entrained solids or return the entrained solids to DOE. If entrained solids are immobilized, then double-shell tank space planned for storage of the solids will be available for storing waste retrieved from single-shell tanks or other waste management activities. The immobilized high-level waste is to be poured into canisters and transferred to a storage area. The waste then would be transferred to DOE for onsite storage pending shipment to a geologic repository for disposal.

1.3 Hanford High-Level Waste Safety Issues

Safety issues related to the Hanford high-level wastes are summarized briefly in the following sections. Detailed discussions were provided in a previous CNWRA report (Pabalan et al., 1999).

1.3.1 Hydrogen Gas Generation

Hydrogen is released from the wastes in all of the Hanford waste tanks (Gephart and Lundgren, 1997). The production of hydrogen should be anticipated in the systems designed to contain and process those wastes. This hydrogen production poses potential for an uncontrolled gas burn that could release radioactive material into the environment (U.S. Department of Energy, 1996d).
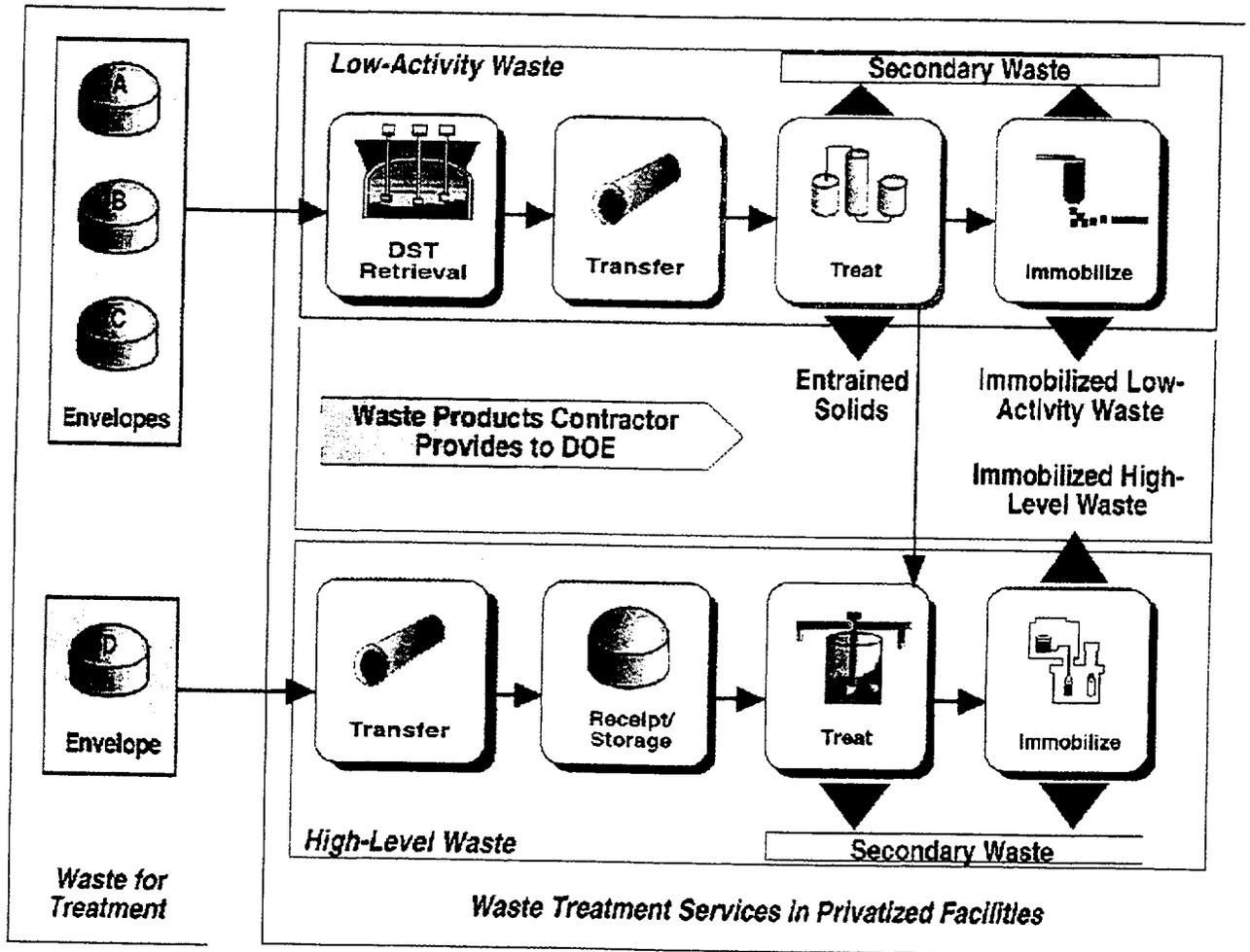
Figure 1-2. Hanford Tank Waste Remediation System Phase I low-activity and high-level waste treatment services (U.S. Department of Energy, 1998b)

Hydrogen is produced by radiolysis of water, organic chemicals, and organic resins. A safety issue occurs when hydrogen is released in amounts producing concentrations in excess of the hydrogen lower explosive limit. The lower explosive limit for hydrogen in air is 4.1 percent (Lewis, 1997).

The radiolysis of water not only produces hydrogen, it also produces hydrogen peroxide. Hydrogen peroxide is unstable and decomposes as shown below to produce oxygen. In pure water, the decomposition is slow, but it is catalyzed by dissolved compounds (Sienko and Plane, 1961). Therefore, in an aqueous waste solution, one might assume that much, if not all, the hydrogen peroxide produced by radiolysis decomposes to produce oxygen, as shown below:

$$H_2O_2(aq) \rightarrow H_2O(l) + \tfrac{1}{2}O_2(g)\uparrow \tag{1-1}$$
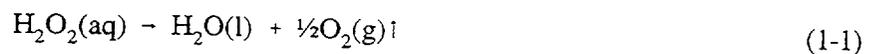
Together with radiolytically produced hydrogen, an explosive mixture of hydrogen and oxygen, in stoichiometric proportions can be produced, which could detonate if an ignition source is present, through the reaction

$$2H_2 + O_2 \rightarrow 2H_2O \qquad (1\text{-}2)$$

When fluids are not flowing through process vessels, hydrogen produced in the vessels should be expected to accumulate. Therefore, vessels containing wastes that could produce hydrogen should remain ventilated, and not sealed. Wastes that could produce hydrogen include aqueous wastes loaded with radioactive materials and organic resins loaded with radioactive materials. Aqueous wastes containing organic chemicals would be expected to produce more hydrogen than the equivalent aqueous waste without organic chemicals.

1.3.2 Exothermic Reactions

Should an exothermic reaction occur, the energy release could pressurize the containment barriers, possibly producing a release of radioactive materials to the atmosphere. In an extreme case, a containment barrier could burst, as in an explosion. The presence of ferrocyanide, organic materials, nitrates, and nitrites establishes a potential for exothermic reactions in the Hanford wastes.

During the 1950s, large quantities of ferrocyanide were added to the Hanford wastes to precipitate cesium-137 and strontium-90. Because wastes have been transferred between tanks and between tank farms, sometimes with few records being kept, ferrocyanide could exist in almost any of the Hanford waste tanks (Gephart and Lundgren, 1997).

One possible exothermic reaction in Hanford wastes involves ferrocyanide [$Fe(CN)_6^{4-}$]. The presence of ferrocyanide establishes a potential for an uncontrolled reaction that could result in release of radioactive material to the environment (U.S. Department of Energy, 1996d). At elevated temperatures, 221–285 °C (430–545 °F), ferrocyanide can react with nitrate ions (NO_3^-) and nitrite ions (NO_2^-) to release large amounts of energy as sensible heat (Gephart and Lundgren, 1997). Because it is a wet phase reaction, and because the necessary temperature is greater than the boiling temperature of the aqueous waste at normal pressures, this reaction is not likely unless the waste is confined and pressurized. Should the reaction occur, the energy release would pressurize the containment even further, possibly causing the containment to burst, as in an explosion. To prevent this from happening, vessels, and sections of waste transfer pipe, containing aqueous wastes should not be isolated by closing valves, because then a pressure build-up could occur by gas evolution or heating. Therefore, the vessels and sections of waste transfer pipe should always be ventilated to prevent a buildup of pressure.

Another example of possible exothermic reactions involves organic materials present in the Hanford wastes. At 221 °C (430 °F), organic materials can react with nitrates and ignite, releasing large amounts of energy (Gephart and Lundgren, 1997). Subsequent pressurization could lead to loss of containment with release of radioactive materials to the environment. In an extreme case, the confinement could burst resulting in equipment damage, personnel injuries, and contamination spread. To prevent these consequences, the temperature should be monitored in any vessels or lengths of waste transfer pipe that contained high-level wastes with organic materials, and which are removed from service for any

13

significant period of time. If decay heat in such vessels or pipes should cause the waste to dry and achieve temperature greater than the boiling temperature of the waste, then steps should be taken to keep the waste wet.

1.3.3 High-Heat Generation

High-heat generation, from decay of fission product radionuclides, could expand gases in the Hanford waste tanks to produce pressurization of the waste containment, possibly resulting in a release of radioactive materials to the atmosphere. Should decay heat evaporate the waste water and subsequently elevate the temperature of the dry waste to above 221 °C (430 °F), the ferrocyanides, organic materials, nitrates, and nitrites in the wastes could react explosively, producing contamination of the environment, damage to equipment, and injury to personnel. Similarly, should hydrogen accumulate and concentrate to above its lower explosive limit, and the decay heat elevate the hydrogen to its auto-ignition temperature, 400 °C (722 °F), an explosion could result.

High-heat generation from radioactive decay establishes a potential for heat-induced structural damage. Damage could result if no external cooling is provided, or if the external cooling system should fail. Structural damage could be followed by release of wastes contained within the tank.

In the Soviet Union during 1957, in a high-level radioactive waste tank with a failed cooling system, decay heat dried the aqueous wastes to dryness, then substantially elevated the temperature of the dry wastes, producing an explosive reaction from organic nitrates. The explosion resulted in the immediate deaths of two guards, damage to equipment, and release of radioactive contamination, requiring the evacuation of an entire community (Vance, 1990).

Heat generated from radioactive decay is a concern for vessels in which hydrogen gas is generated, because the temperature within the vessel must not exceed the auto-ignition temperature of the hydrogen. Hydrogen auto-ignites at 400 °C (752 °F) (Lewis, 1997). Wherever hydrogen generation is a concern, and the waste loading provides a significant source of decay energy, engineering evaluations should be performed to assure that the decay energy cannot overheat the vessel contents.

1.3.4 Plugging of Process Lines

The obvious impact of plugging in a process line is the loss of the intended use of the line. Plugging of process lines also can have the effect of isolating and confining a process vessel or length of piping. Once confined, pressurization can occur by a number of mechanisms (e.g., by gas generation, heating, or both). If pressurized and heated, an exothermic ferrocyanide or organic reaction with nitrates and nitrites could occur. All these mechanisms could lead to failure of the vessel or pipe, and unplanned release of radioactive materials to the environment. To prevent this unplanned release, provisions should be taken to preclude plugging in the system. Waste transfer lines containing significant amounts of undissolved solids should be designed in a way to preclude plugging from an accumulation and subsequent hardening of the solids. Provisions include avoiding low points where solids could accumulate, and operations procedures should require that transfer lines be flushed before being allowed to remain idle for long periods of time.

The temperature of the process lines should be controlled to avoid crystallization during treatment of the fluids. For example, one of the high-level waste transfer lines between the 200-east area and the 200-west area at Hanford became plugged when the pipe temperature decreased so that crystals formed and blocked the flow of wastes in the lines (Gephart and Lundgren, 1997).

In addition, attention should be paid to the compatibility of materials transported through the process lines. For example, one of the high-level waste transfer lines between the 200-east and 200-west areas at Hanford became plugged because a chemical reaction between aluminum and phosphate in the waste produced a "green gunk mixture" that plugged the lines (Gephart and Lundgren, 1997).

Plugging could also occur by a buildup of solids in an ion-exchange column. Therefore, the amount of undissolved solids in the waste should be restricted by filtering the fluids before treating them by ion exchange.

The chemistry in the ion-exchange columns should be studied to assure that dissolved solids do not precipitate in the cells and fill void spaces, causing plugging. For example, aluminum hydroxide is soluble in acid or alkali but practically insoluble at near neutral pH conditions (Lange, 1967). Therefore, to prevent aluminum hydroxide from precipitating and collecting in the ion-exchange columns, the wastes must be kept very acidic or very alkaline.

1.3.5 Radiolysis

Irradiation of water in the aqueous Hanford wastes produces flammable hydrogen gas. Irradiation of organic materials, such as the organics in the Hanford wastes or organic resins used to process the wastes, can produce gases such as carbon dioxide and methane. Irradiation of the nitrates in the wastes can result in the generation of nitrous oxide gas. The generation of hydrogen can pose an explosion hazard. Generation of any of these gases can pressurize the waste confinement to produce a release of radioactive materials to the environment.

When water is irradiated, hydrogen ions (H^+) and hydroxyl ions (OH^-) form. These ions recombine to form water (H_2O) and react with similar radicals to form hydrogen gas (H_2) and hydrogen peroxide (H_2O_2) (Long, 1967):

$$H^+ + OH^- \rightarrow H_2O \tag{1-3}$$

$$2OH^- \rightarrow H_2O_2 + 2e^- \tag{1-4}$$

$$2H^+ + 2e^- \rightarrow H_2 \tag{1-5}$$

Introduction

The production of hydrogen gas and hydrogen peroxide by radiolysis is a hazard.

When organic materials are irradiated, they break down, forming any of a number of smaller molecules. For example, irradiation of the organic ion-exchange resin, resorcinol-formaldehyde, produces carbon dioxide gas (CO_2) and trace amounts of methane gas (CH_4) (Bibler, 1994). Irradiation of nitrates in the presence of organic materials results in the generation of nitrous oxide gas (N_2O) (Bibler, 1994). The generation of gases such as these also poses a hazard.

Vessels containing wastes that could produce significant amounts of gases from radiolysis should be ventilated and not sealed.

1.4   Overview of BNFL Inc. Pretreatment Process

For low-activity waste, BNFL Inc. plans to concentrate the waste feed by evaporation, separate the solids by ultra-filtration, remove cesium-137 by ion exchange with the organic resin SuperLig®-644, and remove technetium-99 by ion exchange with the organic resin SuperLig®-639. The liquid low-activity waste is then to be concentrated by evaporation, and blended with glass formers before being fed to a low-activity waste melter. See figure 1-3, BNFL Inc. process overview. For envelope C wastes only, strontium-90 and transuranic elements are to be removed by precipitation immediately prior to removal of the solids by ultra-filtration.

For high-level wastes, BNFL Inc. plans to separate the liquid from the solids by ultra-filtration, sending the liquid permeate to the low-activity waste pretreatment process described previously. The high-level waste solids are to be combined with the solids ultra-filtered from the low-activity waste, then blended with glass formers before being fed to the high-level waste melter.

1.5   Overview of Lockheed Martin Advanced Environmental Systems Pretreatment Process

The system proposed by LMAES was for low-activity waste only. Solids were to have been removed by centrifuging followed by high-shear rotary filtration. Cesium-137 was to have been removed with resorcinol-formaldehyde resin. Additional cesium-137 was to have been removed by membrane ion exchange. Technetium-99 was to have been removed by electroreduction. The waste was then to have been concentrated by evaporation prior to the addition of glass formers and introduction to the low-activity waste melter.

For envelope C wastes, immediately following cesium-137 removal by membrane ion exchange, the organic materials in the wastes were to have been destroyed by ozonation, followed by removal of strontium-90 and transuranic elements by filtration.

The filtered solids were to have been returned to the DOE as a slurry.

The cesium-137 was to have been eluted from the resorcinol-formaldehyde by an electrochemical ion-exchange process. The eluted resorcinol-formaldehyde resins were then to have been regenerated and reused. The eluted cesium was to have been adsorbed onto inorganic crystalline silicotitanate ion-exchange material, and returned to the DOE in a dry solid form. The technetium-99 was to have been
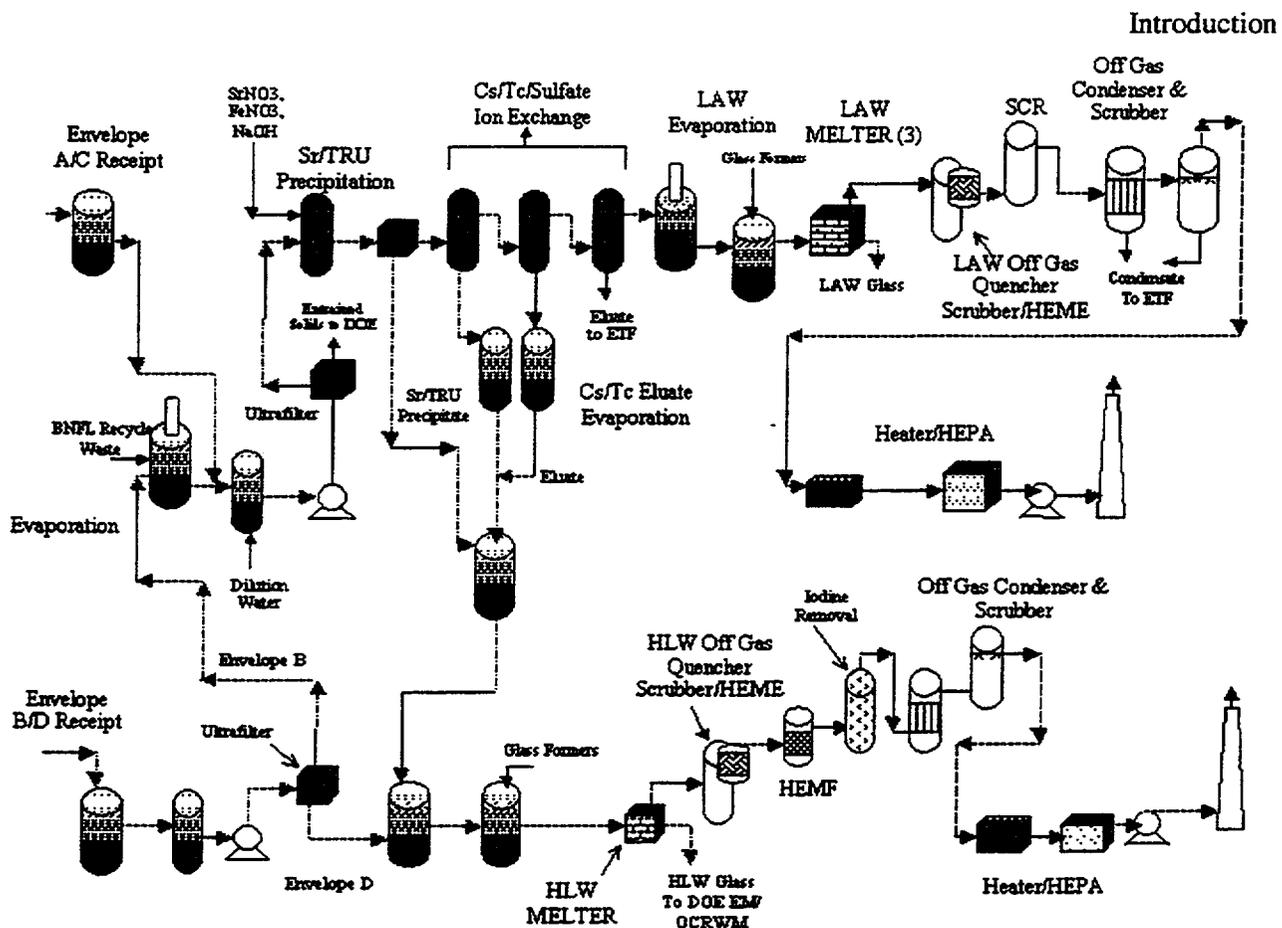
Figure 1-3. BNFL Inc. process overview (Sturm et al., 1999)

removed from the electroreduction system electrode with nitric acid and returned to the DOE in a liquid form.

Detailed descriptions of the centrifuging process, filtration process, cesium-137 ion-exchange process, ozonation and filtration process for strontium-90, transuranic elements removal, technetium electroreduction, and ion-exchange resin management are considered proprietary and have been removed from this version of the report.

1.6   High-Level Waste Pretreatment Experience

1.6.1   West Valley Demonstration Project

The waste in the West Valley Demonstration Project high-level waste storage tank 8D–2 was primarily PUREX process waste that had been neutralized with sodium hydroxide. This neutralized waste consisted of two distinct layers, a precipitated sludge layer consisting mostly of insoluble hydroxides, and a liquid supernatant layer containing soluble nitrates. The water soluble cesium-137 and

nonradioactive sodium were primarily in the supernate. The strontium-90 and other radionuclides were primarily in the sludge.

The West Valley Demonstration Project tank 8D-2 supernate resembles the Hanford neutralized current acid waste, generated by processing spent fuel at PUREX plant. Because the neutralized current acid waste liquid and sludges in Hanford tanks AZ-101 and AZ-102 are categorized as envelope B and D wastes, respectively, the West Valley Demonstration Project supernate and sludge from tank 8D-2 provide a reasonable approximation to the envelope B low-activity waste and envelope D high-level waste to be processed by the TWRS program.

In tables A-6 and A-7, the maximum chemical and radionuclide content limits of the low-activity waste envelope B (U.S. Department of Energy, 1996b) are listed and compared with the measured chemical and radionuclide contents of the supernatant liquid from tank 8D-2 at the West Valley Demonstration Project (Rykken, 1986).

In tables A-8 and A-9, the chemical and radionuclide contents of a composite sludge from Hanford tanks AZ-101 and AZ-102 (Rapko and Wagner, 1997), which will be used as envelope D feed to the TWRS vitrification facility, are listed and compared with chemical and radionuclide contents of the supernatant liquid from tank 8D-2 at the West Valley Demonstration Project (Rykken, 1986). The chemical compositions of these sludges are generally quite similar, with the exception of cadmium. Cadmium is a neutron poison, and more cadmium may have been added at Hanford than at West Valley for criticality control during reprocessing operations. The radionuclide contents of these sludges show distinct similarities in fission products and transuranic elements present, but in some cases the quantities vary significantly. Differences may be due to varying operating histories of the reactors from which the reprocessed fuels came, from varying decay times, or from a difficulty in obtaining representative samples from the sludges.

At the West Valley Demonstration Project, the wastes were pretreated to significantly reduce the volume of the final waste form. See figure 1-4. The high-level waste contained a large amount of nonradioactive sodium that was added to the waste, primarily as sodium hydroxide, to neutralize the waste before it was sent for storage to the underground carbon steel tank, and as sodium nitrite, to inhibit corrosion of the carbon steel tank. In the final waste form, borosilicate glass, the sodium fraction had to be restricted to maintain the desired durability. By removing most of the nonradioactive sodium, only one-sixth the amount of glass was needed to immobilize the radioactive constituents, while maintaining the desired durability.

To remove sodium from the supernate and to retain the radioactive cesium-137, while allowing the sodium to pass from the system with the water, West Valley Demonstration Project adopted an ion-exchange process. A zeolite-based inorganic ion-exchange media (IONSIV® IE-96) was initially selected for the ion-exchange process (Prowse and Schiffhauer, 1992).

Before selecting the zeolite-based ion-exchange system for pretreatment, the West Valley Demonstration Project carefully reviewed and tested several technologies for cesium-137 separation, as shown in table 1-3. The selection of the reference supernatant treatment system was based on a technical ranking using four criteria: (i) process performance, (ii) vitrification and low-level waste processing impacts, (iii) equipment and process complexity, and (iv) safety and environmental considerations. All of the

Low-Level Waste Processing Cycle
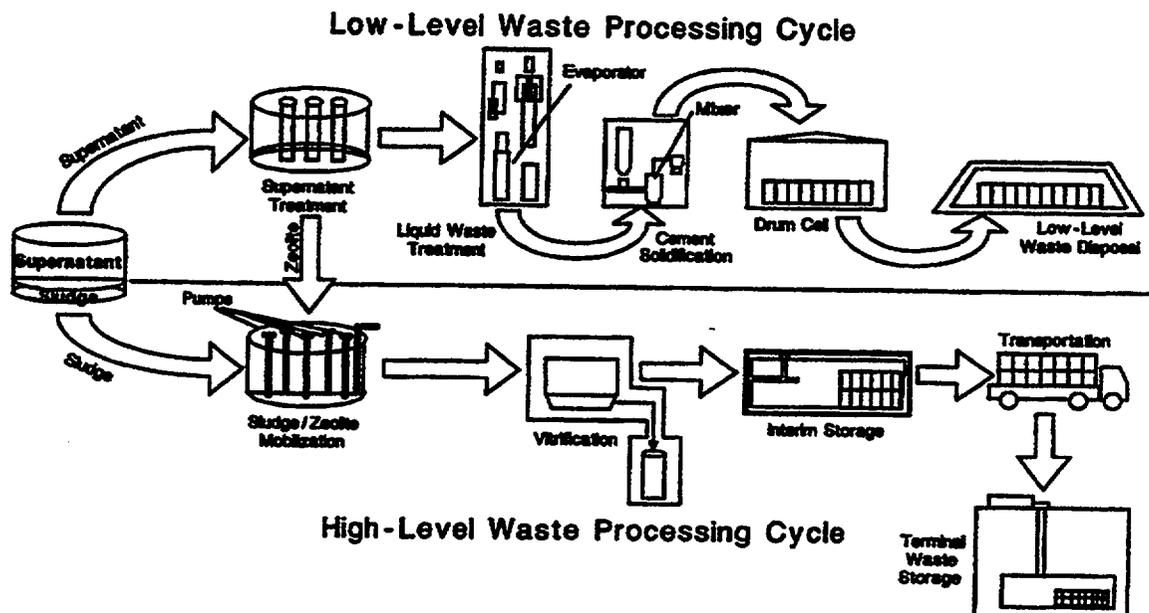
Figure 1-4. West Valley Demonstration Project high-level waste pretreatment process (Ploetz and Leonard, 1988)

processes listed in table 1-3 were capable of satisfactory performance by meeting the minimum cesium-137 decontamination factor of 1,000. In terms of relative technical ranking, the zeolite ion-exchange process was ranked first, followed closely by the phosphotungstic acid precipitation process. Even though the phosphotungstic acid process was complex, it would have had a small impact on the vitrification process. The organic ion-exchange process achieved a low ranking because of (i) its poor decontamination performance, (ii) its high equipment and process complexity, and (iii) its impact on vitrification and low-level waste processing. The sodium tetraphenylborate precipitation process achieved the lowest rating because of the relatively complex processing required for treatment of the precipitate, and the significant impact on vitrification and low-level waste processing.

Based on the previous ranking, the supernatant treatment system was developed (Ploetz and Leonard, 1988). In the West Valley Demonstration Project supernatant treatment system, supernate was transferred from the underground high-level waste storage tank (8D–2) to the supernate feed tank by a submersible vertical turbine pump installed in the tank. Optional filtration was available for when the total solids exceeded 200 ppm. This was for preventing process contamination by removing sludge particles suspended in the supernate. The supernate from the supernate feed tank was transferred through a supernate cooler by a seal-less canned pump at a rate of 130–380 mL/sec (2.0–6.0 gpm). The supernate cooler cooled the supernate to below 13 °C (55 °F). The cooled supernate was pumped through the four ion-exchange columns in series (Ploetz and Leonard, 1988). Each ion-exchange column contained 1.7 m³ (60 ft³) of zeolite having a mass of 1.6 t (3,500 lb). The system was designed to operate with three columns online with one offline and available for recharging, but the batch method of operation allowed

19

Introduction

Table 1-3. Processes considered by West Valley Demonstration Project for cesium-137 retention

Candidates for Pretreatment*	Does the Cesium Decontamination Factor = 1000?	Equipment Complexity	Process Considerations
Inorganic IX Zeolite[†]	Yes, at 25 °C pH = 10 0.6 column volumes per hour	Relatively simple	Easily transferred/melted with glass
Inorganic/Elution	Yes, at 25 °C pH = 10 0.6 column volumes per hour	Moderate	Zeolite not easily decontaminated
Organic IX resins (CS–100, IRC–718)	Yes, at 6 °C pH = 13 80 mesh	Considerable. Vessels, Plumbing	Control formate to prevent metal reduction. Autocatalytic ignition with nitric acid elution possible.
Precipitation (sodium tetraphenylborate)	Yes, with decanted supernate; large incinerator	Considerable. Acid hydrolysis, benzene	Organic destruction
Phosphotungstic acid	Yes, pH = 0 Vessels, filters, pH adjustments	Considerable	pH = 0, precipitate separation critical. Increase low-level waste.

*Other processes examined, but not retained, as leading candidates were ARC–359, IRC–718, IRC–84, IRC–505, charcoal, electrodialysis, hyperfiltration, ferrocyanide, and biosorbents.
[†]Other inorganic media evaluated and not used as being equivalent to, or not as good as, IE–95/96, were Durasil, DeVoe/Holebein compositions, natural zeolites, synthetic zeolites, and variations of IE–95/96.

all four columns to be online at the same time, because the loaded zeolite was changed when the system was not processing. Laboratory analyses were performed to determine the cesium-137 loading in each column. When one column was loaded, after processing a minimum of 57 m^3 (15,000 gal.), the supernate processing was shutdown. All columns were flushed with demineralized water, and the system was placed on recirculation through the second, third, and fourth columns for the remainder of the shutdown period.

The fully loaded zeolite in the first column was replaced with fresh zeolite. The loaded zeolite was first rinsed with residual supernate, and this rinse was sent back to high-level waste tank 8–D2. The rinsed zeolite was then sluiced to the bottom of tank 8D–1 with process water. To sluice the zeolite from the column, the bed was backwashed and expanded. After the column bed was expanded, an outlet valve on the bottom of the column was opened to allow the loaded zeolite bed to fall to the bottom of tank 8D–1. The fresh zeolite was fed to the supernatant treatment system as a water slurry.

During the middle of the pretreatment campaign, zeolite (IONSIV® IE-96) in alternating columns was replaced by a proprietary titanium-coated zeolite (IONSIV® TIE-96), capable of retaining plutonium and strontium-90 along with ion exchanging cesium-137. At the West Valley Demonstration Project, plutonium was present in the high-level waste as an insoluble species. However, with time, as the pretreatment process using zeolite progressed, the waste became dilute and the pH decreased, resulting in a higher solubility for plutonium (Dalton, 1992). The soluble plutonium was carried along with the effluent, passed through the ion-exchange columns, and accumulated in the evaporator. In an attempt to reduce the plutonium carry over, the titanium-coated zeolite (IONSIV® TIE-96) was adopted for the high-level waste pretreatment process.

Following ion exchange, the decontaminated supernate was processed through a sand filter to remove any suspended zeolite fines and then stored in tank 8D-3. The decontaminated supernate was then concentrated and mixed with specially formulated cement for disposal as low-level waste. The loaded zeolite was combined with high-level waste sludge in tank 8D-2 and delivered to the vitrification system.

The supernatant treatment system was provided with instrumentation to monitor flow, pressure, and fluid, temperature, and radiation levels to ensure system operations were controlled and system limitations not exceeded (Borisch and Marchetti, 1987). The majority of the supernatant treatment system equipment was operated from a control room. The system could be remotely started, operated, monitored, and shutdown from the control room. The safety-related systems that provided alarm indications included (i) ventilation system differential pressure monitoring, (ii) radiation monitoring, (iii) effluent monitoring, (iv) leak detection, and (v) pneumatic sample transfer.

The pretreatment process was operated from 1988 to 1995 as shown in table 1-4. During operations, several enhancements that were implemented include

- Cooling of the supernate to 10 °C (50 °F) greatly improved the decontamination factor measured across the zeolite columns.

- Titanium-treated zeolite (TIE-96) removed strontium-90 and plutonium from the supernate, in addition to removing cesium-137.

Some of the lessons learned include

- Pilot-scale testing with nonradioactive simulant is invaluable to develop processes.

- Thorough checking of each piece of equipment is important [e.g., (i) the dump valve in column D failed when it was partially open; (ii) the dump valve in column B failed to stoke, so it was left open and capped to aid future column discharge; (iii) seal leakage occurred due to dump valve actuator failure in columns A, B, and C; and (iv) foreign material—a weld rod—had been left in one of the columns].

- Clear and precise drawings are essential for proper equipment installation (e.g., pump G-001 in tank 8D-2 was oriented in an improper direction).

Table 1-4. West Valley Demonstration Project waste pretreatment history (Dalton, 1997)

Time Period	Material Processed	Volume Processed
May 1988–Nov 1990	PUREX process supernate	560,000 gal.
Apr 1992–May 1994*	PUREX sludge wash #1	410,000 gal.
Jun 1994–Aug 1994	PUREX sludge wash #2	360,000 gal.
Jan 1995–May 1995	THOREX wash[†]	316,000 gal.
		Total of 1,646,000 gal.

*The extended period of time was attributed to equipment problems in other parts of the Integrated Radwaste Treatment System, not to the ion-exchange process.
[†]Similar to PUREX process supernate.

- Monitoring the evaporator influent and effluent is necessary to watch for potential retention of fissile material.

- Monitoring and establishing trends for the chemistry of waste storage tanks, for proper corrosion protection, and for change in solubility of solids, are important.

- As-built drawings are important for operating, troubleshooting, and modifying installed systems.

- Photographing and videotaping soon-to-be inaccessible locations are invaluable if repairs or remote access are necessary.

Vitrification operations began in 1996 after the pretreatment operations had been completed.

1.6.2 Defense Waste Processing Facility

Like the high-level waste at Hanford, the high-level waste at Savannah River was generated by reprocessing fuel from DOE weapons material production reactors. Sodium hydroxide was added to the waste to minimize corrosion in the underground carbon steel waste storage tanks, resulting in strongly alkaline wastes. Sludges, consisting of metal hydroxides and hydrated metal oxides, settled to the bottom of the tanks. Soluble salts and cesium remained in the supernate.

Similarities in waste origin and storage practices between the Savannah River high-level liquid wastes and the TWRS envelope A and B wastes at Hanford are apparent. Similarities in origin of the Savannah River sludges and the TWRS envelope D wastes are also apparent. The Savannah River high-level waste liquids are dissimilar to the TWRS envelope C wastes in the lack of organic complexants.

At the Defense Waste Processing Facility, a process of in-tank precipitation was selected in 1983 as the preferred method for separating radionuclides from the soluble waste. The process would employ in-tank precipitation of cesium-137 with sodium tetraphenylborate and ion exchange of strontium-90 and plutonium onto sodium titanate. The solids, which would retain the radionuclides, would be filtered and

separated from the solution, which would contain the sodium. The sodium solution would be processed into a cement grout called saltstone for disposal as low-level waste. To minimize the amount of hydrocarbons fed to the melter, the tetraphenylborate precipitation products would be decomposed prior to incorporation into the melter feed stream. This decomposition would be accomplished by an acid hydrolysis process using formic acid, hydroxylamine nitrate (to destroy the nitrite corrosion inhibitor that would interfere with the hydrolysis reaction), and a copper catalyst. The resulting organic compounds benzene, phenol, and minor amounts of higher boiling aromatic compounds would be removed by steam stripping and collected for eventual incineration (Carter et al., 1997).

In-tank precipitation operations began in 1995, but higher than expected amounts of vaporized benzene, resulting from decomposition of the sodium tetraphenylborate, were detected, and the in-tank precipitation process was placed on standby in 1996. In February 1998, the DOE formally suspended the use of the in-tank precipitation process for the treatment of Savannah River high-level liquid waste (U.S. General Accounting Office, 1999). Alternative processes are currently being evaluated, including small tank precipitation and ion exchange. The former would use the same chemical as the original in-tank precipitation process, but would use smaller tanks—allowing the process to be completed in 24 hr instead of weeks and reducing the time during which benzene could build up in the tanks. The latter would use a nonelutable crystalline silicotitanate ion exchanger to remove cesium and monosodium titanate to remove the strontium, plutonium, and uranium in the liquid waste.

At the Defense Waste Processing Facility, excess aluminum is removed from the sludge to improve glass processing characteristics, such as melting temperature and melt viscosity (Iverson and Elder, 1992). Removal is by high-temperature dissolution in concentrated sodium hydroxide (Carter et al., 1997). The aluminum-bearing solution is converted into saltstone for disposal as a low-level waste (Carter et al., 1997; Iverson and Elder, 1992).

At the Defense Waste Processing Facility, mercury is removed for corrosion control and chemical contamination control by adding formic acid (Iverson and Elder, 1992). Formic acid reduces the mercuric oxide (HgO) to elemental mercury (Hg), which is subsequently removed by steam distillation, collected, and stored for possible recycle (Iverson and Elder, 1992).

The Savannah River Site has 60,200 m³ (15,900,000 gal.) of salt supernate, plus 53,400 m³ (14,100,000 gal.) of salt cake, which were to be pretreated by in-tank precipitation and filtration. In addition, 15,100 m³ (4,000,000 gal.) of sludge are to be pretreated by washing. While the difficulties associated with in-tank precipitation were being addressed, the Defense Waste Processing Facility began vitrification operations in 1996 using a sludge-only flowsheet.

Some of the lessons learned from the Savannah River Site pretreatment operations include

- Composition of simulants used in process testing should be similar to actual radioactive waste composition. It should include minor constituents, such as noble metals, which could act as catalyst for reactions that could lead to unsafe conditions.

- Final selection of technology and plant design should be made after conducting rigorous tests using actual high-level radioactive waste.

23

Introduction

The Defense Waste Processing Facility pretreatment process as originally conceived is depicted in figure 1-5. The pretreatment processes employed at the West Valley Demonstration Project and at the Defense Waste Processing Facility are compared in table 1-5.

1.7 Future Considerations

The pretreatment flowsheets proposed by BNFL Inc. and LMAES focus on the separation of cesium-137, strontium-90, technetium-99, and transuranics—radionuclides that dominate the inventory of Hanford tank wastes. However, other radionuclides present in significant amounts may also need to be separated from the low-activity waste prior to immobilization. The gamma-emitting radioisotopes europium-154, europium-155, and cobalt-60 are present in significant quantities in Hanford tank wastes. Their estimated total inventories in all the 177 Hanford waste tanks, based on the Hanford best-basis inventory [available online at the Pacific Northwest National Laboratory Tank Waste Information Systems (TWINS) web site http://twins.pnl.gov:8001/TCD/main.html], are listed in table 1-6. For comparison, the estimated inventories of cesium-137, strontium-90, and technetium-99 are also listed in the table. The maximum concentrations of cesium-137, strontium-90, technetium-99, europium-154, europium-155, and cobalt-60 in the low-activity waste envelopes A, B, and C are given in table A-2. BNFL Inc. has not proposed to separate europium and cobalt from the waste stream, but LMAES had planned to investigate unit operations for separation of these elements.

The NRC established no specific quantified limits in Class C low-level waste for europium-154, europium-155, and cobalt-60. Because these gamma-emitting radioisotopes will be incorporated into the immobilized low-activity waste glass and contribute to the radiation dose rate from the immobilized low-activity waste package, practical considerations, such as the effects of external radiation and internal heat generation on transportation, handling, and disposal, may make limiting the concentration of these radionuclides desirable. If the concentrations of these radionuclides in the low-activity waste are deemed sufficient to produce such problems, process unit operations could be installed to remove those from the solution, such as ion exchange or solvent extraction. Alternatively, use of remote handling techniques, or shielding, or both, could be employed. Some ion-exchange methods that may be useful for treating Hanford wastes are discussed briefly in chapter 3.

In addition to radionuclides, separation of other chemical components that could affect production of acceptable waste forms may be needed. An excessive concentration of minor waste species, such as sulfate, could result in increased corrosion of melter components (Jain and Pabalan, 1998). For example, sulfates, in the presence of chlorides in the waste are known to dramatically corrode stainless steel and Inconel® between 500 and 900 °C (932 and 1,652 °F). In addition, because of the limited solubility of sulfur in glass, excessive sulfur concentrations in the waste feed could lead to formation of an immiscible molten sulfate layer on top of the cold-cap in the melter. This sulfate layer, referred to as gall, behaves like a foam (Jain and Pabalan, 1998). At the Pamela vitrification facility (Mol, Belgium), for example, the amount of waste that could be processed into glass was limited by the amount of sulfur in the waste (Weise et al., 1988). BNFL Inc. could reduce the waste loading in the glass formulations for immobilized low-activity waste to avoid formation of the sulfate layer, but this approach would increase the volume of immobilized low-activity waste glass.

The estimated total inventory of sulfate in 177 Hanford tanks is listed and compared to those of nitrate, nitrite, and phosphate in table 1-6. The concentration limits for sulfate in the low-activity waste
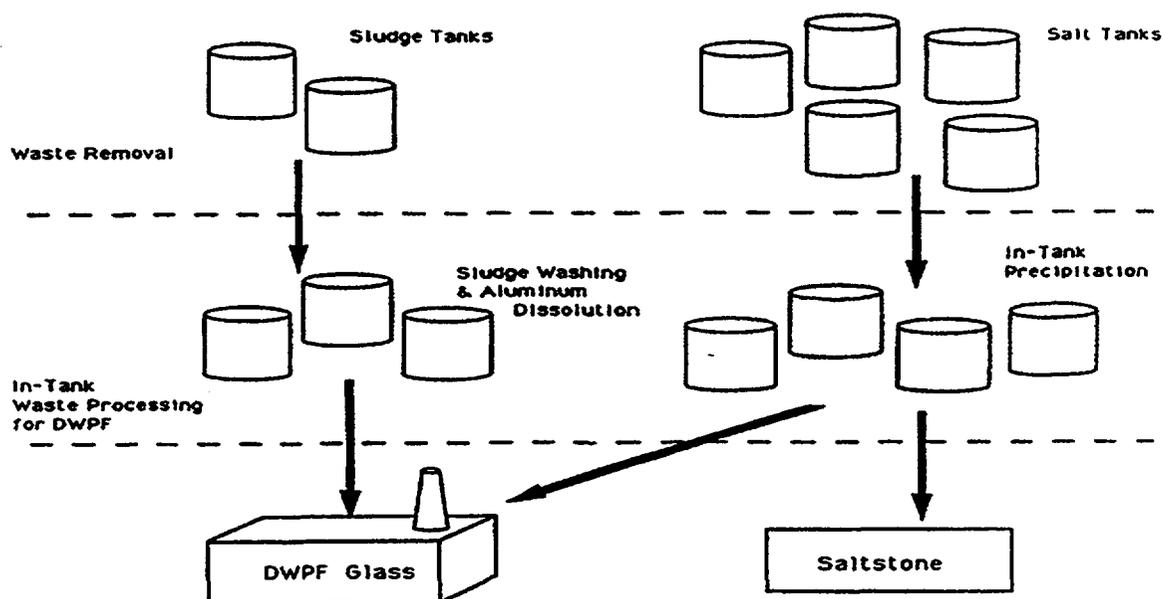
Figure 1-5. Defense Waste Processing Facility (DWPF) high-level waste pretreatment process

Table 1-5. Comparison of West Valley Demonstration Project (WVDP) and Defense Waste Processing Facility (DWPF) waste pretreatment

Pretreatment	Purpose	WVDP Method	DWPF Method
Sodium removal	Waste volume reduction	Ion-exchange pretreatment of supernate with zeolite to retain Cs-137, allowing Na to be removed from the high-level waste with the aqueous solution.	In-tank precipitation of Cs-137 with Na-TPB and ion exchange of Sr-90 and Pu onto sodium titanate, followed by filtration. Na passes from the high-level waste with the filtrate.*
Aluminum removal	Melter operational control	Not applicable.	Concentrated alkaline sludge wash to dissolve/remove the aluminum.
Mercury removal	Chemical contamination control and corrosion control	Not applicable.	Formic acid is used to reduce HgO to Hg, followed by steam distillation to remove Hg.
*Alternative processes are currently being evaluated (U.S. General Accounting Office, 1999)			

25

Table 1-6. Estimated total inventories of predominant radionuclides and anionic components in all the 177 Hanford waste tanks*

Component	Inventory
Cesium-137	53,400,000 Ci
Strontium-90	59,200,000 Ci
Technetium-99	28,600 Ci
Cobalt-60	20,400 Ci
Europium-154	194,000 Ci
Europium-155	177,000 Ci
Nitrate	52,600,000 kg
Nitrite	12,500,000 kg
Phosphate	5,470,000 kg
Sulfate	3,310,000 kg

*Best-basis inventory values taken from the Pacific Northwest National Laboratory Tank Waste Information Systems web site http://twins.pnl.gov:8001/TCD/main.html

envelopes A, B, and C are listed in table A-1. Sulfates tend to be water soluble and can be removed effectively from the high-level waste stream by aqueous sludge washing operations, discussed in chapter 2. Separation of sulfate from the low-activity waste feeds may be possible using ion-exchange or precipitation processes. BNFL Inc. may develop an ion-exchange process to remove sulfate from low-activity waste (Elsden, 1999).

1.8 Summary

Pretreatment processes are an essential part of the TWRS operations for BNFL Inc. to meet the contractual requirements. The process allows the separations of highly radioactive species such as cesium-137, strontium-90, technetium-99 and transuranic elements from the waste. The pretreatment process to separate high-level waste components from the wastes has been successfully conducted at the West Valley Demonstration Project using inorganic ion-exchange media (zeolites). The titanium-coated zeolite was not only able to remove cesium-137 but was also successful in retaining plutonium and strontium. At the Defense Waste Processing Facility, alternatives to the proposed in-tank precipitation process to remove cesium-137 are currently being evaluated because of the higher than expected benzene generation resulting from decomposition of sodium tetraphenylaborate. The pretreatment processes proposed by BNFL Inc. for cesium-137 and technetium-99 make use of organic ion-exchange resins such as SuperLig®-644 and SuperLig®-639 for cesium-137 and technetium-99. Unlike inorganic zeolites, organic ion-exchange resins can be regenerated and reused. In addition, BNFL Inc. has proposed a precipitation process for removing strontium-90 and transuranic elements from the wastes. The

technologies proposed by BNFL Inc. are still developing, and no pilot-scale demonstration has been conducted. The laboratory studies using simulated wastes indicate feasibility of such technologies.

1.9   References

Bibler, N.E. *An Investigation of the Radiolytic Stability of a Resorcinol-Formaldehyde Ion Exchange Resin*. WSRC–RP–94–148. Aiken, SC: Westinghouse Savannah River Company. 1994.

Borisch, R.R., and S. Marchetti. *Selection of the Final Decontamination Method for the Supernatant Treatment System*. DOE/NE/44139–35. West Valley, NY: West Valley Nuclear Services Company. 1987.

Carter, J.T., K.J. Rueter, J.W. Ray, and O. Hodoh. Defense waste processing facility radioactive operations—Part II—Glass making. *Proceedings of Waste Management '97 Conference*. Tucson, AZ: Waste Management Symposia. 1997.

Code of Federal Regulations. *Licensing Requirements for Land Disposal of Radioactive Waste*. Title 10—Energy, Chapter I—Nuclear Regulatory Commission, Part 61. Washington, DC: U.S. Government Printing Office. 1997.

Dalton, W.J. *Qualification Testing of Titanium-Treated Zeolite for Sludge Wash Processing*. White Paper prepared for the U.S. Department of Energy. West Valley, NY: West Valley Nuclear Services Company. 1992.

Dalton, W.J. *Qualification Testing and Full-Scale Demonstration of Titanium-Treated Zeolite for Sludge Wash Processing*. DOE/NE/44139–72. West Valley, NY: West Valley Nuclear Services Company. 1997.

Defense Nuclear Facility Safety Board. *Savannah River Site In-Tank Precipitation Facility Benzene Generation: Safety Implications*. DNFSB/TECH-14 (Revision 2). Washington, DC: Defense Nuclear Facilities Safety Board. 1997.

Ecology. *Hanford Federal Facility Agreement and Consent Order, as amended*. Olympia, WA: Washington State Department of Ecology, U.S. Environmental Protection Agency, and U.S. Department of Energy. 1994.

Elsden, A. Hanford TWRS privatization—The BNFL approach. *American Ceramic Society 101st Annual Meeting Abstracts*. Westerville, OH: American Ceramic Society. 1999.

Gephart, R.E., and R.E. Lundgren. *Hanford Tank Cleanup: A Guide to Understanding the Technical Issues*. PNNL–10773. Richland, WA: Pacific Northwest National Laboratory. 1997.

Iverson, D.C., and H.H. Elder. Defense waste processing facility startup progress report. *Spectrum/92*. Symposium Proceedings. La Grange Park, IL: American Nuclear Society. 1992.

Introduction

Jain, V., and R.T. Pabalan. Review of process safety issues relevant to vitrification of radioactive wastes. *Proceedings of Waste Management '98, March 1–5, 1998.* Tucson, AZ: Waste Management Symposia, Inc. 1998.

Lange, N.A. *Handbook of Chemistry.* New York: McGraw-Hill Book Company. 1967.

Lewis, R.J. *Hazardous Chemicals Desk Reference.* New York: Van Nostrand Reinhold Publisher. 1997.

Long, J.T. *Engineering for Nuclear Fuel Reprocessing.* New York: Gordon and Breach Science Publishers, Inc. 1967.

Nuclear Regulatory Commission. *Branch Technical Position on Concentration Averaging and Encapsulation.* Washington, DC: Division of Waste Management, Office of Nuclear Material Safety and Safeguards, Nuclear Regulatory Commission. 1995.

Pabalan, R.T., M.S. Jarzemba, D.A. Pickett, N. Sridhar, J. Weldy, C.S. Brazel, J.T. Persyn, D.S. Moulton, J.P. Hsu, J. Erwin, T.A. Abrajano, Jr., and B. Li. *Hanford Tank Waste Remediation System High-Level Waste Chemistry Manual.* NUREG/CR–5751. Washington, DC: Nuclear Regulatory Commission. 1999.

Ploetz, D.K., and I.M. Leonard. *Supernatant Treatment System Design through Testing.* DOE/NE/44139–47. West Valley, NY: West Valley Nuclear Services Company. 1988.

Prowse, J.J., and M.A. Schiffhauer. *Safety Analysis Report for Supernatant Treatment System.* WVNS–SAR–004. Revision 7. West Valley, NY: West Valley Nuclear Services Company. 1992.

Rapko, B.M., and M.J. Wagner. *Caustic Leaching of Composite AZ-101/AZ-102 Hanford Tank Sludge.* PNNL–11580. Richland, WA: Pacific Northwest National Laboratory. 1997.

Rykken, L.E. *High-Level Waste Characterization at West Valley.* DOE/NE/44139-14. West Valley, NY: West Valley Nuclear Services Company, Inc. 1986.

Sienko, M.J., and R.A. Plane. *Chemistry.* New York: McGraw-Hill Book Company. 1961.

Sturm, H.F., T.B. Calloway, Jr., C.A. Nash, D.J. McCabe, C.T. Randall, S.T. Wach, D.P. Lambert, C.L. Crawford, S.F. Peterson, R.E. Eibling, W.R. Wilmarth, S.W. Rosencrance, M.S. Hay, M.E. Johnson, and N. Lockwood. *Research and Development Activities in Support of Hanford River Protection—SRTC Program.* WSRC–MS–99–00858. Aiken, SC: Westinghouse Savannah River Company. 1999.

U.S. Department of Energy. *Tank Waste Remediation System Privatization Request for Proposals.* DE–RP06–96RL13308. Richland, WA: U.S. Department of Energy. 1996a.

U.S. Department of Energy. *TWRS Privatization Contract with BNFL Inc.,* DE–AC06–96RL13308. Richland, WA: U.S. Department of Energy. 1996b.

U.S. Department of Energy. *TWRS Privatization Contract with LMAES*. DE–AC06–96RL13309. Richland, WA: U.S. Department of Energy. 1996c.

U.S. Department of Energy. *Tank Waste Remediation System, Hanford Site, Richland, Washington, Final Environmental Impact Statement*. DOE/EIS–0189. Richland, WA: U.S. Department of Energy and Washington State Department of Ecology. 1996d.

U.S. Department of Energy. *Report to Congress—Treatment and Immobilization of Hanford Radioactive Tank Waste Authorization-To-Proceed, Revision 3*. Richland, WA: U.S. Department of Energy. 1998a.

U.S. Department of Energy. *Hanford Site Tank Waste Remediation System Programmatic Environmental Review Report*. DOE/RL–98–54. Revision 0. Richland, WA: U.S. Department of Energy. 1998b.

U.S. General Accounting Office. *Process to Remove Radioactive Waste from Savannah River Tanks Fails to Work*. GAO-RCED-99-69. Washington, DC: U.S. General Accounting Office. 1999.

Vance, R.F. More on Soviet Urals accident. *Nuclear News*. La Grange Park, IL: American Nuclear Society. 1990.

Weise, H., E. Ewest, and M. Demonie. Industrial vitrification of high level liquid waste in the Pamela plant. *Proceedings of Waste Management '88*. Tucson, AZ: Waste Management Symposia, Inc. 1988.

2 SLUDGE WASHING

The wastes in Hanford high-level waste tanks are composed primarily of nonradioactive metal oxides and hydroxides, and insoluble and soluble salts that resulted from plutonium and uranium production operations or nuclear fuel reprocessing. The wastes include sludges formed as a result of neutralization processes performed to allow interim storage of highly acidic process wastes in the underground carbon steel storage tanks. An objective of the Hanford TWRS operations is to convert the tank wastes into waste forms suitable for disposal. Because of the high cost associated with the disposal of high-level waste, minimizing the volume of the high-level waste fraction via pretreatment processes is envisioned.

One of the major pretreatment processes planned for the sludge content of the Hanford waste tanks is sludge washing. The sludge washing process can reduce substantially the amount of high-level waste glass by separating the soluble, nonradioactive components (e.g., aluminum hydroxides and sodium) from the radioactively contaminated solids. Removal of nitrite and nitrate ions would minimize the generation of nitrogen oxide gases during sludge dissolution by acidification or during vitrification of high-level waste. The separation can be achieved by

- Dissolving soluble salts and extracting supernate trapped in the sludge by washing the sludge with corrosion inhibited water (dilute alkaline wash)

- Dissolving aluminum, chromium, and phosphorus components by leaching the sludge with sodium hydroxide solution (enhanced sludge washing)

The aqueous phase resulting from sludge washing can then undergo further pretreatment to separate the radionuclides, such as strontium-90, cesium-137, technetium-99, iodine-129, and transuranic elements from the low-activity waste stream in order for the immobilized low-activity waste to meet NRC Class C limits.

The enhanced sludge washing method focuses on the solubility by caustic leaching of the insoluble metals in the sludge. The elements targeted include aluminum, chromium, iron, calcium, lead, potassium, manganese, bismuth, and sodium, as well as chlorine, silicon, nitrogen, sulfur and phosphorus. Recent DOE reports examined the potential application of this method and established the usefulness of enhanced sludge washing as a pretreatment method that could help reduce the cost of vitrifying Hanford high-level wastes. The enhanced sludge washing procedures tested in these studies include several washing steps and leaching with solutions of different alkalinity. To have a reference for evaluating different variations of the enhanced sludge washing process, Hanford investigators defined a baseline enhanced sludge washing process, shown schematically in figure 2-1 (Rapko et al., 1996a). The baseline method involves an initial wash with inhibited water (e.g., a dilute aqueous solution of sodium hydroxide and sodium nitrite), two subsequent leaching steps with 3 M sodium hydroxide, and a final wash with inhibited water.

This chapter discusses the chemistry of processes relevant to dilute alkaline and caustic washing of Hanford tank sludge, including the chemical mechanisms responsible for sludge dissolution. The method of sludge washing actually employed at Hanford may not be identical to the baseline method. The technologies described by the baseline method, however, are likely to include some that will be used at Hanford.

31
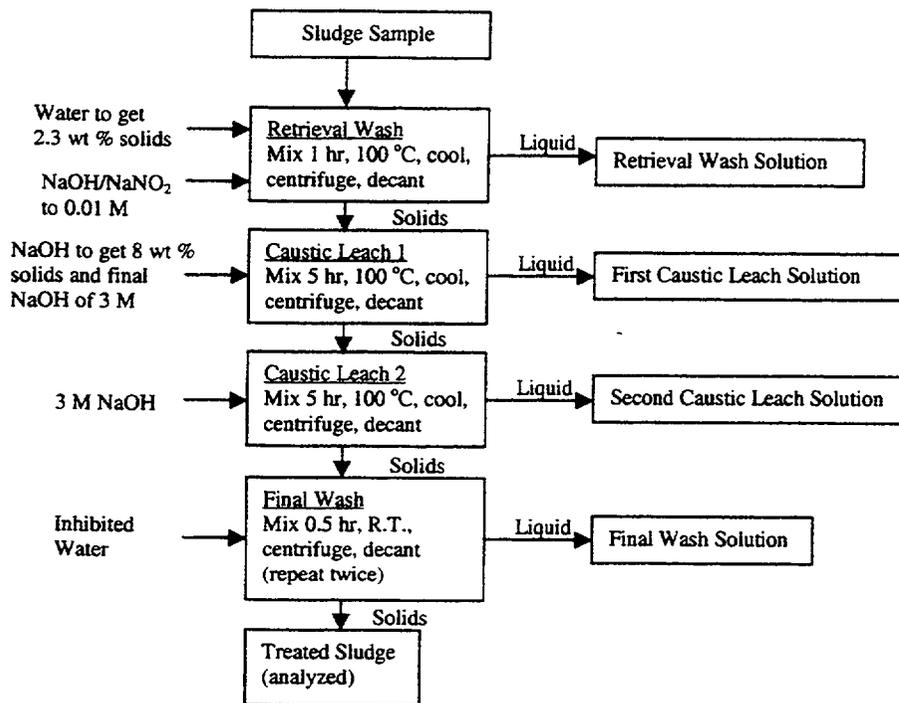
Sludge Washing

Figure 2-1. Schematic of the baseline enhanced sludge washing process (Rapko et al., 1996a)

2.1 Dilute Alkaline Wash

In the retrieval wash step of the baseline sludge washing method, inhibited water is used to remove soluble materials, mainly sodium salts, from the sludge. Dilute aqueous alkaline ($NaOH/NaNO_2$) wash, instead of ordinary water, is used to maintain the ionic strength high enough to avoid formation of colloidal suspensions. If carbon-steel tanks are used, nitrite will aid in protecting the carbon steel from corrosion.

The effectiveness of dilute hydroxide washing for removing the large amounts of sodium from sludges, the minimum pretreatment that will be applied to the Hanford sludges, was examined (Lumetta et al., 1997). The results are summarized in table 2-1. Sodium removal was about 70 percent or greater for all the tanks examined and greater than 90 percent for more than half the tank sludges examined.

Expected separation factors by sludge washing for various elements in 27 single-shell tanks, representing 40 percent of waste types existing in the tank farm inventory, have been reported (Colton, 1995). Values of sludge washing separation factors are summarized in table 2-2 (Colton, 1995). The values given in the table were derived based on a wash step using 100 mL of water per gram of sludge (12 gal./lb).

Table 2-1. Relative amount of sodium (Na) removed by dilute hydroxide washing of several Hanford tank sludges (data from Lumetta et al., 1997)

Tank	Initial Na in Sludge (Wt %)	Total Na Removed (%)
S–101	18	97
S–107	16	93
BY–110	29	98
BY–108	21	96
S–104	18	96
SX–108	23	96
BX–109	20	96
B–201	10	73
U–110	11	69
B–106	20	95
C–109	11	76
C–112	20	73
B–110	23	96
C–106	23	82
B–104	25	93
SX–113	0.2	73
C–104	17	88
C–105	5.3	78

2.2   Caustic Wash

The normality of the caustic solution used is typically about 3 N, but some studies have used solutions up to 10 N. Samples from the Hanford Tanks AZ–101 and AZ–102 indicated little additional leaching occurred using solutions with 1-N sodium hydroxide or higher (Rapko and Wagner, 1997). (Data from Hanford tanks AZ–101 and AZ–102 are of interest because the supernates are to be included in the TWRS envelope B waste stream, and the sludges are to be included in the TWRS envelope D waste stream.) Substantial changes in the concentrations of dissolved components occurred for sodium hydroxide normalities between 0.1 and 1.0. Only a slight improvement in the leaching efficiency was observed with a second caustic wash step (Rapko and Wagner, 1997). Almost all the radioactive and nonradioactive materials removed by caustic leaching were removed by a single 3-N sodium hydroxide leach; only small additional quantities of aluminum (5 percent) and silicon (14 percent) were removed by an additional 3-N sodium hydroxide leach.

Table 2-2. Calculated overall sludge wash separation factors for various ions in single-shell tank sludge (data from Colton, 1995)*

Ion	Form	Removal (%)
Silver	Ag^+	2
Aluminum	Al^{3+}	7
Boron	B^{3+}	59
Barium	Ba^{2+}	<1
Bismuth	Bi^{3+}	<1
Calcium	Ca^{2+}	3
Cadmium	Cd^{2+}	11
Cobalt	Co^{3+}	13
Potassium	K^+	64
Lanthanum	La^{3+}	<1
Magnesium	Mg^{2+}	2
Manganese	Mn^{2+}, Mg^{4+}, Mn^{6+}	<1
Nickel	Ni^{3+}	2
Lead	Pb^{2+}	7
Phosphate	$P_2O_7^{4-}$, PO_4^{3-}	40
Silicon	Si^{4+}	2
Copper	Cu^{2+}	4
Iron	Fe^{3+}	<1
Uranyl	UO_2^{2+}	2
Zinc	Zn^{2+}	3
Chromium	Cr^{3+}, Cr^{6+}	19
Strontium	Sr^{2+}	<1
Zirconium	Zr^{4+}	<4

*The actual wash factors vary from tank to tank

Results from enhanced sludge washing of samples from five Hanford tanks (B–110, B–201, C–109, C–112, and U–110) were reported (Lumetta et al., 1994). (Data from these five tanks are of interest because taken together they encompass several waste types and provide an approximate overall single-shell tank waste, and the double-shell slurry feed to be processed by the TWRS vitrification facility consists of wastes from the single-shell tanks that were concentrated by evaporation.) The study used four wash steps prior to caustic leaching of the sludge. The first two steps involved washing with water at room temperature for a period of ½ hr or 1 hr and with 0.1 M sodium hydroxide for 1 hr at room temperature and 1 hr 100 °C (212 °F). After each wash step, the mixture was centrifuged, the wash solution decanted and brought to room temperature before proceeding to the next step. The caustic leaching step involved mixing the washed solid with 3 M sodium hydroxide or with a mixture of 3 M sodium hydroxide and 2 M sodium carbonate at 100 °C (212 °F) for 5 hr, followed by cooling and solid separation by either gravity settling or centrifugation.

The major constituents in the sludges are given in table 2-3. The results of the previous study, which are given in table 2-4, show large variations in the amount of chromium, aluminum, and phosphorus removed from the different tank samples during the washing steps. Caustic leaching enhanced the removal of chromium, aluminum, and phosphorus, although significant variations for the results of different tank samples are evident. Iron remained insoluble, however, and the small amount of iron removed from some samples was attributed to dissolution of hexacyano-iron salts.

To provide estimated values that can be used for scale-up calculations, weighted average values for removal of aluminum, chromium, iron, and phosphorus based on measurements on samples from the five Hanford tanks (Lumetta et al., 1994) were derived. These values are listed in table 2-5.

Considerable variability in the efficiency of aluminum, chromium, and phosphorus removal by enhanced sludge washing for the 10 different Hanford tank sludges has been reported (Lumetta et al., 1996, 1997) as shown in table 2-6. (Of particular interest are the results from tank AN–104 because the double-shell slurry feed from this tank is included with the envelope A wastes to be processed by the TWRS vitrification facility.) With the exception of tanks AN–104 and BY–110, dilute hydroxide washing was generally ineffective at removing aluminum from most of the tank sludges, but aluminum removal was greatly enhanced by caustic leaching. For tanks AN–104 and BY–110, however, the dilute hydroxide washing was effective for removing aluminum. Much of the chromium and phosphorus was removed by dilute hydroxide washing, with some additional removal during the caustic leach step. The variability observed in chromium removal has been interpreted due to the presence of different chromium-bearing phases (Lumetta et al., 1997). In sludges where chromium is bound in a spinel structure, the structure of the solid phase prevents any oxidant from reaching the chromium. For cases where chromium is bound in aluminum hydroxides, caustic leaching would dissolve the aluminum hydroxide and expose the chromium to any oxidant in solution.

Additional data on the amounts of aluminum, chromium, and phosphorus removed by dilute hydroxide washing (simple wash) and by caustic leaching (enhanced sludge washing) of various Hanford tank sludges were reported. The data for aluminum are in table 2-7, chromium in table 2-8, and phosphorus in table 2-9 (Lumetta et al., 1997). (Of the 22 tank sludges tested, the sludge from double-shell tank

Table 2-3. Major components (wt %) of several Hanford tank wastes (data from Lumetta et al., 1994)

Component	Tank B–110	Tank B–201	Tank C–109	Tank C–112	Tank U–110
Al	0.12	0.49	1.22	1.81	13.80
Bi	2.01	10.34	1.23	N.D.*	1.40
Cr	0.10	0.34	0.02	0.03	0.04
Fe	1.93	1.51	1.89	2.44	1.01
P	1.70	0.59	1.91	2.87	1.43
Si	0.99	2.43	0.90	0.26	1.09
Na	10.00	4.15	8.42	11.80	10.90
Water	57.00	60.00	25.00	42.00	26.00
*Not determined					

AN–104 is of particular interest because the waste from that tank is included in the envelope A waste to be processed by BNFL Inc. in the TWRS vitrification plant.)

A number of studies were performed to determine the efficiency of dilute wash and caustic leaching on removing radionuclides from tank sludges. These studies indicate that only cesium-137 and technetium-99 (dissolved as TcO_4^-) were leached from the sludge to any significant extent. Leaching data shown in table 2-10 indicate that cesium-137 and technetium-99 can be removed up to 100 percent, whereas strontium-90 and the transuranic elements cannot be effectively removed from the sludge. Table 2-11 shows the relative distribution of radionuclides among the various enhanced sludge washing steps. As the data show, cesium-137 and technetium-99 were the primary radioisotopes detected in the leach and wash solutions, and most of those radioisotopes were in the first leach solution. (The data from the seven tanks in table 2-10 and from the five tanks in table 2-11, are of interest because a variety of single-shell tank waste types are included. Collectively these types approximate an overall single-shell tank waste, and the double-shell slurry feed to be processed by the TWRS vitrification facility consists of single-shell tank wastes, which were concentrated by evaporation. The only double-shell tank waste included is from tank SY–103 as listed in table 2-10. This waste is also of interest because it is a concentrated complexant waste with similarities to envelope C waste.)

Results for cesium-137 and technetium-99 leaching by dilute hydroxide washing (simple wash) and by caustic leaching (enhanced sludge washing) of various Hanford tank sludges are listed in table 2-12. (The 22 tank sludges evaluated in table 2-12 are the same as found in tables 2-7, 2-8, and 2-9 previously mentioned, and are of interest for the same reasons.) As much as 100 percent of the cesium-137 partitioned to the wash and leach solutions (Lumetta et al., 1997). Thus, these solutions will require removal of cesium-137 prior to low-activity waste immobilization.

Table 2-4. Major components removed from Hanford tank sludges (data from Lumetta et al., 1994)

Hanford Tank	Element	Removal by Wash (%)	Removal by Wash and Caustic Leaching (%)
B-110	Al	0.00	22.58
	Cr	10.79	55.21
	Fe	0.00	0.00
	P	42.04	98.41
B-201	Al	0.00	39.07
	Cr	41.36	65.69
	Fe	0.00	0.00
	P	14.41	39.53
C-109	Al	8.81	80.69
	Cr	79.91	85.70
	Fe	5.28	5.72
	P	33.05	41.95
C-112	Al	34.91	85.12
	Cr	48.29	88.62
	Fe	3.97	6.70
	P	48.20	84.07
U-110	Al	1.77	85.02
	Cr	67.92	73.45
	Fe	0.00	0.00
	P	90.72	99.05

Table 2-5. Removal of aluminum, chromium, iron, and phosphorus from Hanford tank sludges (data from Lumetta et al., 1994)*

Component	Removal by Washing (%)	Removal by Washing and Leaching (%)
Al	3	83
Cr	31	62
Fe	1	2
P	55	89
*Values listed are weighted averages		-

Table 2-6. Enhanced sludge washing of samples from Hanford tanks (data from Lumetta et al., 1996, 1997)

Hanford Tank	Element	Initial Amount in Sludge (wt %)	Removal by Retrieval Wash (%)	Total Removal after Enhanced Sludge Washing* (%)
BY–104	Al	1.9	65	98
	Cr	0.5	69	71
	P	0.3	93	95
BY–110	Al	3.4	94	96
	Cr	0.4	47	48
	P	0.6	19	23
C–107	Al	9.5	1	78
	Cr	0.1	34	48
	P	1.4	69	94
S–107	Al	20.5	8	73
	Cr	0.6	24	53
	P	0.2	>91	98
SX–108	Al	9.0	6	29
	Cr	0.8	71	78
	P	0.1	9	37
AN–104	Al	2.61	99	100

Table 2-6. Enhanced sludge washing of samples from Hanford tanks (data from Lumetta et al., 1996, 1997) (cont'd)

Hanford Tank	Element	Initial Amount in Sludge (wt %)	Removal by Retrieval Wash (%)	Total Removal after Enhanced Sludge Washing* (%)
	Cr	0.25	34	63
	P	0.12	98	100
BY–108	Al	1.26	63	71
	Cr	0.04	49	43
	P	2.35	73	70
S–101	Al	14.7	12	96
	Cr	0.71	44	89
	P	0.23	87	97
S–104	Al	15.3	2	99
	Cr	0.45	94	99
	P	0.002	>44	>58
S–111	Al	16.0	10	100
	Cr	0.4	18	98
	P	0.2	100	100

*Caustic leaching with 3 M NaOH followed by three washes with inhibited water

Removal of anions from the Hanford tank sludge is also of interest because anions, such as sulfate (SO_4^{2-}), chloride (Cl^-), and fluoride (F^-), have great impact on high-level waste vitrification (Crichton et al., 1995a,b). The results of one study indicate that the majority of anions is removed during the first two steps (Lumetta et al., 1994).

2.3 Chemical Mechanisms of Sludge Dissolution

A number of Hanford tank sludges were studied by DOE investigators to establish the solubility limits of the sludge components in wash and leach solutions. The solubility of the components is an important parameter controlling the removal efficiencies of the various elements. Obviously, a high solubility limit favors dissolution of the sludge components. The results of the DOE studies show that solubility varies with the particular tank sample, with temperature, and with the treatment step.

Table 2-7. Aluminum (Al) removed from Hanford tank sludges by simple wash and by enhanced sludge washing (data from Lumetta et al., 1997)

Hanford Tank	Initial Al in Sludge (wt %)	Al Removed by Simple Wash (%)	Al Removed by Enhanced Sludge Washing (%)
S–101	14.7	12	96
S–111	16	10	100
BY–104	1.88	65	98
BY–108	1.26	63	71
S–104*	15.3	2	99
BX–105	30.5	2	100
BX–109	0.14	61	97
B–201	0.81	0	25
B–202	0.26	<3	19
T–107	5.67	4	78
U–110	18.0	1	82
B–106	0.73	28	86
C–108	15.1	3	94
C–109	16.1	8	81
C–112	3.09	34	85
B–110	0.29	0	18
C–106	4.85	24	47
TY–104	4.28	9	63
SX–113	2.12	0	89
C–104	6.32	9	97
C–105	27.2	0	99
AN–104	2.61	9	90
*Extended leaching time			

2.3.1 Aluminum

Aluminum is present in large quantities in the Hanford tank wastes, primarily as a result of decladding of aluminum-clad, irradiated fuel, and the use of aluminum nitrate as a salting-out agent in a solvent extraction process. A variety of aluminum-bearing species were identified in Hanford tank sludges. These species are listed in tables 2-13 and 2-14.

Table 2-8. Chromium (Cr) removed from Hanford tank sludges by simple wash and by enhanced sludge washing (data from Lumetta et al., 1997)

Hanford Tank	Initial wt % Cr in Sludge (wt %)	Cr Removed by Simple Wash (%)	Cr Removed by Enhanced Sludge Washing (%)
S–101	0.71	44	89
S–111	0.37	18	98
BY–104	0.51	69	71
BY–108	0.04	49	43
S–104*	0.45	94	99
BX–105	0.05	52	96
BX–109	0.03	36	81
B–201	0.73	37	56
B–202	1.12	21	29
T–107	0.07	42	61
U–110	0.1	60	82
B–106	0.07	12	78
C–108	0.06	76	80
C–109	0.03	80	85
C–112	0.04	48	88
B–110	0.23	10	52
C–106	0.31	27	40
TY–104	0.38	72	86
SX–113	0.01	2	40
C–104	0.23	13	52
C–105	0.07	81	86
AN–104	0.25	34	63
*Extended leaching time			

Aluminum solubility can be rationalized in the solubilities of gibbsite and boehmite between 25 and 100 °C (77 and 212 °F). Aluminum, if present as an aluminosilicate phase, is fairly insoluble.

Figure 2-2 illustrates the aluminum solubility limits as a function of sodium hydroxide concentration. The solid curves are based on solubility measurements (Barney, 1976) in solutions saturated with sodium nitrite ($NaNO_2$), sodium nitrate ($NaNO_3$), sodium sulfate (Na_2SO_4), and sodium carbonate (Na_2CO_3), whereas the dashed lines are the calculated solubility limits for the pure Na_2O-Al_2O_3-H_2O system (Volf

41

Table 2-9. Phosphorus (P) removed from Hanford tank sludges by simple wash and by enhanced sludge washing (data from Lumetta et al., 1997)

Hanford Tank	Initial P in Sludge (wt %)	P Removed by Simple Wash (%)	P Removed by Enhanced Sludge Washing (%)
S–101	0.23	87	97
S–111	0.2	100	—[*]
BY–104	0.31	93	95
BY–108	2.35	73	70
S–104[†]	0.002	> 44	> 58
BX–105	0.09	91	100
BX–109	4.50	76	96
B–201	1.25	8	26
B–202	1.00	28	44
T–107	5.42	85	99
U–110	1.1	90	> 98
B–106	5.21	60	94
C–108	5.60	20	93
C–109	2.54	30	42
C–112	4.91	44	84
B–110	3.93	42	98
C–106	0.21	66	68
TY–104	4.04	83	98
SX–113	<0.01	—	—
C–104	0.63	27	89
C–105	0.20	100	100
AN–104	0.12	98	100

[*]No data reported
[†]Extended leaching time

Table 2-10. Partitioning of radionuclides from enhanced sludge washing of several Hanford tank sludges (data from Rapko et al., 1996a)

Hanford Tank	Transuranic[*] Removal (%)	Cesium-137 Removal (%)	Strontium-90 Removal	Technetium-99 Removal
B–111	0	95	0	100
BX–107	0	94	0	99
C–103	0	44	0	88
S–104	0	98	- 0	100
SY–103	1	100	4	85
T–104	0	69	2	—[†]
T–111	0	56	0	12

[*]Primarily plutonium and americium
[†]Below detection limit

and Kuznetsov, 1955). The left-hand solid curve is the solubility curve for the aluminum hydroxide phase gibbsite [Al(OH)$_3$]; the right-hand solid curve is the solubility curve for sodium aluminate (NaAlO$_2$•1.25H$_2$O). At the point of intersection of these two solid curves, the two solid phases are present with the aqueous solution. The curves indicate maximum aluminum solubility (~4 M) occurs at a sodium hydroxide concentration of about 2 M. This maximum aluminum solubility in solutions with chemical compositions similar to Hanford wastes occurs at a much lower sodium hydroxide concentration than in the lower ionic strength solutions of the pure Na$_2$O-Al$_2$O$_3$-H$_2$O system.

Data presented in figure 2-2 indicate that the solubility of aluminum hydroxides is greatly increased at higher ionic strengths, but at sodium hydroxide concentrations greater than 2 M, increasing the aluminum concentration will eventually precipitate sodium aluminate salts. These salts have been commonly observed during evaporator campaigns (Onishi and Hudson, 1996) and in samples from tank SY–101 (Liu et al., 1995). At lower sodium hydroxide concentrations, increases in aluminum concentration eventually result in precipitation of aluminum hydroxides, which may be gibbsite, boehmite, or an amorphous form. The amorphous form is thought to precipitate the quickest, sometimes forming gels that can be particularly troublesome during waste transport (Onishi and Hudson, 1996). The amorphous hydroxide is usually converted in hours or days into a crystalline gibbsite phase. Gibbsite is thought relatively common among the waste aluminum phases and was observed in samples from tank SY–103 (Liu et al., 1995). Boehmite is the thermodynamically favored phase, but it is thought to be less common in the waste.

Caustic leaching is expected to remove a large fraction of the aluminum. Aluminum is removed when aluminum oxides and hydroxides are converted to sodium aluminate (NaAlO$_2$). For example, gibbsite [Al(OH)$_3$] and boehmite (AlOOH) are dissolved according to the following reactions (Weber, 1982):

$$Al(OH)_{3(s)} + NaOH_{(aq)} \rightarrow NaAlO_{2(aq)} + 2H_2O \qquad (2\text{-}1)$$
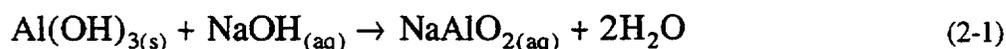
Table 2-11. Distribution of radioactive components among the enhanced sludge washing solutions (data from Lumetta et al., 1994)

Hanford Tank	Nuclide	Retrieval Solution (%)	1st Leach Solution (%)	2nd Leach Solution (%)	Final Wash Solution (%)
S–107	Cs-137	—	79	21	0
	Co-60	—	3	0	0
	Eu-154	—	0	0	0
	Eu-155	—	0	0	0
	Sr-90	—	0	0	0
	Tc-99	—	92	0	6
C–107	Cs-137	13	46	6	7
	Co-60	0	0	0	0
	Eu-154	0	0	0	0
	Eu-155	0	0	0	0
	Sr-90	0	0	0	0
	Tc-90	97	0	0	0
BY–104	Cs-137	100	0	0	0
	Co-60	0	0	0	0
	Eu-154	0	0	0	0
	Eu-155	0	0	0	0
	Sr-90	0	0	0	0
	Tc-99	100	0	0	0
BY–110	Cs-137	—	97	3	0
	Co-60	—	0	0	0
	Eu-154	—	0	0	0
	Eu-155	—	0	0	0
	Sr-90	—	0	0	0
	Tc-99	—	>86	0	<1
SX–108	Cs-137	—	86	1	0
	Co-60	—	0	0	0
	Eu-154	—	<2	0	0
	Eu-155	—	<21	0	0
	Sr-90	—	0	0	0
	Tc-99	—	>55	>3	0

Table 2-12. Cesium-137 removed from Hanford tank sludges by simple wash and by enhanced sludge washing (data from Lumetta et al., 1997)

Hanford Tank	Cs-137 Initially in Sludge (μCi/g)	Cs-137 Removed by Simple Wash (%)	Cs-137 Removed by Enhanced Sludge Washing (%)
S–101	138	97	100
S–111*	0.85	48	96
BY–104	84	100	100
BY–108	1590	3	99
BX–105	58.6	97	100
BX–109	25.3	54	100
B–201	2.3	17	25
B–202	0.11	52	76
T–107	15.6	25	91
U–110	22	5	10
B–106	59.3	51	100
C–108	614	4	99
C–109	950	5	98
C–112	1360	5	98
B–110	35	48	92
C–106	681	38	60
TY–104	128	41	54
SX–113	45.5	3	88
C–104	174	56	100
C–105	293	54	92
AN–104	600	100	100
*Extended leaching time was used			

Table 2-13. Aluminum-bearing solid phases in Hanford tank wastes (data from Lumetta et al., 1997)

Solid Phase	Hanford Tank
AlO(OH) (Boehmite)	S–101, S–14, S–107, S–111, SX–108
AlO(OH) (Diaspore)	S–101
$Al(OH)_{3(am)}$	BX–107, C–106, SY–103, T–104
$Al(OH)_{3(cr)}$	BX–107, BX–113, C–105, C–112, S–101, S–111, SY–103
$Al_2O_3(H_2O)_{(cr)}$	BY–104, C–107, SX–108, SY–103
$AlPO_4$	BX–107, T–104
Aluminosilicate$_{(am)}$*	AN–104, BX–107, BY–104, C–106, C–107, S–101, S–107, SX–108, T–104
Aluminosilicate$_{(cr)}$*	B–111, BX–107, T–104
$Ca_3Al_2O_6$	SX–108
*See table 2-14 for specific composition	

Table 2-14. Molecular formula of aluminosilicate phases found in Hanford tank wastes

Name	Formula
Albite	$NaAlSi_3O_8$
Analcime	$NaAlSi_2O_6 \bullet H_2O$
Natrolite	$Na_2Al_2Si_3O_{10} \bullet 2H_2O$
Nepheline	$NaAlSiO_4$
Cancrinite	$Na_8(AlSiO_4)_6(CO_3)_2$
Montmorillonite	$(Na,Ca)_{0.33}(Al,Mg)_2Si_4O_{10}(OH)_2 \bullet nH_2O$

$$AlO(OH)_{(s)} + NaOH_{(aq)} \rightarrow NaAlO_{2(aq)} + H_2O \qquad (2\text{-}2)$$
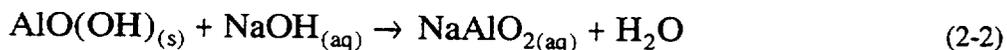
The rate of dissolution for boehmite (10^{-9} mole/cm^2·sec) is slower than the rate (10^{-7} mole/cm^2·sec) for gibbsite (Su et al., 1997). These values can be considered as limits for the dissolution rates of other aluminum solids, such as aluminosilicates. For example, nepheline ($NaAlSiO_4$) has a dissolution rate of 10^{-8} mole/cm^2·sec and is likely to be dissolved during the standard enhanced sludge washing process, whereas analcime ($NaAlSi_2O_6 \bullet H_2O$) and albite ($NaAlSi_3O_8$), which both have a dissolution rate of about 10^{-11} mole/cm^2·sec, will likely remain insoluble during the enhanced sludge washing process. Thus, the efficiency of enhanced sludge washing in removing aluminum from the waste will be influenced by the composition of the solids in the sludge.
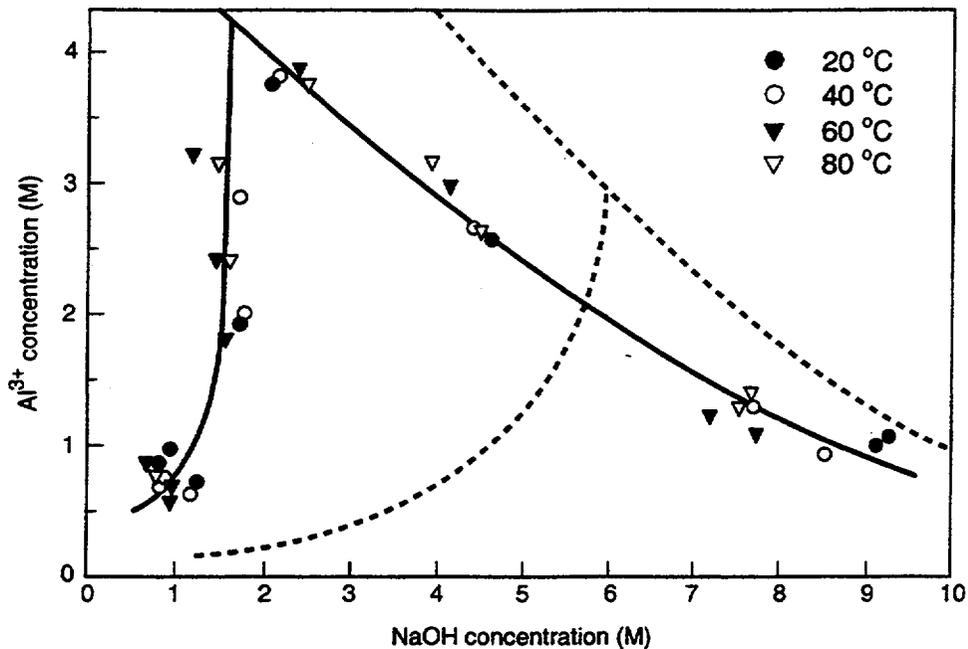
Figure 2-2. Aluminum solubility as a function of NaOH concentration. The solid curves represent aluminum solubility in solutions saturated with $NaNO_2$, $NaNO_3$, $NaAlO_2$, Na_2SO_4, and Na_2CO_3 (Barney, 1976). The dashed curves represent aluminum solubility in the Na_2O-Al_2O_3-H_2O system (Volf and Kuznetsov, 1955). The left-hand curves are the solubility curves for $Al(OH)_3$ (gibbsite); the right-hand curves are the solubility curves for $NaAlO_2 \cdot 1.25H_2O$. The symbols are experimental data at various temperatures taken from Barney (1976).

Su et al. (1997) studied the formation of aluminosilicates in solutions with aluminum to silicon ratios resembling those of Hanford tank wastes. The structure and composition of the aluminosilicates were characterized by x-ray powder diffraction, nuclear magnetic resonance, and Raman spectroscopy. The study provided information that could be useful in predicting the solubility and dissolution behavior of aluminum in sludge and designing effective pretreatment methods. The results show that the sodium nitrate concentration in solution has a significant effect on the nature of the insoluble aluminosilicates produced. At high pH (13.5) and high salt content (5 M $NaNO_3$), cancrinite [$Na_8(AlSiO_4)_6(CO_3)_2$] is the only phase formed regardless of the initial aluminum-to-silicon ratio used (Su et al., 1997). At the same pH but lower salt concentrations (1 M $NaNO_3$), a range of aluminosilicate zeolites is formed with different silicon-to-aluminum ratios, depending on the initial ratio of silicon to aluminum. Amorphous cement material forms at lower pH (12.5) with low initial silicon and aluminum concentration ($\sim 10^{-2}$ M) or at higher pH (13.5) with high initial silicon and aluminum concentration (~ 2 M).

2.3.2 Chromium

Because of potential melter problems caused by the presence of chromium, the concentration of chromium allowed in the melter feed is low, and a relatively small amount of chromium in the sludge can have a relatively large impact on the volume of high-level waste glass produced. Thus, the efficiency of its removal by sludge washing and caustic leaching is important. The chromium solubilities can be modeled fairly well by the solubility of amorphous chromium hydroxide $[Cr(OH)_3]$. Based on the known amphoteric behavior of chromium (III), chromium is expected to dissolve in highly alkaline solutions due to the formation of tetrahydroxochromium anions $[Cr(OH)^-_4]$ through the reaction (Rai et al., 1987)

$$Cr(OH)_{3(s)} + NaOH_{(aq)} \rightarrow Na[Cr(OH)_4]_{(aq)} \qquad (2\text{-}3)$$
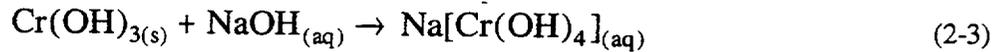
Recent studies (Lumetta et al., 1996; Rapko et al., 1996a; Rapko and Wagner, 1997) indicated a more complex chemistry for chromium dissolution during the caustic leaching process. Specifically, ultraviolet-visible spectroscopy of caustic leach solutions shows that the dissolved chromium is present as Cr^{6+}, not Cr^{3+}, indicating that chromium oxidation occurs during the caustic leach process. Hence, chromium removal is likely sensitive to the redox chemistry (i.e., the presence of oxidants) of the waste itself and of the washing or leaching solution. Data from leach tests also indicate that kinetics can play a role in the efficiency of chromium removal (Lumetta et al., 1997).

Chromium (III) can be oxidized by any manganese dioxide (MnO_2) that is present in the sludge:

$$2Cr(OH)_3 + 3MnO_2 + 4OH^- \rightarrow 2CrO_4^{2-} + 3Mn(OH)_2 + 2H_2O \qquad (2\text{-}4)$$
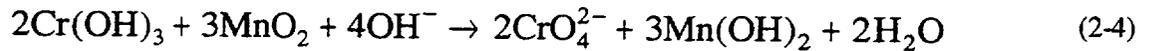
although manganese exists in the sludge mainly in the hydroxide form. In addition, enhancement of chromium removal can be obtained by adding oxidants, such as permanganate (MnO_4^-), ozone (O_3), or hydrogen peroxide (H_2O_2), to the leachant solution to oxidize chromium (III) to chromium (VI) via the following electrochemical reactions:

$$Cr(OH)_3 + 5OH^- \rightarrow CrO_4^{2-} + 4H_2O + 3e^- \qquad E = 0.12V \qquad (2\text{-}5)$$

$$MnO_4^- + 2H_2O + 3e^- \rightarrow MnO_2 + 4OH^- \qquad E = 0.588V \qquad (2\text{-}6)$$

$$HO_2^- + H_2O + 2e^- \rightarrow 3OH^- \qquad E = 0.87V \qquad (2\text{-}7)$$

$$O_3 + H_2O + 2e^- \rightarrow O_2 + 2OH^- \qquad E = 1.24V \qquad (2\text{-}8)$$
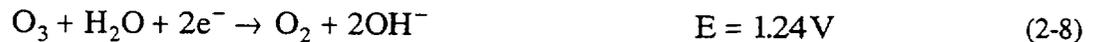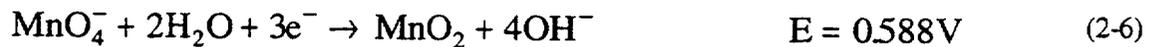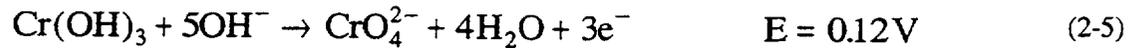
For example, caustic leaching removed only 12 percent of the chromium from tank SY–103 sludge, whereas approximately 90 percent of the chromium was removed with addition of permanganate or ozone to the leachant solution (Rapko et al., 1995).

Table 2-15 lists the chromium-containing phases that were identified in Hanford sludges by microscopic examination coupled with x-ray powder diffraction. In several cases, the chromium is bound with other transition metals in spinel-type structures. Dissolving the chromium contained in such phases would be difficult, even under oxidative conditions, because the structure of these mineral phases would physically prevent the oxidant from reaching the chromium. For cases where chromium is bound in aluminumhydroxides, caustic leaching would dissolve the aluminum hydroxide matrix and expose the chromium to any oxidant.

Table 2-16 presents several results of chromium leaching of Hanford tank wastes. Two features are apparent from these results. First, except for tank BX–107, excellent correlation is shown between the percent of chromium (VI) in the sludge and the amount of chromium removed in the retrieval wash. Second, in all cases, after the sludge wash and caustic leach treatment, the chromium remaining in the sludge is chromium (III). Additional data based on ultraviolet spectroscopic measurements of the caustic leach solutions reveal that the dissolved chromium is present as chromium (VI), not chromium (III), indicating that further chromium oxidation occurs during the caustic leach (Rapko and Wagner, 1997).

Note that while caustic solutions can dissolve chromium (III) at room temperature, precipitation of the solid phase guyanaite [CrO(OH)], which does not dissolve readily in aqueous caustic media, can occur at elevated temperatures (Lumetta et al., 1997). Under these conditions, the addition of oxidants to the leachant solution will be needed to enhance formation of chromium (VI). Also, in the low-activity waste stream and prior to solidification and disposal, having chromium in the 3+ oxidation state is preferable because of its lower mobility compared to the 6+ oxidation state. Reduction of chromium (VI) to chromium (III) could be done with hydroxylamine, although addition of organics could pose other problems, such as hydrogen gas generation.

The efficient removal of chromium from high-level waste sludges requires the baseline enhanced sludge washing process be improved. Specific considerations for chromium leaching have been studied in experiments with two oxidizing agents on two samples taken from the tanks B–111 and SY–103, samples that were previously treated with the baseline enhanced sludge washing (Rapko et al., 1996b). Both the kinetic and equilibrium aspects of chromium dissolution were studied. Five tests were conducted on each tank sample. These tests included reactions with stoichiometric potassium permanganate ($KMnO_4$), three-fold excess potassium permanganate, sub-stoichiometric (0.1) potassium permanganate plus ozone, ozone only, and blank (0.1 M NaOH). Table 2-17 shows the kinetics of chromium dissolution for both tank samples. In general, the solutions exhibited significant decreases in pH during the course of the tests. The decrease in pH of the blank solutions was usually less than that observed for the leach solutions. Thus, the pH decrease cannot be ascribed to environmental effects, such as the uptake of carbon dioxide gas from the atmosphere. The observed pH decreases appear consistent with the stoichiometry for the following chromium oxidation reactions:

$$Cr(OH)_3 + MnO_4^- + OH^- \rightarrow CrO_4^{2-} + MnO_2 + 2H_2O \qquad (2\text{-}9)$$

49
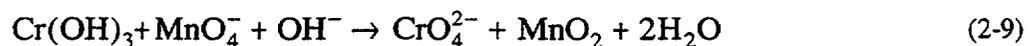
Table 2-15. Chromium-containing phases identified in Hanford sludges (data from Lumetta et al., 1997)

Phase	Hanford Tank
$Bi_{38}CrO_{60}$	B–111
CrO(OH) (Grimaldiite)	BY–110
$Al/Cr(OH)_{3(am)}$ *	BY–104, BY–110, T–111
$NaAlO_2/Cr(OH)_{3(am)}$ †	AN–104
Ca/Cr phase	AN–104
$(Fe^{2+},Mg)(Cr,Fe^{3+})_2O_4$ (Donathite)	BY–104
$FeCr_2O_4$	S–111
$MnCr_2O_4$	S–111
$Mn_{1.5}Cr_{1.5}O_4$	S–111

*Cr associated with amorphous Al hydroxide
†Cr associated with amorphous sodium aluminate

Table 2-16. Oxidation state of chromium in sludge and amount removed by wash and caustic leaching (data from Rapko et al., 1996b)

Hanford Tank	Cr in Untreated Sludge		Cr Removed by Retrieval Wash	Cr Remaining in Washed Sludge*		Cr Removed by Caustic Leaching†
	% Cr^{3+}	% Cr^{6+}	%	% Cr^{3+}	% Cr^{6+}	%
B–111	73	27	27	>95	>5	41
BX–107	91	9	21	>95	>5	29
S–104	>5	>95	90	—	—	96
SY–103	>95	>5	5	>95	>5	13
T–104	84	16	17	>95	>5	27
T–111	78	22	24	>95	>5	64

*Determined by x-ray absorption spectroscopy
†Sludge reacted with retrieval wash, followed by two leaching steps at 100 °C (212 °F) with 3 M NaOH and three washes at room temperature

Table 2-17. Removal of chromium from enhanced washed Hanford sludge by additional treatment (data from Rapko et al., 1996b)

Hanford Tank	Test[*]	pH		Chromium Removed After Selected Times					
		Initial	Final	1 hr (%)	7 hr (%)	16 hr (%)	23 hr (%)	30 hr (%)	37 hr (%)
SY–103	A	11.3	10.3	53.8	62.3	67.0	81.0	74.8	77.3
	B	11.6	12.3	n.p.[†]	n.p	n.p	n.p	n.p	n.p
	C	11.3	9.4	72.7	72.4	78.9	70.0	76.6	77.7
	D	11.4	9.1	12.3	64.1	75.3	81.9	77.1	76.8
	E	11.4	10.4	14.6	18.0	21.4	20.7	19.1	22.9
B–111	A	11.7	7.7	15.9	14.2	15.2	19.4	21.3	20.0
	B	n.p	n.p	n.p	n.p	n.p	n.p	n.p	n.p
	C	12.0	7.0	3.6	11.9	16.6	20.3	25.8	29.5
	D	12.0	6.5	4.6	8.3	17.5	15.7	15.3	14.1
	E	12.0	11.4	5.5	6.4	7.5	8.0	9.0	10.4

[*]A: Stoichiometric $KMnO_4$
B: Three times stoichiometric $KMnO_4$
C: 10 % of stoichiometric $KMnO_4$, plus ozone
D: Ozone
E: 0.1 M NaOH
[†]Not performed

$$2Cr(OH)_3 + 3O_3 + 4OH^- \rightarrow 2CrO_4^{2-} + 3O_2 + 5H_2O \qquad (2\text{-}10)$$
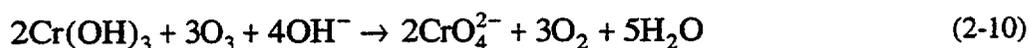
For both chromium oxidations, hydroxide ions are consumed and would lead to a decrease in solution pH as the reaction proceeds. In addition, since more hydroxide is consumed during ozone oxidation of chromium compared to permanganate oxidation, reaction (2-10) would result in much greater decrease in pH compared to reaction (2-9). Consistent with this explanation, the ozone leach tests show a lower final pH compared to the permanganate tests.

2.3.3 Phosphorus

Most of the phosphorus found in tank sludges appears present as sodium phosphate (Rapko et al., 1996a), and a small amount of sodium phosphate is predicted to dissolve from the sludge. The solubility of sodium phosphate in the wash and leach solutions is inhibited by the high sodium concentration in the

solutions. An equation that relates sodium phosphate solubility to aqueous sodium concentration and to temperature is (Onishi and Hudson, 1996)

$$[PO_4^{3-}] = \frac{A}{[Na^+]^3} + \frac{B}{[Na^+]^2} + \frac{C}{[Na^+]} + D \tag{2-11}$$

where brackets denote concentrations in molality (moles/kg of water), and A, B, C, and D are constants with the following temperature dependence:

$$A \text{ or } B \text{ or } C \text{ or } D = a_0 + a_1 T + a_2 T^2 \tag{2-12}$$

Values of a_0, a_1, and a_2 are given in table 2-18.

A significant portion of the phosphorus is expected to be removed from the sludge when water-insoluble metal phosphate $[(M)_m(PO_4)_n]$ salts metathesize (double decompose) to insoluble hydroxide salts and soluble tribasic sodium phosphate (Na_3PO_4), as in the following reaction:

$$(M^{n+})_3(PO_4^{3-})_{n(s)} + 3nNaOH_{(aq)} \rightarrow 3(M^{n+})(OH)_{n(s)} + 3nNa^+ + n(PO_4)_{(aq)}^{3-} \tag{2-13}$$
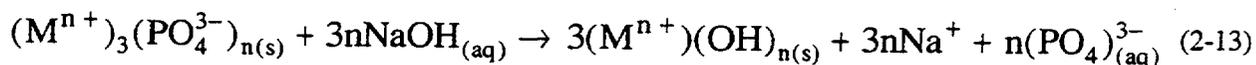
Phosphorus that does not leach from the sludge is assumed to exist as an alkaline earth phosphate [e.g., $Ca_3(PO_4)_2$], for which the above metathesis reaction is thermodynamically unfavorable (Lumetta et al., 1994). Other phosphate phases that exist in the sludge are lanthanum pyrophosphate $[La_4(P_2O_7)_3]$ and hydroxyapatite $[Ca_5(OH)(PO_4)_3]$. Table 2-19 shows the various phosphate phases that were identified in Hanford tank wastes. At present, no data suggest that appreciable removal of the phosphorus present as alkaline earth phosphates will occur under the proposed processing conditions (Rapko et al., 1996a). Note that adequate volumes of a final, low-sodium wash (e.g., figure 2-1) are required to remove phosphorus from the sludge because of the limited solubility of tribasic sodium phosphate at the high sodium concentrations of the caustic leach steps. During the caustic leaching steps, the high sodium concentration drives the reaction shown in Eq. (2-13) to the left, resulting in less phosphate being removed. The use of low sodium concentration during the final wash helps drive the reaction to the right.

2.3.4 Iron

The removal of iron from the sludge could reduce the overall mass of high-level waste solids because it is a major nonradioactive component of Hanford tank sludges. Iron exists as ferric hydroxide $[Fe(OH)_3]$. The baseline caustic leaching method is not capable of removing it. Neither BNFL Inc. nor LMAES included iron leaching in their proposed processes. The feasibility of selectively leaching iron from Hanford sludges by treatment with various iron-complexing agents, however, was of interest to Hanford investigators. The efficacy of acetohydroxamic acid and disodium 4,5-dihydroxy-1,3-benzenedisulfonate (Tiron®) as iron-leaching agents using nonradioactive ferric hydroxide was evaluated. Two series of experiments were performed (Lumetta, 1997) to establish the efficiency of the leaching agents. The first

Table 2-18. Values a_0, a_1, and a_2 are parameters that describe the temperature dependence of constants A, B, C, and D according to Equation (2-12) (taken from Onishi and Hudson, 1996)

	A	B	C	D
a_0	-5181.902	2656.08	-425.7586	20.71154
a_1	180.5396	-95.25732	15.53686	-0.7619675
a_2	-1.219804	0.697907	-0.1187975	0.006032556

Table 2-19. Phosphorus-containing solid phases in Hanford wastes (data from Lumetta et al., 1997)

Solid Phase	Hanford Tank
$AlPO_4$	BX–107, B–111, T–104
Bi/Fe Phosphate	T–111
$Ca_5(OH)(PO_4)_3$	BY–104, BY–110, T–111
$Ca_xSr_{10-x}(PO_4)_6(OH)_2$ (x = 8 or 9)	BY–108
$Ca_3(PO_4)_2$	C–112
$La_4(P_2O_7)_3$	T–111
$Pb_5(OH)(PO_4)_3$	C–107
Na_3PO_4	B–111, BX–107, T–104, T–111
U Phosphate	C–112

series used ferric hydroxide [$Fe(OH)_3$] that was formed by adding potassium hydroxide (KOH) to a solution of ferric chloride ($FeCl_3$), whereas the ferric hydroxide in the second series was formed by adding ferric nitrate [$Fe(NO_3)_3$] to a solution of sodium hydroxide (NaOH). In the former, the precipitated ferric hydroxide was washed with water and dried [termed "aged" $Fe(OH)_3$] at 105 °C (221 °F) for several days, whereas in the latter, the ferric hydroxide was allowed to stand in the sodium hydroxide solution at room temperature for 3 days and not dried [termed "*in situ*" $Fe(OH)_3$]. Cycles of tests were performed for these two types of ferric hydroxide at different temperatures [room temperature, 50 °C (122 °F), and 100 °C (212 °F)]. Results of the first and second series of tests are shown in tables 2-20 and 2-21.

As shown in table 2-20, the relative amount of iron leached from aged ferric hydroxide ranged from 20 to approximately 30 percent, with the exception of test number Fe–A2. Heating up to 100 °C (212 °F) had no effect on the amount of iron dissolved. Possibly the remaining 70 to 80 percent of the iron that was not dissolved consisted of phases resistant to dissolution. Transmission electron microscopy (Lumetta, 1997) indicated the presence of needle-like particles (most likely goethite) and round particles (most likely hematite) in the aged ferric hydroxide.

Table 2-20. Iron leaching of "aged" Fe(OH)₃ (data from Lumetta, 1997)

Test	Material	Concentration (M)	Temperature (°C)	Initial pH	Final pH	Fe Dissolved (%)
Fe–A1	AHA*	0.1	R.T.†	5.63	7.79	20
Fe–A2	AHA	0.1	R.T.	9.59	9.76	12
Fe–A3	AHA	0.1	R.T.	1.70	1.90	21
Fe–A4	AHA	0.25	R.T.	5.51	7.15	21
			50	5.51	4.70	29
			100	5.51	4.34	23
Fe–A5	AHA	0.25	R.T.	9.40	9.41	20
			50	9.40	8.78	25
			100	9.40	5.80	20
Fe–T1	Tiron®‡	0.25	R.T.	11.31	11.17	21

*AHA = acetohydroxamic acid
†R.T. = room temperature
‡Tiron® = disodium 4,5-dihydroxy-1,3 benzenedisulfonate

Table 2-21. Iron leaching tests using Fe(OH)₃ precipitated *in situ* (data from Lumetta, 1997)

		Leach Conditions			Fe Dissolved		
Test	Material*	Concentration (M)	Initial pH	Final pH	After 24 hr (%)	After 72 hr (%)	After 168 hr (%)
Fe–A8	AHA	0.25	9.09	9.17	32	33	33
Fe–A9	AHA	0.25	11.04	11.46	22	23	24
Fe–A10	AHA	0.25	12.93	13.04	9	9	7
Fe–T2	Tiron®†	0.25	9.00	8.17	32	33	33
Fe–T3	Tiron®†	0.25	11.08	10.67	31	32	32
Fe–T4	Tiron®†	0.25	12.80	13.46	39	45	53

*AHA = acetohydroxamic acid
†Tiron® = disodium 4,5-dihydroxy-1,3-benzenedisulfonate

The Tiron® solution appears promising for removing iron from the Hanford sludges. The amount of iron dissolved in the presence of acetohydroxamic acid decreased with increased pH. These results are shown in table 2-21 and illustrated in figure 2-3, where the iron concentration is approximately 700 mg/L (~5.8 × 10⁻³ lb/gal.) with the pH at 9, but only about 200 mg/L (1.7 × 10⁻³ lb/gal.) when the pH is 13. Leaching with acetohydroxamic acid for longer than 24 hr did not significantly increase the amount of iron dissolved. The acetohydroxamic acid leaching at pH of 9 dissolved 33 percent of the iron, similar to the results for leaching with Tiron® at pH values of 9 and 11. Improved iron dissolution, however, was obtained with Tiron® at pH of 13 (figure 2-4). In the latter case, kinetics was important in determining the amount of iron dissolved from ferric hydroxide. About 53 percent of the iron was dissolved after 168 hr, and the data suggest that further dissolution could occur at longer times.

Both acetohydroxamic acid at pH of 9 and Tiron® at pH of 13 completely dissolved freshly precipitated solid [i.e., Fe(OH)₃] that was not allowed to stand for 3 days (Lumetta, 1997). This result supports the conclusion that iron dissolution by acetohydroxamic acid and Tiron® are kinetically impaired for "aged" iron hydroxide solids.

2.3.5 Manganese

Manganese is considered insoluble under the baseline enhanced sludge washing treatment. A test, however, in which sludge waste from Hanford tank U–110 was leached with Tiron® at pH 13 indicated that caustic leaching with Tiron® is effective in removing manganese from the sludge. Tiron® leaching reduced the manganese concentration in the sludge by about 95 percent from an initial concentration of 4,680 ppm (Lumetta, 1997).

2.3.6 Lead

Lead is considered insoluble under the baseline enhanced sludge washing treatment.

2.4 Application to Hanford Wastes

The baseline sludge pretreatment flowsheet involves retrieval of the sludge by sluicing and pumping with inhibited water (0.01 M NaOH + 0.01 M NaNO₂) and then leaching the sludge with caustic (3 M NaOH). Caustic leaching is expected to remove a large fraction of aluminum, which is present in large quantities in Hanford tank sludges. A significant portion of the phosphorus and chromium is also expected to be removed from the sludge. The baseline caustic leaching is not capable of removing iron, which is also a major nonradioactive component of Hanford tank sludges. It should be noted that data on sludge washing of Hanford wastes are based on limited sets of laboratory experiments involving small samples taken from large tanks. Thus, caution should be used in extrapolating the results of these studies to the actual conditions of Hanford tank waste processing.

2.4.1 Operational Considerations

Retrieval of the waste sludge by sluicing and pumping with a dilute aqueous solution of sodium hydroxide and sodium nitrate (0.01 M NaOH+ 0.01 M NaNO₂) is appropriate for the Hanford wastes because the Hanford waste tanks are lined with carbon steel. Keeping the solution alkaline with dilute
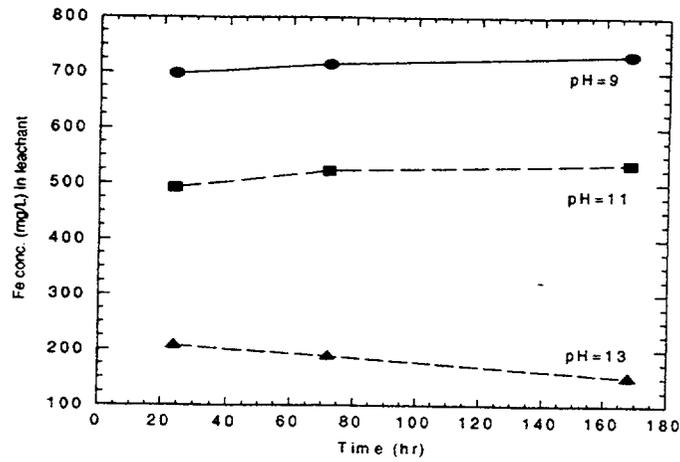
Figure 2-3. Results of Fe(OH)$_3$ leaching with acetohydroxamic acid solution as a function of time and pH (data from Lumetta, 1997)
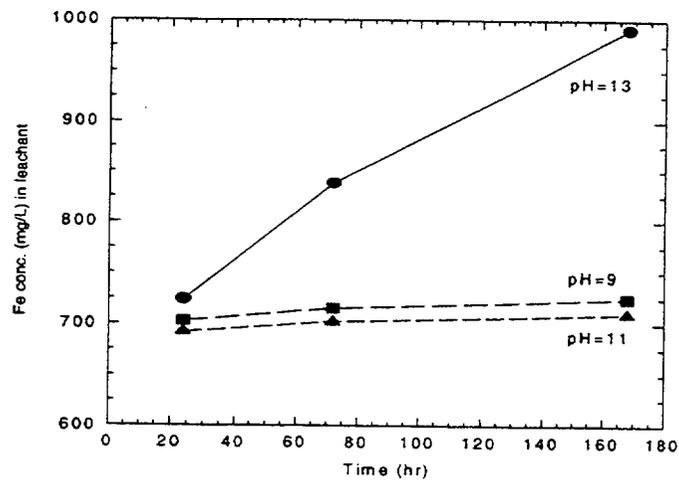
Figure 2-4. Results of Fe(OH)$_3$ leaching with Tiron® solution as a function of time and pH (data from Lumetta, 1997)

sodium hydroxide, and including a small amount of sodium nitrite as a corrosion inhibitor, will protect the carbon steel liners from corrosion. If the dilute aqueous solution is decanted from the sludge, it will carry much of the water soluble materials away from the sludge, including nonradioactive sodium (Na^+), nitrates (NO_3^-), nitrites (NO_2^-), and cesium-137. Removal of the sodium can have the benefit of reducing the volume of the final, solidified, high-level waste product (Krause et al., 1994). Removal of the nitrites can have the benefit of avoiding nitrogen oxide gas (NO_x) generation when the sludge is acidified in preparation for vitrification. Removal of the nitrates can have the benefit of reducing the amount of NO_x generated when the slurry is delivered to the melter. The cesium-137, however, would need to be selectively removed from the solution and returned to the high-level waste stream for processing into the final high-level waste form.

Leaching the sludge with concentrated sodium hydroxide (3 M NaOH) will dissolve compounds from the sludge, such as aluminum hydroxide, silica, and silicates, and will convert phosphates into soluble hydroxides. Subsequent washing of the leachate from the sludge would remove the nonradioactive aluminum, silica, silicates, sulfates and phosphates from the high-level waste (Krause et al., 1994). Removal of these materials can have the benefit of reducing the volume of the final, solidified high-level waste product.

Laboratory-scale testing of caustic leaching on Hanford Plutonium Finishing Plant sludges using sodium hydroxide followed by potassium permanganate ($KMnO_4$) has been demonstrated to remove greater than 95 percent of the aluminum, chromium, phosphorus, and sulfur (Krause et al., 1994).

2.4.2 Safety Considerations

2.4.2.1 Sodium Hydroxide

Sodium hydroxide, also known as caustic soda and lye, is soluble in water. It is a corrosive irritant to skin, eyes, and mucous membranes, causing a significantly corrosive action on all body tissue, including burns and, frequently, deep ulceration. Mists, vapors, and dusts cause small burns, and contact with the eyes rapidly causes severe damage to its delicate tissue. Ingestion causes serious damage to the mucous membranes and other tissues with which contact is made. Inhalation of the dust or concentrated mist can cause damage to the upper respiratory tract and to lung tissue. Mutation data have been reported (Lewis, 1997). Therefore, appropriate protective clothing should be worn whenever sodium hydroxide is handled.

For sodium hydroxide, the Occupational Safety and Health Administration (OSHA) Permissible Exposure Level (PEL), the American Conference of Governmental Industrial Hygienists (ACGIH) Threshold Limit Value (TLV), and National Institute for Occupational Safety and Health (NIOSH) Recommended Exposure Level (REL) ceiling values are all 2 mg/m^3. This is the amount to which workers can be exposed for a normal 8-hr day, 40-hr work week, without ill effects (Lewis, 1997).

Sodium hydroxide is a strong base that can react violently with many substances (Lewis, 1997). Therefore, it should never be combined with other chemicals unless the possible reactions have been adequately investigated and appropriate precautions taken. When mixing with water, the high heat of mixing needs to be considered also.

57

Sludge Washing

Sodium hydroxide is reported in the Environmental Protection Agency (EPA) Toxic Substances Control Act (TSCA) Inventory and is subject to controls under the Comprehensive Environmental Response, Compensation and Liability Act of 1986 (CERCLA). A release of 450 kg (1,000 lb) or more of sodium hydroxide must be reported to the National Response Center and to state and local government officials as well.

Sodium hydroxide should be handled only in well-ventilated areas. When handling sodium hydroxide solutions, workers should wear a mist respirator, impervious gloves, chemical goggles, full face shield, apron, boots, and gauntlets.

2.4.2.2 Sodium Nitrite

Sodium nitrite is soluble in water. It is a human poison by ingestion. It is a possible carcinogen that may react with organic amines in the body to form carcinogenic nitrosamines. Systemic effects from ingestion include motor activity changes, nausea, vomiting, coma, and other effects. It is an eye irritant. Mutation data have been reported (Lewis, 1997). Therefore, appropriate protective clothing should be worn whenever sodium nitrite is handled.

Sodium nitrite is a strong flammable oxidizing agent. In contact with organic matter, it will ignite by friction. It may explode on contact with cyanides, ammonium salts, cellulose, and other materials (Lewis, 1997). Therefore, it should never be combined with other chemicals unless the possible reactions have been adequately investigated and appropriate precautions taken.

Sodium nitrite, when heated to decomposition, emits toxic fumes of NO_x and sodium oxide (Na_2O). Decomposition occurs at 320 °C (608 °F). Therefore, precautions should be taken to prevent exposure to fire or other high-temperature sources, when stored or handled.

Sodium nitrite is reported in the EPA TSCA Inventory and subject to controls under CERCLA. A release of 45 kg (100 lb) or more must be reported to the National Response Center and state and local government officials.

When handling sodium nitrite, workers should wear a dust respirator, rubber gloves, goggles and face shield, rubber shoes, apron, and clothing to protect skin from dust.

2.4.2.3 Radiological

Waste slurries are radioactive. Therefore, appropriate radiological controls must be in place when taking samples, performing maintenance on slurry handling equipment, or decommissioning slurry handling equipment. Radiological controls include wearing appropriate anti-contamination clothing, using shielding, limiting the time workers spend near equipment containing the radioactive materials, and monitoring radiation.

2.4.2.4 Industrial

When pumps are in operation, appropriate industrial practices for safety near rotating equipment must be practiced.

If the pumps are operated by electrical motors, appropriate industrial practices for safety around electrical equipment must be practiced.

Remote operation will reduce many of the risks.

2.4.3 Comparable Operations in Existence

2.4.3.1 West Valley, New York

Large quantities of sodium were present in the high-level PUREX process waste supernate at West Valley. Most of it was added as sodium hydroxide when the former nuclear fuel reprocessing plant was operational. To prevent corrosion of the tank, the sodium hydroxide was added to neutralize the acidic waste before being sent to the carbon steel high-level waste tank for storage. Removal of much of the sodium was necessary to minimize the borosilicate glass needed to immobilize the high-level waste.

Sulfate salts were present in the PUREX process sludge. These needed to be removed because, in the final borosilicate glass waste form, sulfate was limited to 0.3 wt % to assure adequate glass quality.

The West Valley Demonstration Project removed sodium from the supernate and soluble sulfate salts from the sludge in successive campaigns using the Integrated Radwaste Treatment System. The Integrated Radwaste Treatment System consisted of an ion-exchange system, an evaporator, a cement solidification system, and a shielded, aboveground low-level waste storage facility.

From May 1988 to November 1990, the West Valley Demonstration Project processed 2,100 m³ (560,000 gal.) of liquid high-level waste supernate, retaining the cesium-137 on zeolite ion-exchange material, while expelling the sodium with the decontaminated liquid. The decontaminated liquid was subsequently concentrated by evaporation, solidified by cementation in square 1.9-m³ (71 gal.) drums and stored in the aboveground low-level waste storage facility. The zeolite loaded with cesium-137 was eventually vitrified with the rest of the high-level waste.

Washing the sulfates from the sludge began during November 1991 and accomplished by two washes. For each wash, demineralized water was added to the high-level waste storage tank. To minimize the solubility of the uranium and plutonium in the sludge, 20 wt % sodium hydroxide solution was added to control the solution pH to within the range of 11.8–12.5.

The sludge was mobilized and agitated using five mixing pumps. The pumps were supported by steel trusses, which spanned the top of the tank. The trusses rested on concrete piers with none of the load imparted to the top of the tank or to the concrete vault housing the tank. The pumps were deep well, long shafted, low pressure, high flow, centrifugal pumps. A 15.2-m (50-ft) long stainless steel pipe column, 360 mm (14 in.) in diameter, housed each pump drive shaft. Each pump was energized by a 112-kW (150-hp) motor located above the tank. Each pump had two 2.27-m³/min (600-gpm) discharge nozzles located approximately 250 mm (10 in.) above the tank floor, and the nozzles rotated at 0.5 rpm (Vance et al., 1997).

The solids were allowed to settle, and the water was decanted from the sludge. Decanting was accomplished using centrifugal, multistage, turbine-type pumps. Each pump consisted of a series of pump

bowls housing the impeller and a vertical column through which the pump shaft rose to the motor. The pumps were sized to make transfers at rates from 0.23 to 0.27 m^3/min (60–70 gpm). These flow rates provided fluid velocities from 1.8 to 2.1 m/sec (6 to 7 ft/sec), sufficient to prevent settling of any solids in the line during transfer (Vance et al., 1997).

Processing of the 1,550 m^3 (410,000 gal.) of solution from the first sludge wash through the Integrated Radwaste Treatment System began during April 1992 and completed in May 1994. Eight campaigns were required to process the solution, with each campaign defined as the process between ion-exchange column recharging/realignment operations. Processing of the 1,347 m^3 (355,850 gal.) of solution from the second sludge wash through the Integrated Radwaste Treatment System began in June 1994 and was completed in August 1994. The wash solution was passed through three ion-exchange columns arranged in series, with the alternate columns containing zeolite with titanium and zeolite without titanium. Each column contained 1.29 t (3,600 lb) of the ion-exchange material, with a volume of approximately 1.9 m^3 (67 ft^3). The zeolite without titanium was effective for removing the cesium-137. Zeolite with titanium was used to remove not only cesium-137, but also sufficient plutonium such that the resulting low-level waste form would contain less than the 100 nCi/g (45.4×10^{-6} Ci/lb). Overall system decontamination factors were consistently greater than the design values of 1,000 for cesium and 10 for plutonium (Dalton, 1997).

Subsequent to sludge washing activities, other wastes were transferred to the carbon steel high-level waste tank, and sodium nitrite was added for corrosion control. Corrosion of the carbon steel high-level waste tank was inhibited. A video recording of the interior of the high-level waste storage tank, taken after the high-level waste vitrification campaign was completed, revealed no interior corrosion below the original liquid level.

The addition of sodium nitrite had an impact on high-level waste vitrification operations. Batches of the high-level waste from the tank containing the nitrite were pretreated for melter feed operations by concentration, acidification, and addition of glass-forming chemicals. When acidified, the nitrites were rapidly converted to oxide gases of nitrogen (NO_x). Because the batches were relatively large and acidified rapidly, surges of NO_x gases were generated that entered the vessel ventilation system. The vessel ventilation system directed these gases to the NO_x abatement equipment in the melter offgas treatment system. Because the surges of NO_x exceeded the design capacity of the abatement equipment, NO_x gases were able to penetrate the NO_x abatement equipment. On release to the atmosphere, visible orange plumes of NO_x gases were temporarily visible (Kutina and Walters, 1998). These visible plumes occurred no more than once per melter feed preparation cycle. Each such plume was visible for a period of several minutes.

Because the washing was performed to remove soluble salts, the experience at West Valley is applicable to the TWRS at Hanford, where the sludges are to be washed for the same purpose (Jain and Barnes, 1989).

2.4.3.2 Savannah River, South Carolina

The Savannah River Site intends to process 15,000 m^3 (4 million gal.) of sludge, including soluble salts, and aluminum.
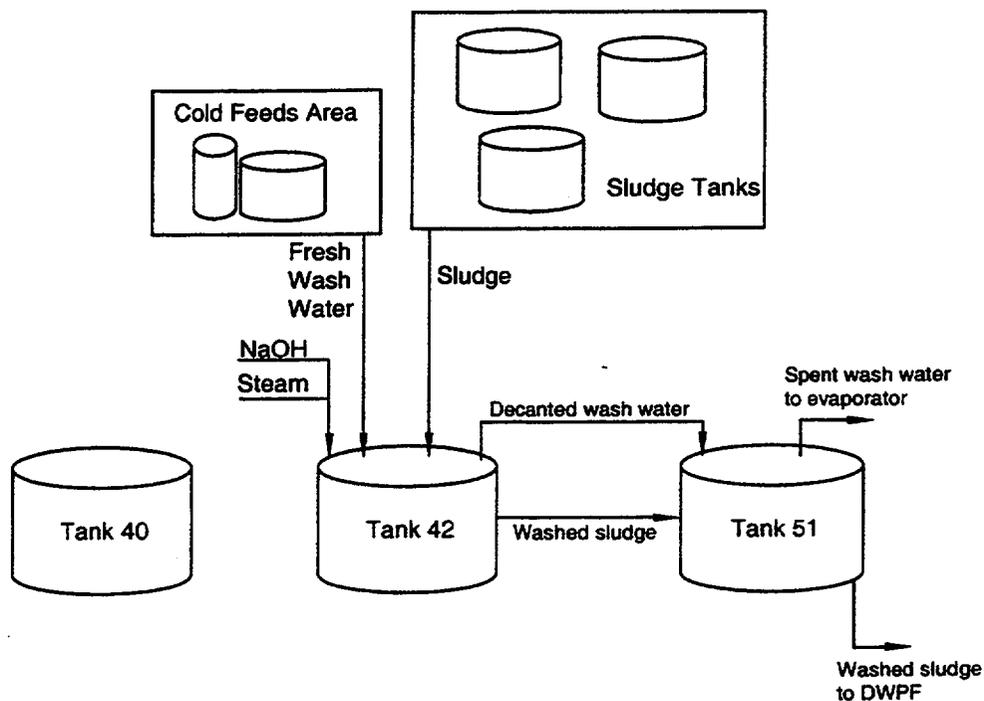
Figure 2-5. Defense Waste Processing Facility (DWPF) sludge washing schematic

The pretreatment process will consist of sludge washing and aluminum dissolution, to remove much of the aluminum and soluble salts. The aluminum will be removed to improve glass processing characteristics, such as melting temperature and melt viscosity (Carter et al., 1997). The soluble salts are to be removed to reduce the volume of glass necessary to immobilize the sludge. This process is being retrofitted into three existing waste tanks—40, 42, and 51 (see figure 2-5).

To remove aluminum, the sludge will be mixed with 3 M caustic and heated to 90 °C (190 °F). Heat will be provided by introducing steam through spargers. This process is designed to dissolve the aluminum.

The sludge will be allowed to settle, and the aluminum will be removed by decanting the liquid. The aluminum-bearing solution will be converted into a cement grout called saltstone for disposal as a low-level waste (Carter et al., 1997; Iverson and Elder, 1992).

To remove the soluble salts, water will be added, and the resulting slurry will be agitated. Then the slurry will be allowed to settle, and the soluble salts will be removed by decanting the liquid. This procedure will be repeated as necessary. The decontaminated wash solution also will be disposed of as saltstone.

The process will be sized to produce approximately 2,650 m³ (700,000 gal.) of sludge over a period of 2 yr. This quantity is enough to feed the West Valley Demonstration Project for about 2.5 yr.

Sludge Washing

The sludge washing step at Savannah River Site is comparable to the sludge washing operations planned for the Hanford TWRS. No similar aluminum dissolution step is currently planned for the TWRS, however.

2.4.4 Sludge Washing Proposed by BNFL Inc.

Following concentration of envelope A, B, and C wastes by evaporation, and precipitation of strontium and transuranic elements from envelope C wastes, BNFL Inc. proposes to collect the solids into a slurry by ultrafiltration, then wash the slurry with water to reduce the concentration of sodium below a certain limit.

More than 70 percent of the sodium in numerous single-shell tank sludges was shown to be removed by a single dilute alkaline wash, and the removal was greater than 90 percent for more than half of the tanks examined. The sodium in the wastes has therefore been shown easily dissolved and removed from the sludge. The BNFL Inc. target sodium concentration is clearly achievable by repetitive water washes of the alkaline sludge.

With a sodium concentration in the envelope A, B, and C wastes of up to 14 M, the sodium content can be as much as 322 g/L (2.69 lb/gal.). Only the nitrate content would be greater, but the nitrate will be driven from the wastes as a gaseous effluent and will not become part of the glass matrix. Therefore, removal of the sodium will significantly reduce the amount of glass necessary to solidify the low-activity waste. In relative terms, removal of other elements from the waste would have only a small impact on the volume of the final glass waste form. Apparently consistent with this analysis, BNFL Inc. proposed no wash steps to selectively remove other materials, such aluminum, chromium, phosphorus, or iron. Removal of chromium by sludge washing or other means may have to be reconsidered by BNFL Inc., however, if melter problems due to excessive concentrations of chromium are encountered.

2.5   References

Barney, G.S. *Vapor-Liquid-Solid Phase Equilibria of Radioactive Sodium Salt Wastes at Hanford.* ARH–ST–133. Richland, WA: Atlantic Richfield Hanford Company. 1976.

Carter, J.T., K.J. Reuter, J.W. Ray, and O. Hodoh. Defense waste processing facility radioactive operations–Part II–Glass making. *Proceedings of Waste Management '97 Conference.* Tucson, AZ: Waste Management Symposia. 1997.

Colton, N.J. *Sludge Pretreatment Chemistry Evaluation: Enhanced Sludge Washing Separation Factors.* PNL–10512. Richland, WA: Pacific Northwest Laboratory. 1995.

Crichton, S.N., T.J. Barbieri, and M. Tomozawa. Solubility limits for troublesome components in a simulated low level nuclear waste glass. *Ceramic Transactions* 61: 283–290. 1995a.

Crichton, S.N., M.F. Savage, and M. Tomozawa. Volatilization rates of troublesome components from a simulated low level nuclear waste glass. *Ceramic Transactions* 61: 291–298. 1995b.

Iverson, D.C., and H.H. Elder. Defense waste processing facility startup progress report. *Spectrum/92 Symposium Proceedings.* La Grange Park, IL: American Nuclear Society. 1992.

Jain, V., and S.M. Barnes. *Waste Description and Previtrification Treatment Activities at WVDP, HWVP, and DWPF*. DOE/NE/44139-57. West Valley, NY: West Valley Nuclear Services Company. 1989.

Krause, T.R., J.C. Cunnane, and J.E. Helt. *Sludge Technology Assessment*. ANL-94/45. Argonne, IL: Argonne National Laboratory. 1994.

Kutina, L., and B. Walters. NO$_x$ reductions in sight. *Perspective*. May 29, 1998. West Valley, NY: West Valley Nuclear Services. 1998.

Lewis, R.J. *Hazardous Chemicals Desk Reference*. New York: Van Nostrand Reinhold Publisher. 1997.

Liu, J., L.R. Pederson, and L.Q. Wang. *Solid-Phase Characterization in Flammable-Gas-Tank Sludges by Electron Microscopy*. PNNL-10723. Richland, WA: Pacific Northwest Laboratory. 1995.

Lumetta, G.J. *Leaching of Iron from Hanford Tank Sludge: Results of FY 1997 Studies*. PNNL-11779. Richland, WA: Pacific Northwest National Laboratory. 1997.

Lumetta, G.J., B.M. Rapko, and N.G. Colton. *Washing and Caustic Leaching of Hanford Tank Sludges*. PNL-SA-23598. Richland, WA: Pacific Northwest Laboratory. 1994.

Lumetta, G.J., B.M. Rapko, M.J. Wagner, J. Liu, and Y.L. Chen. *Washing and Caustic Leaching of Hanford Tank Sludges: Results of FY 1996 Studies*. PNL-11278. Richland, WA: Pacific Northwest National Laboratory. 1996.

Lumetta, G.J., I.E. Burgeson, M.J. Wagner, J. Liu, and Y.L. Chen. *Washing and Caustic Leaching of Hanford Tank Sludges: Results of FY 1997 Studies*. PNNL-11636. Richland, WA: Pacific Northwest National Laboratory. 1997.

Onishi, Y., and J.D. Hudson. *Waste Mixing and Diluent Selection for the Planned Retrieval of Hanford Tank 241-SY-102: A Preliminary Assessment*. PNNL-10927. Richland, WA: Pacific Northwest National Laboratory. 1996.

Rai, D., B.M. Sass, and D.A. Moore. Chromium(III) hydrolysis constants and solubility of chromium(III) hydroxide. *Inorganic Chemistry* 26: 345–349. 1987.

Rapko, B.M., and M.J. Wagner. *Caustic Leaching of Composite AZ-101/AZ-102 Hanford Tank Sludge*. PNNL-11580. Richland, WA: Pacific Northwest National Laboratory. 1997.

Rapko, B.M., G.J. Lumetta, and M.J. Wagner. *Washing and Caustic Leaching of Hanford Tank Sludges: Results of FY 1995 Studies*. PNNL-10712. Richland, WA: Pacific Northwest Laboratory. 1995.

Rapko, B.M., D.L. Blanchard, N.G. Colton, A.R. Felmy, J. Liu, and G.J. Lumetta. *The Chemistry of Sludge Washing and Caustic Leaching Processes for Selected Hanford Tank Wastes*. PNNL-11089. Richland, WA: Pacific Northwest National Laboratory. 1996a.

Sludge Washing

Rapko, B.M., G.J. Lumetta, and M.J. Wagner. *Oxidative Dissolution of Chromium from Hanford Tank Sludge Under Alkaline Conditions.* PNNL–11233. Richland, WA: Pacific Northwest National Laboratory. 1996b.

Su Y., L. Wang, B.C. Bunker, and C.F. Windisch. Spectroscopic studies of aluminosilicate formation in tank waste simulants. *Materials Research Society Symposium Proceedings.* Pittsburgh, PA: 465: 465–472. 1997.

Vance, R.F., B.A. Brill, D.E. Carl, H.S. Dhingra, R.A. Meigs, and M.G. Studd. *Design of Equipment Used for High-Level Waste Vitrification at the West Valley Demonstration Project.* DOE/NE/44139–73. West Valley, NY: West Valley Nuclear Services Company. 1997.

Volf, F.F., and S.I. Kuznetsov. Equilibrium phase diagram of the system Al_2O_3-Na_2O-H_2O. *Journal of Applied Chemistry of the U.S.S.R.* 26: 265–269. 1955.

Weber, E.J. *Aluminum Hydroxide Dissolution in Synthetic Sludges.* DP–1617. Aiken, SC: Savannah River Laboratory. 1982.

3 ION EXCHANGE

One of the first steps in most pretreatment scenarios will be saltcake dissolution and sludge wash (and leach) followed by a solids/liquid separation. Most of the radionuclides, including cesium-137 and technetium-99, are expected in the aqueous liquids resulting from these steps. These solutions are the focus of the ion-exchange removal process. The ion-exchange process has the goal of removing enough of the radionuclides from the low-activity waste feed so the resulting immobilized low-activity waste will meet the Class C standards of Title 10 of the Code of Federal Regulations Part 61. The separated radionuclides are proposed to be immobilized in a borosilicate glass matrix. BNFL Inc. plans to remove cesium-137 and technetium-99 from Hanford tank waste supernates and sludge wash solutions using ion exchange. LMAES had also proposed to use ion exchange to remove cesium-137 from Hanford tank wastes.

Ion exchange is a partitioning technology that has been extensively used in the nuclear industry. Ion-exchange systems have the advantage of simplicity of equipment and operation together with the potential to provide many processing stages that occupy a relatively small facility space. Numerous studies investigated the potential application of ion-exchange technology to cesium recovery from high-level alkaline wastes and sludge wash waters, including those from the Hanford site (Bray et al., 1993; Brown et al., 1995), the Savannah River Site (Bibler et al., 1990), and the West Valley Demonstration Project (Bray et al., 1984). Investigators from various national laboratories evaluated several commercial and experimental adsorbents.

3.1 Ion-Exchange Equilibria—Theory

3.1.1 Equilibrium Constant

Ion exchange is a stoichiometric process, where an ion removed from solution is replaced by another ion from the solid. This process is normally represented by the reaction

$$z_B A^{z_A+} + z_A \overline{B} \Leftrightarrow z_A B^{z_B+} + z_B \overline{A} \tag{3-1}$$

where A and B are ions in the liquid phase, $\overline{A}$ and $\overline{B}$ are ions in the solid phase, and z_A+ and z_B+ are the valence of ions A and B, respectively.

The thermodynamic equilibrium constant, K_{eq}, for the ion-exchange reaction can be calculated from

$$K_{eq} = \frac{(\overline{a}_A)^{z_B}(a_B)^{z_A}}{(a_A)^{z_B}(\overline{a}_B)^{z_A}} \tag{3-2}$$

where $\overline{a}_A$ and $\overline{a}_B$ are the chemical activities of ions A and B, respectively, in the solid phase, and a_A and a_B are the chemical activities of ions A and B, respectively, in the liquid phase.

For ion exchange involving alkali cations, such as the cesium ion (Cs^+) and the sodium ion (Na^+), z_A+ and z_B+ are equal to one, and Eq. (3-2) can be rewritten as

$$K_{eq} = \frac{\bar{a}_A \, a_B}{a_A \, \bar{a}_B} \tag{3-3}$$

The chemical activity of an ion in the liquid phase can be defined as $C \times \gamma$, where C and γ are the concentration and activity coefficient, respectively, of the ion in the liquid phase. Similarly, the chemical activity of the same ion in the solid phase can be defined as $q \times \bar{\gamma}$, where q and $\bar{\gamma}$ are the concentration and activity coefficient, respectively, of the ion in the solid phase. Substituting these relationships for ions A and B into Eq. (3-3) produces the following equation for the equilibrium constant of a monovalent ion-exchange reaction

$$K_{eq} = \frac{q_A \bar{\gamma}_A \, C_B \gamma_B}{C_A \gamma_A \, q_B \bar{\gamma}_B} \tag{3-4}$$

3.1.2 Distribution Coefficient

A relationship commonly used to evaluate the performance of an ion-exchange material is the distribution coefficient or distribution factor, K_d. For example, for ion A, $K_{d,A}$ is defined as the ratio of the equilibrium concentration of A in the solid phase (q_A) to the equilibrium concentration of A in the liquid phase (C_A), that is,

$$K_{d,A} = \frac{q_A}{C_A} \tag{3-5}$$

Values of $K_{d,A}$ are typically given in units of milliliters per gram (mL/g). Substituting $K_{d,A}$ for q_A/C_A in Eq. (3-4), the ion exchange equilibrium constant, K_{eq}, can also be expressed in terms of the distribution coefficient, as in

$$K_{eq} = K_{d,A} \frac{\bar{\gamma}_A \, C_B \gamma_B}{\gamma_A q_B \bar{\gamma}_B} \tag{3-6}$$

In a real process situation, in which the solid phase is initially free of the ion in the solution, the concentration of the ion in the solid phase at equilibrium, q_A, can be expressed as the amount of the ion removed from the solution divided by the weight of the solid, or

$$q_A = \frac{C_{i,A} - C_{f,A}}{W} \tag{3-7}$$

where $C_{i,A}$ and $C_{f,A}$ denote the initial and final solution concentrations of A and W is the dry weight of the ion-exchange material.

The corresponding equilibrium concentration of ion A in the liquid phase, C_A, is the amount of A remaining in solution divided by the volume, V, of the solution, or

$$C_A = \frac{C_{f,A}}{V} \tag{3-8}$$

Substituting Eq. (3-7) and (3-8) into Eq. (3-6) gives

$$K_{d,A} = \frac{C_{i,A} - C_{f,A}}{C_{f,A}} \cdot \frac{V}{W} \tag{3-9}$$

This distribution coefficient represents the theoretical volume of the solution that can be processed per unit mass of ion-exchange material under equilibrium conditions. Eq. (3-9) is useful for calculating the distribution coefficient because it is expressed in terms of easily obtained experimental data.

An alternative distribution coefficient, λ, describes the volume of solution that can be processed by a given volume of ion-exchange material. Values of λ are obtained by multiplying K_d by the bed density (ρ_b, gram of adsorbent per milliliter of adsorbent in solution) of the ion-exchange material, as in

$$\lambda_A = K_{d,A} \times \rho_b \tag{3-10}$$

This alternate volumetric distribution coefficient is often called the lambda value or lambda parameter to distinguish it from the mass-based distribution coefficient, K_d. The λ value provides a method of comparing the ion-exchange performance of a wide variety of materials on a volume basis, which allows the process engineer to estimate the ion loading with respect to the column size required. Because the units of the lambda value are volume per volume, it is a dimensionless number if a consistent set of units is used. In theory, λ represents the number of exchanger bed volumes of feed that can be loaded on an exchanger. In practice, it is difficult to achieve 100 percent loading of a column. Under certain conditions, however, λ is approximated by the bed volumes processed when 50 percent breakthrough is achieved during column loading.

The selectivity of an ion-exchange medium for a particular ion depends on the solution pH, the relative amounts of competing ions, and temperature. The effect of a competing ion on the selectivity of an adsorbent for a particular ion can be important. For example, the abundant sodium ion (Na^+) present in Hanford tank wastes would be expected to compete with cesium ions (Cs^+) for the ion-exchange sites of the adsorbent. Increases in both the sodium ion concentration and the sodium/cesium ratio are expected to reduce the ion-exchange selectivity for cesium. Another competing ion present in significant amounts in Hanford wastes is potassium (K^+).

Ion Exchange

3.1.3 Isotherm Modeling

Extensive experimental studies are reported in the literature that systematically evaluated the effects of various parameters on the distribution coefficient. The results of a suite of experiments studying the effect of aqueous concentration on adsorption while other parameters are held constant are called adsorption or ion-exchange isotherms. Adsorption isotherms used to model experimental ion-exchange data on Hanford wastes include the Langmuir, Freundlich, Langmuir-Freundlich, and Brunauer-Emmett-Teller isotherms.

3.1.3.1 Langmuir Isotherm

The Langmuir isotherm was originally used to describe the adsorption of gas molecules onto homogeneous solid surfaces (crystalline material) that exhibit one type of adsorption site (Langmuir, 1918). Many investigators have extended the Langmuir isotherm to describe the adsorption of aqueous species onto solid substrates, including heterogeneous solids. The Langmuir isotherm is expressed as

$$\frac{q_A}{C_A} = \frac{q_o K_1}{1 + K_1 C_A} \tag{3-11}$$

where K_1 is the Langmuir isotherm constant, and q_o is the total ion-exchange capacity of the adsorbent. If the Langmuir isotherm constant and the total ion-exchange capacity of the adsorbent are known, the distribution coefficient for any equilibrium concentration of ion A, C_A, can be calculated from

$$K_{d,A} = \frac{q_o K_1}{1 + K_1 C_A} \tag{3-12}$$

because $K_{d,A} = q_A/C_A$ [see Eq. (3-5)].

3.1.3.2 Freundlich Isotherm

An alternative equation is the Freundlich isotherm (Freundlich, 1926), defined by

$$q_A = K_f C_A^n \tag{3-13}$$

where K_f and n are the model parameters. The Freundlich isotherm can be transformed to a linear equation by taking the logarithms of both sides of Eq. (3-13):

$$\log q_A = \log K_f + n \log C_A \tag{3-14}$$

When $\log q_A$ is plotted on the y-axis and $\log C_A$ on the x-axis, the best-fit straight line has a slope of n, and $\log K_f$ is its intercept. When n = 1, the Freundlich isotherm reduces to a linear relationship, and because q_A/C_A is the ratio of the amount of solute adsorbed to the equilibrium solution concentration (the definition of K_d), the Freundlich K_f is equivalent to the value of K_d.

3.1.3.3 Langmuir-Freundlich Isotherm

Unlike the Langmuir isotherm, which assumes a limited number of sorption or ion-exchange sites, the Freundlich isotherm does not consider an upper limit for the adsorbent ion-exchange capacity. Thus the Freundlich isotherm applies strictly to adsorption data obtained for low values of C_A. To overcome this limitation, a combination of the Langmuir and Freundlich isotherms is also used to represent ion-exchange data.

The Langmuir-Freundlich isotherm is expressed as

$$q_A = \frac{K_1 C_A^m}{K_2 + C_A^m} \tag{3-15}$$

where K_1, K_2, and m are empirical parameters. This equation has the characteristics of both the Langmuir and Freundlich isotherms and can be used to model ion-exchange data over a wide range of aqueous concentrations. At low aqueous concentrations of A, the equation exhibits a Freundlich behavior, whereas it shows a saturation (Langmuir-type behavior) at high aqueous concentration.

3.1.3.4 Brunauer-Emmett-Teller Isotherm

Another isotherm used for batch equilibrium modeling is the Brunauer-Emmett-Teller equation

$$\frac{C_A}{(C_{A,S} - C_A)q_A} = \frac{1}{K_B q_A^o} + \frac{K_B - 1}{K_B q_A^o} \cdot \frac{C_A}{C_{A,S}} \tag{3-16}$$

where C_A is the equilibrium concentration of A in solution, $C_{A,s}$ is the saturation concentration of A in solution, K_B is an empirical constant, q_A is the equilibrium concentration of A in the solid, and q_A^o is the concentration of sorbed A required to complete a monolayer on the surface of the sorbent (Bostick et al., 1996).

3.1.3.5 Usefulness of the Isotherm Equations

A large amount of cesium ion equilibrium data on ion exchange involving a phenol-formaldehyde-based resin and a resorcinol-formaldehyde resin has been correlated using the Langmuir, Freundlich, and Langmuir-Freundlich isotherms (Kurath et al., 1996). The Langmuir isotherm did not fit the equilibrium data well and is not recommended for use. Experimental data below a cesium concentration of 10^{-4} M were represented well by the Freundlich isotherm, but the more complicated Langmuir-Freundlich isotherm was required to model the full range of equilibrium data for the resorcinol-formaldehyde resin.

Bostick et al. (1996) used the Brunauer-Emmett-Teller equation to fit equilibrium data on strontium sorption on a resorcinol-formaldehyde resin. In that study, the value of $C_{A,s}$ for strontium saturation concentration was chosen as 7.5×10^{-5} mol/L, representing the uppermost strontium concentration found in typical groundwaters. Figure 3-1 compares experimental and model results and shows that calculated
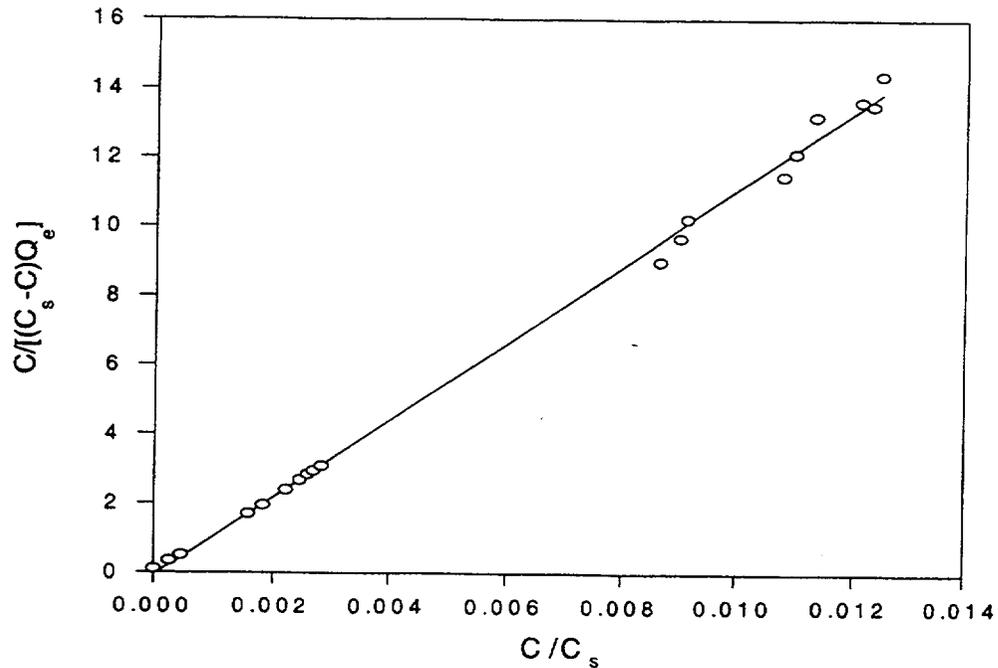
Figure 3-1. Strontium sorption data characterized with the Brunauer-Emmett-Teller isotherm (Bostick et al., 1996)

values fit the experimental data well for the range evaluated $(0 < C_A/C_{A,s} < 0.012)$, with a regression coefficient of 0.997 (Bostick et al., 1996).

3.1.4 Column Modeling

3.1.4.1 Column Dynamics

The following model is presented for column dynamics studies (Klavetter et al., 1994). The model incorporates axial dispersion and mass transfer resistances due to film (interparticle) and pore (intraparticle) diffusion and assumes dynamic localized equilibrium. For one-dimensional flow, the mass balance equation in the bulk phase is given by

$$\frac{\partial C}{\partial \tau} - \frac{1}{Pe_b}\frac{\partial^2 C}{\partial z^2} + v\frac{\partial C}{\partial z} + \frac{1-\varepsilon}{\varepsilon}\frac{3L}{R_p}\frac{Bi}{Pe_p}(C - C_s) = 0 \qquad (3-17)$$

and the mass balance equation for the particle is given by

$$\left(\varepsilon_p + \rho_p\frac{\partial q}{\partial C_p}\right)\frac{\partial C_p}{\partial \tau} = \frac{1}{Pe_p}\frac{L}{R_p}\frac{1}{\rho^2}\frac{\partial}{\partial\rho}\left(\rho^2\frac{\partial C_p}{\partial\rho}\right) \qquad (3-18)$$

where the subscript p denotes the properties of the particle. The following boundary conditions are used by the model:

$$\frac{\partial C}{\partial z} = Pe_b(C - C_{inlet}) \qquad \text{at } z = 0 \qquad (3\text{-}19)$$

$$\frac{\partial C}{\partial z} = 0 \qquad \text{at } z = 1 \qquad (3\text{-}20)$$

$$\frac{\partial C_p}{\partial \rho} = Bi(C - C_s) \qquad \text{at } \rho = 1 \qquad (3\text{-}21)$$

$$\frac{\partial C_p}{\partial \rho} = 0; \quad \frac{\partial q}{\partial \rho} = 0 \qquad \text{at } \rho = 0 \qquad (3\text{-}22)$$

The mass balance is solved after assuming an isotherm equation

$$q = f(C_p) \qquad (3\text{-}23)$$

The following dimensionless variables and dimensionless numbers are used in the model:

$$z = \frac{x}{L}; \; \rho = \frac{r}{R_P}; \; \tau = \frac{tv}{L} \qquad (3\text{-}24)$$

$$Pe_b = \frac{Lv}{D_L} \qquad (3\text{-}25)$$

$$Pe_p = \frac{R_p v}{De_p} \qquad (3\text{-}26)$$

$$Bi = \frac{R_p k_f}{De_p} \qquad (3\text{-}27)$$

where the Peclet numbers are Pe_b for the bulk phase and Pe_p for the particle, and Bi is the Biot number. L and r are the length and radius of the column, v is the interstitial velocity, R_p is the particle radius, D_L is the diffusion coefficient for the bulk phase, De_p the effective diffusion coefficient for the particle phase and k_f is the film mass transfer coefficient. For low Pe_b values, backmixing occurs, and the elution curve

71

Ion Exchange

becomes a broad S-shaped curve with elution of the species (e.g., cesium) occurring within a few column volumes. For large Pe_b values, conditions are in the plug flow regime. The Biot number is a measure of the resistance to film diffusion. As the Biot number increases, the resistance to intraparticle (pore) diffusion becomes more significant than the interparticle (film) diffusion.

Modeling results for a base case system and its variants, all using cesium and a crystalline silicotitanate ion exchanger, are shown in figure 3-2 (Klavetter et al., 1994). The values of time on the x-axis of figure 3-2 were not specified in the original reference (Klavetter et al., 1994). The figure illustrates the effects on the breakthrough of cesium through the ion-exchange column of varying the values of the lambda parameter ($\lambda = K_d \rho_b$) and the effective diffusivity within the particle. Curve 1 is the base case, with $D_L = 5 \times 10^{-8}$ m²/s, $k_f = 6.6 \times 10^{-2}$ m/s, $De_p = 1.37 \times 10^{-11}$ m²/s, and $\lambda = 241$. For curve 2, the λ value is 5 percent higher relative to the base case, shifting the elution curve to slightly later times. Curve 3 used a factor of ten higher value for De_p relative to the base case. As expected, with less intraparticle resistance, the solute elutes later than the base case. Curve 4 is the same as curve 3, but with lower value for the λ parameter resulting in earlier cesium breakthrough compared to curve 3. Thus, increasing the value of λ results in the shift of the elution curve to later times or to higher column volumes. None of the model curves describes the full range of experimental data well, rather, just portions of the data. Therefore, although useful, the model should be used with caution.

3.1.4.2 Transfer Units

For engineering applications, simpler empirical equations are typically applied. For example, the total number of mass transfer units is defined as

$$N = 4 \frac{\left(\dfrac{\partial X_A}{\partial T} \right)_{0.5}}{1 - R} \tag{3-28}$$

where the partial derivative denotes the slope of the breakthrough curve at the 50 percent breakthrough point (Brunson et al., 1994). T is the throughput parameter, given as the ratio of the adsorbent volume to the total column volume of solution that passed through at the 50 percent breakthrough point, and x_A is the ratio of the concentration of component A in the input solution to its concentration in the output solution. That is,

$$X = \frac{C_{A,in}}{C_{A,out}};$$

$$T = \frac{\text{Column Volume}}{\text{Column Volume @ 50\% Breakthrough}} \tag{3-29}$$

The variable R is a scaled separation factor for component A at trace levels ($x_A \ll 0.1$) and is calculated from the equation
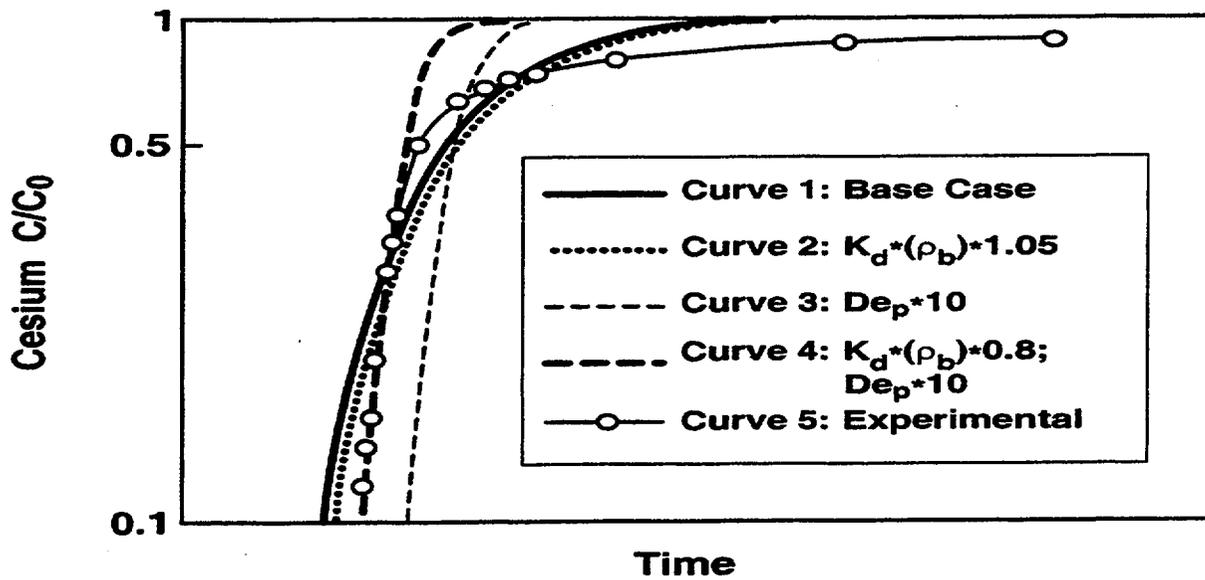
Figure 3-2. Comparison of experimental data and results of ion-exchange modeling showing effects of changes in effective diffusivity and distribution coefficients on cesium elution (Klavetter et al., 1994)

$$R = \frac{1}{1 + (x_A)_o (1/r - 1)} \qquad (3\text{-}30)$$

The parameter r is a normal separation factor based on the fluid and solid concentrations, as shown in the equation

$$r = \frac{x_A (1 - y_A)}{y_A (1 - x_A)} \qquad (3\text{-}31)$$

where the concentration of species A in the fluid is x_A and in the adsorbent is y_A.

3.1.4.3 Mass Transfer Coefficient

Based on the number of transfer units, N, the bulk mass transfer coefficient, k_b, can be calculated from the equation

$$k_b = \frac{N}{K_d (v/f)} \qquad (3\text{-}32)$$

73

Ion Exchange

where K_d is the equilibrium distribution coefficient and v/f is the ratio of the adsorbent volume to the volumetric flow rate (Brunson et al., 1994).

3.1.5 Scale-Up Considerations

A minimum column diameter of 30 adsorbent particle diameters is considered necessary to prevent peak velocities near the wall of the column (Brooks et al., 1996). For example, for the recorcinol-formaldehyde resin with 0.34-mm (0.013 in.) average particle diameter, a 1.0-cm (0.39-in.) diameter or larger column should be used. This conclusion is based on particle Peclet number measurements, which are shown to be higher near the walls for diameter columns that are smaller than 30 particle diameters (Brooks et al., 1996).

Another important parameter is the mass transfer coefficient for bulk diffusion, $k_b a$. This parameter becomes important in smaller size columns, and it is defined as

$$k_b a = \frac{2.62 (D_L v)^{0.5}}{(d_p)^{1.5}} \tag{3-33}$$

where D_L is the diffusivity in the liquid, v is the superficial velocity, and d_p is the particle diameter (Brooks et al., 1996). Ideally, d_p should have large values so that the mass transfer of the solute into the particle will be the rate-limiting step. The mass transfer coefficient for the solute transfer into the particle, $k_p a$,

$$k_p a = \frac{60 D_p}{(d_p)^2} \tag{3-34}$$

where D_p is the diffusivity of the solute in the solid.

The reciprocal sum of $k_b a$ and $k_p a$ gives the overall mass transfer coefficient. Bulk diffusion becomes important in shorter columns.

The previous mass transfer coefficient equations can be used to determine the number of mass transfer units (N) for a given volume of ion-exchange material from

$$N = \frac{60 K_d \rho_b D_p V}{(d_p)^2 f} \tag{3-35}$$

where ρ_b is the bed density, V is the bed volume, and f is the flowrate.

3.2 Ion-Exchange Materials

A number of ion-exchange media was developed in commercial, government, and academic laboratories targeting specific elements for separation applications. Table 3-1 lists some of the various ion exchangers that were studied, along with information on the supplier company. The crystalline silicotitanate ion

74

Table 3-1. Source companies for selected ion-exchange materials

Material	Company	Description
Crystalline silicotitanate ion exchangers	UOP Molecular Sieves Mt. Laurel, NJ	IONSIV® IE-910, powder form IONSIV® IE-911-08, spherical form IONSIV® IE-911-38B, granular form
Resorcinol-formaldehyde resins	Boulder Scientific Mead, CO	BIB-DJ SLR-DJ SRR Resorcinol-formaldehyde (BSC-210)
Superligands (Macrocyclic polymer resins)	IBC Advanced Technologies American Fork, UT	SuperLig®-639 SuperLig®-644
	3M St. Paul, MN	SLIG-644 WWL WEB
Zeolites (Alkali-metal aluminosilicates)	UOP Molecular Sieves Mt. Laurel, NJ	IONSIV® IE-96 IONSIV® TIE-96, titanium coated
	Steelhead Spokane, WA	Chabazite, natural occurring zeolite

exchangers were originally developed in powder form by R.G. Dosch (Sandia National Laboratories) and R.G. Anthony (Texas A&M University). The powdered and the engineered crystalline silicotitanates (IONSIV® IE-910 and IONSIV® IE-911, respectively) are being developed and commercialized by UOP Molecular Sieves (Mt. Laurel, New Jersey). The crystalline silicotitanate material was previously considered by BNFL Inc. for a low-activity waste-only facility to readsorb cesium-137 that would have been eluted from the primary ion-exchange system of SuperLig®-644. A disadvantage of the crystalline silicotitanate material is that it cannot be regenerated.

Resorcinol-formaldehyde is a commercially available organic ion-exchange resin. It was considered by LMAES for use in removing cesium-137 from the Hanford low-activity waste.

SuperLig®-644 and SuperLig®-639 are two versions of the covalently bound Superligand® macrocyle family of sequestering ligands from IBC Advanced Technologies (American Fork, Utah). SuperLig®-644 has been shown highly selective for cesium even in the presence of excess sodium or potassium (Brown et al., 1995). SuperLig®-644 is planned by BNFL Inc. to be the ion-exchange medium to remove cesium-137. BNFL Inc. plans to use SuperLig®-639 as the ion-exchange medium to remove technetium-99 from the Hanford waste stream.

The IE-96 material is a high-capacity aluminosilicate zeolite produced by UOP Molecular Sieves with relatively high selectivity for cesium over other alkali metals. TIE-96 is a modified version of IE-96 capable of removing strontium and plutonium from alkaline solutions, in addition to remove cesium (Brown et al., 1996b).

75

Ion Exchange

A more complete listing of ion-exchange material is given in table B-1. Several of these materials are still under development, and those that have been tested on Hanford wastes by DOE investigators may not have been in optimal form.

3.2.1 Physical Considerations

The particle size, density, F-factor (ratio of dry weight to wet weight), and swelling resistance of several ion-exchange media are shown in table 3-2. The values in the table show that organic resins have lower densities than the inorganic ion exchangers, but inorganic adsorbents do not change density (swell) significantly during hydration or with changes in solution pH (Braun et al., 1996).

3.2.2 Performance

3.2.2.1 Ion-Exchange Selectivity

The selectivity of the adsorbents for cesium generally follows the order crystalline silicotitanate powder ≈ crystalline silicotitanate granules > resorcinol-formaldehyde ≈ SuperLig®-644 > zeolite (Brown et al., 1996a,b). For strontium, the general order of selectivity is crystalline silicotitanate granules > crystalline silicotitanate powder > zeolite > SuperLig®-644 > resorcinol-formaldehyde. Both forms of crystalline silicotitanate sorbent demonstrate high affinity for cesium and strontium, based on experiments using actual or simulated double-shell slurry feed wastes. The organic resins exhibit relatively low affinity for strontium and would not be useful for strontium removal (Brown et al., 1996a,b).

Crystalline silicotitanate can also remove plutonium from solution. However, in solutions containing organic material, plutonium, as well as strontium, are complexed and crystalline silicotitanate cannot efficiently remove these elements from solution (Bray et al., 1993).

3.2.2.2 Distribution Coefficients

Batch ion-exchange tests are used to evaluate K_d values as a function of time. In these tests, a small amount of ion adsorbent is mixed with a known volume of the solution of interest in a batch reactor. After time to reach equilibrium, the solid ion-exchange material and the liquid phase are separated, and samples of the solution are taken for analysis of the equilibrium ion concentration. The amount of time required to reach equilibrium and the rate of approach to equilibrium are typically determined by taking aqueous samples at different time intervals.

Hanford Double-Shell Slurry Feed and Neutralized Current Acid Waste Simulants

Hanford double-shell slurry feed and neutralized current acid wastes are representative of TWRS envelope A waste and TWRS envelope B waste, respectively.

Comparisons of cesium and strontium uptake from a double-shell slurry feed simulant and from an actual double-shell slurry feed waste (see table 3-3) are presented in tables 3-4 and 3-5. In table 3-4, volumetric

Table 3-2. Physical properties of selected ion-exchange materials (data from Brown et al., 1996a,b; Lee et al., 1997; UOP Molecular Sieves, 1997a,b)

Material	Particle Size (μm)	Density Dry (g/mL)	F-Factor (dry wt/wet wt)	Swelling (H⁺ to Na⁺ form)
Crystalline silicotitanate powder	<1	0.7738 (measured) 0.960 (as shipped)	0.9680	Resistant to swelling
Crystalline silicotitanate spheres	250–590 (30–60 mesh)	0.8999 (measured) 0.960 (as shipped)	0.8990	Resistant to swelling
Crystalline silicotitanate granules	250–590 (30–60 mesh)	1.1300 (measured)	0.8870	Resistant to swelling
Resorcinol-formaldehyde	210–355 (45–70 mesh)	0.3044 (measured)	0.8070	43–54 %
SuperLig®-644*	355–840 (20–45 mesh)	0.2238 (measured)	0.9751	40–50 %
Zeolite	297–840 (20–50 mesh)	0.880 (as shipped)	no data	Resistant to swelling
Zeolite, with titanium	297–840 (20–50 mesh)	0.7672 (measured) 0.960 (as shipped)	0.8338	Resistant to swelling
*No published information was found on SuperLig®-639.				

distribution coefficients (λ) for the double-shell slurry feed simulant at two sodium/cesium ratios and different sodium ion concentrations are shown (Brown et al., 1996a,b). The data suggest the benefit of dilution for feed streams to inorganic adsorbents, since the change in λ value increases substantially with decreasing aqueous sodium concentration for the inorganic adsorbents. Values of strontium λ based on experiments that used some of the same adsorbents and actual double-shell slurry feed are shown in table 3-5. Over the range of conditions investigated, the concentration of cesium generally had little effect on the strontium λ. This is not surprising since both cesium and strontium are present in low concentrations and generally do not compete for the same exchange sites (Brown et al., 1996b). This result means that the equilibrium system can be approximated as if it is two binary ion-exchange interactions.

A comparison of ion exchanger performance for removal of plutonium, cesium, and strontium from a double-shell slurry feed waste stream (pH > 14) based on batch experiments is given in table 3-6. The table lists the equilibrium distribution coefficients for the zeolite, titanium-impregnated zeolite, and crystalline silicotitanate ion-exchange media at 10 and 40 °C (50 and 104 °F) (Bray et al., 1993). Cesium distribution coefficients (λ) at various sodium concentrations based on column tests using the zeolite, resorcinol-formaldehyde, and crystalline silicotitanate ion-exchange materials are listed in table 3-7. This table indicates that more simulant volumes can be treated continuously with crystalline silicotitanate compared with the other ion exchangers.

Table 3-3. Double-shell slurry feed (DSSF) waste and simulant compositions (data from Brown et al., 1996a)

Constituent[*]	Units	DSSF Waste[†,‡]	DSSF Simulant[§]
Cs-137	μCi/mL	150	0
Sr-90	μCi/mL	0.16	0
Total Organic Carbon	g/L	2.16	0
Total Inorganic Carbon	mol/L	0.13	0.14
OH	mol/L	2.01	2.17
F	mol/L	below detection limit	0.0433
Cl	mol/L	6×10^{-4}	0.065
NO_2	mol/L	0.81	0.94
NO_3	mol/L	1.34	1.49
PO_4	mol/L	0.016	0.0175
SO_4	mol/L	0.01	0.0126
Na	mol/L	4.67	5.00
K	mol/L	0.44	0.475
Al	mol/L	0.46	0.497
Cr	mol/L	0.0019	0
Si	mol/L	0.0019	0
Sr	mol/L	$1.3 \times 10^{-5§}$	7.14×10^{-8}
B	mol/L	0.0058	0
Ca	mol/L	2.4×10^{-4}	2.41×10^{-4}
Ba	mol/L	$<1.45 \times 10^{-5§}$	5.91×10^{-7}

[*]Other constituents are present in the actual waste at less than 10^{-3} mol/L, but were not added to the waste simulant: Mo, Pb, Ni, Zr, Zn, Fe, Cd, and Be. The published analyses also listed S and P, in addition to SO_4 and PO_4, in essentially the same molar concentrations as the SO_4 and PO_4.
[†]A composite of 70, 20, and 10 vol % from Hanford tanks AW–101, AP–106 and AP–102, respectively.
[‡]Analysis performed by Westinghouse Hanford Company, except as noted.
[§]Analysis performed by Pacific Northwest National Laboratory.

Table 3-4. Effect of sodium/cesium ratio and sodium concentration on cesium volumetric distribution coefficient (λ)* (data from Brown et al., 1996a,b)

Ion-Exchange Material	Na/Cs	λ in 0.2 M Na (mL/mL)	λ in 1 M Na (mL/mL)	λ in 3 M Na (mL/mL)	λ in 5 M Na (mL/mL)
Crystalline silicotitanate powder	10^4	21,100	3,710	918	521
Crystalline silicotitanate granules	10^4	14,100	¯2,940	755	505
Resorcinol-Formaldehyde	10^4	870	224	88	67
SuperLig®-644	10^4	890	175	70	30
Zeolite, titanium-coated	10^4	1,030	164	44	22
Crystalline silicotitanate powder	10^6	52,200	8,120	2,100	1,120
Crystalline silicotitanate granules	10^6	27,900	6,890	2,420	1,320
Resorcinol-Formaldehyde	10^6	2,660	712	293	245
SuperLig®-644	10^6	2,490	666	346	248
Zeolite, titanium-coated	10^6	1,100	182	46	22

*From double-shell slurry feed simulant

Table 3-9 shows the comparative performance of the SuperLig®-644 resin to the resorcinol-formaldehyde resins for cesium uptake from Hanford neutralized current acid waste simulants, with compositions given in table 3-8. Based on the cesium equilibrium distribution coefficient (K_d) alone, the SuperLig®-644 appears the superior cesium adsorbent material. After accounting for absorbent material. After accounting for differences in the equilibrium sodium/cesium ratio for the resins, the equilibrium cesium loading of SuperLig®-644 per unit mass is only slightly greater compared to resorcinol-formaldehyde at the same equilibrium sodium/cesium ratio. Thus, the resorcinol-formaldehyde and the SuperLig®-644 resins have similar performance for cesium uptake from a neutralized current acid waste simulant (Brown et al., 1995).

Table 3-5. Effect of sodium/cesium ratio on strontium volumetric distribution coefficient (λ)*
(data from Brown et al., 1996a,b)

Ion-Exchange Material	Na/Cs	λ (mL/mL)
Crystalline silicotitanate, granules	105	1,090
	1,760	1,100
	48,600	1,090
	387,000	1,160
Crystalline silicotitanate, powder	106	378
	2,690	420
	78,500	559
	431,000	636
	646,000	615
Zeolite, with titanium	105	216
	1,090	193
	11,800	197
	82,700	199
Resorcinol-formaldehyde	104	17
	1,150	20
	18,300	20
	183,000	17

*In actual double-shell slurry feed waste

Table 3-6. Equilibrium distribution coefficients (K_d) for plutonium, cesium, and strontium* (data from Bray et al., 1993)

Ion-Exchange Material	Temp (°C)	K_d for Pu (mL/g)	K_d for Cs (mL/g)	K_d for Sr (mL/g)
Zeolite	10	<1	132	73
	40	106	60	3,100
Zeolite, with titanium	10	602	109	2,753
	40	5,724	47	2,571
Crystalline silicotitanate	10	412	295	>10^5
	40	2,729	147	>10^5

*From double-shell slurry feed waste

Table 3-7. Cesium equilibrium volumetric distribution coefficients (λ) at various sodium concentrations* (data from Bray et al., 1993)

Ion-Exchange Material	λ in 0.2 M Na (mL/mL)	λ in 1 M Na (mL/mL)	λ in 3 M Na (mL/mL)	λ in 5 M Na (mL/mL)
Resorcinol-formaldehyde	3,100	1,800	300	180
Crystalline silicotitanate	—	5,300	1,500	850
Zeolite	1,900	300	80	42
*Double-shell slurry feed waste, Na/Cs molar ratio = 10^4, T = 25 °C				

The equilibrium distribution coefficients for cesium uptake from two tank waste simulants, neutralized current acid waste and double-shell slurry feed (using resorcinol-formaldehyde and zeolite), are shown in table 3-10 (Brooks et al., 1996). The initial cesium concentration ranged from 7×10^{-5} to 7.37×10^{-4} M, and the sodium concentration ranged from 1.8 to 8.7 M. Better results were obtained with the resorcinol-formaldehyde resin.

The effects of total sodium concentration and sodium-to-cesium concentration ratio on the cesium volumetric distribution coefficient for a neutralized current acid waste simulant are shown in table 3-11. Values are given for zeolite and resorcinol-formaldehyde ion exchangers.

Melton Valley Storage Tank Waste

Batch experiments were conducted on cesium, strontium, and technetium removal from supernates from two tanks of the Melton Valley Storage Tank Facility at Oak Ridge National Laboratory (Collins et al., 1995). These supernates are characterized by alkaline pH and high salt concentrations, similar to Hanford tank wastes. The composition of tank W–25 and tank W–29 supernates are given in table 3-12. Isotherm cesium data for different ratios of tank W–25 supernate to crystalline silicotitanate adsorbent are given in table 3-13.

Jubin et al. (1998) conducted batch sorption studies using Melton Valley Storage tank W–25 supernate with a pH of 12.6, a sodium concentration of 3.9 M, and a nitrate concentration of 3.8 M. The experiments resulted in cesium distribution coefficients (K_ds) of 138–764 mL/g (16.5–91.6 gal./lb) using resorcinol-formaldehyde, and 451–958 mL/g (54.0–114 gal./lb) using crystalline silicotitanate.

3.2.2.3 Ion-Exchange Kinetics

Hanford Tank AW–101 Simulant

Hanford tank AW–101 contains a double-shell slurry feed waste (Brown et al., 1996a). Double-shell slurry feed supernate is typical of TWRS envelope A waste.

Batch kinetic experiments were conducted using a Hanford tank AW–101 waste simulant and various ion-exchange materials (Braun et al., 1996). The compositions of typical AW–101 simulants are shown

81

Table 3-8. Neutralized current acid waste (NCAW) simulant compositions (in mol/L) (data from Brown et al., 1995; Lumetta et al., 1993; Bray et al., 1996)

Constituent	NCAW Simulant of Brown et al., 1995	NCAW Simulant of Lumetta et al., 1993	NCAW Simulant of Bray et al., 1996[*]
Na	5.00	5.92	5.92
K	0.12	0.14	0.14
Rb	5.00×10^{-5}	1.3×10^{-4}	1.3×10^{-4}
Cs	5.00×10^{-4}	varied	0
Al	0.43	0.52	0.52
SO_4	0.15	0.18	0.18
OH (total)	3.40	—	—
OH (free)	1.68	2.0	2.0
CO_3	0.23	0.24	—
NO_2	0.43	1.87	0.52
NO_3	1.67	0.52	1.87
F	0.089	0.107	0.107
PO_4	0.025	—	—
[*]Target composition			

Table 3-9. Comparison of cesium uptake[*] on the SuperLig®-644 and resorcinol-formaldehyde resins (data from Brown et al., 1995)

Parameter	Units	SuperLig®-644		Resorcinol-Formaldehyde	
Initial cesium concentration	mol/L	5×10^{-4}		5×10^{-4}	
Initial sodium concentration	mol/L	5		5	
Initial sodium/cesium	mol/mol	1×10^{4}		1×10^{4}	
Final cesium concentration	mol/L	4.3×10^{-5}	5.4×10^{-5}	1.1×10^{-4}	1.1×10^{-4}
Equilibrium sodium/cesium	mol/mol	9.2×10^{4}	1.2×10^{5}	4.7×10^{4}	4.7×10^{4}
Measured K_ds	mL/g	1,176	1,509	633	614
Calculated λs	mL/mL	264	339	231	224
[*]From Hanford neutralized current acid waste simulant					

Table 3-10. Cesium distribution coefficients from two simulant wastes (data from Brooks et al., 1996)

Ion-Exchange Material	K_d for Neutralized Current Acid Waste (mL/g)	K_d for Double-Shell Slurry Feed (mL/g)
Resorcinol-Formaldehyde	450–1200	236–650
Zeolite	45	12

Table 3-11. Effect of sodium/cesium ratio on the cesium volumetric distribution coefficient (λ) (data from Lumetta et al., 1993)*

Na⁺ Concentration (mol/L)	Zeolite		Resorcinol-Formaldehyde	
	[Na⁺]/[Cs⁺] (mol/mol)	λ (mL/mL)	[Na⁺]/[Cs⁺] (mol/mol)	λ (mL/mL)
0.2	1.12×10^5	2,440	376	596
	1.16×10^6	2,900	1.49×10^6	22,758
	1.28×10^7	3,170	2.02×10^7	26,909
	—	—	1.89×10^8	26,759
1	2.38×10^4	467	77.5	44
	2.34×10^5	469	6.06×10^3	797
	2.47×10^6	531	2.88×10^5	4,484
	—	—	4.44×10^6	6,803
	—	—	6.00×10^7	7,760
3	9.41×10^3	125	61.7	15
	9.52×10^4	135	1.21×10^3	110
	9.90×10^5	152	7.46×10^4	996
	—	—	1.48×10^6	2,359
	—	—	2.22×10^7	2,939
5	6.96×10^3	61	56.9	11
	7.80×10^4	71	889	55
	7.33×10^5	74	2.97×10^4	391
	—	—	5.76×10^5	925
	—	—	1.56×10^7	1,991

*In neutralized current acid waste simulant.

Table 3-12. Compositions of Melton Valley tanks W–25 and W–29 supernates (data from Collins et al., 1995)

Constituent	Units	Tank W–25 Supernate	Tank W–29 Supernate
Cs-134	Bq/L	7.4×10^6	3.4×10^6
Cs-137	Bq/L	2.5×10^8	2.2×10^8
Co-60	Bq/L	6.3×10^6	4.0×10^5
Eu-154	Bq/L	1.1×10^5	BDL*
Sr-90	Bq/L	1.0×10^6	2.4×10^6
Tc-99	Bq/L	2.1×10^4	2.0×10^4
Al	mg/L	453	0.43
Ba	mg/L	1.2	0.36
Ca	mg/L	9.5	3.5
Cs	mg/L	0.19	0.57
Cr	mg/L	51	2.2
Cu	mg/L	0.7	0.2
K	mg/L	14,000	11,400
Na	mg/L	89,000	102,000
Pb	mg/L	12.8	7.1
Sr	mg/L	0.4	1.0
Tc	mg/L	0.032	0.031
Th	mg/L	0.3	<0.1
U	mg/L	4.3	1.3
Zn	mg/L	9.5	61
B^-	mg/L	345	<50
Cl^-	mg/L	3,740	3,000
F^-	mg/L	371	<5
NO_3^-	mg/L	236,000	280,000
PO_4^{2-}	mg/L	BDL*	<50
SO_4^{2-}	mg/L	2,370	670
*Below detection limit			

Table 3-13. Cesium (Cs) isotherm data for crystalline silicotitanate* at different ratios of supernatant volume to ion-exchanger mass (S/E) (data from Collins et al., 1995)

Ion-Exchange Material	S/E (mL/g)	Cs Loading (meq/kg)	Cs Loading (meq/L)	K_d (mL/g)	Removal (%)
Crystalline silicotitanate	5,000	1.9	1.0×10^{-3}	1,850	27.0
	2,000	0.79	6.4×10^{-4}	1.020	54.9
	400	0.39	4.5×10^{-4}	640	67.6
	200	0.22	3.2×10^{-4}	670	78.7
	100	0.13	1.3×10^{-4}	840	91.2
*Using Melton Valley tank W–25 supernate					

in table 3-14. The reported values of cesium volumetric distribution coefficient (λ) as a function of time are shown in table 3-15. Note that after about 18 hr, the ion-exchange capacity of the solids for cesium was reached and the loading on the ion exchangers remained relatively constant. Table 3-15 shows the crystalline silicotitanate ion exchangers outperformed the other adsorbents, with an order of magnitude higher cesium loading capacity. Also, the effect of crystalline silicotitanate particle size on the distribution coefficient was apparent at early times. For example, for crystalline silicotitanates at 0.02 hr, the λ value for the powder is greater than that of the granules by a factor of about 50. Other data not shown in the table however, indicate that the use of smaller particle size leads to a higher pressure drop.

Melton Valley Storage Tank Waste

The composition of Melton Valley Storage tank W–25 and tank W–29 supernates is given in table 3-12. Table 3-16 gives the percent removal and the cesium K_d for crystalline silicotitanate and SuperLig®-644 as a function of time. Values as a function of time of the strontium distribution coefficient and the percent removal from tank W–29 supernate using crystalline silicotitanate are given in table 3-17.

3.2.2.4 Ion-Exchange Capacities

Superligand®, Resorcinol-Formaldehyde, and Crystalline Silicotitanate on Melton Valley Storage Tank Supernates

SuperLig®-644, resorcinol-formaldehyde, and crystalline silicotitanate were tested with actual supernate from Melton Valley storage tank W–27 (Lee et al., 1997). The column used was 15 cm (5.9 in.) high with a 1.5 cm (0.59 in.) diameter, and contained 10–12 mL (6.1–7.3 in.^{3}) of adsorbent. Adjustments of pH and cesium concentration were performed on the received waste, and two different samples were prepared. The compositions of these samples are given in table 3-18. The results for all adsorbents tested are shown in figures 3-3 and 3-4. The results show that the crystalline silicotitanate materials exhibit better performance than the other adsorbents. The crystalline silicotitanate materials were able to maintain the

Table 3-14. Hanford tank AW–101 simulants and simulated supernatant compositions (in mol/L) (data from Bibler, 1994; Crawford et al., 1993)

Species	AW–101 Simulant of Bibler, 1994	AW–101 Simulant of Crawford et al., 1993	Simulated High-Level Waste Supernate
NaOH	7.1	5.10	2.90
$Al(NO_3)_3$	0.5	0.50	0.38
$NaNO_3$	2.4	2.40	1.20
$NaNO_2$	1.1	2.20	0.71
Na_2CO_3	0.21	0.21	0.20
Na_2SO_4	0.01	0.01	0.17
KNO_3	—	—	0.015
$CsNO_3$	1.4×10^{-4}	—	2.4×10^{-4}
$Zn(NO_3)_3$	0.001	—	—
KOH	1.1	1.10	—
Cs-137	trace	—	trace

Table 3-15 Cesium volumetric distribution coefficients $(\lambda)^*$ as a function of time (data from Braun et al., 1996)

Ion Exchanger Material	λ after 0.02 hr	λ after 0.03 hr	λ after 0.13 hr	λ after 0.50 hr	λ after 1.85 hr	λ after 18.7 hr	λ after 67.9 hr	λ after 117 hr
Crystalline silicotitanate, powder	112	126	262	217	473	1,429	990	1,462
Crystalline silicotitanate, spheres	4.51	—	—	20.9	—	716	—	—
Crystalline silicotitanate, granules	2.23	—	12.7	—	—	887	776	1,146
Resorcinol-formaldehyde	1.4	1.79	5.66	14.5	47.1	110.4	97.5	99.6
SuperLig®-644	8.08	3.27	9.21	30.89	—	165	180	173
Zeolite, with Ti	—	—	4.53	11.9	15.5	22.8	23.3	—

*With Hanford tank AW–101 waste

Table 3-16. Cesium distribution coefficient (Cs K_d) and removal from Melton Valley supernates as a function of time (data from Collins et al., 1995)

Ion-Exchange Material and Test Waste	Cs K_d and Removal at 0.25 hr		Cs K_d and Removal at 2 hr		Cs K_d and Removal at 24 hr		Cs K_d and Removal at 72 hr		Cs K_d and Removal at 144 hr	
	(mL/g)	(%)	(mL/g)	(%)	(mL/g)	(%)	(mL/g)	(%)	(mL/g)	(%)
Crystalline silicotitanate with W–25 supernate	451	71.5	662	77.4	672	-77.5	672	77.7	958	83.8
Crystalline silicotitanate with W–29 supernate	616	76.0	847	82.0	1,188	85.0	1,078	86.5	1,247	86.2
SuperLig®-644 with W–29 supernate	125	39.4	385	67.3	549	73.8	1,098	84.6	1,300	88.0

Table 3-17. Strontium distribution coefficient (Sr K_d) and removal from Melton Valley supernate as a function of time (data from Collins et al., 1995)

Ion-Exchange Material and Test Waste	Sr K_d and Removal at 0.25 hr		Sr K_d and Removal at 2 hr		Sr K_d and Removal at 24 hr		Sr K_d and Removal at 144 hr	
	(mL/g)	(%)	(mL/g)	(%)	(mL/g)	(%)	(mL/g)	(%)
Crystalline silicotitanate with tank W–29 supernate	518	72.6	24,000	99.2	24,900	92.2	903	82.3

column effluent at less than one percent for longer periods of time than the other adsorbents. The best kinetic performance of crystalline silicotitanates was at about three column volumes per hour. Table 3-19 lists the number of column volumes until breakthrough occurs for several ion exchangers for the Melton Valley tank W–27 waste stream. The organic resins resorcinol-formaldehyde and SuperLig®-644 exhibited volume changes during certain stages of the operation (Lee et al., 1997). No problems were observed for the crystalline silicotitanate.

Table 3-18. Melton Valley tank W-27 waste supernatant composition (in mg/L) (data from Lee et al., 1997)

Constituent	pH 13.3 Sample	pH 14.02 Sample
Al	0.847	<0.146
As	0.0089	<0.250
Ba	8.04	5.61
Ca	89.1	3.1
Cd	0.22	<0.11
Cr	2.96	3.49
Cs	0.935	9.95
Cu	<0.0319	0.15
Hg	0.09	0.117
K	10,300	12,000
Na	113,000	127,000
Ni	1.22	0.73
Pb	0.0092	<10
Rb	1.1	2.06
Si	—	29.3
Sr	—	26.3
U	<1.0	0.485
Zn	0.473	<0.148
Br	288	<50.0
Cl	3,180	2,960
NO_2	—	2,720
NO_3	322,000	298,000
SO_4	1,540	1,380
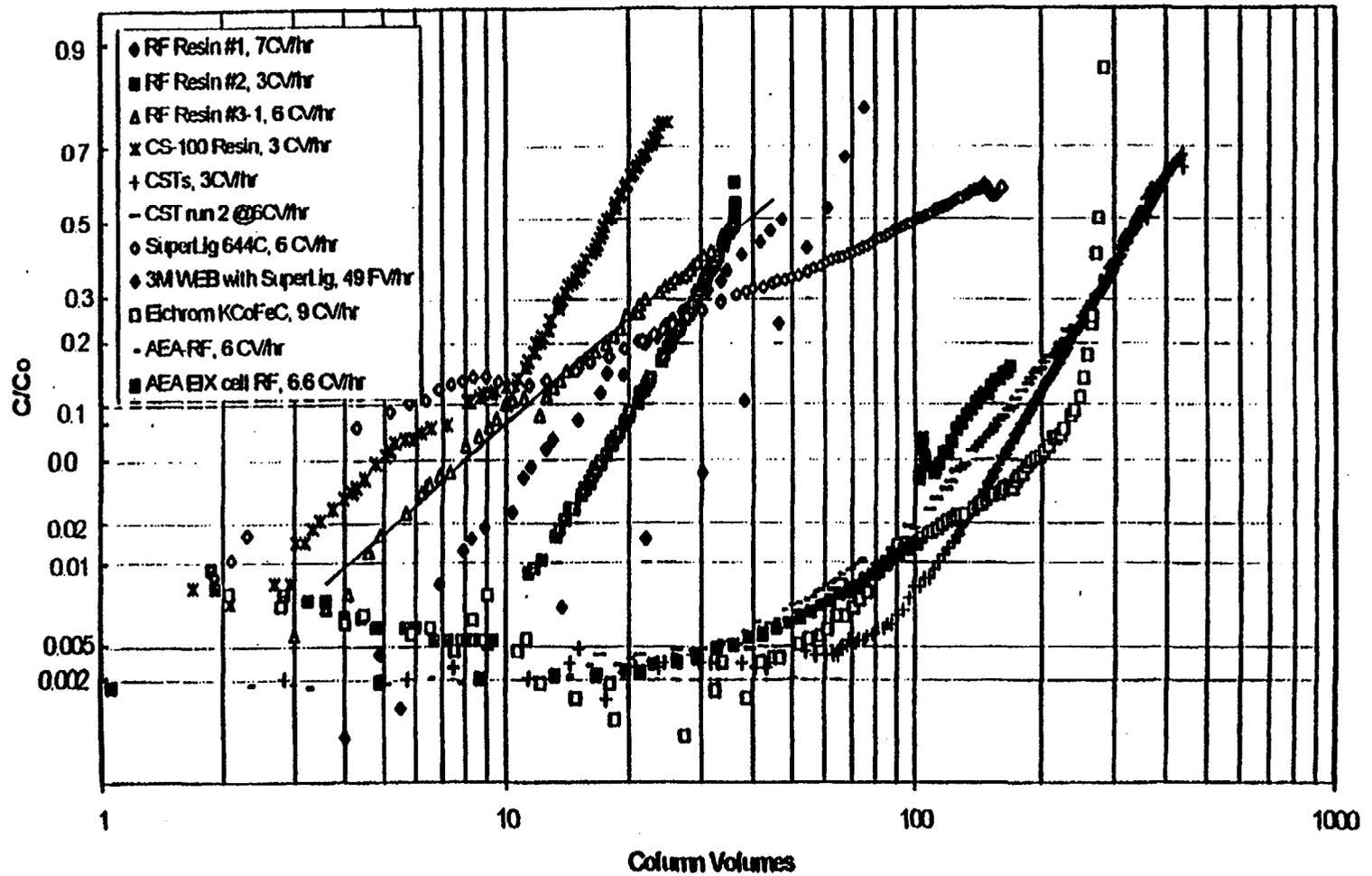
Figure 3-3. Comparison of cesium sorbents using a Melton Valley storage tank W–27 waste simulant (pH 13.3) (from Lee et al., 1997)
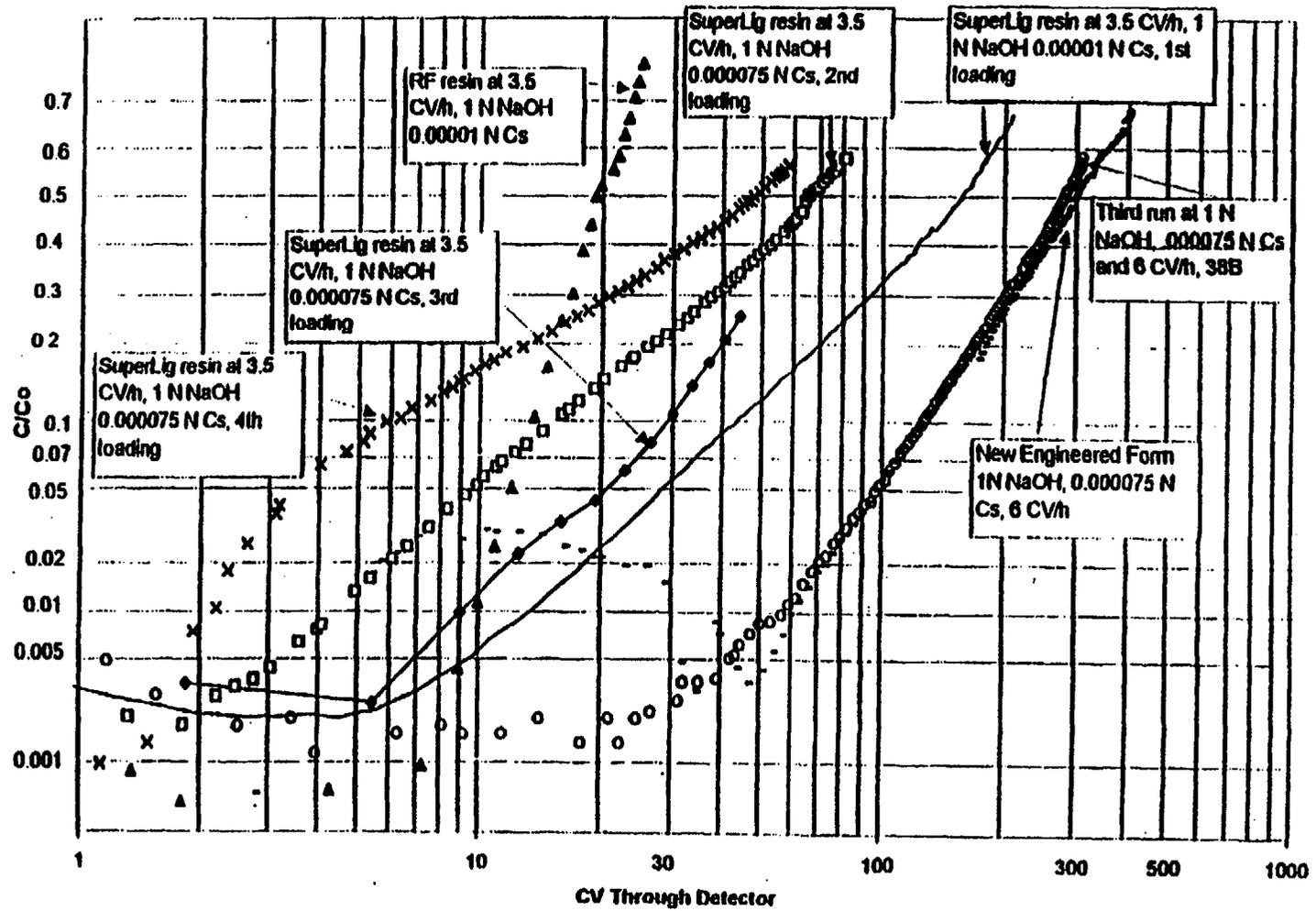
Figure 3-4. Comparison of cesium sorbents using a Melton Valley storage tank W–27 waste simulant (pH 14.0) (from Lee et al., 1997)

Batch studies using Melton Valley Storage tank W–25 supernate with a pH of 12.6, a sodium concentration of 3.9 M, and a nitrate concentration of 3.8 M, revealed loading capacities of 8 g of cesium/kg of resorcinol-formaldehyde, and 15 g of cesium/kg of crystalline silicotitanate (Jubin et al., 1998).

Resorcinol-Formaldehyde on Simulated Wastes

Experiments were conducted on four simulant wastes using the resorcinol-formaldehyde resin (Bibler, 1994). The composition of the Hanford tank AW–101 simulant used in the experiments is given in table 3-14. The compositions of the other simulants—Savannah River Site and Melton Valley tanks W–25 and W–29—are given in table 3-20. Breakthrough curves for these simulants are shown in figures 3-5 and 3-6. As can be seen from the graphs, the 50 percent breakthrough point for the Melton Valley tank W–25 simulant was approximately 205 column volumes, whereas it was only 30 column volumes for the tank W–29 simulant. This difference could be attributed to the much higher potassium concentration of the tank W–29 waste simulant compared to the tank W–25 simulant. These data show that competition from potassium ions could degrade the efficiency of the resin, leading to earlier breakthrough. The breakthrough curve for the Hanford tank AW–101 simulant (figure 3-6) was not as sharp as the other breakthrough curves. It is interesting to note that with this waste stream, characterized by highly alkaline conditions, the second resorcinol group became active and capacity of the resin doubled as the loading operation proceeded. This allowed loading of the first column up to 90 percent, at the point where the second column reached 50 percent loading. Thus, with four columns in series, the first column can be kept online until about 200 column volumes have passed through the system.

Crystalline Silicotitanate on Simulated Wastes

Column ion-exchange tests were performed by Braun et al. (1996) to simulate actual system performance and evaluate the effectiveness of crystalline silicotitanite (granular form) for removing cesium from tank wastes. Figure 3-7 shows experimental results for simulants of double-shell slurry feed waste and Melton Valley wastes, which had initial cesium concentrations of 10 ppm. The figure shows the relative concentration of cesium in the effluent versus the amount of waste processed expressed in terms of column volumes. The adsorbent capacity (equilibrium saturation) in these tests was estimated at the 50 percent point of the breakthrough curve. In figure 3-7, this point was reached at about 500 column volumes of double-shell slurry feed waste or Melton Valley wastes for the first column of the crystalline silicotitanate. A separate experiment using an improved crystalline silicotitanite material resulted in 660 column volumes processed to 50 percent breakthrough in double-shell slurry feed simulant. The high capacity and high selectivity for cesium shown by these results demonstrate that crystalline silicotitanate has a level of performance sufficient to allow use without regeneration or further concentration. Eliminating the regeneration or elution step would result in significant cost savings in the construction of a large-scale unit.

3.2.2.5 Important Operating Parameters

The important operating parameters for a given ion-exchange application include the concentration of the solute of interest, the concentration of competing ions, the pH, and the temperature of the feed solution.

Table 3-19. Capacities of selected ion-exchange materials for cesium removal from Melton Valley tank W–27 (data from Lee et al., 1997)

Ion-Exchange Material	Feed		Flow Rate $(CV/hr)^*$	Loading Cycles (each)	Breakthrough		
	Alkalinity (pH)	Cesium Concentration (mol/L)			1 % $(CV)^\dagger$	10% (CV)	50% (CV)
Resorcinol-formaldehyde	13.3	7.5×10^{-6}	3	1	12	20	35
Resorcinol-formaldehyde	13.3	7.5×10^{-6}	6	5	4	11	40
Resorcinol-formaldehyde	13.3	7.5×10^{-6}	7	1	7.5	17	48
Resorcinol-formaldehyde	14	1.0×10^{-5}	6	1	10	14	18
Resorcinol-formaldehyde	13.3	7.5×10^{-6}	6	1	65	140	—
SuperLig®-644	13.3	7.5×10^{-6}	3	1	20	65	—
SuperLig®-644	13.3	7.5×10^{-6}	6	1	1	10	100
SuperLig®-644	14	1×10^{-5}	3.5	4	15	46	166
		7.5×10^{-5}			4.5	16	70
		7.5×10^{-5}			15	31	70
		7.5×10^{-5}			2	6	50
SLIG-644 WWL	13.3	7.5×10^{-6}	49.8	1	18	38	60
Crystalline silicotitanate, granular	13.3	7.5×10^{-6}	3	1	114	192	350
Crystalline silicotitanate, granular	13.3	7.5×10^{-6}	6	1	82	174	342
Crystalline silicotitanate, granular	14	7.5×10^{-5}	6	1	55	123	273
Crystalline silicotitanate[‡]	14	7.5×10^{-5}	6	1	60	129	296
Crystalline silicotitanate[‡]	12.6	4.4×10^{-6}	6	1	100	226	505

*Column volumes (CV) per hour
†Column volumes
‡Engineered form (nonpowder)

Table 3-20. Savannah River Site and Melton Valley tanks W–25 and W–29 simulant compositions (in mol/L) (data from Bibler, 1994)

Constituent	Savannah River Site	Melton Valley Tank W–25	Melton Valley Tank W–29 Simulant
NaOH	2.9	0.24	0.06
$Al(NO_3)_3$	0.38	0.005	1.6×10^{-4}
$NaNO_3$	1.2	4.0	3.2
$NaNO_2$	0.71	0.1	—
Na_2CO_3	0.20	—	0.1
Na_2SO_4	0.17	—	0.052
KNO_3	0.012	0.25	0.43
$CsNO_3$	2.4×10^{-4}	8.7×10^{-6}	2.6×10^{-6}
KOH	—	—	—
$Zn(NO_3)_3$	—	—	—
$CaCO_3$	—	0.001	—
Cs-137	Trace	Trace	Trace
Total [Na^+]	5.6	4.3	3.6

Competing Ions

Resorcinol-formaldehyde resin and zeolite were tested using two Hanford simulant wastes: neutralized current acid waste and complexant concentrate. Both were highly alkaline simulants, and the neutralized current acid waste contained low concentrations of organic species. The composition of the neutralized current acid waste is given in table 3-8, and the complexant concentrate composition is given in table 3-21. The effect of sodium concentration on the cesium distribution coefficient is shown in table 3-22. As expected, an increase in initial sodium concentration decreased the cesium removal efficiency. The resorcinol-formaldehyde resin exhibited superior performance compared to the zeolite. No significant effect was observed on the adsorbent performance of cesium/rubidium molar ratios from
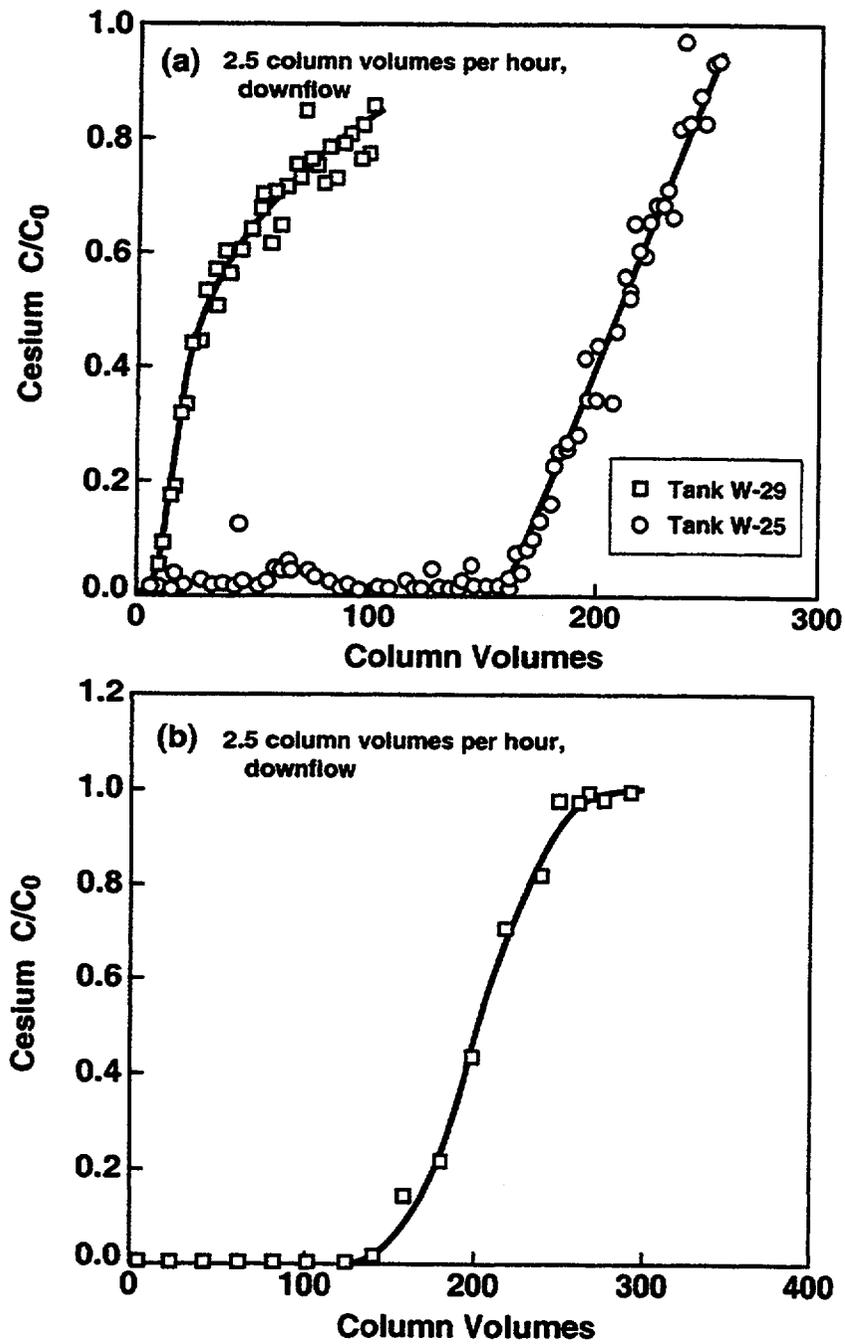
Figure 3-5. Breakthrough curves for (a) two Melton Valley storage tank wastes and (b) one Savannah River Site waste simulant (Bibler, 1994)
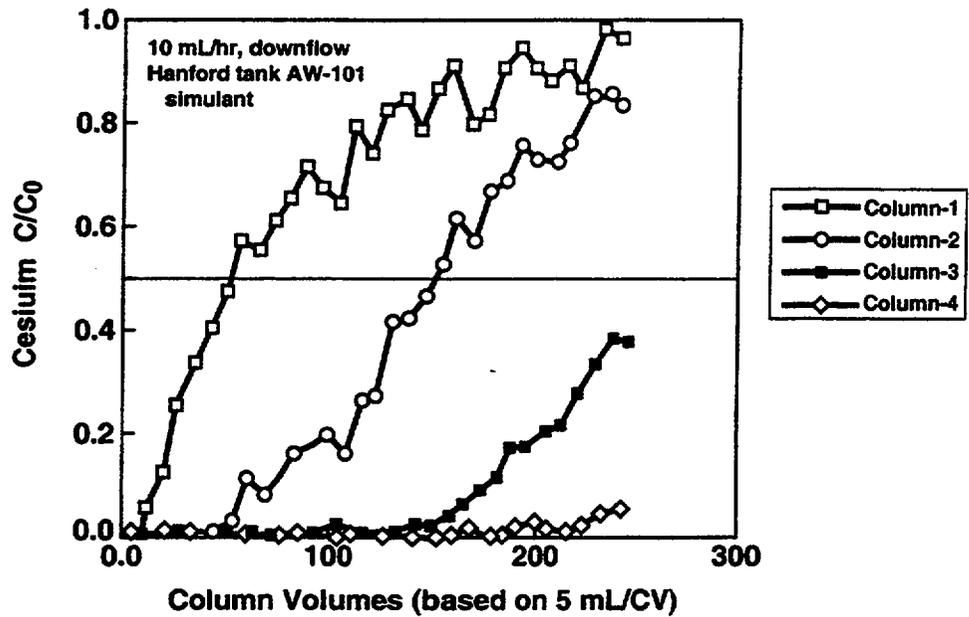
Figure 3-6. Breakthrough curves for a Hanford tank AW-101 simulant waste through four column in series (Bibler, 1994)
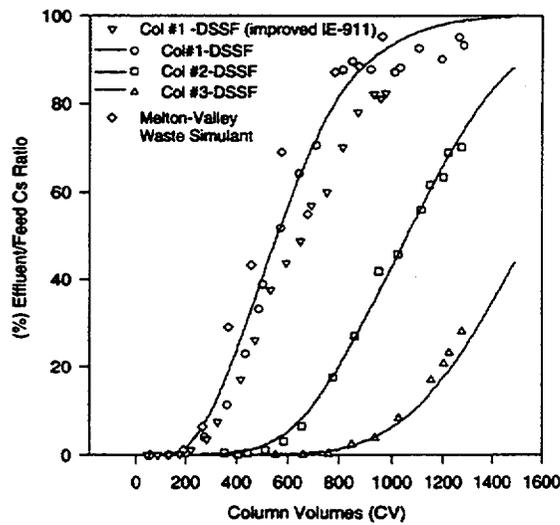
Figure 3-7. Column testing for the IE-911-38B crystalline silicotitanate resin in double-shell slurry feed and Melton Valley waste simulants (Braun et al., 1996)

95

Table 3-21. Complexant concentrate composition (data from Bray et al., 1996)*

Constituent	Concentration (mol/L)[†]
Al	0.5
Ca	0.02
Fe	0.06
K	0.05
La	0.001
Mg	0.01
Mn	0.02
Mo	0.005
Na	10.0
Ni	0.01
Si	0.005
Sr	0.0007
Zn	0.002
Zr	0.002
CO_3	0.64
F	0.15
Cl	0.10
NO_2	1.50
NO_3	4.62
PO_4	0.03
OH (free)	0.5
TOC	46[†]

*Target composition
[†]Total organic carbon (TOC) in units of grams per liter (g/L)

Table 3-22. Effect of sodium ion concentration on cesium volumetric distribution coefficient (λ) (data from Bray et al., 1996)[*]

Ion-Exchange Material	Waste Simulant	Sodium Ion Concentration (mol/L)	Cesium Volumetric Distribution Coefficient (λ) (mL/mL)
Resorcinol-Formaldehyde	Complexant Concentrate	3	369
		5	269
		7	176
	Neutralized Current Acid Waste	0.2	5,482
		1	1,265
		3	417
		5	249
Zeolite	Complexant Concentrate	3	164
		5	82
		7	47
	Neutralized Current Acid Waste	0.2	2,245
		1	448
		3	124
		5	62
[*]Sodium/cesium ratio = 1×10^4			

0.2 to 92 (Bray et al., 1996). On the other hand, potassium was shown to effectively compete with cesium for the ion-exchange sites, as shown by data in figure 3-5.

Resorcinol-formaldehyde resin data shown in table 3-23 demonstrate that as the initial concentration of the competing cation increased, the sorption of strontium and cesium decreased (Bostick et al., 1996).

pH

The feed pH controls the capacity of the adsorbents for specific solutes. For example, a cesium K_d equaled 2,400 mL/g for the crystalline silicotitanate ion exchanger and a Hanford simulant waste [double-shell slurry feed at pH = 14 and 25 °C (77 °F)]. The distribution coefficient, however,

Table 3-23. Effect of competing cations calcium (Ca), sodium (Na), potassium (K), and magnesium (Mg) on cesium (Cs) and strontium (Sr) distribution coefficients (K_d) for resorcinol-formaldehyde resin (data from Bostick et al., 1996)

Initial Cs concentration: 2.6×10^{-6} meq/L							
Init.[Ca]	meq/L	1.80	1.81	3.81	5.14	5.88	6.82
K_d(Cs)	mL/g	11,400	10,700	5,500	4,900	4,300	3,900
Init.[Na]	meq/L	0.57	1.64	2.96	4.21	—	—
K_d(Cs)	mL/g	12,000	11,100	10,100	9,600	—	—
Init.[K]	meq/L	0.014	0.242	0.472	0.718	0.963	—
K_d(Cs)	mL/g	12,300	11,400	11,100	10,700	9,990	—
Init.[Mg]	meq/L	0.467	1.58	3.22	6.45	9.69	—
K_d(Cs)	mL/g	11,900	8,150	5,290	4,340	3,820	—
Initial Sr concentration: 0.00228 meq/L							
Init.[Ca]	meq/L	1.83	1.84	3.83	5.18	5.90	6.88
K_d(Sr)	mL/g	438,000	326,000	3,900	2,140	1,690	1,070
Init.[Na]	meq/L	0.626	1.72	2.98	4.26	5.94	—
K_d(Sr)	mL/g	553,000	379,000	281,000	222,000	151,000	—
Init.[K]	meq/L	0.0092	0.238	0.486	0.993	—	—
K_d(Sr)	mL/g	466,000	409,000	320,000	292,000	—	—
Init.[Mg]	meq/L	0.500	1.61	3.23	6.48	9.72	—
K_d(Sr)	mL/g	352,000	99,100	6,080	2,230	1,080	—

exceeded 20,000 mL/g after the feed pH was adjusted to 10.8 with carbon dioxide (Dosch et al., 1996).Thus, partial neutralization of the waste could enhance the removal efficiency up to one order of magnitude.

In another study of a crystalline silicotitanate ion exchanger, cesium distribution coefficients for double-shell slurry feed simulants with different pHs were reported by Bray et al. (1993). The distribution coefficient values are listed in table 3-24. Note that the cesium distribution coefficient for a solution with a pH of 10 is 25 times higher compared to a solution with a pH of 14.

Table 3-24. Effect of pH on cesium distribution coefficient (Cs K_d)* (data from Bray et al., 1993)

Ion-Exchange Material	pH	Cs K_d
Crystalline silicotitanate	14.1	290
	13.1	490
	12.8	890
	10.9	4,800
	10.2	8,000
*From double-shell slurry feed simulant		

Two other crystalline silicotitanate adsorbents were tested at various pH values by Bray et al. (1993). These tests used double-shell slurry feed simulants with a sodium ion concentration of 5 M and initial cesium or strontium concentrations of 10^{-4} M. The contact time for these experiments was 72 hr, and results are shown in table 3-25. The data show that as the pH was increased from 0 to 13, the strontium distribution coefficient increased from less than 10 to about 5,000. The cesium distribution coefficient varied from greater than 1,300 to about 78,000, with a maximum distribution coefficient at a pH of about five.

Temperature

The effect of temperature on resorcinol-formaldehyde resin and zeolite were tested using two Hanford simulant wastes: neutralized current acid waste and complexant concentrate, with compositions shown in tables 3-8 and 3-21, respectively. The results are shown in table 3-26 for the two simulants at various sodium concentrations. The data show that the effect of temperature was prominent for the zeolite. As the temperature increased, the volumetric distribution coefficient (λ) decreased. The effect of temperature on the resorcinol-formaldehyde resin was not as pronounced as on the zeolite.

Bray et al. (1993) reported cesium and strontium distribution coefficients for three ion exchangers—a zeolite, a titanium-coated zeolite, and a crystalline silicotitanate—measured at 10 and 40 °C (50 and 104 °F) in experiments using a synthetic double-shell slurry feed. The results listed in table 3-27 show that the cesium distribution coefficient for the three ion exchangers doubled as the temperature decreased from 40–10 °C (104–50 °F). On the other hand, no substantive improvement in the strontium distribution coefficient was observed at the lower temperature. In fact, the strontium distribution coefficient for the zeolite decreased by a factor of 40 when the temperature decreased from 40–10 °C (104–50 °F).

3.2.2.6 Regeneration/Reversibility

Organic Resins

The regeneration of the resorcinol-formaldehyde resin after an adsorption-elution cycle with a simulant waste containing cesium was investigated (Brunson et al., 1994). After stripping cesium from the resin

Table 3-25. Variation of strontium and cesium distribution coefficients (Sr K_d* and Cs K_d) with pH for crystalline silicotitanate (data from Bray et al., 1993)

Strontium Concentration Initially 10^{-4} Molar											
pH	0	0.6	4.6	7	7.7	8.1	8.9	9.1	9.7	11.9	12.8	13.0
Sr K_d (mL/g)	6.9	8.0	31	88	160	240	320	420	520	2,200	4,900	5,300

Cesium Concentration Initially 10^{-4} Molar											
pH	0.3	1.4	4.9	7.6	8.5	9.4	10.2	12.9	—	—	—	—
Cs K_d (mL/g)	10,000	31,000	78,000	53,000	23,000	6,800	2,900	1,300	—	—	—	—

*Double-shell slurry feed simulant solutions with sodium ion concentration of 5 M. Temperature = 25 °C; contact time = 72 hr

Table 3-26. Temperature effects on the strontium volumetric distribution coefficient (λ) (data from Bray et al., 1996)

Waste Simulant	Sodium Concentration (mol/L)	Temperature (°C)	λ for Resorcinol-Formaldehyde (mL/mL)	λ for Zeolite (mL/mL)
Neutralized Current Acid Waste	0.2	10	5,311	2,189
		25	3,617	1,950
		40	3,870	1,334
	3	10	380	121
		25	302	81
		40	285	54
Complexant Concentrate	3	10	352	164
		25	282	96
		40	342	62
	5	10	258	81
		25	205	44
		40	225	27
	7	10	174	47
		25	145	28
		40	148	20

Table 3-27. Cesium and strontium distribution coefficients* (Cs K_d and Sr K_d) at 10 and 40 °C (data from Bray et al., 1993)

Material	Cs K_d (mL/g)		Sr K_d (mL/g)	
	10 °C	40 °C	10 °C	40 °C
Zeolite	132	60	73	3,100
Zeolite, Ti-coated	109	47	2,753	2,571
Crystalline silicotitanate	295	147	$>10^5$	$>10^5$
*Double-shell slurry feed simulant				

with hydrochloric acid, the resin was converted to the hydrogen form. The resin was subsequently washed with 4 column volumes of water to remove any remnants of the stripping solution, and then 12 column volumes of 2-M sodium hydroxide solution were passed through the bed to regenerate the column. Nine of the 12 column volumes were passed in an upflow direction, and the last three column volumes were passed in a downflow direction. The caustic solution was left in the resin for 18 hr to ensure full conversion of the resin to the sodium form. The regeneration step returned the organic resin to its original volume.

Elution studies were also performed by Brunson et al. (1994) using a 2-M hydrochloric acid solution. The majority of cesium was eluted in three column volumes, and the stripping operation was completed in 16 column volumes. The highest cesium concentration during elution was observed after 1.5–2 column volumes of the strip solution passed through the resin. The resin was found stable after many regeneration cycles.

One-half molar nitric acid was used to elute cesium from the resorcinol-formaldehyde resin in experiments using simulants of Hanford tank AW–101 and Melton Valley tank W–25 wastes. The elution was performed with an upflow rate of 2.5 column volumes per hr. The results for the Melton Valley tank W–25 simulant are shown in table 3-28. The data indicate that elution was complete at 10 column volumes. The results of experiments on elution of cesium, potassium, and sodium loaded from a Hanford tank AW–101 simulant are shown in figures 3-8 to 3-10. As the figures show, all the alkali metals were completely eluted from the resin at about the same number of column volumes.

Elution experiments were performed to compare the performance of the resorcinol-formaldehyde and SuperLig®-644 resins (Brown et al., 1995). A 0.5-M nitric acid solution was used to elute cesium previously loaded from a Hanford neutralized current acid waste simulant. Each resin required approximately 1.2 column volumes to neutralize and displace the column void volume. Cesium concentration increased 2–3 orders of magnitude and then decreased exponentially below the detection limit. Experimental results, along with physical properties of the resins, are shown in table 3-29. The data indicate that the SuperLig®-644 resin exhibits higher cesium loading per unit mass (0.20 mmole/g) and required less eluant volume (3.5 column volumes) than the resorcinol-formaldehyde resin.

Table 3-28. Cesium elution from resorcinol-formaldehyde with 0.5 M nitric acid (data from Bibler, 1994)*

Eluent volume	CV	2.5	5	7.5	10
Eluted Cs	μCi	0	0.023	0.0008	0

*Loaded from Melton Valley tank W–25 simulant; eluted at 2.5 column volumes (CVs) per hour

In the study by Lee et al. (1997), the performance of SuperLig®-644 resins in adsorbing cesium from Melton Valley tank W–27 waste simulant was shown to degrade with the number of loadings. The Lee et al. (1997) data, plotted in figure 3-4, show that the resin performance deteriorated from the first to the second loading and from the third to the fourth loading, as indicated by the earlier breakthrough of cesium. For example, the 0.1 breakthrough point dropped from 43 column volumes during the first loading to 15 during the second loading and from 30 column volumes during the third loading to 6 during the fourth loading. An increase in the resin performance from the second to the third loading was observed, which was described by Lee et al. (1997) to further conditioning[1] of the resin.

The regeneration of organic resins results in large quantities of acidic waste that must be concentrated and then processed as low-activity waste. After the degradation of the resin from radiation and chemical reactions, it must be disposed.

Inorganic Ion-Exchange Material

The crystalline silicotitanate ion exchangers are not designed for regeneration (Braun et al., 1996). Cesium, for example, could not be eluted from crystalline silicotitanate with several eluants, such as 3-M nitric acid, 3-M formic acid, 8-M ammonium nitrate, or 2-M calcium nitrate. Also, no elution of cesium was observed from crystalline silicotitanates in either highly caustic solutions or solutions exposed to large amounts of radiation (Klavetter et al., 1994). However, crystalline silicotitanates have compositions suitable for high-level waste vitrification.

3.2.3 Stability

In using ion exchange to pretreat actual wastes, other factors such as the chemical, thermal, and radiation stability of the adsorbent should be addressed in addition to sorption and desorption behaviors.

3.2.3.1 Chemical

The study by Brown et al. (1996c) indicated the SuperLig®-644 resin that was nonirradiated but exposed to the neutralized current acid waste simulant exhibited a much lower value of cesium distribution coefficient ($K_d \sim 80$ mL/g at a sodium to cesium molar ratio of 50,000) compared to the SuperLig®-644

---

[1]The exchange capacity and density of a resin are invariably affected by the first service cycles. In actual operations, a fresh resin is typically subjected to several exchange cycles to stabilize its characteristics, [i.e., size, distribution, capacity, and density (Dorfner, 1991b)].
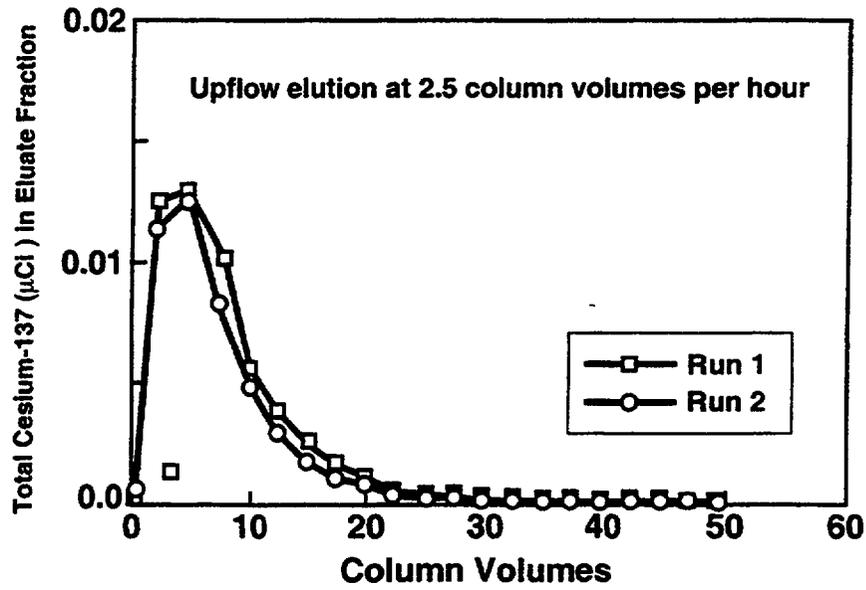
Figure 3-8. Cesium elution from the resorcinol-formaldehyde resin with 0.5 M nitric acid (Bibler, 1994)
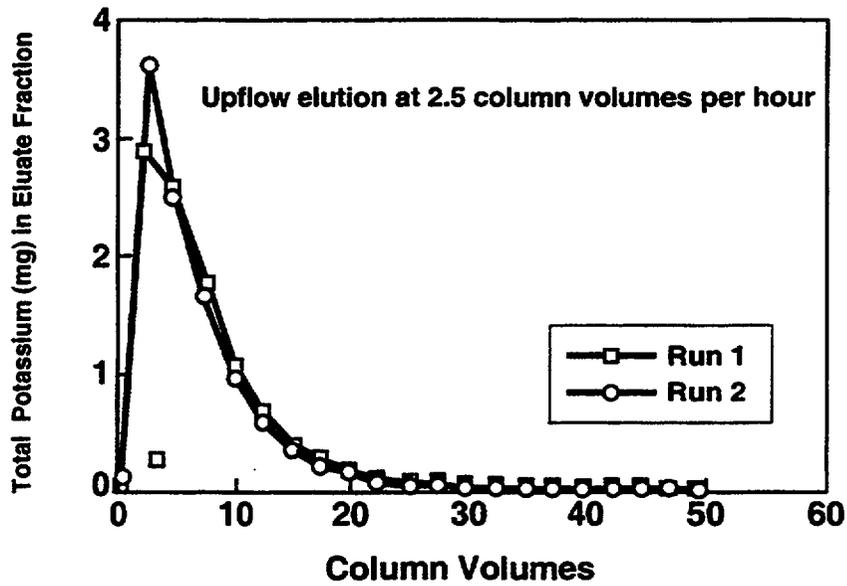
Figure 3-9. Elution curves for potassium from the resorcinol-formaldehyde resin with 0.5 M nitric acid (Bibler, 1994)
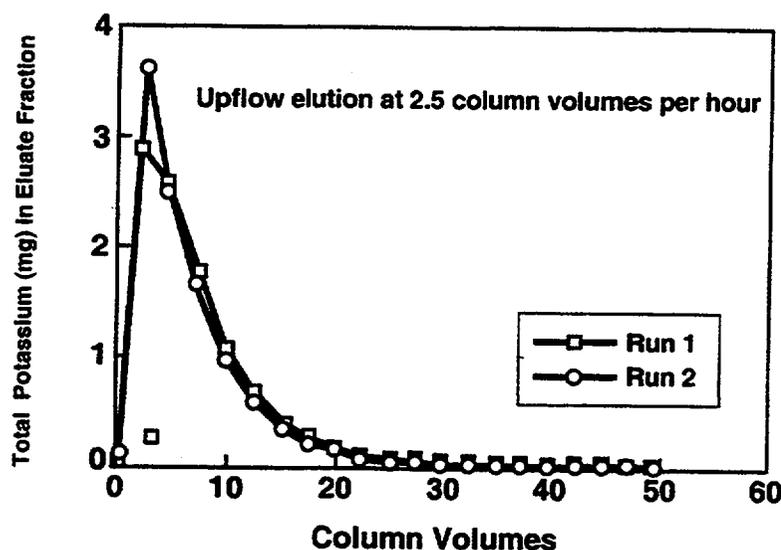
Figure 3-10. Elution curves for sodium from the resorcinol-formaldehyde resin with 0.5 M nitric acid (Bibler, 1994)

resin that was nonirradiated and exposed to pure water or 0.5-M nitric acid solution (~300 mL/g at a sodium to cesium molar ratio of 50,000). This lower distribution coefficient was attributed to the reduced chemical stability of the SuperLig®-644 material in caustic solutions.

A problem with the resorcinol-formaldehyde resin is that oxidation of the resin can occur, resulting in quinone, ketone, and ether groups on the primary ring of the resin along with a simultaneous decrease in the phenolic and hydroxyl exchange groups (Hubler et al., 1996). A particle size of 297–840 μm (20–50 mesh) should be used because for smaller, 297-μm (50-mesh) particles, the surface area is more easily oxidized, and for larger, 840-μm (20-mesh) particles, the exchange process is limited by intragranular diffusion.

The powdered crystalline silicotitanate ion-exchange material shows no deterioration in performance in the pH range of 0–14 (Braun et al., 1996). The same holds for the granular crystalline silicotitanate, which contains an inert binder highly resistant to chemical attack. Both granular and powdered crystalline silicotitanate material have rigid inorganic structures that resist significant shrinkage or swelling. Such variations in structure can cause uneven flow distribution and bed plugging. Table 3-30 gives the distribution factors for cesium on crystalline silicotitanate from a highly alkaline double-shell slurry feed simulant [pH > 14, 40 °C (104 °F)] as a function of time. The data show no noticeable deterioration in the performance of the crystalline silicotitanate ion exchanger. Other results of chemical stability tests on a crystalline silicotitanate ion-exchange material are listed in table 3-31 (Klavetter et al., 1994).

Table 3-29. Cesium elution characteristics* using 0.5 M nitric acid (data from Brown et al., 1995)

Resin Properties	Units	Resorcinol-Formaldehyde	SuperLig®-644
Resin F Factor	dry mass/wet mass	0.8419	1.000
Resin Mass in Column	g	91.20	47.12
Resin Mass in Column	g, dry	76.78	47.12
Initial Column Volume	mL	210	210
Resin Particle Size	mesh	45–70	20–45
Average Resin Particle Size	mesh	60	35
Resin Density	g/mL	0.37	0.22
Cs Loading	mmole/g	0.18	0.20
Cs Loading	mmole/mL	0.070	0.045
Loading Volume to 0.5 C/C_o	—	139	93.6
Elution Volume to 0.1 C/C_o	—	7.0	3.5
Peak Cs Concentration C/C_o	—	38.5	185
Volume Compression at 0.1 C/C_o	—	20	27
Elution Composite	Na/Cs	20.6	10.5

*Resins loaded from neutralized current acid waste simulant

Table 3-30. Chemical stability of crystalline silicotitanates in a warm, highly alkaline solution* as measured by changes in the cesium distribution coefficient (Cs K_d) with time (data from Bray et al., 1993)

Time (days)	1	5	15	21	42	84
Cs K_d (mL/g)	152	164	143	159	155	146

*Double-shell slurry feed simulant; T = 40 °C; pH = 14

Table 3-31. Chemical stability of crystalline silicotitanates in a warm, alkaline solution* measured by changes in the cesium distribution coefficient (Cs K_d) with time (data from Klavetter et al., 1994)

Time (days)	1	23	69	80
Cs K_d (mL/g)	742	734	709	710

*Double-shell slurry feed simulant; T = 25 °C; 1.3 molar free OH⁻

Ion Exchange

3.2.3.2 Thermal

The crystalline silicotitanate ion exchangers should be maintained under 60 °C (140 °F) when exposed to concentrated acid or caustic solutions (>6 molar) (Braun et al., 1996). In acid or caustic conditions, some leaching of titanium occurs at elevated (>60 °C) temperature. At ambient temperatures, the crystalline silicotitanates show no loss in structural integrity or performance in concentrated acid/base solutions.

For resorcinol-formaldehyde resin, curing temperatures above 135 °C (275 °F) decompose the resin (Hubler et al., 1996).

3.2.3.3 Radiation

One of the key parameters in the assessment of ion-exchange materials is its useful lifetime in the radioactive environment encountered during waste processing. Ionizing radiation of 10^4 Gray (10^6 rad) or more are known to change both the mechanical and chemical properties of ion exchangers, particularly the organic resins (Pillay, 1982). The degree to which these changes affect the process applications of ion exchangers is dependent on several factors: the chemical nature of the exchanger; the radiation dose rate; the nature of adsorbed ions within the exchanger; and the environment of the exchanger, such as temperature, solution pH, and solution composition. For organic resins, the consequences of radiation can manifest in agglomeration of the resin, gas evolution, pH changes, desorption of adsorbed ions, partial dissolution of the decomposition products in water, phase separation between liquids and solids, corrosion of the containers, and eventual migration of the radionuclides from the resin matrix to the environment (Pillay, 1982).

Various studies have been conducted by the DOE on the effects of ionizing radiation on ion-exchange materials. Results of those studies relevant to pretreatment of Hanford tank wastes are summarized in the following sections.

Organic Resins

Superligands

For SuperLig®-644 resin, gamma irradiation of the material in either pure water or 0.5-M nitric acid solution up to 10 million Gray (10^9 rad) essentially has no effect on resin performance as measured by cesium uptake (Brown et al., 1996c). Table 3-32 shows the results for different experimental conditions. The data in the table show that irradiation in water did not appreciably affect the performance of the SuperLig®-644 resin, except at the highest dose of 20 million Gray (2×10^9 rad), which reduced performance by about 20 percent. Irradiation in a dilute acid solution caused the performance to deteriorate by about 20 percent at 10 million Gray (10^9 rad). A decrease in performance starts at a dose of 1 million Gray (10^8 rad) for the air irradiation case and is substantially lower at 20 million Gray (2×10^9 rad). The results for air irradiation imply a chemical instability of the resin in air, in contrast to the water case where free oxygen was not present and a free radical transfer to a water molecule might have occurred. The results in neutralized current acid waste have similar trends to those in ambient air. Evidently, resin performance is severely reduced at high irradiation levels. It should be noted that an

Table 3-32. Radiolytic stability of SuperLig®-644* as determined by changes in cesium adsorption (data from Brown et al., 1996c)

Irradiation Environment	Dose	Measure				
Distilled Water	Unirradiated	Na/Cs (final)	580	8,400	140,000	2,200,000
		K_d (mL/g)	23	103	280	520
	10^6 Rad	Na/Cs (final)	570	8,400	130,000	2,100,000
		K_d (mL/g)	25	107	268	514
	10^7 Rad	Na/Cs (final)	572	8,300	154,000	2,100,000
		K_d (mL/g)	23	100	302	478
	10^8 Rad	Na/Cs (final)	609	8,800	144,000	2,100,000
		K_d (mL/g)	33	118	287	478
	10^9 Rad	Na/Cs (final)	586	8,300	132,000	1,800,000
		K_d (mL/g)	27	104	250	450
	2×10^9 Rad	Na/Cs (final)	561	7,400	117,000	1,650,000
		K_d (mL/g)	20	75	221	367
0.5 M HNO_3	Unirradiated	Na/Cs (final)	595	8,400	142,000	1,970,000
		K_d (mL/g)	28	113	269	438
	10^6 Rad	Na/Cs (final)	588	8,900	149,000	2,100,000
		K_d (mL/g)	26	116	313	458
	10^7 Rad	Na/Cs (final)	585	8,400	126,000	2,200,000
		K_d (mL/g)	25	111	242	484
	10^8 Rad	Na/Cs (final)	585	8,400	149,000	2,170,000
		K_d (mL/g)	25	108	297	476
	10^9 Rad	Na/Cs (final)	552	7,600	122,000	1,830,000
		K_d (mL/g)	16	78	236	404
	2×10^9 Rad	Na/Cs (final)	552	7,100	114,000	1,740,000
		K_d (mL/g)	15	67	215	357

Table 3-32. Radiolytic stability of SuperLig®-644* as determined by changes in cesium adsorption (data from Brown et al., 1996c) (cont'd)

Irradiation Environment	Dose	Measure				
Air	Unirradiated	Na/Cs (final)	575	9,100	154,000	2,100,000
		K_d (mL/g)	23	122	354	478
	10^6 Rad	Na/Cs (final)	581	9,100	160,000	2,110,000
		K_d (mL/g)	26	129	344	542
	10^7 Rad	Na/Cs (final)	574	8,400	136,000	2,170,000
		K_d (mL/g)	25	105	290	520
	10^8 Rad	Na/Cs (final)	548	7,250	123,000	1,780,000
		K_d (mL/g)	17	72	233	402
	10^9 Rad	Na/Cs (final)	515	6,100	78,700	1,240,000
		K_d (mL/g)	8	34	101	231
	2×10^9 Rad	Na/Cs (final)	506	5,130	58,000	670,000
		K_d (mL/g)	4	8	22	47
Neutralized Current Acid Waste	Unirradiated	Na/Cs (final)	526	5,480	70,000	1,020,000
		K_d (mL/g)	7	19	70	158
	10^6 Rad	Na/Cs (final)	520	5,600	67,000	1,010,000
		K_d (mL/g)	6	22	61	152
	10^7 Rad	Na/Cs (final)	517	5,500	71,000	980,000
		K_d (mL/g)	6	18	74	153
	10^8 Rad	Na/Cs (final)	512	5,400	63,900	876,000
		K_d (mL/g)	4	15	51	116
	10^9 Rad	Na/Cs (final)	503	5,060	52,000	570,000
		K_d (mL/g)	3	5	11	27
	2×10^9 Rad	Na/Cs (final)	505	4,900	48,000	490,000
		K_d (mL/g)	1	1	1	1

*Manufactured with a proprietary web-like matrix called WWL (3M, St. Paul, Minnesota)

irradiation level of 20 million Gray (2×10^9 rad) is high and is not representative of typical process conditions. Table 3-33 presents the cesium distribution factors for the SuperLig®-644 (at a constant sodium/cesium molar ratio of 10^5) irradiated in a neutralized current acid waste simulant (Brown et al., 1996c). The maximum dose of 20 million Gray (2×10^9 rad) required about 8 wk of exposure at a rate of 16,000 Gray/hr (1.6×10^6 rad/hr). As the table shows, the resin was stable for all conditions at radiation doses up to 1 million Gray (10^8 rad). Above this limit, major degradation of the resin occurred in ambient air, but even more so in neutralized current acid waste. From the data given in the table and by comparing the ambient air and the neutralized current acid waste cases, one can conclude that the difference is due to the chemical degradation of the resin in the highly caustic solution. To minimize this chemical degradation and to avoid organic-nitrate oxidation reactions that could damage the ion-exchange systems, the resin should be converted after elution to the sodium form with sodium hydroxide. For a loading cycle of 50 hr, a 6 column volumes/hr flowrate, ten loading cycles before resin disposal, and assuming a radiation dose rate of 2,700 Gray/hr (2.7×10^5 rad/hr), one-to-two months of continuous operation is possible before reaching a radiation dose high enough to significantly degrade the SuperLig®-644 performance.

Resorcinol-Formaldehyde Resin

Resorcinol-formaldehyde resin is highly selective for cesium in highly alkaline solutions. In studies by Crawford et al. (1993) and Bibler and Crawford (1994), the resin was irradiated for different time periods in either pure deionized water or in Hanford tank AW–101 waste simulant. The composition of the tank AW–101 simulant is given in table 3-14. The irradiation dose rates ranged from 7,000–26,000 Gray/hr (0.7×10^6–2.6×10^6 rad/hr), and the temperatures during irradiation reached 40 °C (104 °F) due to gamma radiation heating. To determine the possible effects of reactions, such as hydrolysis, occurring in the absence of radiation, slurries identical to those being irradiated were stored in the tank AW–101 simulant or in pure water for time periods identical to the irradiation times. After the resin was irradiated or stored in the tank AW–101 simulant or pure water, K_d values were determined for the irradiated and unirradiated resins. Two different test solutions were used to determine distribution coefficients. One test solution was a 1.5-M sodium hydroxide solution containing 4.5-M sodium nitrate, along with trace quantities of nonradioactive and radioactive cesium. The other was a caustic simulated high-level waste supernate containing a total sodium ion concentration of 5.6 M, a nonradioactive cesium concentration of 2.5×10^{-4} M, and a trace amount of cesium-137. The composition of this simulated supernate is given in table 3-14. The resulting distribution coefficients are given in table 3-34 for the sodium/potassium form of the resin and in table 3-35 for the potassium form of the resin. The data in the tables indicate that radiation doses up to 1 million Gray (10^8 rad) did not greatly affect the performance of the resin, at least for the duration of the experiments (up to 45 hr). Also, the resin appeared more resistant to radiation in pure water than in the tank AW–101 simulant.

Another measure of the resistance of the resin to radiolytic or hydrolytic degradation is the amount of carbon that can be leached from the resin after it is irradiated or stored. Table 3-36 shows the concentrations of organic and inorganic (carbonate and bicarbonate) carbon leached from the resorcinol-formaldehyde resin irradiated or stored in Hanford tank AW–101 simulant. The data indicate that a large amount of organic and inorganic carbon was leached from the irradiated resin, with the concentration of leached carbon increasing with time. In the absence of radiation, the resin degraded slightly with storage; the concentration of leached carbon remained relatively constant with time. Radiolysis does not affect

Ion Exchange

Table 3-33. SuperLig®-644* cesium distribution coefficients for various doses and environments of irradiation[†] (data from Brown et al., 1996c)

Irradiation Environment		Measured					
Distilled Water	Dose (rad)	10^5	10^6	10^7	10^8	10^9	2×10^9
	K_d (mL/g)	279	258	300	387	261	224
0.5 M nitric acid	Dose (rad)	10^5	10^6	10^7	10^8	10^9	2×10^9
	K_d (mL/g)	263	314	299	234	238	217
Air	Dose (rad)	10^5	10^6	10^7	10^8	10^9	2×10^9
	K_d (mL/g)	308	298	250	207	105	29
5 M Neutralized Current Acid Waste	Dose (rad)	10^5	10^6	10^7	10^8	10^9	2×10^9
	K_d (mL/g)	79.0	81.5	70.3	60.3	14.1	0.804

*Manufactured with a proprietary web-like matrix called WWL (2M, St. Paul, Minnesota
[†]Sodium/cesium ratio = 1×10^5

Table 3-34. Cesium distribution coefficient (Cs K_d) for resorcinol-formaldehyde resin* as a function of irradiation and storage time[†] (data from Bibler and Crawford, 1994)

Irradiation or Storage Time (hr)		0.5	1	20	52	96	120	258	451
Dose (rad)		5×10^5	1×10^6	2×10^7	5.3×10^7	1.2×10^8	2.5×10^8	6.7×10^8	1.2×10^9
AW-101 Simulant/ 1.5 M NaOH + 4.5 M NaNO₃	K_d (mL/g) Irradiated	1,400	2,500	3,000	2,600	1,700	470	150	80
	K_d (mL/g) Unirradiated	1,500	3,500	1,800	2,900	2,900	1,500	670	670
AW-101 Simulant/ Simulated Supernate	K_d (mL/g) Irradiated	360	530	770	670	190	63	21	12
	K_d (mL/g) Unirradiated	490	810	570	>1000	>1,000	290	150	78
Pure Water/ 1.5 M NaOH + 4.5 M NaNO₃	K_d (mL/g) Irradiated	1,200	1,200	1,700	2,000	2,700	920	750	880
	K_d (mL/g) Unirradiated	1,500	1,200	2,500	1,100	2,100	1,000	900	970
Pure Water/ Simulated Supernate	K_d (mL/g) Irradiated	140	130	150	210	>1,000	54	97	83
	K_d (mL/g) Unirradiated	110	140	300	110	380	160	110	84

*Sodium/potassium form
[†]The resin was irradiated or stored in an tank AW-101 simulant or in pure water. The distribution coefficients were determined using a 1.5 M NaOH+4.5 M NaNO₃ solution or a simulated high-level waste supernate.

Table 3-35. Cesium distribution coefficient for resorcinol-formaldehyde resin[*] as a function of irradiation and storage time[†] (data from Crawford et al., 1993)

Irradiation or Storage Time (hr)		22	94
Dose (rad)		5.4×10^7	2.3×10^8
AW–101 Simulant/1.5 M NaOH + 4.5 M NaNO$_3$	K_d (mL/g) Irradiated·	1,400	1,300
	K_d (mL/g) Unirradiated	2,000	2,400
AW–101 Simulant/Simulated Supernate	K_d (mL/g) Irradiated	> 1,000	250
	K_d (mL/g) Unirradiated	450	440
Pure Water/1.5 M NaOH + 4.5 M NaNO$_3$	K_d (mL/g) Irradiated	680	1,700
	K_d (mL/g) Unirradiated	1,400	1,400
Pure Water/Simulated Supernate	K_d (mL/g) Irradiated	140	220
	K_d (mL/g) Unirradiated	150	340

[*]Potassium form
[†]The resin was irradiated or stored in a tank AW–101 simulant or in pure water. The distribution coefficients were determined using a 1.5 M NaOH+4.5 M NaNO$_3$ solution or a simulated high-level waste supernate.

Table 3-36. Carbon leached from resorcinol-formaldehyde[*] that was irradiated or stored in waste simulant[†] (data from Bibler and Crawford, 1994)

Irradiation or Storage Time (hr)	Dose (rad)	Organic Carbon (ppm)		Inorganic Carbon (ppm)	
		Irradiated Resin	Unirradiated Resin	Irradiated Resin	Unirradiated Resin
96	2.5×10^8	329	254	629	739
258	6.7×10^8	621	224	819	535
451	1.2×10^9	1,029	322	1,315	526

[*]Sodium/potassium form
[†]AW–101 waste simulant

111

resin water retention properties or thermal stability (Crawford et al., 1993; Bibler and Crawford, 1994). On the other hand, radiolysis of the potassium form of the resin increases its swelling capacity.

Inorganic Ion-Exchange Material

The radiation stability of crystalline silicotitanate was studied by Klavetter et al. (1994) by exposing samples of the ion exchanger to radiation doses of 10^5, 10^6, and 10^7 Gray (10^7, 10^8, and 10^9 rad) corresponding to 7.0, 70.2, and 698 hr of exposure from a Co–60 source. The test materials included dry powders, powders in Hanford tank AW–101 simulant solution, cesium-loaded crystalline silicotitanate in AW–101 simulant solution, cesium- and strontium-loaded crystalline silicotitanate in AW–101 simulant solution, and cesium-loaded crystalline silicotitanate in 2-M nitric acid solution. Stability was determined by examining the cesium or strontium distribution coefficients and the x-ray diffraction patterns of the materials before and after exposure to the radiation fields. The results show the distribution coefficients before and after radiation exposure were the same within experimental uncertainties. Specifically, the distribution coefficients of the crystalline silicotitanate dry powders, the powders in the AW–101 simulant, and the cesium-loaded crystalline silicotitanate generally showed less than 5 percent variation in the distribution coefficients before and after radiation exposure. No effect on performance was noted, even after exposure to 10^7 Gray (10^9 rad) (Klavetter et al., 1994).

3.3 Application to Hanford High-Level Waste Pretreatment

The use of ion exchange for the pretreatment of Hanford tank wastes requires the adsorbents to satisfy several requirements. These requirements include high selectivity and capacity for cesium-137 and technetium-99 from solutions that are highly alkaline and have high concentrations of the sodium ion. Removal efficiency of cesium and other radionuclides should be high enough to produce a final immobilized low-activity waste form that meets the NRC Class C limits. The ion-exchange material must also have good chemical and radiation stability. In addition, the ion-exchange medium has to be compatible with the final waste form (glass) if it is to be incorporated with the glass matrix.

BNFL Inc. plans to remove cesium-137 from the low-activity waste feed using SuperLig®-644 ion-exchange material. For the low-activity waste-only flowsheet, the cesium-137 would be eluted from the SuperLig®-644 with acid, then readsorbed onto crystalline silicotitanate for return to the DOE as a free-flowing solid. For the low-activity waste/high-level waste flowsheet, the separated cesium would be blended into the feed for the high-level waste melter. Following cesium removal from the low-activity waste melter feed, the technetium would be adsorbed by the SuperLig®-639 ion-exchange resin, and eluted with acid. The eluate would be transferred to the technetium eluate evaporator for volume reduction and nitric acid recovery. Crystalline silicotitanate would not be used with the low-activity waste/high-level waste flowsheet.

LMAES planned to remove cesium-137 from the low-activity waste feed using a resorcinol-formaldehyde ion-exchange resin. The cesium-137 would have been eluted from the resin with acid solution in an electrochemical ion-exchange process. After elution of the cesium, the resin would have been regenerated using caustic solution. The eluted cesium would have been readsorbed onto crystalline silicotitanate for return to the DOE.

In general, the crystalline silicotitanate ion exchangers show superior ability to remove cesium and strontium compared to other ion-exchange media. Crystalline silicotitanate distribution coefficients for cesium greater than 2,000 mL/g (240 gal./lb) for an alkaline Hanford waste simulant have been reported (Dosch et al., 1996). With a pH adjustment between 1 and 10, the distribution coefficient exceeds 10,000 mL/g (1,200 gal./lb). In addition, the crystalline silicotitanates were found to have distribution coefficients greater than 100,000 mL/g (12,000 gal./lb) for strontium and 2,000 mL/g (240 gal./lb) for plutonium from Hanford waste simulants.

Zeolite ion-exchange material is presently used elsewhere within the nuclear industry to remove cesium-137 from alkaline wastes, but was not considered by either BNFL Inc. or LMAES.

3.3.1 Operational Considerations

3.3.1.1 Superligands

Superligands are being developed, as adaptations of other commercially available products, for adsorption of cesium-137 and technetium-99 from wastes at Hanford. SuperLig®-644 is being developed for cesium-137 adsorption, and SuperLig®-639 is being developed for technetium-99 adsorption. SuperLig®-644 and SuperLig®-639 are being tailor-made by IBC Advanced Technologies for service in solutions having a high pH. While some laboratory studies on the SuperLig®-644 to remove cesium-137 have been published and are discussed in this chapter, no publicly available performance data could be located for SuperLig®-639.

Selectivity

SuperLig®-644 has the capability to selectively remove cesium-137 from alkaline wastes and would be useful for that purpose. It exhibits a relatively low affinity for strontium-90 removal and would not be useful for that purpose (Brown et al., 1996b).

Information on the selectivity of SuperLig®-639 for technetium-99 was not readily available from published literature. In the highly alkaline Hanford waste solutions, technetium-99 exists as the stable pertechnetate ion, TcO_4^- (Schultz, 1980). Therefore, the SuperLig®-639 will need to be selective for technetium in this form.

Capacity

Each volume of SuperLig®-644 ion-exchange resin has the capacity to effectively remove cesium-137 from 80–90 bed volumes of simulated Hanford neutralized current acid waste or about 220 mL of waste per gram of resin (26 gal./lb) (Brown et al., 1996a,b). This information, together with knowledge of the waste characteristics and column operating dynamics, is useful for optimizing the ion-exchange column size and regeneration cycle frequency.

Information on the capacity of SuperLig®-639 to remove technetium-99 was not readily available from the published literature.

Ion Exchange

Temperature

Information on the temperature effects on the performance of the superligands was not readily available from the published literature. In general, but not always, increases in temperature tend to produce decreases in the selectivity of ion-exchange material (Moghissi et al., 1986). Therefore, if the waste is prone to become warm from decay heat, provision to cool the waste before it is treated should be considered.

pH

Information on the effects of pH on the performance of the superligands was not readily available in the published literature.

Sodium Concentration

Increasing the sodium concentration increases the number of volumes of Hanford waste that can be treated by a given mass of SuperLig®-644 ion-exchange resin (Brown et al., 1996a,b). Therefore, the number of load/elute cycles can be minimized by processing concentrated waste streams (Brown et al., 1996b).

The effects of sodium concentration on the performance of SuperLig®-639 were not readily available from the published literature.

Kinetics

Kinetics information for the superligands was not readily available from the published literature. For ion-exchange resins in general, flow rates of 3.4–6.8 L/sec per square meter of cross-sectional area (5–10 gpm/ft^2) are recommended. Higher flow rates produce a decrease in residence time available for diffusion into the resin particle, and may require resin beds deeper than the typical depth of 610–1,220 mm (2–4 ft) (Moghissi et al., 1986). This information is useful for designing the ion-exchange column.

Swelling

Swelling of the SuperLig®-644 ion-exchange resin occurs in caustic solutions (Brown et al., 1996a,b). Swelling of 40–50 percent has been observed (Lee et al., 1997; Jubin et al., 1998). Therefore, provision should be made to elute and regenerate the SuperLig®-644 *in-situ*, to shrink the material before trying to remove it from the column. Further, upward flow should be employed to minimize the effect of any channels produced between the resin and the walls of the column resulting from shrinkage during elution and regeneration.

Information on swelling of SuperLig®-639 was not readily available from the published literature.

114

Chemical Stability

Prolonged storage in a caustic solution will probably significantly degrade the SuperLig®-644 ion-exchange resin (Brown et al., 1996a,b). If used to process alkaline wastes, provisions will need to be made for periodic replacement of SuperLig®-644.

Information on the chemical stability of SuperLig®-639 was not readily available from the published literature.

Thermal Stability

Information on the thermal stability of superligand resins was not readily available from the published literature.

Radiation Stability

The study by Brown et al. (1996c) shows that gamma irradiation of the SuperLig®-644 ion-exchange resin in Hanford neutralized current acid waste simulant up to 1 million Gray (10^8 rad) had no significant effect on resin performance. However, the observed cesium distribution coefficients decreased by at least an order of magnitude between 1–20 million Gray (10^8 and 2×10^9 rad). For example, results for a sodium-to-cesium molar ratio of 50,000 indicate a reduction in the cesium distribution coefficient from 70 mL/g at 1 million Gray to about 0.8 mL/g at 20 million Gray. Other data indicate that the resin is more susceptible to radiation damage in the Hanford waste simulant than it is in air or in water (Brown et al., 1996a,b).

The results at high-irradiation doses only portray upper bounding limits and should not be considered representative of typical ion-exchange process conditions. Nevertheless, if the SuperLig®-644 resin is used for treating Hanford wastes, procedures should be in place to remove the resin from use before being exposed to more than one million Gray (10^8 rad). This should permit 1–2 mo of continuous operation per bed (Brown et al., 1996a,b). Because of its instability following exposure to high doses of gamma radiation, SuperLig®-644 probably should not be used for long-term storage of radioactive materials removed from Hanford wastes.

Information on the radiation stability of SuperLig®-639 was not readily available from the published literature.

Although no irradiation studies specific to gas generation from superligand ion-exchange resins are available in the public literature, it can reasonably be expected this material would produce gases similar to those produced from other organic resins, such as anionic and cationic styrene-divinyl copolymers and resorcinol-formaldehyde resins. The most significant gas generated from irradiation of these resins is hydrogen (Crawford, 1995). The irradiation effects for both SuperLig®-639 and -644 should be independently evaluated to establish operating parameters.

Ion Exchange

Elution/Regeneration

Elution of cesium from SuperLig®-644 can be accomplished with 3.5 volumes of 0.5 M nitric acid per volume of resin (Brown et al., 1995). A reaction with nitrates deteriorates the resin, so it should be regenerated with caustic as soon as possible following elution with nitric acid.

Information on elution and regeneration of technetium-99 from SuperLig®-639 was not readily available from the published literature.

3.3.1.2 Resorcinol-Formaldehyde

Selectivity

Resorcinol-formaldehyde ion-exchange resin has the capability to selectively remove cesium-137 from alkaline wastes, and would be useful for that purpose. Resorcinol-formaldehyde resin exhibits a relatively low affinity for strontium-90 removal and would not be useful for that purpose (Brown et al., 1996b).

Capacity

Each volume of resorcinol-formaldehyde ion-exchange resin has the capacity to treat 190 volumes of simulated Hanford neutralized current acid waste, or 160 volumes of double-shell slurry feed waste. Testing with a simulant of a third Hanford waste—complexant concentrate waste—indicated that the ion-exchange capacity may not be affected by the presence of organic complexants (Kurath et al., 1994). This information, together with knowledge of the waste characteristics and column operating dynamics, is useful for optimizing the ion-exchange column size and regeneration cycle frequency.

Each kilogram of resorcinol-formaldehyde can capture approximately 8 g of cesium (Jubin et al., 1998).

Temperature

Decreasing the temperature increases the volume of waste that can be treated by a given volume of resorcinol-formaldehyde ion-exchange resin. The volume of simulated neutralized current acid and complexant concentrate wastes that can be treated has been shown to increase by a factor of about 1.4 when the temperature is decreased from 40–10 °C (104–50 °F) (Kurath et al., 1994). Therefore, if the waste is prone to become warm through decay heat, provision to cool the waste before it is treated should be considered.

pH

Increasing the pH increases the number of volumes of waste that can be treated by a given volume of resorcinol-formaldehyde ion-exchange resin. The optimum pH for cesium-137 loading is greater than 12 (Kurath et al., 1994). This characteristic is well suited for processing the alkaline wastes at Hanford.

Sodium Concentration

Increasing the sodium concentration slightly increases the number of volumes of Hanford waste that can be treated by a given volume of resorcinol-formaldehyde ion-exchange resin (Bray et al., 1996; Kurath et al., 1994). Thus, the number of load/elute cycles can be minimized by processing concentrated waste streams (Brown et al., 1996b). The Hanford wastes probably should not be diluted before being treated by the resorcinol-formaldehyde resin.

Kinetics

Reducing the liquid flow rate produces a steeper cesium operating curve, which is the concentration of cesium-137 in the effluent versus volume of waste treated. When processing a simulated neutralized current acid waste, a reduction in the flow rate from 9–3 column volumes per hour delayed the breakthrough of detectable cesium in the effluent, from after 100 column volumes to after 160 column volumes had been treated (Kurath et al., 1994). Therefore, the ion-exchange column should be sized to operate at a waste flow rate of approximately 3 column volumes per hour.

Swelling

Swelling of resorcinol-formaldehyde ion-exchange resin occurs as the pH or salt concentration of the solution increases. The resin shrinks by 30–35 percent during acid elution (Kurath et al., 1994). If resorcinol-formaldehyde is to be used for treating Hanford wastes, this swelling and shrinking of the resin, which could result in formation of preferred pathways for the waste feed, would need to be taken into account when designing the ion-exchange columns.

Chemical Stability

Resistance of the resorcinol-formaldehyde ion-exchange resin to most acids is excellent. Resistance to alkaline conditions, such as those of Hanford wastes, is also good (Kurath et al., 1994).

Thermal Stability

The maximum allowable temperature for the resorcinol-formaldehyde ion-exchange resin is probably about 80 °C (180 °F) (Kurath et al., 1994). If the Hanford wastes are cooled before treatment to improve the resorcinol-formaldehyde loading characteristics, thermal stability would not become a significant issue.

Radiation Stability

Radiation doses up to one million Gray (10^8 rad) do not affect the performance of the resorcinol formaldehyde ion-exchange resin (Bibler, 1994; Carlson et al., 1995). Gamma radiation doses of 1–10 million Gray (10^8–10^9 rad) produce moderate degradation of the resin. When irradiated in the presence of simulated neutralized current acid waste, radiolytically-induced oxidation converts some of the ion-exchange sites (hydroxyl functionality) into quinone and carboxylic functionalities (Hubler et al., 1995). Therefore, some minor degradation of resin performance as a result of exposure to radiation

117

Ion Exchange

should be anticipated when treating the highly radioactive Hanford wastes, and provisions should be made to replace the resin periodically.

Following irradiation testing of resorcinol-formaldehyde resin in a static state in the presence of simulated Hanford neutralized current acid waste, a layer of inorganic salts was observed deposited on a stainless steel surface. The deposit apparently resulted from the degradation of salts in the simulated waste solution. If this phenomenon occurs routinely while processing actual Hanford wastes on a production scale, equipment could plug, valves could fail, and the degree to which processing equipment becomes contaminated could increase (Carlson et al., 1995).

Elution/Regeneration

Elution/regeneration of resorcinol-formaldehyde ion-exchange resins is relatively inefficient. When resorcinol-formaldehyde is eluted with an acidic solution, the resin shrinks by about 35 percent as sodium, potassium, and cesium ions are replaced with hydrogen ions. The shrinkage causes the resin to pull away from the walls of the column, allowing channeling of the elution solution along the column walls (Bray et al., 1996). Elution of resorcinol-formaldehyde loaded from operation with simulated neutralized current acid wastes and double-shell slurry feed wastes required eight or more column volumes of 1-M formic acid, 8 or more column volumes of 0.4-M nitric acid (Kurath et al., 1994), or 7 column volumes of 0.5-M nitric acid (Brown et al., 1995).

The estimated ion-exchange capacity loss from each elution/regeneration cycle is about 3 percent (Kurath et al., 1994). Therefore, provision should be made to replace the resin periodically.

3.3.1.3 Crystalline Silicotitanates

Selectivity

Crystalline silicotitanates can selectively remove cesium, strontium, and plutonium from alkaline wastes, unless organic complexants are present, and would be useful for that purpose. Crystalline silicotitanate has a higher capacity to remove cesium and strontium from solution than resorcinol-formaldehyde resin, macrocyclic organic resin such as SuperLig®-644, or aluminosilicate zeolite ion-exchange material (Bray et al., 1993; Brown et al., 1996b).

Capacity

When the engineered form (nonpowder) was used to treat actual waste from Melton Valley tank W–27, a 50 percent breakthrough of cesium occurred at 350 column volumes. A test at Melton Valley with actual waste (pH = 11.5) demonstrated a capacity of over 400 column volumes without breakthrough. A capacity of 660 column volumes was observed when using Hanford double-shell slurry feed simulant (Braun et al., 1996). The scatter in these data suggest that the capacity of the crystalline silicotitanate is sensitive to the actual composition of the waste, and the higher capacity data point should be used only with caution. This information, together with knowledge of the waste characteristics and column operating dynamics, is useful for optimizing the ion-exchange column size and crystalline silicotitanate replacement frequency.

Each kilogram of crystalline silicotitanate can capture approximately 15 g of cesium (Jubin et al., 1998).

Temperature

As the liquid temperature is decreased, the number of volumes of Hanford waste that can be treated by a given volume of crystalline silicotitanate increases. The volume that can be treated doubles when the temperature is decreased from 40–10 °C (104–50 °F) (Bray et al., 1993). Therefore, if the waste is prone to become warm through decay heat, provision to cool the waste before it is treated should be considered.

pH

Cesium-137 adsorption by crystalline silicotitanate is sensitive to pH in the pH region of 10–14. At a pH of 10.2, 1 g of crystalline silicotitanate could treat 8,000 mL (1 lb could treat 959 gal.) of simulated Hanford waste, whereas at a pH of 13.1, 1 g could treat only 490 mL (1 lb could treat only 59 gal.) (Bray et al., 1993). Therefore, lowering the pH of the waste before using crystalline silicotitanate to capture cesium-137 would tend to minimize the amount of the material needed.

Strontium-90 adsorption by crystalline silicotitanate is also sensitive to pH, being most efficient in the acidic pH range of 4–7. Nonetheless, for pH values in the range of 10–14, 1 g of crystalline silicotitanate could treat more than 1,000 mL (1 lb could treat 120 gal.) of simulated Hanford waste (Bray et al., 1993).

Sodium Concentration

The volume of Hanford waste that can be treated by a given volume of crystalline silicotitanate increases as the sodium concentration decreases. For a 5-M sodium solution, only 850 volumes of simulated Hanford waste could be treated by a given volume of crystalline silicotitanate, whereas for a 1-M sodium solution, 5,300 volumes could be treated (Bray et al., 1993). Therefore, the amount of exchange material required can be minimized by processing dilute streams (Brown et al., 1996b).

Kinetics

The best kinetics performance for crystalline silicotitanates occurs at flow rates of about 3 column volumes per hour (Lee et al., 1997). Therefore, the ion-exchange system should be designed to operate at that flow rate.

The powdered form gives the highest mass transfer rate, but produces higher resistance to flow and, therefore, greater pressure differentials. The engineered form, with particle sizes in the range of 250–590 μm (30–60 mesh) is considered optimal (Braun et al., 1996).

Swelling

Crystalline silicotitanate resists significant swelling or shrinkage with changes in temperature, pH, and ion exchange (Braun et al., 1996). Therefore, swelling and shrinkage are not significant design concerns when using this ion-exchange material.

Ion Exchange

Chemical Stability

Crystalline silicotitanate is stable in caustic fluids [i.e., it does not dissolve or degrade (Bray et al., 1993)]. Long-term exposure to concentrated nitric acid (≥ 6 M) results in leaching of some titanium (Braun et al., 1996). Therefore, from a chemical stability perspective, crystalline silicotitanate can be used to collect and store cesium-137 from Hanford wastes.

Thermal Stability

Dry heating of cesium-loaded crystalline silicotitanate to several hundred degrees should not cause any loss in the retention of the cesium. However, temperatures should be maintained at less than 60 °C (140 °F) when crystalline silicotitanate is exposed to concentrated acids or extremely alkaline solutions for extended times (Braun et al., 1996). Therefore, if used to store the collected cesium-137, the loaded crystalline silicotitanate should be dried.

Radiation Stability

Samples of crystalline silicotitanate have been exposed to 10 million Gray (10^9 rad) of radiation in various solutions with no loss of structure or performance (Braun et al., 1996). Therefore, from a radiation stability perspective, crystalline silicotitanate appears suitable for prolonged storage of collected cesium-137.

Elution/Regeneration

Cesium cannot be reasonably eluted from crystalline silicotitanate and the crystalline silicotitanate cannot be regenerated (Brown et al., 1996b). Thus, crystalline silicotitanate must be used on a once-through basis.

According to the manufacturer (UOP Molecular Sieves, Mt. Laurel, New Jersey), strontium-90 can be eluted by the use of a suitable salt solution.

3.3.1.4 Zeolite

Selectivity

Inorganic ion-exchange materials such as zeolite, an aluminosilicate material, are highly selective for cesium-137 separation (Jain and Barnes, 1989). Compared to unmodified zeolite material, the titanium-coated zeolite has a higher capacity for the removal of strontium-90 and plutonium, in addition to cesium-137 (Bray et al., 1993). Therefore, zeolite can be useful for capturing cesium-137 from liquid wastes, and might be useful for capturing strontium-90 and plutonium.

Capacity

At the West Valley Demonstration Project, about 100 m^3 (26,460 gal.) of undiluted alkaline high-level waste supernate, containing about 2 Ci/L (8 Ci/gal.) was processed by a lead column containing 1.7 m^3 (60 ft^3) of titanium-impregnated zeolite, before the column experienced breakthrough of approximately

85 percent (Ploetz and Leonard, 1988). This result indicates a distribution coefficient (λ) of about 59, for a loading of about 100,000 Ci/m^3 (3,000 Ci/ft^3). This information, together with knowledge of the waste characteristics and column operating dynamics, is useful for optimizing the ion-exchange column size and the zeolite replacement frequency.

Temperature

Solution temperature exerts a strong influence on the decontamination factor for zeolite (Jain and Barnes, 1989). The number of volumes of Hanford waste that can be treated by a unit volume of zeolite, with or without titanium (as TiO$_2$) coating, increases as the liquid temperature decreases. The volume that can be treated doubles when the temperature is decreased from 40–10 °C (104–50 °F) (Bray et al., 1993; 1996). Therefore, if the waste is prone to become warm through decay heat, provision to cool the waste before it is treated should be considered.

pH

The pH of the liquid exerts a strong influence on the decontamination factor for zeolite. An alkaline pH of 10–11 is preferred for optimum cesium-137 removal (Jain and Barnes, 1989). Higher pH values could cause deterioration of the zeolite in ion-exchange columns or during storage (Jain and Barnes, 1989).

Sodium Concentration

As the sodium concentration decreases, the number of volumes of Hanford waste that can be treated by a given volume of zeolite increases. For a 5-M sodium solution, only 42 volumes of simulated Hanford double-shell slurry feed waste could be treated by a given volume of zeolite, whereas for a 1-M sodium solution, 300 volumes could be treated (Bray et al., 1993). Therefore, the amount of zeolite material required can be minimized by processing dilute streams (Brown et al., 1996b).

Kinetics

An appropriate fluid flow rate to achieve high adsorption of cesium onto zeolite is approximately 0.6 column volumes per hour (Ploetz and Leonard, 1988).

Swelling

Zeolites, because of their rigid aluminosilicate crystal structure, are generally believed to resist swelling. No study on the swelling characteristics of zeolites was found in published literature. However, experience at the West Valley Demonstration Project provides some evidence of zeolite swelling resistance. Following pretreatment of the alkaline West Valley high-level waste supernate using zeolite, the cesium-loaded zeolite was successfully dumped remotely by opening a discharge valve. Dumping of the zeolite in this manner would not have been possible had the zeolite become significantly swollen.

Ion Exchange

Chemical Stability

Zeolite deteriorates in highly alkaline solutions, particularly at a pH greater than 13 (Jain and Barnes, 1989). Therefore, zeolite would not be appropriate for processing Hanford wastes having a pH greater than 13.

Thermal Stability

Information on the thermal stability of zeolite ion-exchange material is not readily available in the published literature. Because zeolites have been applied on an industrial scale, such as at the West Valley Demonstration Project (Jain and Barnes, 1989) and given that no observation regarding thermal decomposition has been reported, it can be surmised that thermal degradation will not be a problem at typical waste processing temperatures.

Radiation Stability

Zeolite ion-exchange material is far more resistant to radiation damage than selected organic ion-exchange resins commonly used in the nuclear industry during the early 1980's, based on studies at the Los Alamos National Laboratory (Pillay, 1982). Measurements included comparative changes in pH of immersion water before and after irradiation, tendency to agglomerate as a result of irradiation damage, and gas evolution as a result of irradiation (Pillay, 1982).

After exposure to 4.4 million Gray (4.4×10^8 rad) of gamma irradiation from cobalt-60, the pH of 10 mL (0.3 fluid oz) of deionized water mixed with 2 g (0.07 oz) of zeolite increased nominally from 8.0–9.0. In contrast, after an irradiation exposure of about an order of magnitude less [700,000 Gray (7×10^7 rad)], the cationic organic resin having sulfonic functionality groups produced a large decrease in pH, from 3.4–1.5, apparently because of a significant release of acidic ions (HSO_3^+) from the functional groups. Similarly the cationic organic resin having a quaternary amine functionality produced a tremendous decrease in pH, from 8.5–2.5, apparently due to a major release of acidic ions (NH_4^+) from the functional groups (Pillay, 1982).

To measure agglomeration, several 2-cm (0.8-in.) diameter and 20-cm (8-in.) long columns were filled with an inorganic zeolite, an anionic organic resin, or a cationic organic resin. After exposure to 220 million Gray (2.2×10^9 rad) of gamma irradiation from a cobalt-60 source, fluids would flow through the columns filled with zeolite only, not the columns filled with ion-exchange resins. The agglomeration/plugging of the organic resins was attributed to the generation of gases within the organic resin matrices (Pillay, 1982)

Gas evolution from irradiation of zeolites was tested using eight different samples having different moisture contents; four were loaded with cesium. All the samples were irradiated to 1.4 million Gray (1.4×10^8 rad). In all the samples, the gases generated were attributed to radiolysis of water, not deterioration of the zeolite. In two samples, an unexplained amount of methane was observed (Pillay, 1982).

Therefore, from a radiation stability perspective, zeolite appears suitable for prolonged storage of collected cesium-137. However, the material should be dried prior to prolonged storage to prevent gas generation from radiolysis of water.

Elution/Regeneration

Zeolite ion-exchange material is not typically eluded or regenerated. According to the manufacturer, however, it can be regenerated with a sodium chloride solution (UOP Molecular Sieves, 1997b).

3.3.2 Safety Considerations

3.3.2.1 Superligands (SuperLig®-644 and SuperLig®-639)

Historically, runaway organic-nitrate oxidation reactions have caused significant damage to ion-exchange systems. Therefore, following elution with nitric acid, the superligand resins should be converted to the sodium form as quickly as possible (Brown et al., 1996c).

Hydrogen is produced from radiolysis of water. Therefore, hydrogen gas would be produced if the loaded superligand resin were to be stored wet. Other gases, such as carbon dioxide, may be produced by the radiolytic decomposition of the resin, as has been observed for other organic resins. These gases can cause the resin storage container to pressurize. The time necessary to create a flammable concentration of hydrogen from radiolysis in a sealed storage container is directly proportional to the free volume in the container and inversely proportional to the amount of resin present and to the dose rate to the resin from the radionuclides sorbed on it (Crawford, 1995). Theoretically, depending on the specific set of circumstances, a flammable concentration in a storage container could be reached after only a few days.

3.3.2.2 Resorcinol-Formaldehyde Resin

Hydrogen, a flammable gas, will be generated from radiolysis at a rate of about 0.11 molecules per 100 eV in a system of resorcinol-formaldehyde resin stored in Hanford waste that contains 3.9-M nitrate. The sum of all gases generated in such a system is 0.13 molecules per 100 eV (Bibler, 1994).

The formation of hydrogen gas results from radiolysis of water, not from radiation interacting with the resin. Carbon dioxide is produced from decomposition of the resin, as are lesser amounts of carbon monoxide and methane gases. Nitrous oxide is produced by radiolysis when nitrate, or nitric acid, is present in the system (Bibler, 1994).

Formation of these gases can pressurize a container storing radionuclide-loaded resorcinol-formaldehyde. The time necessary to form a flammable concentration of hydrogen in a sealed storage container due to radiolysis is directly proportional to the free volume in the container and inversely proportional to the amount of resin present and to the dose rate to the resin from the radionuclides sorbed on it (Crawford, 1995). Theoretically, depending on the specific set of circumstances, a flammable concentration in a storage container could be reached after only a few days.

3.3.2.3 Crystalline Silicotitanates

No unusual safety considerations were identified for the inorganic crystalline silicotitanates.

3.3.2.4 Zeolite

Commercial zeolite ion-exchange material (IE-96 and TIE-96) contains a small amount (<4 wt %) of crystalline silicon dioxide (quartz). Crystalline silicon dioxide inhaled in the form of quartz is carcinogenic to humans (Lewis, 1997). Therefore, when handling the dry material, suitable respiratory protection should be used.

3.3.3 Comparable Operations in Existence

3.3.3.1 Superligands

Superligand ion-exchange materials are commercially available. SuperLig®-644 and SuperLig®-639 are presently being tailored by the manufacturer for removal of cesium-137 and technetium-99 from alkaline high-level waste. While some laboratory studies on the SuperLig®-644 to remove cesium-137 have been published and referenced here, no performance data are publicly available for SuperLig®-639. Neither SuperLig®-644 nor SuperLig®-639 has been used on an industrial scale, and it is unclear whether the large quantities of Superligands the TWRS ion exchange facility would require will be available in time.

3.3.3.2 Resorcinol-Formaldehyde

Resorcinol-formaldehyde ion-exchange resin is commercially available and has been studied extensively for use in removing cesium-137 from alkaline high level wastes. However, it has not been used on an industrial scale.

3.3.3.3 Crystalline Silicotitanates

During 1996 and 1997, an engineering scale process at the Oak Ridge National Laboratory demonstrated the application of crystalline silicotitanate for removing cesium from actual radioactive waste. The modular, mobile process was designated as the Cesium Removal Demonstration (Lee et al., 1997). During four runs, using 0.038 m³ (1.34 ft³) beds in various column configurations, 116 m³ (30,600 gal.) of supernate from Melton Valley Storage tank W-29 were processed through crystalline silicotitanate. Approximately 1,142 Ci of cesium-137 were captured on 0.26 m³ (9.4 ft³) of the crystalline silicotitanate. Feed rates of 3- and 6-bed volumes per hour were employed, with 50-percent cesium breakthroughs being observed after processing approximately 500 column volumes. The loaded material, in a dry state, was to be placed in temporary storage at the Oak Ridge National Laboratory (Jubin et al., 1998).

3.3.3.4 Zeolite

At the West Valley Demonstration Project, zeolite and titanium-impregnated zeolite were used to remove more than 99.9 percent of the cesium-137 (Valenti et al., 1997) from the high-level waste supernatant. Each of 4 ion-exchange columns, arranged in series, contained 1.7 m³ (60 ft³) of the zeolite material. The

undiluted alkaline supernatant, containing about 2 Ci/L of cesium-137 (about 8 Ci/gal.) and cooled to about 12 °C (54 °F), was pumped into the ion-exchange system at a maximum rate of 320–420 mL/sec (5.1–6.7 gpm). During the first campaign, 100 m^3 (26,460 gal.) was processed before the lead column experienced breakthrough of approximately 85 percent. The decontamination factor for cesium-137 removal by the entire system for the first campaign was greater than 23,000. The decontamination factor for strontium-90 was 4. The zeolite did not show any appreciable removal of plutonium, uranium, or technetium-99 (Ploetz and Leonard, 1988). The cesium-loaded zeolite was blended with the high-level waste sludge and fed to the high-level waste melter to become part of the vitrified high level waste. The treated supernatant was processed by evaporation and cementation for aboveground disposal as a low-level waste.

The use of inorganic zeolite ion-exchange material was not considered a viable alternative for pretreating high-level waste supernatant at the Defense Waste Processing Facility because the high alkalinity of their wastes (pH = 13) could cause deterioration of the zeolite in the ion-exchange columns, or during storage (Jain and Barnes, 1989).

3.3.4 Waste Ion-Exchange Material Management

3.3.4.1 Organic Resins (SuperLig®-644, SuperLig®-639, and Resorcinol-Formaldehyde)

Historically, runaway organic-nitrate oxidation reactions have caused significant damage to ion-exchange systems. Therefore, following elution with nitric acid, organic resins should be converted to the sodium form as quickly as possible (Brown et al., 1996c).

Radiation from adsorbed radionuclides act on the liquid left within, and adhering to, the resins to produce hydrogen gas. The radiation also causes degradation of the organic resins to produce other gases such as carbon dioxide. To prevent the gas generation from pressurizing the resin containers, the storage containers should be vented.

Radiolytically produced hydrogen should not be permitted to accumulate in the resin storage container and reach flammable concentration. The lower explosive limit for hydrogen in air is 4.1 percent (Lewis, 1997). Therefore, the containers should be vented by a method that prevents accumulation of a flammable concentration of hydrogen. One way is to store the containers upright with the filtered vent at the top. Natural diffusion of the gases through a dry filter should limit the accumulation of hydrogen to less than 1 percent. Studies specific to proposed TWRS operations are recommended to verify this.

To make spent organic resin stable for permanent disposal, the resin should be thoroughly dried.

3.3.4.2 Inorganic Ion-Exchange Material (Crystalline Silicotitanates, and Zeolites)

Radiation from adsorbed radionuclides acts on the liquid left within, and adhering to, the ion-exchange material to produce hydrogen. To prevent the gas generation from pressurizing the storage containers, the containers should be vented.

Radiolytically produced hydrogen should not be permitted to accumulate in the resin storage container and reach flammable concentration. The lower explosive limit for hydrogen in air is 4.1 percent (Lewis, 1997). Therefore, the containers should be vented by a method that prevents accumulation of a flammable concentration of hydrogen. One way is to store the containers upright with the filtered vent at the top. Natural diffusion of the gases through a dry filter should limit the accumulation of hydrogen to less than 1 percent. Studies specific to proposed TWRS operations are recommended to verify this.

To permanently dispose of spent inorganic ion-exchange material, vitrification and subsequent permanent disposal with the high-level waste, should be considered. This was successfully done at the West Valley Demonstration Project and should be equally applicable for spent inorganic ion-exchange materials at Hanford.

3.4   Ion-Exchange Proposed by BNFL Inc.

3.4.1   Cesium Removal

3.4.1.1   The Process

BNFL Inc. proposed ion exchange to remove cesium-137 from the concentrated and ultrafiltered low-activity waste stream using SuperLig®-644. Loading the cesium-137 onto the SuperLig®-644 would be accomplished by passing the low-activity waste stream through ion-exchange columns until the concentration of cesium-137 in the effluent approaches a certain limit. The column would then be rinsed with caustic solution and elution of the cesium-137 would be accomplished by passing an acid solution through the ion-exchange columns.

For the low-activity waste/high-level waste flowsheet, the eluate containing the cesium-137 would be blended into the high-level waste for vitrification in the high-level waste melter.

For the low-activity waste-only flowsheet, the acidic eluate with the cesium-137 would be neutralized with caustic, then fed through crystalline silicotitanate columns to recover the cesium-137. The loaded crystalline silicotitanate would then be dried and returned to the DOE for storage.

3.4.1.2   SuperLig®-644 Resin

For operation at 25 °C (77 °F), SuperLig®-644 will be appropriately selective for the cesium ion in an alkaline solution, even in the presence of 5 M of the competing ion, sodium. However, whether SuperLig®-644 will be appropriately selective for cesium in the presence of organic complexants is uncertain because no published information was found on the performance of SuperLig®-644 in solutions containing significant amounts of organic material.

The capacity of the SuperLig®-644, in terms of column volumes of waste that can be processed per column volume of the resin, is not precisely established because testing has not been performed on precise simulants. The impact of not knowing the exact capacity may leave some uncertainty regarding the amount of waste resin that eventually will need to be managed. It will not otherwise adversely affect the overall chemistry of the BNFL Inc. vitrification process flowsheet.

The stability of SuperLig®-644 in alkaline solution is probably limited. Therefore, once placed into service, the SuperLig®-644 should be used until loaded, after which it should be eluted immediately with acid. If the pretreatment process is shutdown for any significant period of time, the alkaline solution should either be flushed from the SuperLig®-644 or the resin should be eluted with acid, regardless of its loading state.

The thermal stability of SuperLig®-644 is not a concern if the operating temperature is 25 °C (177 °F).

Radiologically, SuperLig®-644 has been shown to withstand a dose of 10 million Gray (10^9 rad) without significant impact on its performance, as measured by cesium uptake. At higher doses, the performance of the resin deteriorates. Ten million Gray (10^9 rad) is a greater dose than would be expected during normal continuous operation. Assuming a radiation dose rate of 2,700 Gray/hr (2.7×10^5 rad/hr), 1–2 mo of continuous operation is possible.

Overall, SuperLig®-644 should perform its intended function well with envelope A and B wastes. Whether it will work well with envelope C waste is uncertain because of the presence of organic materials in the envelope C waste.

3.4.1.3 SuperLig®-644 Column Size and Dynamics

Kinetics data for SuperLig®-644 are not readily available from the published literature, so no definitive statement can be made about the kinetics associated with the BNFL Inc. resin column design.

SuperLig®-644 is known to swell when converted from the hydrogen ion form to the alkali metal form. Because swelling could create difficulty in removing the unregenerated resin from the ion-exchange column, elution of the cesium loading from the resin within the ion-exchange column is probably necessary. Because the elution step would produce shrinkage of the previously swollen resin, channels around or through the resin bed would likely be produced by the elution step. To ensure the liquid waste efficiently contacts the resin following elution and regeneration, and does not simply flow through the channels, the waste should be introduced into the bottoms of the resin columns.

Elution of cesium from SuperLig®-644 using 3.5 column volumes of 0.5-M nitric acid has been demonstrated.

SuperLig®-644 can be regenerated, but it deteriorates significantly from the third to fourth loading so it will probably need to be replaced after about three regeneration cycles.

3.4.1.4 Crystalline Silicotitanate Ion-Exchange Material

For operation at 25 °C (77 °F), crystalline silicotitanate will be appropriately selective for cesium ion from the neutralized eluate.

The capacity of crystalline silicotitanate, in terms of column volumes of eluate that can be processed per column volume of the ion-exchange material, is not precisely established because testing has not been performed on precise simulants. The impact of not knowing the exact capacity may leave some uncertainty regarding the amount of loaded ion-exchange material that eventually will need to be

returned to the DOE. It will not otherwise adversely affect the overall chemistry of the BNFL Inc. low-activity waste vitrification process flowsheet.

Crystalline silicotitanate is stable in caustic fluids. Therefore, neutralization of the acidic eluate before introducing the eluate to the columns containing the crystalline silicotitanate, is appropriate.

When exposed to extremely alkaline solutions, crystalline silicotitanate should be kept below 60 °C (140 °F). Operation of the ion-exchange column at 25 °C (77 °F) is appropriate. Dry heating of cesium-loaded crystalline silicotitanate to several hundred degrees should not cause any loss in the retention of the cesium. Therefore, the BNFL Inc. plan for a low-activity waste-only facility to return the cesium-loaded crystalline silicotitanate to the DOE for storage is appropriate from a thermal stability perspective because the decay heat from the cesium-137 will not deteriorate the ion-exchange material.

Samples of crystalline silicotitanate have been exposed to 10 million Gray (10^9 rad) of radiation with no loss of structure. However, after the cesium-137 loaded material is returned to the DOE for storage, a total radiation dose much greater than 10 million Gray (10^9 rad) should be anticipated. This greater dose would be because of the heavy loading with radioactive cesium and the undefined period of exposure to cesium-137. Therefore, no definitive statements can be made at this time regarding the potential long-term effects of ionizing radiation on the dry, cesium-137 loaded crystalline silicotitanate during storage.

Overall, crystalline silicotitanate should perform its intended function well, at least in the near term. If the cesium-137 is loaded onto crystalline silicotitanate and returned to the DOE for storage, the DOE should proactively pursue vitrification or other appropriate processing of the material to preempt any unanticipated complications that might result from overexposure of crystalline silicotitanate to ionizing radiation.

3.4.1.5 Crystalline Silicotitanate Column Size and Dynamics

Crystalline silicotitanate has been shown to function well with a process flow rate of about three column volumes per hour.

Crystalline silicotitanate resists significant swelling with changes in pH, temperature, or ion exchange. Therefore, discharging the loaded ion-exchange material from the column should not pose a problem.

3.4.2 Technetium Removal

3.4.2.1 The Process

Following removal of the cesium, BNFL Inc. proposed ion exchange to remove technetium-99 from the low-activity waste stream using SuperLig®-639. Loading the technetium-99 onto the SuperLig®-639 would be accomplished by passing the low-activity waste stream through an ion-exchange column until the concentration of technetium-99 in the effluent approaches a certain limit. The column then would be rinsed with a caustic solution and elution of the technetium-99 from the SuperLig®-639 would be accomplished by passing acidic solution through the ion-exchange columns, followed by a rinse with

demineralized water. Regeneration of the SuperLig®-639 would not be performed because the SuperLig®-639 is not required to be in a sodium form.

3.4.2.2 SuperLig®-639 Resin

SuperLig®-639 resin is being tailor-made by IBC Advanced Technologies for removal of technetium-99 from solutions having a high pH. No performance data, however, were readily available in the published literature. Therefore, no definitive statements can be made at this time regarding the suitability of SuperLig®-639 for its intended use.

3.4.2.3 SuperLig®-639 Column Size and Dynamics

Kinetics data for SuperLig®-639 were not readily available from the published literature, so no definitive statement can be made about the kinetics associated with the BNFL Inc. resin column design.

No data on SuperLig®-639 swelling were readily available in the published literature. SuperLig®-639 is likely to behave as other similar organic resins and swell when being loaded. Because swelling could create difficulty in removing the unregenerated resin from the ion-exchange column, elution of the technetium from the resin is probably necessary. Because the elution step would likely produce shrinkage of the previously swollen resin, channels around or through the resin bed would likely be produced by the elution step. To ensure the liquid waste efficiently contacts the resin following elution, and does not simply flow through the channels, the fluid should be introduced into the bottoms of the resin columns.

Because no data on elution of technetium from SuperLig®-639 are readily available in the published literature, no definitive statements can be made regarding the appropriateness of the technetium elution scheme proposed by BNFL Inc.

Overall, insufficient published information was available to assess adequately the dynamics of the technetium removal process proposed by BNFL Inc.

3.5 Future Considerations

As pointed out in chapter 1, although the pretreatment flowsheet proposed by BNFL Inc. focuses on separation of the dominant radionuclides in Hanford tank wastes—cesium-137, strontium-90, technetium-99, and transuranics, removal of other radionuclides such as europium-154, europium-155, and cobalt-60, as well as nonradioactive components such as sulfate, may become necessary. The gamma-emitting radioisotopes of europium and cobalt would contribute to the radiation dose rate from the immobilized low-activity waste package and affect the required thickness of the immobilized low-activity waste package wall. Sulfates pose problems for vitrification because of the low solubility in silicate glasses and the tendency to form molten salt phases that accumulate on the surface of the glass melt pool.

BNFL Inc. has not proposed to separate europium-154, europium-155, and cobalt-60 from the low-activity waste stream, although LMAES had planned to investigate unit operations for separation of cobalt and europium. Because separation of europium-154, europium-155, cobalt-60, and sulfate could

still become important, published studies related to the separation of these components from Hanford wastes are briefly discussed in this section.

3.5.1 Europium/Cobalt Removal

None of the ion-exchange materials discussed in previous sections appear to have been evaluated for use in europium and cobalt separation. Two adsorbents that could potentially be useful are sodium titanate and diphonix.

3.5.1.1 Ion Exchange with Sodium Titanate

Sodium titanate is an inorganic ion-exchanger ($NaTi_2O_5H$) produced by Allied Signal of Des Plaines, Illinois. It is used primarily for strontium removal and is effective for that purpose. Testing with actual double-shell slurry feed waste from Hanford tank AW–101 revealed a high volumetric distribution coefficient (λ) for strontium—1,200 unit volumes of liquid processed per unit volume of sodium titanate (Brown et al., 1996a,b). Actually, sodium titanate has a great affinity and capacity for adsorbing cations with valences of +2, +3, and +4 from alkaline media (Schultz, 1980). Thus, although no specific studies conducted on the use of sodium titanate for removal of cobalt or europium, these elements (Co^{+2}, Co^{+3}, Eu^{+2}, and Eu^{+3}) would be good candidates for adsorption by sodium titanate, along with other multivalent cations. However, the affinity of the titanate exchanger for multivalent cationic radionuclides is so high that no satisfactory way of eluting absorbed radionuclides has been found (Schultz, 1980).

The titanate exchanger can be used as a 105–420 μm (40–140 mesh) powder or as titanate-loaded macroreticular anion-exchange resin beads that have diameters in the range 297–840 μm (20–50 mesh). The powdered form has a bulk density of 0.58 g/mL (36 lb/ft^3) (Brown et al., 1996a,b). Hydraulic properties of the beads are far superior to those of the powder (Schultz, 1980).

3.5.1.2 Ion Exchange with Diphonix

Diphonix™ is a commercially available ion-exchange resin manufactured by Eichrom Industries Inc. (Darien, Illinois). The resin is polyfunctional and constructed of a polystyrene/divinylbenzene matrix in a spherical bead form with diphosphonic and sulfonic groups bonded to the polymer matrix. The resin displays metal ion selectivity and rapid rates of complexation over a wide range of solution pH. It has been shown capable of complexing 98.3 percent of europium (Eu^{3+}) from a 1-N nitric acid solution after 30 min of contact. In the presence of sodium the resin was still able to complex 96.5 percent of the europium from a 1-N nitric acid solution to a 0.4-N sodium nitrate solution (Lawrence and Kurath, 1994).

3.5.2 Sulfate Removal

Sulfate can be removed from aqueous solutions using anion exchange. Usually, strong base anion-exchange resins, which derive their functionality from quaternary ammonium exchange sites, are recommended for this purpose. A variety of strong base anion-exchange resins are commercially available [Appendix I in Dorfner (1991a)]. The two main groups of strong base anion resins are Type 1 and Type 2, depending on the type of amine used in making the resins. Type 1 has three methyl groups in

the quaternary ammonium exchanges sites, whereas in Type 2 an ethanol group replaces one of the methyl groups. Type 1 resins are recommended for solutions that have high silica and carbonate concentrations; Type 2 resins give best results on solutions that predominately contain free mineral acids—chlorides and sulfates (DeSilva, 1995). Type 2 resins, however, have relatively unstable functional groups and are not recommended for use at elevated temperatures or in radiation fields (Kuhne, 1991).

No published studies on sulfate removal from Hanford wastes were available. Published information on sulfate removal typically involves purification of drinking water derived from surface and groundwaters, particularly those with elevated sulfate concentrations stemming from gypsum deposits in the aquifer. For example, the CARIX® process, which uses a mixed bed of weak acid resin in the free acid form and an anion-exchange resin in the bicarbonate form, has been used successfully to remove hardness, sulfate, and nitrate up to raw water salinities of 1,000 mg of total dissolved solids per liter of solution (Holl and Flemming, 1991). Because of the unique—and complex—chemical composition of Hanford tank wastes, it is not possible to extrapolate information derived from studies on demineralization of drinking water to the removal of sulfate from Hanford wastes. BNFL Inc. is currently developing an ion-exchange process to remove sulfate from the low-activity waste stream (Elsden, 1999). However, problems in developing this process can be expected due to the high concentrations in Hanford wastes of nitrate (NO_3^-), nitrite (NO_2^-), and hydroxide (OH^-) anions as well as the significant concentrations of other anionic species such as phosphate (PO_4^{3-}), silicate (SiO_3^{2-}), aluminate [$Al(OH)_4^-$], chloride (Cl^-), and chromate (CrO_4^{2-}). These anions would compete with sulfate for the anion-exchange sites of the resin and could make the anion-exchange process inefficient for sulfate removal. The developmental efforts by BNFL Inc. will need to be evaluated when information becomes available, particularly with respect to the effectiveness of the resin to remove sulfate and also determination of its chemical and radiation stability.

3.6   References

Bibler, N.E. *Cesium Removal from High-Level Waste Using a Resorcinol-Formaldehyde Ion Exchange Resin*. WSRC–MS–94–0409. Aiken, SC: Westinghouse Savannah River Company. 1994.

Bibler, N.E., and C.L. Crawford. *An Investigation of the Radiolytic Stability of a Resorcinol-Formaldehyde Ion Exchange Resin*. WSRC–RP–94–148. Aiken, SC: Westinghouse Savannah River Company. 1994.

Bibler, J.P., R.M. Wallace, and L.A. Bray. Testing a new cesium-specific ion exchange resin for decontamination of alkaline high-activity waste. R.G. Post, ed. *Proceedings of Waste Management '90*. Volume 2. Tucson, AZ: Waste Management Symposia, Inc.: 747–751. 1990.

Bostick, D.T., W.D. Arnold, Jr., B. Guo, M.W. Burgess, D.R. McTaggart, and P.A. Taylor. *Evaluation of Improved Techniques for the Removal of ^{90}Sr and ^{137}Cs from Process Wastewater and Groundwater: FY 1995 Status*. ORNL/TM–13099. Oak Ridge, TN: Lockheed Martin Energy Research Corporation. 1996.

Ion Exchange

Braun, R., T.J. Dangieri, D.J. Fenelly, J.D. Sherman, W.C. Schwerin, R.R. Willis, N.E. Brown, J.E. Miller, R.G. Anthony, C.V. Philip, L.A. Bray, G.N. Brown, D.D. Lee, T.T. Borek, W.J. Connors, A.S. Behan, R.W. Fisher, N. Greenlay, F.G. Portenstein, T.M. Reynolds, W. Zamechek, E.A. Klavetter, J.L. Krumhansi, J.E. Reich, S.G. Thoms, and D.E. Trudell. *Ion-Exchange Performance of Commercial Crystalline Silico-Titanates for Cesium Removal.* SAND96–0656C. Albuquerque, NM: Sandia National Laboratories. 1996.

Bray, L.A., L.K. Holton, T.R. Myers, G.M. Richardson, and B.M. Wise. *Experimental Data Developed to Support the Selection of a Treatment Process for West Valley Alkaline Supernatant.* PNNL–4969. Richland, WA: Pacific Northwest Laboratory. 1984.

Bray, L.A., K.J. Carson, and R.J. Elovich. *Initial Evaluation of Sandia National Laboratory-Prepared Crystalline Silico-Titanates for Cesium Recovery.* PNNL–8847. Richland, WA: Pacific Northwest Laboratory. 1993.

Bray, L.A., K.J. Carson, R.J. Elovich, and D.E. Kurath. *Equilibrium Data for Cesium Ion Exchange of Hanford CC and NCAW Tank Waste.* PNNL–11123. Richland, WA: Pacific Northwest National Laboratory. 1996.

Brooks, K.P., A.Y. Kim, and D.E. Kurath. *Assessment of Commercially Available Ion Exchange Materials for Cesium Removal from Highly Alkaline Wastes.* PNNL–11121. Richland, WA: Pacific Northwest National Laboratory. 1996.

Brown, G.N., R.J. Elovich, and L.A. Bray. *Evaluation and Comparison of SuperLig 644, Resorcinol-Formaldehyde and CS-100 Ion Exchange Materials for the Removal of Cesium from Simulated Alkaline Supernate.* PNNL–10486. Richland, WA: Pacific Northwest Laboratory. 1995.

Brown, G.N., L.A. Bray, C.D. Carlson, K.J. Carson, J.R. DesChane, R.J. Elovich, F.V. Hoopes, D.E. Kurath, L.L. Nenninger, and P.K. Tanaka. *Comparison of Organic and Inorganic Ion Adsorbents for Removal of Cesium and Strontium from Simulated and Actual Hanford 241–AW–101 DSSF Tank Waste.* PNNL–10920. Richland, WA: Pacific Northwest Laboratory. 1996a.

Brown, G.N., L.A. Bray, C.D. Carlson, K.J. Carson, J.R. DesChane, R.J. Elovich, F.V. Hoopes, D.E. Kurath, L.L. Nenninger, and P.K. Tanaka. *Comparison of Organic and Inorganic Ion Adsorbents for Removal of Cesium and Strontium from Simulated and Actual Hanford 241–AW–101 DSSF Tank Waste.* PNNL-11120. Richland, WA: Pacific Northwest National Laboratory. 1996b.

Brown, G.N., K.J. Carson, J.R. DesChane, R.J. Elovich, and P.K. Berry. *Chemical and Radiation Stability of a Proprietary Cesium Ion Exchange Material Manufactured from WWL Membrane and SuperLig 644.* PNNL–11328. Richland, WA: Pacific Northwest National Laboratory. 1996c.

Brunson, R.R., D.F. Williams, W.D. Bond, D.E. Benker, F.R. Chattin, and E.D. Collins. *Removal of Cesium from Aluminum Decladding Wastes Generated in Irradiated Target Processing Using a Fixed-Bed Column of Resorcinol-Formaldehyde Resin.* ORNL/TM–12708. Oak Ridge, TN: Martin Marietta Energy Systems, Inc. 1994.

Carlson, C.D., L.A. Bray, S.A. Bryan, J.A. Franz, D.E. Kurath, S.R. Adami, G.N. Brown, J.R. Deschane, R.J. Elovich, J.C. Linehan, W.S. Shaw, and M.R. Telander. *Radiation Testing of Organic Ion Exchange Resins.* PNNL–10767. Richland, WA: Pacific Northwest Laboratory. 1995.

Collins, J.L., B.Z. Egan, K.K. Anderson, C.W. Chase, and J.T. Bell. *Batch Test Equilibration Studies Examining the Removal of Cs, Sr, and Tc from Supernatants from ORNL Underground Storage Tanks by Selected Ion Exchangers.* CONF–9505101–1. Oak Ridge, TN: Oak Ridge National Laboratory. 1995.

Crawford, C.L. *Radiolytic Hydrogen Production During the Long Term Storage of Spent Organic Ion Exchange Resins.* WSRC–MS–95–0013. Aiken, SC: Westinghouse Savannah River Company. 1995.

Crawford, C.L., N.E. Bibler, and J.P. Bibler. *An Investigation of the Radiolytic Stability of a Resorcinol-Formaldehyde Ion Exchange Resin.* WSRC–MS–93–550. Aiken, SC: Westinghouse Savannah River Company. 1993.

Dalton, W.J. *Qualification and Full-Scale Demonstration of Titanium-Treated Zeolite for Sludge Wash Processing.* DOE/NE/44139–72. West Valley, NY: West Valley Nuclear Services. 1997.

DeSilva, F.J. Essentials of ion exchange. *Water Quality Association Annual Convention, Nashville, Tennessee, March 15, 1995.* 1995.

Dorfner, K., ed. *Ion Exchangers.* Berlin, Federal Republic of Germany: Walter de Gruyter. 1991a.

Dorfner, K. Synthetic ion exchange resins. *Ion Exchangers.* K. Dorfner, ed. Berlin, Federal Republic of Germany: Walter de Gruyter: 189–396. 1991b.

Dosch, R.G., E.A. Klavetter, H.P. Stephens, N.E. Brown, and R.G. Anthony. *Crystalline Silicotitanates-New Ion Adsorbent for Selective Removal of Cesium and Strontium from Radwastes.* SAND96–1929. Albuquerque, NM: Sandia National Laboratories. 1996.

Elsden, A. Hanford TWRS privatization—The BNFL approach. *American Ceramic Society 101st Annual Meeting Abstracts.* Westerville, OH: American Ceramic Society. 1999.

Freundlich, H. *Colloid and Capillary Chemistry.* London, England: Methuen. 1926.

Holl, W., and H.-C. Flemming. Treatment of drinking water with ion exchange resins. *Ion Exchangers.* K. Dorfner, ed. Berlin, Federal Republic of Germany: Walter de Gruyter: 835–844. 1991.

Ion Exchange

Hubler, T.L., J.A. Franz, W.J. Shaw, S.A. Bryan, R.T. Hallen, G.N. Brown, L.A. Bray, and J.C. Linehan. *Synthesis, Structural Characterization, and Performance Evaluation of Resorcinol-Formaldehyde (R-F) Ion-Exchange Resin.* PNNL–10744. Richland, WA: Pacific Northwest National Laboratory. 1995.

Hubler, T.L., W.J. Shaw, G.N. Brown, J.C. Linehan, J.A. Franz, T.R. Hart, and M.O. Hogan. *Chemical Derivation to Enhance the Chemical/Oxidative Stability of Resorcinol-Formaldehyde (R-F) Resin.* PNNL–11327. Richland, WA: Pacific Northwest National Laboratory. 1996.

Jain, V., and S.M. Barnes. *Waste Description and Previtrification Treatment Activities at WVDP, HWVP, and DWPF.* DOE/NE/44149–57. West Valley, NY: West Valley Nuclear Services Company, Inc. 1989.

Jubin, R.T., D.D. Lee, E.C. Beahm, J.C. Collins, D.J. Davidson, B.Z. Egan, A.J. Mattus, R.D. Spence, and J.F. Walker. Tank Waste Treatment R&D Activities at Oak Ridge National Laboratory. *Proceedings of Waste Management '98, March 1–5, 1998.* Tucson, AZ: Waste Management Symposia, Inc. 1998.

Klavetter, E.A., N.E. Brown, D. Trudell, R.G. Anthony, D. Gu, and C.T. Erkey. *Ion-Exchange Performance of Crystalline Silico-Titanates for Cesium Removal from Hanford Tank Waste Simulants.* SAND–94–0680C. Albuquerque, NM: Sandia National Laboratories. 1994.

Kuhne, G. Ion exchangers in nuclear technology. *Ion Exchangers.* K. Dorfner, ed. Berlin, Federal Republic of Germany: Walter de Gruyter: 873–902. 1991.

Kurath, D.E., L.A. Bray, K.P. Brooks, G.N. Brown, S.A. Bryan, C.D. Carlson, K.J. Carson, J.R. DesChane, R.J. Elovich, and A.Y. Kim. *Experimental Data and Analysis to Support the Design of an Ion-Exchange Process for the Treatment of Hanford Tank Waste Supernatant Liquids.* PNNL–10187. Richland, WA: Pacific Northwest Laboratory. 1994.

Kurath, D.E., L.A. Bray, K.P. Brooks, C.D. Carlson, and A.Y. Kim. *Analysis of Equilibrium Data for Cesium Ion Exchange of Hanford CC and NCAW Supernatant Liquid: Status Report.* PNNL–11117. Richland, WA: Pacific Northwest National Laboratory. 1996.

Langmuir, I. The adsorption of gases on plane surfaces of glass, mica, and platinum. *Journal of the American Chemical Society* 40: 1,361–1,403. 1918.

Lawrence, W.E., and D.E. Kurath. *Preliminary Survey of Separations Technology Applicable to the Pretreatment of Hanford Tank Waste.* PNNL–9426. Richland, WA: Pacific Northwest Laboratory. 1994.

Lee, D.D., J.F. Walker, Jr., P. A. Taylor, and D.W. Hendrickson. Cesium Removal flow studies using ion exchange. *American Institute of Chemical Engineers Spring National Meeting.* Houston, TX: American Institute of Chemical Engineers. 1997.

Lewis, R.J. *Hazardous Chemicals Desk Reference*. New York: Van Nostrand Reinhold Publisher. 1997.

Lumetta, G.J., J.L. Swanson, and L.A. Bray. *Radionuclide Separations for the Reduction of High-Level Waste Volume*. PNNL–SA–21389. Richland, WA: Pacific Northwest Laboratory. 1993.

Moghissi, A.A., H.W. Godbee, and S.A. Hobart. *Radioactive Waste Technology*. New York: American Society of Mechanical Engineers. 1986.

Pillay, K.K.S. Radiation Effects on Ion Exchange Materials Used in Waste Management. *Three Mile Island Cleanup: Experiences, Waste Disposal and Environmental Impact*. L.J. King and J.H. Opelka, eds. New York: American Institute of Chemical Engineers. 1982.

Ploetz, D.K., and I.M. Leonard. *Supernatant Treatment System Design through Testing*. DOE/NE/44139–47. West Valley, NY: West Valley Nuclear Services Company. 1988.

Schultz, W.W. *Removal of Radionuclides from Hanford Defense Waste Solutions*. RHO–SA–51. Richland, WA: Rockwell Hanford Operations. 1980.

UOP Molecular Sieves. *IONSIV® IE-910 Ion Exchanger Series*. Product Information Sheet, IE-910 Literature. Mt. Laurel, NJ: UOP Molecular Sieves. 1997a.

UOP Molecular Sieves. *IONSIV® TIE-96 Ion Exchanger*. Product Information Sheet, IE-95 Literature, UOP Molecular Sieve Adsorbents. Des Plaines, IL: UOP Molecular Sieves. 1997b.

Valenti, P.J., J. Paul, and R.S. Roberts. Vitrification operational experiences at the West Valley Demonstration Project. *Proceedings of Waste Management '97 Conference*. Tucson, AZ: Waste Management Symposia, Inc. 1997.

4 ELECTROCHEMICAL METHODS

LMAES had proposed to use two electrochemical methods to pretreat low-activity waste received from the DOE—electrochemical ion exchange and electroreduction. The electrochemical ion-exchange process was to enhance elution of the loaded resorcinol-formaldehyde resin, subsequent to the use of that resin for removing cesium-137 by conventional ion exchange. The electroreduction process was to be used for removing technetium-99 from the low-activity waste.

Many applications of the electrochemical processes are possible. Westinghouse Electric Company employed electrolysis of uranyl tetrafluoride dissolved in a mixture of salts to produce the first pure uranium for the Manhattan Project. The United States, the United Kingdom, and the former Union of Soviet Socialist Republics have all employed electrolysis of fused salts to produce thorium (Benedict et al., 1981). At the Idaho Chemical Processing Plant, electrolysis was developed for spent nuclear fuel dissolution (Long, 1978). To improve plutonium partitioning from dissolved nuclear fuel, Allied General Nuclear Services developed a special electrocell for the Barnwell Nuclear Plant in which plutonium was reduced from the organic-soluble tetravalent state to the organic-insoluble trivalent state. Electrolysis has been employed to enrich deuterium, for final separation by other processes, in Norway, Switzerland, and India (Benedict et al., 1981).

4.1 Electrochemical Ion Exchange

The concept of electrochemically controlled ion exchange was first developed as a possible method for desalinating brackish waters (Evans, 1965, 1970). The concept was based on local pH changes induced at an electrode surface by the passage of small electrolytic currents. When the electrode contained weakly acidic cation-exchange groups, these became activated sites for cation adsorption at cathodic potentials. Conversely, at anodic potentials, the process was reversed, and the adsorbed cations were eluted. Electrochemical ion exchange was subsequently investigated and developed at the Harwell Laboratory of AEA Industrial Technology (Oxfordshire, United Kingdom) for potential treatment of liquid waste streams containing soluble radioactive species (Bridger et al., 1991; Turner et al., 1992).

An electrochemical ion-exchange electrode, based on the Harwell design, consists of an ion-exchange powder incorporated into the electrode structure by an appropriate binder. The combination of the electrochemical ion-exchange electrode and a counter electrode make up the electrochemical ion-exchange cell. The ion-exchange material used in the construction of electrochemical ion-exchange electrodes are, generally, weak acid cation-exchangers or basic anion-exchangers. The process of resin activation involves ionization of the respective active group within the material. The ion-exchange process is controlled by applying a potential difference between the electrochemical ion-exchange electrode and the counter electrode—ions are adsorbed on the ion-exchange membrane from which they may be eluted by polarity reversal. This method achieves large volume reduction factors because the exchanger can be reused over several adsorption/elution cycles with the use of a small amount of eluant. The method involves a minimum of added chemicals and can lead to remote automatic control and increased safety due to the ability of using the applied potential as an additional process control variable (Jones et al., 1992).

The electrochemical ion-exchange operation is favorable for contaminant adsorption from low concentration waste streams where flocculation and evaporation techniques are not suitable. It has also been shown to perform well for removing colloidal and dissolved radionuclide activity following a

filtration step. Electrochemical ion-exchange offers the flexibility of using various cationic–anionic electrochemical ion-exchange combinations to achieve control of the effluent pH—an important parameter in treatment schemes for mixtures containing a variety of solutes.

A schematic diagram of an electrochemical ion-exchange cell is shown in figure 4-1 in which the power supply unit and monitoring instrumentation (e.g., pH meter) are included. It consists of two similar electrochemical ion-exchange electrodes mounted to face each other with process liquid upflowing between them at the center of the cell. The electrochemical ion-exchange electrode consists of a platinized titanium electrode onto which a membrane has been cast. The membrane could be made from zirconium phosphate powder having a typical particle size of 0.1 mm (0.004 in.) held together by a binder, such as polybutadiene or polystyrene. Zirconium phosphate powder is a weak cation-exchanger available in hydrogen form. The counter electrode can be a platinized titanium mesh mounted against the surface of the electrochemical ion-exchange electrode and in direct contact with the liquid being treated.

The fabrication of the electrochemical ion-exchange electrode involves a step of mixing an ion-exchange material with a synthetic rubber (e.g., Kraton, a polystyrene-butadiene copolymer) in a solvent (e.g., trichloroethane). The resulting slurry is poured into a mould containing a platinized titanium mesh electrode and the solvent allowed to evaporate overnight. The membrane attains a porous structure resulting from evaporation of the solvent. Uncoated mesh is used for the counter electrode. Plastic clips clamp the electrodes together, forming the electrochemical ion-exchange module. The module can be immersed in a stirred electrolyte solution (batch mode) or contained in a flow cell through which electrolytes can pass. The electrochemical ion-exchange method offers the option of putting cation- and anion-exchange electrodes in the same cell, where at low potentials the cation electrochemical ion-exchange electrode acts as the counter electrode to the anion electrochemical ion-exchange electrode, and vice-versa.

Various inorganic and organic exchangers are possible candidates for an electrochemical ion-exchange application. Table 4-1 provides a list of exchangers that have been evaluated for treatment of radionuclide-containing waste streams (Turner et al., 1992). In evaluating the use of electrochemical ion-exchange for waste treatment operations, the selected exchanger material should be thoroughly tested through repeated adsorption/elution cycles to identify the suitable ranges of operating parameters. For example, among the four IRA- and IRN-series adsorbers, which are organic anion-exchangers, listed in table 4-1, IRA910 and IRN78L electrodes were selected for further testing because the other two had high electrical resistance (Turner et al., 1992). In addition, kinetic and equilibrium experiments should be accomplished over wide ranges of various operating parameters to identify operating conditions that yield acceptable selectivity coefficients.

4.1.1 Theory

The electrochemical ion-exchange process involves a pH perturbation caused by the applied potential, activation of the resin and ion migration (adsorption and elution) from the resin (Bridger et al., 1991).

138
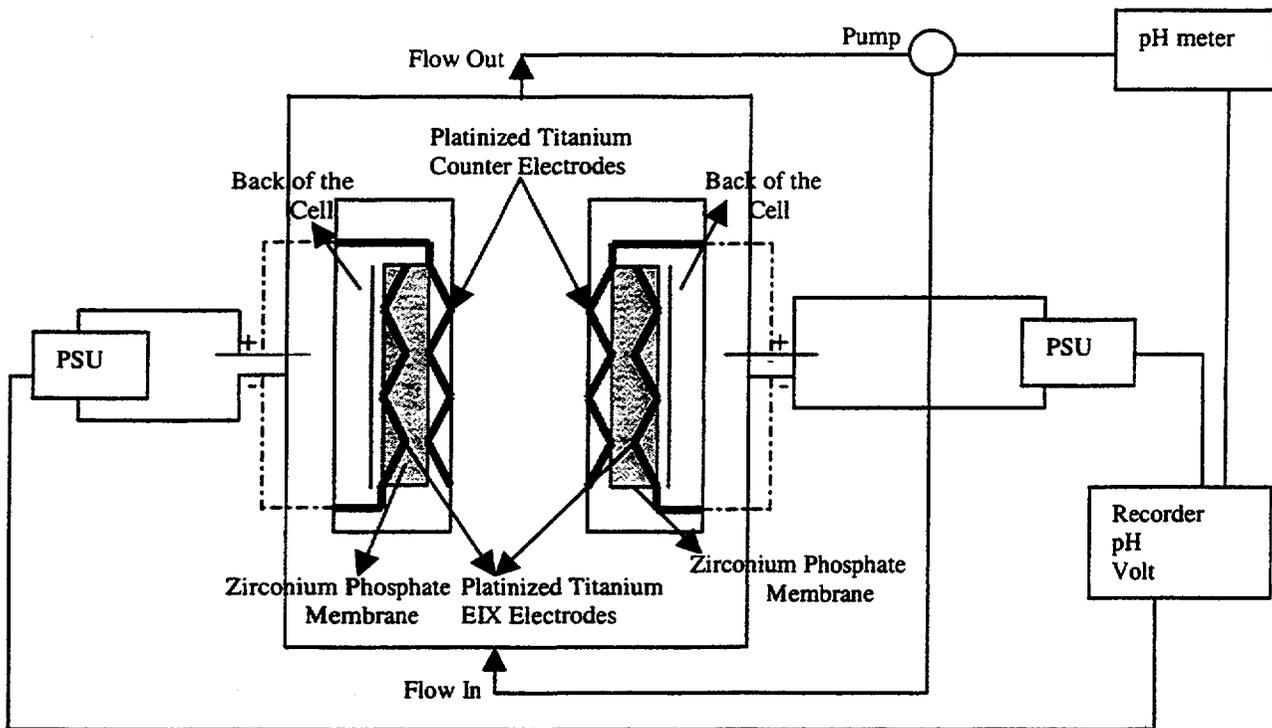
Figure 4-1. Cross section of an electrochemical ion-exchange (EIX) cell (Cumming et al., 1997; Jones et al., 1992)

4.1.1.1 Electrochemical pH Perturbation

By applying a suitable potential across the electrode system, water is either oxidized or reduced depending on the potential of the electrode. At the anode, water is oxidized according to the reaction:

$$2H_2O \rightarrow O_2 + 4H^+ + 4e^- \tag{4-1}$$

producing oxygen and lowering the pH of the solution. At the cathode, water is reduced according to the reaction:

$$2H_2O + 2e^- \rightarrow H_2 + 2OH^- \tag{4-2}$$

resulting in hydrogen evolution and an increase in solution pH.

4.1.1.2 Activation of Ion-Exchange Material

During cation exchange, the active group on the exchange resin, typically a carboxylic acid group, is deprotonated to give an overall negative local charge:

Table 4-1. List of exchangers evaluated for application to radionuclides separation (Turner et al., 1992)

Adsorber	Structure	Size (μM)	Moisture (% Max)	pH Range	Swelling (vol %)	pK$_a$	Ion-Exchange Capacity (meq/g)		Density (g/cm³)
							Dry	Wet	
IRC84	Crosslinked acrylic -COOH	400	40–46	4–14	65	5.3	10	4.0	1.19
IRC50	Methacrylic divinylbenzene -COOH	450–500	43–53	5–14	75–100	6.1	10	3.5	1.25
IRN78L	Styrene divinylbenzene gel -N(C₃)₃	410–480	43–49	0–14	18–22	—	3.8	1.4	1.1
IRA910	Styrene divinylbenzene Type II Dimethyl-ethanolamine	410–550	55–60	0–14	12–17	—	3.8	1.0	1.09
IRA94S	Styrene divinylbenzene macroreticular	370–470	55–60	0–9	12–14	—	4.2	1.25	1.05
IRA68	Acrylic gel	350–450	46–52	0–7	15	—	8.7	3.3	1.1
ZrP	Hydrous zirconium phosphate	50	15	1–11	0	—	5–7	—	2.76
ZrO₂	Hydrous zirconium oxide	80	60	1–11	0	—	—	—	3.25

$$R - COOH + OH^- \rightarrow H_2O + R - COO^- \tag{4-3}$$

where R represents the resin structure. For anion exchange, the reaction involves protonation of secondary or tertiary ammonium groups on the resin:

$$R - N(CH_3)_2 + H^+ \rightarrow R - \left[NH(CH_3)_2\right]^+ \tag{4-4}$$

4.1.1.3 Adsorption-Elution

In a cation exchange process, a cation is adsorbed on the resin to maintain the charge balance after deprotonation of the resin:

$$R - COO^- + M^+ \rightarrow R - COO^-M^+ \tag{4-5}$$

Elution of the cation is achieved by reversing the polarity. The elution process is effectively a neutralization reaction, involving reprotonation of the active group:

$$R - COO^-M^+ + H^+ \rightarrow R - COOH + M^+ \tag{4-6}$$

Similarly, an anion is adsorbed after protonation of the resin:

$$R - \left[NH(CH_3)_2\right]^+ + A^- \rightarrow R - \left[NH(CH_3)_2\right]^+ A^- \tag{4-7}$$

whereas, under a cathodic potential on the electrochemical ion-exchange electrode, the adsorbed anion is eluted:

$$R - \left[NH(CH_3)_2\right]^+ A^- + OH^- \rightarrow R - \left[N(CH_3)_2\right] + H_2O + A^- \tag{4-8}$$

By applying a potential across the cell, anions migrate toward the anode, and cations migrate toward the cathode. Changes in pH are controlled by reactions in the counter electrode. Thus, during cation adsorption, the pH of the solution is decreased, whereas during cation elution, the pH is increased. Similarly, the pH is increased during anion adsorption and decreased during anion elution.

4.1.1.4 H^+-OH^- Competition

The electrochemical ion-exchange method suffers from interference problems because, during cation adsorption, hydrogen ions produced at the anode interfere with the adsorption of metal ions (M^+) and, eventually, deactivate the deprotonated sites. For example, data given in table 4-2 show that the

Table 4-2. Values of cesium concentration remaining in solution as a function of time and pH*

5<pH<8.6	Time (min)	3.6	12	32	43	57	69	—	—
	Cs (ppm)	67	32	5.4	2.1	0.6	0.4	—	—
3<pH<6.8	Time (min)	1.9	11	19	37	48	66	81	115
	Cs (ppm)	87	50	24	12	10	7.2	6.5	5.3
2.8<pH<3.7	Time (min)	4.2	14	24	39	74	112	159	—
	Cs (ppm)	62	52	46	38	22	18	12	—
2.4<pH<2.9	Time (min)	9.7	36	66	85	127	—	—	—
	Cs (ppm)	83	67	54	46	39	—	—	—

*Cesium was adsorbed onto a CG50 cationic electrochemical ion-exchange electrode at a cathodic current density of 2 mA/cm^2 (Turner et al., 1992)

efficiency and kinetics of cesium removal by a CG50[1] resin decrease as the pH decreases. Similarly, deprotonation of the resin occurs by reaction with hydroxyl ions generated at the cathode during cation elution. For these reasons, the performance of the electrochemical ion-exchange method depends on the pH of the feed solution, as well as its buffering capacity. For cation electrochemical ion-exchange processes, feed solutions that have alkaline pH or contain a basic salt could neutralize the hydrogen ions

produced on the counter electrode and result in high-cell efficiency. An alternative way of dealing with competitive reactions is to use a combined cationic–anionic electrochemical ion-exchange configuration, which is good for maintaining pH control.

4.1.1.5 Factors Affecting Cell Performance

For a given solution containing a number of ions, the performance of the cell depends on four process variables:

(i) Cell current (A): For current density in the range of 1 to 5 mA/cm^2 (6–30 mA/in.^{2}), an increased cell current leads to an improved cell performance. At higher values of current density, the extra evolved gas disturbs the uniformity of flow through the cell, leading to a decrease in cell performance.

(ii) Flow rate (F): Increases in flow rate generally lead to a proportionately reduced performance due to shorter residence time of feed in the cell.

(iii) Feed concentration (M): For a particular cell current and flow rate, an increase in the feed concentration of the ions of interest and of the background ions will lead to a rise in the effluent concentration and, hence, early breakthrough.

---

[1]The CG50 resin is a preground form of the IRC50 ion-exchange resin, commercially produced by Rohm and Haas (Philadelphia, Pennsylvania) and is commonly used in metal recovery and biochemical applications.

(iv)   Cell efficiency (E): Cell efficiency depends on several factors, including adsorption kinetics, feed pH, flow cell design, and possibly on the degree of loading of the electrode.

The performance of the cell can be defined as a single parameter, CP, which is proportional to the four process variables:

$$CP \propto \frac{(A)(E)}{(F)(M)} \qquad (4\text{-}9)$$

The CP is used to assess the likely performance of a cell and make comparisons of cells using differing values of feed flow and current density (Bridger et al., 1991; Jones et al., 1992; Fletcher et al., 1992). The higher the CP, the better the cell performance. Note that equation (4-9) is valid only for a limited range of cell current (e.g., 1–5 mA/cm^2) because hydrogen gas evolution above that range will significantly disturb the plug flow pattern in the flow cell.

If X is the number of milliequivalents (meq) of the ion requiring adsorption in 1 hr, then

$$X = F(L / hr) \times M(meq / L) \qquad (4\text{-}10)$$

Also, the number of coulombs (C) passing through the cell in an hour is 3,600 × A, and the number resulting in cation adsorption is 3,600 × A × E. Noting that 96,487 C, which corresponds to the Faraday constant, are required for the adsorption of 1,000 meq, the parameter Y, which is the number of milliequivalents adsorbed, can be defined as:

$$Y = \frac{(A)(3,600)(E)(1,000)}{96,487} \qquad (4\text{-}11)$$

The CP parameter, which can be defined as the ratio of the milliequivalents of ions adsorbed to the milliequivalents of ions requiring adsorption, can be calculated from the equation:

$$CP = \frac{Y}{X} = \frac{(A)(3,600)(E)(1,000)}{(F)(M)(96,487)} \qquad (4\text{-}12)$$

Thus, in this simple manner, the cell performance can be determined as operated in various modes and for various ions of interest. Note that values of CP higher than one would indicate the need to use electrodes with higher surface area due to the adsorption of competing ions.

4.1.1.6 Modeling Electrochemical Ion-Exchange Processes

Detailed modeling of electrochemical ion-exchange processes has been undertaken by Cumming et al. (1997). A simplified representation of a small section of half the flow cell is shown in figure 4-2. In the figure, C denotes concentration, and J_i is the flux of species i, resulting from gradients in species concentration and cell potential. For a one-dimensional flow-through operation, a convective flow term can be added and an equation for the flux of species i can be written as

143
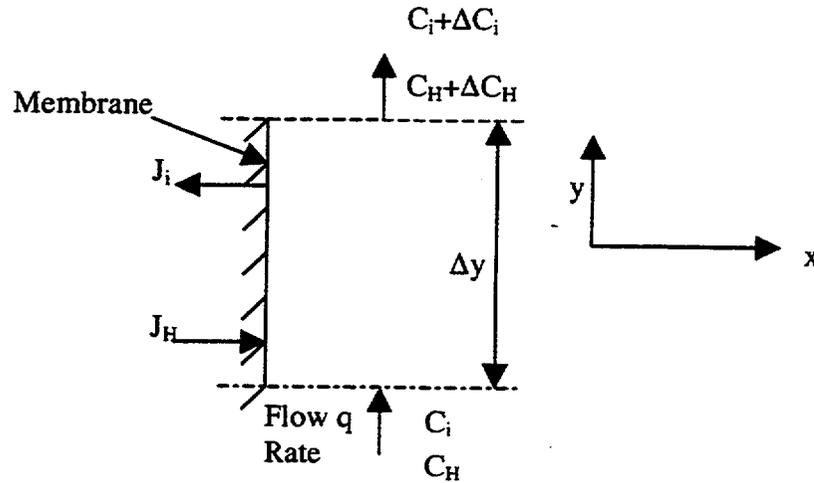
Figure 4-2. Schematic of a differential part of the membrane in an electrochemical ion-exchange cell (Reproduced from Transactions of the Institution of Chemical Engineers, Vol. 75, Cumming, I., H. Tai, and M. Beier, A model to predict the performance of an electrochemical ion exchange cell, pp. 9–13, with permission from the Institution of Chemical Engineers).

$$J_i(y) = -D_i \left| \frac{dc_i}{dx} + z_i c_i \frac{F}{RT} \frac{d\varphi}{dx} \right| + c_i v \qquad (4\text{-}13)$$

where F is the Faraday constant, R is the gas constant, T is the absolute temperature, z is the ionic charge, v is the convection velocity toward the membrane, D is the diffusion coefficient, and φ is the potential between the cell center and the membrane surface. The three terms in the equation arise, respectively, from diffusion due to a concentration gradient, electrical migration due to a potential gradient, and convective flow.

By assuming a constant potential gradient, b, for x values near the membrane surface, and assuming either no concentration gradient or convective flow, the equation for the flux of species i can be simplified as[2]

---

[2] A comparison by Cumming et al. (1997) of experimental data and model predictions for removal of zinc, copper, and nickel over a range of current densities indicate reasonable predictions can be obtained using these assumptions. They recommend, however, detailed experiments to evaluate the effects of cell potential and convective flow on the flux to help design scale-up operations.

$$J_i(y) = -D_i z_i c_i \frac{F}{RT} b \qquad (4\text{-}14)$$

Based on this flux, the local current density (I) carried by the ions can be calculated from Faraday's law as

$$I(y) = F \sum_i z_i J_i(y) \qquad (4\text{-}15)$$

For the cell illustrated in figure 4-1 (a two-electrode electrochemical ion-exchange configuration), the mass balance for the segment of the cell shown in figure 4-2 for all components, excluding hydrogen ions and any anions, is

$$c_i q - (c_i + \Delta c_i) q + 2J_i(y) w \Delta y = 0 \qquad (4\text{-}16)$$

or, in the differential form,

$$q \, dc_i = 2J_i(y) w \, dy = -2w D_i z_i c_i \frac{F}{RT} b \, dy \qquad (4\text{-}17)$$

where q is the volumetric liquid flow through the cell, and w is the cell width. The flux term is doubled because the module contains two electrochemical ion-exchange cells, one on each side of the module.

By integrating Eq. (4-17) from entrance conditions (c_i^f, 0) to a point in the y-axis (c_i, y), the resulting equation is

$$c_i(y) = c_i^f \exp\left[-2w D_i z_i \frac{F}{qRT} b y \right] \qquad (4\text{-}18)$$

The introduction of the electroneutrality condition

$$\sum_i z_i c_i = 0 \qquad (4\text{-}19)$$

allows one to derive the hydrogen concentration at the exit:

$$c_H^0 - c_H^f = \sum_i z_i \left(c_i^f - c_i^0 \right) \qquad (4\text{-}20)$$

Electrochemical Methods

Also, the cell current over a length of the cell is

$$\Delta I = 2I(y)w\Delta y = 2w\Delta yF\sum_i z_i J_i(y) = -2w\Delta yF\sum_i z_i^2 D_i c_i \frac{F}{RT}b \tag{4-21}$$

The hydrogen ion can be considered separately from the other cations, and a differential equation can be written:

$$
\begin{aligned}
dI = & -2wdyF\sum_i z_i^2 D_i c_i^f \frac{F}{RT}b \ \exp\left(-\frac{2wz_iFbD_iy}{RTq}\right) \\
& -2wdyD_H\frac{F^2b}{RT}\left\{c_H^f + \sum_i z_i c_i^f\left[1 - \exp\left(-\frac{2wz_iFbD_iy}{RTq}\right)\right]\right\}
\end{aligned}
\tag{4-22}
$$

By integration over the length of the cell, the total cell current is derived:

$$
\begin{aligned}
I = & -2wF\sum_i z_i^2 D_i c_i^f \frac{F}{RT}b\ \frac{\exp\left(-\dfrac{2wz_iFbD_iL}{RTq}\right)-1}{\dfrac{2wz_iFbD_i}{RTq}} \\
& -2wD_H\frac{F^2b}{RT}\left\{c_H^fL + \sum_i z_i c_i^f\left[L+\frac{\exp\left(-\dfrac{2wz_iFbD_iL}{RTq}\right)-1}{\dfrac{2wz_iFbD_i}{RTq}}\right]\right\}
\end{aligned}
\tag{4-23}
$$

or,

$$
\begin{aligned}
I = & -2wF\left\{\sum_i -z_i\frac{qc_i^f}{2w}\left[\exp\left(-\frac{2wz_iFbD_iL}{RTq}\right)-1\right]+D_H\frac{Fb}{RT}c_H^fL\right\} \\
& -2wF\left\{LD_H\frac{Fb}{RT}\sum_i z_i c_i^f + \frac{q}{2w}\sum_i\frac{D_H}{D_i}c_i^f\left[\exp\left(-\frac{2wz_iFbD_iL}{RTq}\right)-1\right]\right\}
\end{aligned}
\tag{4-24}
$$

Eq. (4-24) can be simplified to

$$I = -2wF\left\{\sum_i\left(\frac{D_H}{D_i}-z_i\right)\frac{qc_i^f}{2w}\left(\exp\left[-\frac{2wz_iFbD_iL}{RTq}\right]-1\right)+D_H\frac{FbL}{RT}\left(c_H^f + \sum_i z_i c_i^f\right)\right\} \tag{4-25}$$

which can be rewritten as

146

$$I = -2wF\left\{\sum_i \left(\frac{D_H}{D_i} - z_i\right)\frac{q}{2w}\left(c_i^o - c_i^f\right) + D_H \frac{FbL}{RT}\left(c_H^f + \sum_i z_i c_i^f\right)\right\}$$

(4-26)

Either of the two equations [(4-24) or (4-26)] has to be solved by trial and error for b with the use of a set of experimental data. Subsequently, b can be substituted into Eq. (4-18) and (4-20) to solve for the concentration profile and pH. Figure 4-3 shows experimental measurements and model predictions for the performance of an electrochemical ion-exchange cell treating water containing 390–450 ppm sodium, with pH from 1 to 3 (Cumming et al., 1997). The liquid flow rate was in the range of 5.6×10^{-2}–4.4×10^{-1} cm³/sec. The figure illustrates that the model reasonably agrees with the experimental data on the percentage removal of sodium. The figure also shows that lower flow rates enhance sodium removal, and that lower pH deteriorates cell performance significantly. This decline in performance, which becomes significant at a pH of 3 or less, is due to competition from the hydrogen ions, and establishes a low pH limit for a cationic electrochemical ion-exchange adsorption operation. Similarly, the anionic electrochemical ion-exchange adsorption operation has an upper pH limit of about 11.5 because of competition from hydroxyl ions present in high concentrations under alkaline conditions. Other data, not included in the figure, demonstrate that higher current densities enhance sodium removal (Cumming et al., 1997).

4.1.1.7 Tafel and Butler-Volmer Equations

In the foregoing analysis, the cell was assumed to operate under galvanostatic conditions (constant current), and the relationship between cell current and cell potential was not considered explicitly. The cell potential (potential difference between the two platinum-coated titanium electrodes) will be governed by the polarization of the two electrodes and ohmic potential drop between the two electrodes:

$$E_{cell} = E_a - E_c - IR_{cell}$$

(4-27)

where E_a is the anode potential (measured with respect to a reference electrode), E_c is the potential of the cathode, I is the cell current, and R_{cell} is the cell resistance. The cell resistance depends on the cell geometry, solution conductivity, and porosity of the ion-exchange membrane surrounding the cathode. The polarization of the anode and cathode depend on the specific electrochemical reactions. For the cathode, the main reaction is the reduction of proton (for acidic solutions) or the reduction of water (for near-neutral solution) to hydrogen. The current-potential relationship for the proton reduction may be expressed by a generalized Butler-Volmer reaction kinetics that includes activation or charge transfer controlled forward and reverse reaction rates:

$$I_{H=si_{0_H}}\left[\exp\left(\frac{\alpha_a F}{RT}\left(E_c - E_{eq}\right)\right) - \exp\left(\frac{-\beta_c F}{RT}\left(E_c - E_{eq}\right)\right)\right]$$

(4-28)

where s is the surface area; i_{0_H} is the exchange current density for proton reduction on the platinum-coated titanium electrode; α_a the anodic and the β_c cathodic transfer coefficients; F the Faraday
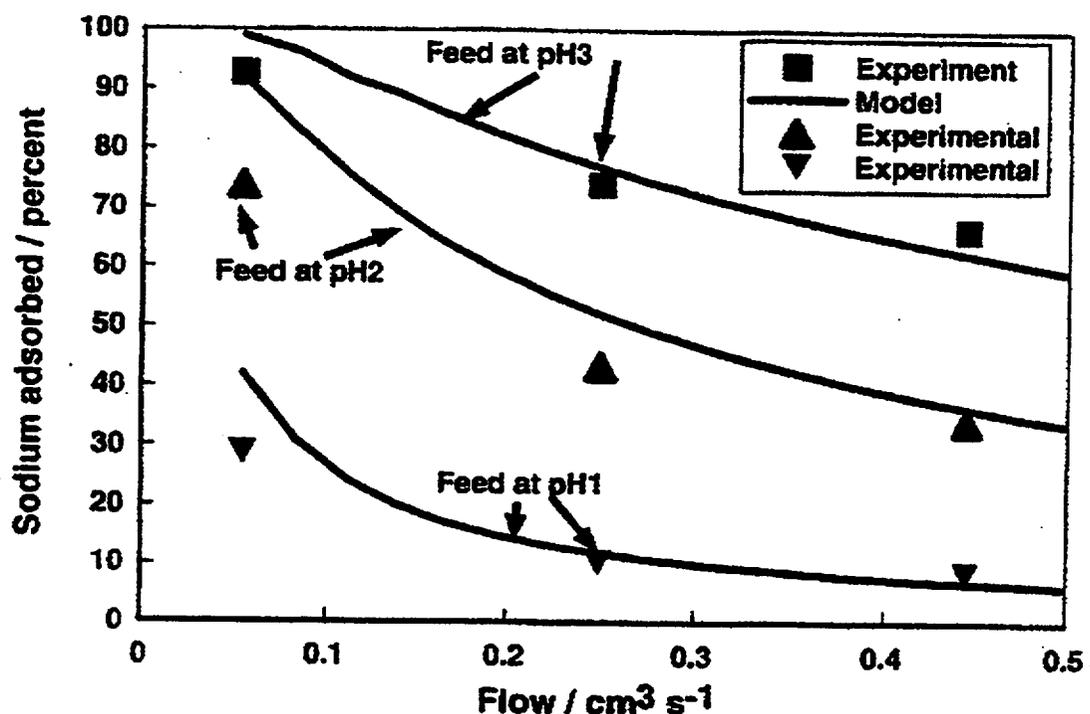
Figure 4-3. Comparison of experimental data (symbols) and model predictions (solid lines) for removal of Na^+ by electrochemical ion exchange (Reproduced from Transactions of the Institution of Chemical Engineers, Vol. 75, Cumming, I., H. Tai, and M. Beier, a model to predict the performance of an electrochemical ion exchange cell, pp. 9–13, with permission from the Institution of Chemical Engineers).

constant; R the gas constant; T the absolute temperature; and E_{eq} the equilibrium potential of the proton reduction reaction. The term (E_c-E_{eq}) represents the overpotential.

It can be seen from Eq. (4-28) that, at potentials far below the equilibrium potential, the first term vanishes, leading to a Tafel type relationship:

$$I_H = -si_{0_H}\left[\exp\left(\frac{-\beta_c F}{RT}(E_c - E_{eq})\right)\right]$$

(4-29)

where the negative sign indicates a cathodic current. The Tafel relationship indicates that the current becomes larger as the overpotential is increased in magnitude. In acidic solutions, however, a limiting current is reached governed by the rate of mass transfer of protons to the electrode surface. A more generalized Tafel expression that includes mass transfer controlled process is given by

$$I_H = -si_{0_H} \frac{\left[\exp\left(\dfrac{-\beta_c F}{RT}(E_c - E_{eq})\right)\right]}{\left[1 + \dfrac{i_{0_H}}{i_{lim}}\exp\left(\dfrac{-\beta_c F}{RT}(E_c - E_{eq})\right)\right]}$$ (4-30)

where i_{lim} is the limiting current density for proton reduction. The exchange current density, i_{0_H}, is a function of pH and decreases with an increase in pH. At near-neutral pH, water reduction reaction replaces the proton reduction reaction as the cathodic process. Since access of water to the electrode surfaces is typically not transport limited (except in extremely concentrated or nonaqueous solutions), the current for water reduction obeys the Tafel relationship shown in Eq. (4-29). The exchange current density, however, is different from that of the proton reduction reaction. At the anode of the cell, a similar relationship to Eq. (4-30) is likely to hold for the oxidation of water—the limiting current density being dictated by the transport of protons away from the electrode. Finally, as the cell current increases, the ohmic drop may dominate the cell potential depending on the cell resistance. Together, these factors will govern the power requirements for the process and the needs for heat dissipation (due to ohmic heating).

4.1.2 Performance

Table 4-3 lists the distribution coefficient values, K_d, for several inorganic exchangers effective in selective removal of cesium from sodium-containing waste streams by conventional ion exchange. Note that the separation factors vary with the pH and sodium concentration of the solution—two of the important operating parameters to consider in the application of ion-exchange technology (discussed in chapter 3). The ion exchangers listed in the table were investigated for use in electrochemical ion-exchange applications (Turner et al., 1992), specifically with respect to their selectivity, capacity, and chemical stability. Turner et al., (1992) concluded, based on the study, that zirconium phosphate is the most attractive for further development in electrochemical ion-exchange applications. Zirconium phosphate has the additional advantage it does not swell during hydration or subsequent adsorption of cations—unlike organic resins that can swell up to 100 percent of the original volume, depending on the structure and degree of crosslinking of the polymeric backbone.

4.1.3 Operating Parameters

As the analysis given in the preceding section suggests, for a given cell design and feed solution, the two main degrees of freedom in an electrochemical ion-exchange application are the applied current and the flow rate. Small-scale experiments have to be performed to determine the optimum values of these two parameters for the application of interest.

4.1.3.1 Solution Chemistry

To ensure the success and longevity of the electrochemical ion-exchange application, the chemistry of the solution treated must be well known. For example, changes in pH could result in chemical reactions that change the oxidation states of the ions. The effect of high concentrations of salts in solution must be evaluated because competition for adsorption sites by other ions could lead to low cell efficiency.

149

Table 4-3. Effect of pH and sodium concentration on cesium distribution coefficient (K_d) values for various inorganic exchangers (Turner et al., 1992)

Adsorber	Na Concentration (g/L)	pH Range Where $K_d<10^3$	pH Range Where $10^3<K_d<10^4$	pH Range Where $10^4<K_d<10^5$
Zeolon 500[*]	0.23	0–0.97	0.97–3.03	3.03–12
	1.0	0–1.33	1.33–12	—
	10.0	0–6.25	6.25–12	—
IE-96[†]	0.23	0–2.48	2.48–3.04	3.04–12
	1.0	0–2.73	2.73–12	—
	10.0	0–4.44	4.44–12	—
Titanium Phosphate (TiP)	0.23	11.35–12	0–11.35	—
	1.0	10.1–12	0–10.1	—
	10.0	7.57–12	0–7.52	—
Zirconium Phosphate (ZrP)	0.23	—	0–1.07, 8.43–12	1.07–8.43
	1.0	10.15–12	0–1.25, 5.47–10.15	1.25–5.47
	10.0	9.00–12	0–7.83	—
Ammonium Phospho-Tungstate+ZrP	0.23	—	8.72–12	0–8.72
	1.0	—	6.61–10.2	0–6.61
	10.0	—	4.59–9.00	0–4.59

[*]Zeolon is an aluminosilicate zeolite with a mordenite-type structure.
[†]IE-96 is a high-capacity aluminosilicate zeolite produced by UOP Molecular Sieves (Mt. Laurel, New Jersey) with relatively high selectivity for cesium over other alkali metals.

The effects of high ionic strength can be alleviated to some extent by the use of a different adsorbent material. For example, the results of a test comparing waste treatment using an amorphous zirconium phosphate and a γ-zirconium phosphate adsorbent in a flow-through cell indicate that the performance of electrodes made from γ-zirconium phosphate is generally better than that of those made from amorphous zirconium phosphate, especially at low flow rates (Turner et al., 1992). A combined cation/anion electrochemical ion-exchange unit (e.g., using a combination of a γ-zirconium phosphate cation-exchanger and an IRA910 anion-exchanger) produces enhanced contaminant removal for the waste stream at low flow rates, as well as providing a better control of the pH.

Knowledge of the solution chemistry helps to predict the various precipitates that could form due to solubility limits and, thus, avoid misinterpretation of the results or mistakes in selecting the cell design. For example, high concentrations of cobalt in solution can lead to cobaltous hydroxide [$Co(OH)_2$] precipitation on the electrode. Thus, for application of cathodic electrochemical ion-exchange to removal of cobalt from such solutions, the concentration of cobalt should be adjusted to levels below the solubility limit of the hydroxide, 3.2 mg/L (2.7×10^{-5} lb/gal.) (Allen et al.,1992). Alternatively, anionic electrochemical ion-exchange, which is effective for adsorption of the cobalt hydroxyl anion, can be used. Anionic electrochemical ion-exchange is also useful for removal of the uranium and plutonium hydroxyl anions. Other types of pretreatment methods might be required before an electrochemical ion-exchange application. Examples of pretreatment include electrolytic oxidation of oxalate to carbon dioxide and neutralization of nitric acid with ammonia, followed by electrolytic reduction to ammonium nitrite and thermal decomposition to nitrogen gas at 70 °C (158 °F) (Jones et al., 1992).

Another important factor with respect to the effect of solution chemistry on electrochemical ion-exchange processes is the possible interference of complexing agents present in solution. For example, complexation of cobalt by ethylenediaminetetra-acetic acid (EDTA) changes the cationic cobalt (II) species to an anionic cobalt-EDTA complex. However, the anionic EDTA-complex can be efficiently removed by anionic electrochemical ion exchange. An alternative solution is to photochemically decompose the chelating complex to release cobalt as a cation and proceed with cationic electrochemical ion-exchange adsorption.

General patterns for selectivity between certain groups of ions and specific adsorbers have been established. For example, γ-zirconium phosphate exhibits higher selectivity for the adsorption of divalent cobalt compared to monovalent lithium and cesium. Selectivity coefficients for cation decontamination of various waste streams using zirconium phosphate (ZrP), butyl-ammonium zirconium phosphate (Bu-am ZrP), hexyl-ammonium zirconium phosphate (Hex-am ZrP), γ-zirconium phosphate (γ-ZrP), IRC–50, and hydrous titanium oxide (HTiO) are listed in table 4-4.

Knowledge of solution chemistry is important not only in optimizing the adsorption process, but also in designing an efficient separation scheme for the elution step. For example, lithium, sodium, and cesium all have soluble hydroxides at any pH, whereas cobalt has a limited solubility at high pH due to the formation of solid cobaltous hydroxide. This observation can help one to establish an elution scheme for separating the alkalies from cobalt. For example, the alkali ions can be eluted at pH 11—a condition in which cobalt will not be readily eluted from the electrode. Subsequently, cobalt can be released from the adsorber at a pH of 1.5.

The ion-exchange capacity of some adsorbers changes with pH. For example, the exchange capacity of hydrous titanium oxide changes from 2 meq/g at a pH of 12 to 1.5 meq/g at a pH of 4. Thus, the need for pH control has to be evaluated for electrochemical ion-exchange applications.

4.1.3.2 Performance Variables

Key performance variables are the choice of adsorber, the current density, the solution pH, and the flow rate. The effects of the first three variables on cell efficiency are studied using batch experiments, whereas the effect of flow rate is studied using flow experiments. Identifying an optimum current density, where the decontamination factor is maximized, is possible.

Table 4-4. Selectivity coefficients from batch cationic electrochemical ion-exchange adsorption experiments (data from Turner et al., 1992)

Adsorber	Magnox[*] (Cs^{+} versus Na^{+})	PWR[*] (Co^{2+} versus Li^{+})	MTR[*] (Co^{2+} versus Cs^{+})
ZrP	2	0.86	1.64
Bu-am ZrP	1.63	1	0.42
Hex-am ZrP	0.7	1.86	1.14
γ-ZrP	1.71	11.1	20.0
IRC-50	1.66	10.0	2.1
HTiO	1.9	1.2	0.42
[*]Magnox, PWR, and MTR are waste streams from spent fuel storage pond waters of different reactor types.			

Other factors affecting the overall performance of the cell are the electrical resistance of the adsorber, its coulombic efficiency, and the lowest adsorbance level that can be achieved. For adsorbers with low electrical resistance, using high current densities with a low voltage (<60 V) is possible. In practice, the cell resistance might increase after a number of cycles, and, thus, the current density will decrease at a constant externally applied potential. The coulombic efficiency of the cell can be determined by measuring the time required to remove 95 percent of the cesium from a 1-L solution with an initial cesium concentration of 200 ppm. High efficiency indicates that the current passing through the cell is used to create adsorption sites on the exchanger. Determining the decontamination factor achievable for a given configuration is important. A test can be designed to identify the lowest adsorbance level in a 1-L solution of 200 ppm cesium at a current density of 5 mA/cm^2 (30 mA/in.^{2}) (Turner et al., 1992).

A combination of electrodes could be used to improve the efficiency of an electrochemical ion-exchange cell. For example, an adsorber with high resistance but high capacity can be used in combination with a low-resistance electrode. Usually, organic adsorbers have higher resistance and higher capacity (75 percent of the theoretical limit) compared to inorganic adsorbers, which have lower resistance and lower capacity (11 percent of the theoretical). The kinetics of ion exchange on these inorganic adsorbers are usually slower than on organic adsorbers, which indicates that the mobility of ions in the internal structure of the inorganic adsorber is slow.

Experimental studies are needed to evaluate the effects of adsorption/elution time periods on the performance of the electrochemical ion-exchange systems. For example, the net sodium adsorption from a cesium/sodium solution can be minimized by using a 20-sec elution time (slower elution kinetics) and 10-sec adsorption cycle (decontamination factor = 1.5), but better performance can be achieved with 10-sec adsorption and 10-sec elution cycles (decontamination factor = 7.5).

4.1.3.3 Cell Potential

The cell potentials listed in table 4-5 are typical for electrochemical ion-exchange applications. The cell potential is increased as the flow rate increases to maintain constant current density, but a maximum

Table 4-5. Batch electrode performance parameters for electrochemical ion exchange (EIX) (data from Turner et al., 1992)

| Electrode | EIX Construction* | | Cell Potential (V) | Coulombic Efficiency (min) | Lowest Adsorbance Level (ppm) |
	EIX Layer	Outer Layer			
BJ/123	15 g CG50 0.5 g Graphite	5 g CG50 Viledon	60	30	0.05
BJ/124	15 g CG50 0.5 g Graphite	None	60	60	5.0
BJ/126	15 g IRC84 0.5 g Graphite	5 g IRC84 Viledon	16	50	1.0
BJ/128	15 g IRC84 0.5 g Graphite	5 g CG50 Viledon	17	53	1.0
BJ/130	7.5 g CG50 7.5 g IRC84 0.5 g Graphite	2.5 g CG50 2.5 g IRC84	31	32	0.1
BJ/131 (2 part electrode)	Upper: 7.5 g CG50, 0.25 g Graphite Lower: 7.5 g IRC84, 0.25 g Graphite	Upper: 2.5 g CG50 Viledon Lower: 2.5 g IRC84 Viledon	23	16	5.0
BJ/132	20 g IRP64 0.5 g CG50	Viledon	42	64	3.0
BJ/136	20 g IRC84 5.0 g CG50	6 g IRC84 Viledon	36	22	0.1
BJ/137	12.5 g IRC84	5 g IRC84	35	60	0.2
BJ/142	20 g ZrP Silicon binder	None	60	1,000	5.0
BJ/144	30 g ZrP	None	12	25	0.1
BJ/146	45 g ZrP	None	20	24	<0.1
*The binder is Kraton unless indicated otherwise. Viledon is a microporous polyimide cloth.					

value (<60V) is established for safety reasons. In a typical electrochemical ion-exchange application, the applied potential controls the effluent pH as ions are released in the counter electrode. Table 4-6 shows the results of a multicell cathodic electrochemical ion-exchange application on a Magnox waste stream.

Caution should be exercised in applications where the electrochemical ion-exchange electrode is an anode (e.g., in anion-exchange application). At high anodic potentials, anions could be oxidized. For example, the chloride ion can turn into the hypochlorite ion, which causes degradation of the resin. Thus, in this type of application, the wire metal in the electrochemical ion-exchange electrode is surrounded by a thin coating of a cation-exchange membrane, and the anion-exchange resin is cast around the electrode. The water decomposition reaction in this design occurs at the boundary of the cation and anion resins.

4.1.3.4 Regeneration

The electrochemical ion-exchange method does not suffer from regeneration costs as the conventional ion-exchange method. However, the electrochemical ion-exchange adsorber material loses part of its activity after a long period of adsorption/elution cycles. For example, for the zirconium phosphate cation-exchanger, a hydrolysis reaction can convert it to hydrous zirconia:

$$Zr(HPO_4)_2 + 6OH^- \rightarrow Zr(OH)_4 + 2PO_4^{3-} + 2H_2O \qquad (4\text{-}31)$$
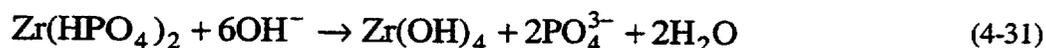
This reaction limits the useful life of a zirconium phosphate electrode to about 6 yr, which is still a long period of operation.

Nevertheless, one study indicated that the exchanger could be regenerated by converting hydrous zirconia to zirconium phosphate. This regeneration is achieved by absorption of phosphoric acid while the electrode is poised at an anodic potential. This procedure not only restores the ion-exchange behavior of the electrode, but also enhances its removal efficiency (Allen et al., 1992).

4.1.4 Application to Hanford Wastes

Experimental use of an electrochemical ion-exchange system for cesium-137 and cobalt-60 removal from a reactor/fuel (Magnox) pond water (100 ppm Na and pH of 11.5) produced cesium-137 decontamination factors of 100 to 5,000 using a zirconium phosphate electrode over a 25-day period at a throughput of greater than 5.5 bed volumes per hr (equivalent to 64 percent loading of the resin). Decontamination factors greater than 11 for plutonium and equal to 70 for americium in wastes from the production of nuclear fuels were also reported (Jones et al., 1992). Results for decontamination of cesium-137 from a nuclear waste stream containing 100 g/m^3 sodium (8 × 10^{-4} lb/gal.) and 10 g/m^3 cesium (8 × 10^{-5} lb/gal.) included decontamination factors of 5,000 for cesium and 133 for sodium and a volume reduction factor greater than 100 (Allen et al., 1992). A thorough study of electrochemical ion-exchange on various waste streams, including reactor fuel wastes, produced the results summarized in table 4-7 (Turner et al., 1992). These results indicate that large decontamination factors can be achieved. Thus, electrochemical ion exchange is a promising method for treatment of Hanford wastes to reduce radionuclideconcentrations to within acceptable contamination limits for disposal. An advantage of electrochemical ion exchange over conventional ion-exchange technology for processing Hanford wastes is the small amount of eluant

Table 4-6. Decontamination factors (DFs) for cesium and sodium as a function of flow rate*

	Cesium		Sodium		Voltage (V)	pH	Flow Rate (L/hr)
	ppb	DF	ppm	DF			
Feed	860		89				
Effluent	<3	>287	1.1	81	6.6–7.9	2.45	8
	<3	>287	0.7–2.4	37–127	8.0–9.9	2.7	19
Feed	720		70				
Effluent	<3	>240	1.0	70	12.5–13.9	3.06	42
	<3	>240	0.69	101	15.1–16.7	3.18	64
Feed	630		68				
Effluent	<3	>210	0.79	99	17.4–18.8	3.26	98.7
	<3	>210	1.1	62	19.5–20.9	3.4	140

*From a simulated Magnox pond water using a five-module electrochemical ion-exchange plant with zirconium phosphate electrodes (data from Turner et al., 1992)

solution needed, which significantly reduces the amount of secondary waste to be treated. No chemicals, such as nitric acid or formic acid, would be needed for electrochemical elution following treatment of Hanford wastes. No neutralization step after elution would be required because the electrochemical elution process would produce hydroxyl ions, and because no acidic solutions would be used for the elution (Bontha et al., 1994) unless elution of cobalt-60 is also needed, a process that would require acidic pH (see table 4-7). Elution could be accomplished with a much smaller volume of solution, perhaps 30 percent or less than that required for conventional chemical elution, and elution could be accomplished in a period of about 3 hr (Bontha et al., 1994).

However, the use of electrochemical ion-exchange has a disadvantage relative to conventional ion-exchange technology. The resorcinol-formaldehyde to be used in the electrochemical elution process proposed by LMAES may need to be modified into a macroporous foam by the addition of binders such as polystyrene and polybutadiene. (The electrical conductivity of the macroporous structure allows sufficient electrical current to pass through and elute the resin, whereas the low electrical conductivity of conventional resorcinol-formaldehyde resin requires the application of weak acid solutions for elution.) Studies show that the presence of the binder can reduce cesium ion uptake from a Hanford neutralized current acid waste by about 60 percent. This reduction results from the relatively small amount of ion exchanger in the foam, and possibly in a decrease in the effective surface area of the resin due to the presence of the binders (Bontha et al., 1994). Therefore, cesium-137 removal rate from the Hanford low-activity waste by an electrochemical ion-exchange process would be slower than for resorcinol-formaldehyde in a conventional ion-exchange process due to the presence of the binders, and a cesium-137 decontamination factor of 7–10 is expected.

4.1.4.1 Operational Considerations

In electrochemical ion-exchange applications, the possible swelling of organic electrochemical ion-exchange adsorbers needs to be taken into account because disturbance of the plug flow and

Table 4-7. Electrochemical ion-exchange performance for treatment of various waste streams (data from Turner et al., 1992)

Waste Stream	Flow Rate (L/hr)	Adsorber	Cell Potential (V)		Current Density (mA/cm^2)	Decontamination Factor	Elution Conditions	VRF*
			Adsorption	Elution				
PWR Low-level Waste	0.16–0.68	ZrP	23	12	3–5	50–31	Li: pH 11 Co: pH 1.5–2	—
	0.16	IRN78L	5–10	4	3	170		
	0.32	IRN78L	5–10	—	3	>100		
	0.16	IRN78L/ZrP	7.5–23	4–12	3–5	375		
PWR Drain	2.5	ZrP	20	12	3	>125	Li: pH 11 Co: pH 1.5–2	>270
MTR Pond	4.5	ZrP	23	12	3	>100	pH 1.5–2.0	>2,600
	45	ZrP	23	12	3	>500 (Co), >85 (Cs)		
	750	ZrP	23	12	3	>100		
Magnox	1	ZrP	19	12	3	>500	Water	—
	11	ZrP	19	12	3	>80		
	300	ZrP	19	12	3	>100		
Harwell Low-level Waste	0.16	IRN78L/ZrP	15/7.5	12/4	3	>8 (Cs), >75 (Co)' >7 (Cs, Co)	pH 1.5–2	—
	5	IRC50/IRA910	15/4	7/4	3			
Harwell MLW†	0.25	γ-ZrP/IRA910	13/14	2/4	3	11–26	pH 1.5–2	—

*Volume reduction factor.
†Medium level waste.

entrapment of gases will deteriorate cell performance. For example, swelling of CG50 could be as high as 50 percent.

The ion-exchange selectivity of the adsorber has to be investigated for a better understanding of cell behavior. For example, the amorphous zirconium phosphate adsorber shows preference for cesium over sodium for occupancies of less than 0.19, whereas sodium is more strongly adsorbed for occupancies greater than 0.62. The crossover in preferences is found at 0.34. This behavior can be explained by noting that large cavities in the adsorber preferentially adsorb the hydrated cesium ion, which is smaller than the hydrated sodium ion. The dehydrated sodium ion, which is smaller than the dehydrated cesium ion, is adsorbed preferentially onto the smaller cavities (Turner et al., 1992).

Knowledge of the waste streams to be treated is required for selecting an optimum adsorber. Low capacity adsorbers, such as the zirconium phosphate (11 percent maximum capacity of its theoretical), are good for low-concentration streams or for selective adsorption through potential reversal.

The mode of operation is also important. For example, an anionic–cationic electrochemical ion-exchange treatment mode for a 0.01-M potassium nitrate solution could give only 85 percent cation removal efficiency and result in low effluent pH (1.5). When the two electrodes were combined in the same cell, the efficiency rose to 99.45 percent, and in a four-electrode configuration, the efficiency was 97.5 percent. The difference in performance of the four and two cationic–anionic electrochemical ion-exchange modes is probably due to the absence of gas production in the latter configuration. A way to increase the efficiency in the four-electrode cationic-anionic electrochemical ion-exchange mode is to pass higher current density through the anionic electrochemical ion-exchange half cell.

Experiments using a zirconium phosphate electrochemical ion-exchange electrode show that a few cycles are required at startup to achieve optimum performance of the cell (Turner et al., 1992). The initial cycle, during which the kinetics were slower and the electrode had a higher starting potential, served to condition the electrode. This is probably due to the progressive hydration of the zirconium phosphate. The second and subsequent cycles had faster kinetics and lower cell voltages.

Another important operational consideration is the observed increase of the lowest adsorbance level if repeated aliquots of cesium were adsorbed without intermediate elution. Although the lowest adsorbance level of a zirconium phosphate electrode was less than 0.1 ppm, experiments have indicated that the 24th aliquot of cesium corresponded to a loading of only 11 percent (Turner et al., 1992). Compared to organic resins, where a similar decline in performance was not observed until 75 percent loading, this is a significant disadvantage of electrochemical ion exchange. However, when the electrochemical ion-exchange electrode had been fully eluted, its adsorption characteristics were found to be restored—both in terms of kinetics and lowest adsorbance level—giving decontamination factors greater than 2,000. The decrease in decontamination factor with increased loading is interpreted due to the low internal mobility of adsorbed cation within the electrode (Turner et al., 1992). The low mobility resulted in local concentration of occupied sites that had risen more rapidly at the surface of the electrode, inhibiting the rate of further adsorption beyond a mean of approximately 10 percent.

Regarding the pH, feed streams with salt concentrations less than 1 meq/L are good candidates for a cationic electrochemical ion-exchange application. For feed streams with concentrations higher than 1.5 meq/L, the nature of the counter ion becomes important. For example, 100 ppm sodium carbonate salt

Electrochemical Methods

solution contains 4.4 meq/L and the pH is about 3 because of the buffering capacity of the carbonate ion. However, for a non-buffering salt solution (e.g., Na_2SO_4), the pH would be 2.4 and cationic electrochemical ion-exchange would be inappropriate. The decrease of pH below 3 should be controlled by using a combination of the cationic electrochemical ion-exchange electrode with an anionic electrochemical ion-exchange electrode.

Also, chemical stability tests should be conducted to ensure the durability of the material during a long, continuous period of operation.

The unique ability to reuse the cell continuously, with controlled elution on the same eluant volume, results in a small volume of secondary waste for disposal, as well as a long time cycling operation. For example, for 30,000 m^3 (8,000,000 gal.) of treated waste with a volume reduction factor of 3,000, only 10 m^3 (2,600 gal.) of secondary waste are generated by an immobilization process that results in 18 m^3 (640 ft^3) of cement material for disposal (Turner et al., 1992).

Studies ranging from benchtop batch cells to pilot plant flow-through cells were conducted by Turner et al. (1992). The studies used radioactive waste stream simulants and actual low-level waste stream samples. The power requirements in these types of studies depend on a number of factors, including electrode design, cell current density, and solution conductivity. For example, in one study involving treatment of a plutonium-containing waste stream, the electrical energy requirements ranged from 0.03 to 0.22 kW-hr/L. Turner et al. (1992) estimated the power consumption for the treatment of a number of waste streams. For an effluent rate of 1,000 L/hr, the total power requirement ranged from 0.0024 to 0.206 kW-hr/L, depending on the waste stream composition. This estimated range of power requirement does not include power consumption by pumps and ventilators. However, it was suggested by Turner et al. (1992) that because of the relatively small size of the plants, the power requirements of the auxiliary systems will not add significantly to the power requirements for the electrochemical ion-exchange system.

It must be noted that the current densities employed in an electrochemical ion-exchange process are relatively small, approximately 3–5 mA/cm^2. The conductivities of the solutions range from 8 to 800 μS/cm. The ohmic heating will be proportional to i^2R, where i is the current density and R is the resistance (inverse of conductance). Assuming the lowest conductivity and highest current density, an ohmic energy of about 3 W/cm^3 can be calculated. The potential ohmic heating of the electrochemical cell by this amount of energy will depend on the specific cell configuration (e.g., flow rate).

4.1.4.2 Safety Considerations

The process control capability afforded by the extra variable (potential) makes the electrochemical ion-exchange operation particularly attractive because of the minimal safety considerations. The electrochemical ion-exchange cells are compact and easily controlled from an operations room. The performance of the method can be remotely monitored by the effluent pH, activity, and conductivity. Small volumes of sample can be drawn periodically for laboratory analysis.

Replacement of the electrodes seems an important safety issue, but only after years of operation. In cases where the electrodes need replacement early because of radiation damage (organic adsorbers) or osmotic shocks (inorganic adsorbers), the complete module can be replaced, which reduces the potential for

158

exposure of maintenance staff to ionizing radiation. When performing maintenance, industrial practices for safety in radiological environments should be observed.

In general, electrochemical ion exchange does not require high pressures to operate. Also, electrochemical ion-exchange requires a minimal number of moving parts (low speed pumps and fluid valves), which results in more reliable operation. The electrochemical ion-exchange process itself will employ direct electrical current, and circulating equipment such as pumps will likely employ an alternating electrical current. Therefore, appropriate industrial practices for safety around electrical equipment, both alternating current and direct current, should be observed.

Electrochemical treatment of alkaline water can produce hydrogen and oxygen gases. Accumulations of these gases can be flammable or even explosive. Therefore, steps should be taken to ventilate the process and remove such gases for discharge to the atmosphere, where the flammable hydrogen can become diluted to noncombustible concentrations.

4.1.4.3 Comparable Operations in Existence

The major industrial use for electrodialysis, a variant of electrochemical ion exchange, to date has been to demineralize brackish water, but electrodialyzers containing mixtures of cation- and anion-exchange resins have proven useful for decontaminating water slightly contaminated with radioactive material (Perry and Green, 1984). Electrodialysis/electroosmosis has also been used to remove spend nuclear fuel pool and magnesium cladding fines at the British Nuclear Fuels Ltd. reprocessing facility at Sellafield, United Kingdom.

A typical electrodialysis system for demineralizing brackish water, which contains 3,000 ppm sodium chloride, at a rate of 628 m^3/day (167,000 gal./day) would require about 29 kW of direct current at about 640 V (Perry and Green, 1984).

Electrochemical elution of cesium-137 from the resorcinol-formaldehyde ion-exchange resin is developmental, studied recently in bench-scale experiments by AEA Technology of the United Kingdom (Bontha et al., 1994). These studies, however, were conducted specifically to evaluate the potential application of the technology to Hanford wastes.

4.2 Electroreduction

LMAES had proposed to remove technetium-99 by electroreduction process. Technetium-99 and other metallic species, such as chromium, in the waste stream would be electrolytically plated onto the cathode and separated from the high sodium ion content of the waste stream. Once electroreduction was complete, the deposited metals would then be recovered from the electrode in a separate bath by dissolution in an acid solution.

4.2.1 Theory

Electrodeposition is the process of cathodically depositing a metal ion onto a conductive substrate (Dini, 1991). For example, deposition of cupric ions onto a substrate to form copper occurs by the reaction

$$Cu^{2+} + 2e^- \rightarrow Cu \qquad E^0 = 0.34 \text{ V (SHE)} \qquad (4\text{-}32)$$

If multiple metal ions are present in solution, multiple metals may be deposited onto the cathode, depending on the potential. Selectivity of the species deposited during electroreduction is determined by the electrochemical kinetics and mass transport of those species in solution. For example, figure 4-4 illustrates the general considerations of electroreduction for two metals, M_1 and M_2, with equilibrium potentials $V_{0,1}$ and $V_{0,2}$, respectively, where $V_{0,1}$ is more positive than $V_{0,2}$. At the electroreduction potential, V_{dep}, the reduced composition is determined by the ratio of the currents for the two metals, provided V_{dep} is negative of $V_{0,1}$ and $V_{0,2}$. In a system represented by figure 4-4(a), the Tafel lines are parallel and M_1 is preferentially deposited. In figure 4-4 (b), the Tafel lines diverge, so M_1 is preferentially deposited. In figure 4-4(c), the Tafel lines converge, and either M_1 or M_2 is preferentially deposited, depending on V_{dep}. In Region (I) of figure 4-4(c) (above the intersection), M_1 is preferentially deposited; in Region (II) (below the intersection), M_2 is preferentially deposited. For a system represented by figure 4-4(d), the deposition of M_1 becomes mass transport limited. This fourth case is similar to the converging Tafel line case and either M_1 or M_2 is preferentially deposited, depending on V_{dep}.

Similarly, side reactions of water electrolysis occurring at the cathode during the electroreduction process can result in a low-current efficiency and high power consumption. For example, some of the reactions that can occur at the cathode are

$$2H^+ + 2e^- \rightarrow H_2 \qquad (4\text{-}33)$$

$$O_2 + 2H_2O + 4e^- \rightarrow 4OH^- \qquad (4\text{-}34)$$

$$4H_2O + 4e^- \rightarrow 2H_2 + 4OH^- \qquad (4\text{-}35)$$

Figure 4-5 shows that for acid solutions, the relative electrochemistry of the competing hydrogen evolution and metal deposition reactions determine the percentage of the applied current applied to the metal deposition reaction for a given applied deposition potential. In Region I, hydrogen evolution is favored, whereas in Region II, metal deposition consumes the higher percentage of the applied current.
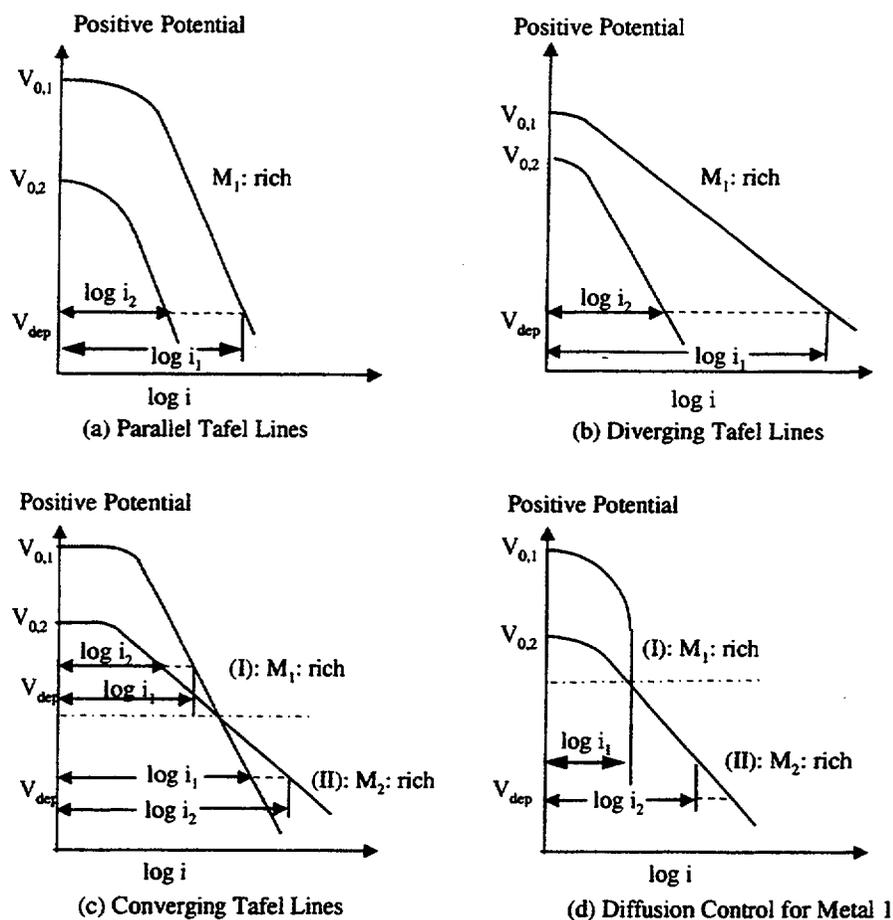
Figure 4-4. Electroreduction of metals M_1 and M_2 in which $V_{0,1}$ is more positive than $V_{0,2}$

4.2.2 Stability Diagrams (Pourbaix Diagrams)

The curves depicted in figures 4-4 and 4-5 will be affected by the chemistry of the environment, such as changes in solution pH. Therefore, to accurately assess the effect of solution chemistry on the preferential deposition of metal ions from waste stream solutions, or on the possible consumption of applied current by water electrolysis reactions occurring at the cathode, multiple current-potential curves should be determined using electrochemical techniques in a variety of solutions.

Based on a survey of literature, it appears that such work has not been done. Also, the application of electroreduction methods to the pretreatment of Hanford wastes would require accurate knowledge of the chemistry of the waste stream. However, an effective method of quickly evaluating the electrochemistry of a metal species in an aqueous system, such as that of technetium-99 in waste solutions, is through the use of a potential-pH diagram. Potential-pH diagrams, more commonly known as Pourbaix diagrams, are
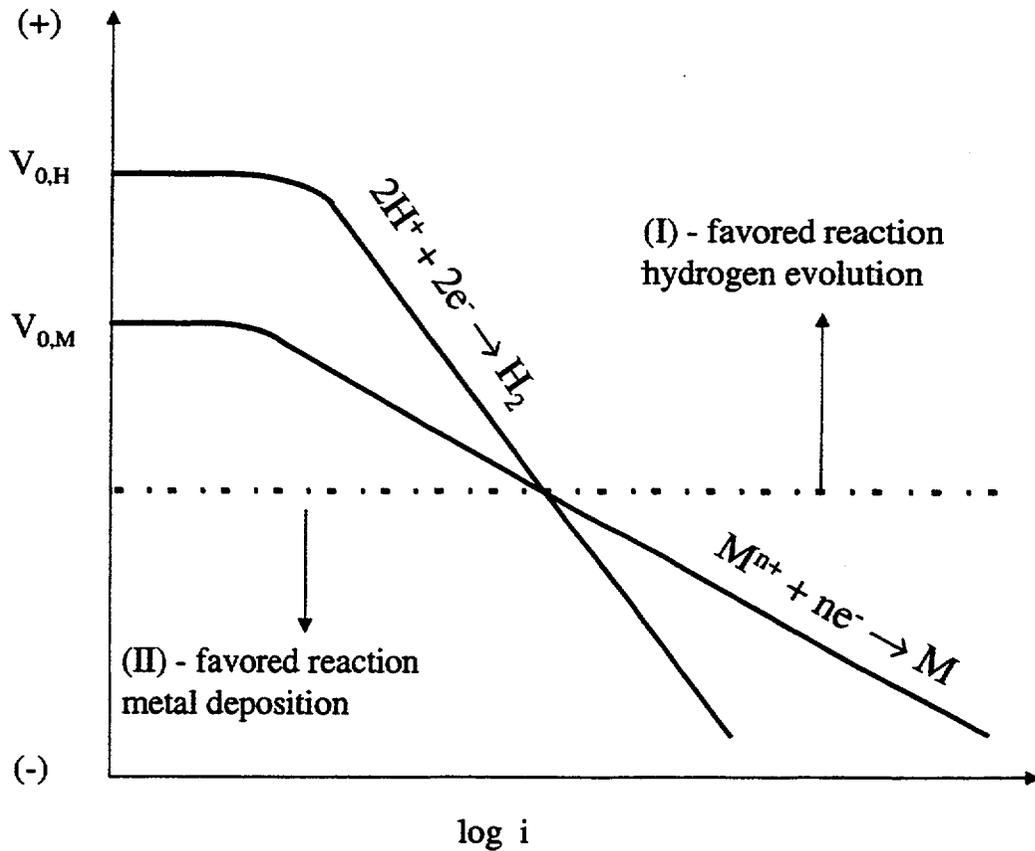
Figure 4-5. Distribution of current for either metal deposition or hydrogen evolution during an electroreduction process in an acid solution

used to predict the equilibrium behavior of a metal species in contact with an aqueous environment. In the simplest form, the diagrams show the regions of stability for species in solution, including the compounds and complexes formed in that environment. The advantage of using a Pourbaix diagram is that, for a given solution pH, the redox potential between various species in the system can be determined at a glance. Therefore, an approximate range of electrode potentials that could be used for the electrodeposition of technetium-99 from waste stream solutions onto a cathode can be determined quickly and compared with the likely electrodeposition potentials for other species in the waste solution.

Pourbaix diagrams are constructed from the free-energy change of the chemical reactions between species likely to occur in the system. Typically included in the Pourbaix diagram are regions of stability for oxygen, water, and hydrogen, allowing rapid determination of the possible competing hydrogen evolution/water reduction reactions on an electrochemical process. The construction of Pourbaix diagrams has been covered extensively by a number of authors and not repeated here (Pourbaix, 1974; ASM International Handbook Committee, 1987). One of the limitations of the diagrams listed in Pourbaix (1974) is the lack of considerations of ligands other than water—derived species such as OH^-.

162

Note, however, that software programs, such as the Corrosion Simulation Program[3] produced by OLI Systems, Inc. (Morris Plains, New Jersey), can rapidly construct these diagrams, given the appropriate free-energy data for the species in the system. This sophisticated modeling software allows changes in environment chemistry (including formation of complexes) to be assessed by the effect on possible competing metal deposition and water electrolysis reactions, without the need for experimental effort.

There are two characteristics of Pourbaix diagrams that must be taken into account during construction and use. First, these diagrams are temperature and concentration dependent. Any change in the temperature of the system under consideration or change in concentration of the species present will require the construction of a separate diagram. Free-energy data of each species in the system at higher temperatures can be calculated with knowledge of changes in the free energies ($\Delta G°_{298}$) and entropies ($\Delta S°_{298}$) at 298 K and with expressions for the heat capacity ($C°_p$) of each species. Concentration changes can be taken into account, and lines for various concentration levels are included in the diagram.

Second, the Pourbaix diagram gives no indication of reaction kinetics (i.e., how fast species form and how long it takes the system to come to equilibrium). Any difference in predicted and experimentally determined results may be because (i) the system may not have reached equilibrium conditions or (ii) some species may have been present in the system not accounted for in the construction of the Pourbaix diagram.

Figure 4-6 shows a Pourbaix diagram for an aqueous solution of technetium-99 at room temperature (Pourbaix, 1974). This diagram was generated in the mid-1970s and could be updated with more recently obtained data to ensure accuracy. To provide an indication of the effectiveness of an electroreduction approach to technetium-99 removal from alkaline waste streams, it is adequate.

4.2.3 Operating Parameters

Electroreduction is comparable to the publicly accepted process of electroplating.

4.2.3.1 Chemistry

Technetium can be removed electrolytically from acidic wastes (Kolarik, 1991; Krause et al., 1994) and from alkaline wastes (Hobbs, 1994). In an alkaline solution, the half-cell reaction is as shown next (Hobbs, 1994):

$$TcO_4^- + 2H_2O + 3e^- \rightarrow TcO_2 + 4OH^- \tag{4-36}$$

The pertechnetate anion, TcO_4^-, is the stable form of technetium in oxygen-saturated solutions at most pH values, as illustrated in figure 4-6 (Pourbaix, 1974). Pertechnetate would also be the likely form of technetium in Hanford tank wastes, due to the presence of nitrate and nitrite ions. As illustrated in

---

[3]A brief description of OLI Software is provided in the report by Pabalan et al. (1999).
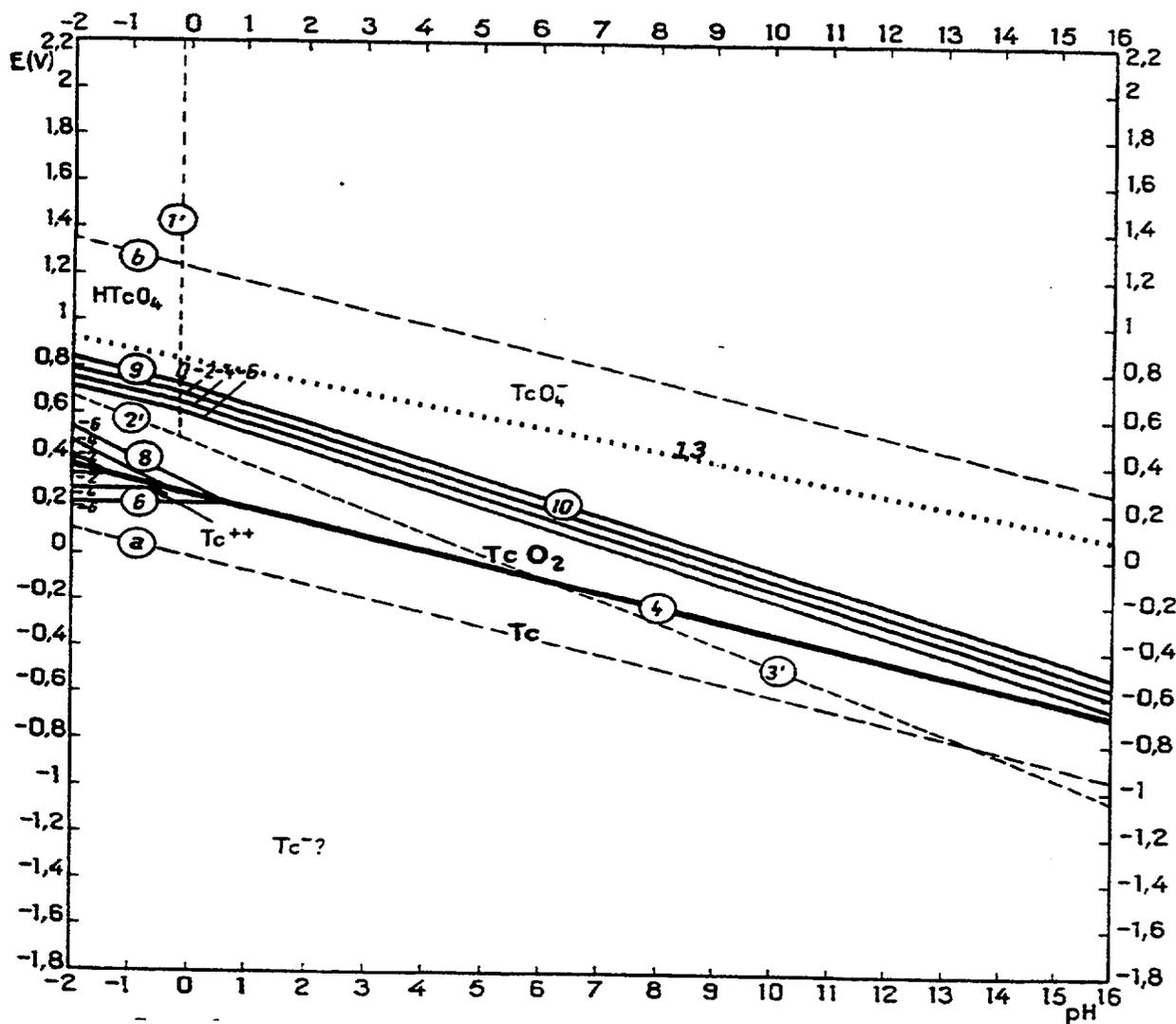
Figure 4-6. Potential-pH diagram for Tc-H$_2$O at ambient temperature (taken from Pourbaix, 1974, with permission from the editors: NACE and CEBELCOR). The numbers represent the following reactions:

1: $HTcO_4 \rightarrow TcO_4^- + H^+$

2: $Tc^{2+} + 4 H_2O \rightarrow HTcO_4 + 7 H^+ + 5 e^-$

3: $Tc^{+2} + 4 H_2O \rightarrow TcO_4^- + 8 H^+ + 5 e^-$

4: $Tc + 2 H_2O \rightarrow TcO_2 + 4 H^+ + 4 e^-$

5: $TcO_2 + H_2O \rightarrow TcO_3 + 2 H^+ + 2 e^-$

6: $Tc \rightarrow Tc^{2+} + 2 e^-$

7: $Tc + 4 H_2O \rightarrow TcO_4^- + 8 H^+ + 7 e^-$

8: $Tc^{2+} + 2 H_2O \rightarrow TcO_2 + 4 H^+ + 2 e^-$

9: $TcO_2 + 2 H_2O \rightarrow HTcO_4 + 3 H^+ + 3 e^-$

10: $TcO_2 + 2 H_2O \rightarrow TcO_4^- + 4 H^+ + 3 e^-$

11: $TcO_3 + H_2O \rightarrow HTcO_4 + H^+ + e^-$

12: $TcO_3 + H_2O \rightarrow TcO_4^- + 2 H^+ + e^-$
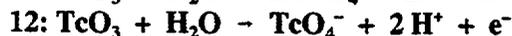
The dotted line (13) represents Eh-pH conditions imposed at equal concentrations of nitrate and nitrite by the half reaction: $\frac{1}{2}NO_2^- + \frac{1}{2}H_2O \rightarrow \frac{1}{2}NO_3^- + H^+ + e^-$; conditions will vary negligibly when the concentrations of these two anions are within two orders of magnitude, as they typically are in Hanford supernates (Agnew, 1997).

figure 4-6, nitrate and nitrite would buffer the oxidation potential of the aqueous phase to be within the stability field of TcO_4^-.

Tests indicate that about 95 percent (decontamination factor = 20) of the technetium in an alkaline solution (1–3 M sodium hydroxide) can be collected on a cathode in 20 hr of electrolytic operation, and about 99.98 percent (decontamination factor = 5,000) can be removed in 48 hr of electrolytic operation (Hobbs, 1994).

In a 48-hr test on actual decontaminated salt solution at the Savannah River Site, using virgin nickel electrodes and a current density of 1,080 A/m^2 (100 A/ft^2), only 56 percent (decontamination factor = 2.3) of the technetium-99 was removed. The major chemical constituents of the waste were 5.5 M sodium ion, 0.95 M hydroxide ion, 2.7 M nitrate ion, and 0.25 M nitrite ion. The test was to study nitrate and nitrite destruction, not the removal of technetium-99 (Hobbs, 1994).

Electrolytic deposition of technetium-99 from alkaline wastes is still under development. A comprehensive program of laboratory studies followed by bench- and pilot-scale testing will be needed to support development and implementation (Krause et al., 1994). The significant operating parameters that must be studied include waste composition, electrode materials, nature of electrode surface, electrode spacing, current density, and temperature (Hobbs,1994).

Tests suggest that greater than 95 percent of the technetium-99 plated on the cathode can be removed from the cathode by reversing the cell potential, followed by electrolysis for a brief period of time. This converts the technetium oxide deposit to pertechnetate, which rapidly dissolves, as shown next:

$$TcO_2 + 4OH^- \rightarrow TcO_4^- + 2H_2O + 3e^- \tag{4-37}$$

As an alternative, tests suggest that greater than 95 percent of the technetium-99 plated on the cathode can be removed from that electrode by turning off the power and soaking the electrode in a strongly alkaline solution (Hobbs, 1994).

4.2.3.2 Preferential Electrodeposition of Technetium-99

For the following discussion, the pH of the waste being treated by the electroreduction process is assumed in the range of 10 to 14. The pH of the bath used for dissolution of the deposited metals from the cathode could be controlled to optimize that final treatment process. Because there is little publicly available data on the electroreduction of aqueous technetium-99 species to metallic technetium in alkaline solutions, the Pourbaix diagram shown in figure 4-6 is used for this initial assessment. An updated version of this Pourbaix diagram could be generated using software programs, such as the Corrosion Simulation Program produced by OLI Systems, Inc., once the chemistry of the waste stream has been accurately defined. Although the actual pH of the waste is unknown at this stage, a pH of 12 will be used for this discussion.

A discussion of preferential electrodeposition of technetium-99 from waste streams must first begin with a determination of the valence state of the reduced technetium. If the technetium-99 is electrodeposited in its metallic state, the electrochemical potential required to achieve this reduction process will be more negative than if the technetium-99 is deposited as a technetium (IV) oxide, and the process could

165

encounter interference from competing deposition reactions or water electrolysis reactions such as hydrogen evolution. For example, at pH 12, the equilibrium potential for reduction of technetium (VII), for the particular case of 10^{-4} M TcO_4^- to technetium (IV) is approximately -0.28 V [standard hydrogen electrode (SHE)] (line 1, number 4, in figure 4-6); the equilibrium potential for reduction of technetium (IV) to metallic technetium (line 4 in figure 4-6) is approximately -0.45 V (SHE). At the same pH value, the equilibrium potential for reduction of iron (III) to iron (II) is approximately -0.45 V (SHE), with the further reduction of iron (II) to metallic iron occurring at approximately -0.77 V (SHE) (lines 16 and 12), in the Pourbaix diagram for the iron-water system shown in figure 4-7.

Comparisons among (i) the electroreduction potential of technetium (IV) to metallic technetium, (ii) the electrochemical potential for the hydrogen evolution reaction, and (iii) the potential for the reduction of iron suggest that extraction of technetium-99 from the waste stream by electroreduction may be compromised by the hydrogen evolution reaction and, possibly, by the reduction of iron (III) to iron (II). If, however, the electroreduction step removes technetium-99 from the waste stream using the technetium (VII) to technetium (IV)-oxide transition, the process could be better optimized solely for technetium-99 removal. However, because of the complex chemistry of the Hanford wastes, an evaluation of the process could be facilitated by thermodynamic calculations of Pourbaix diagrams that account for the presence of other chemical species in solution.

The percentage of the current that would be consumed by the technetium-99 electroreduction reaction, as opposed to the hydrogen evolution oriron (III)–iron (II) reduction reactions, cannot be determined from the Pourbaix diagrams, which illustrate thermodynamic stability only. Consequently, additional studies would need to be conducted to determine the relative deposition kinetics of all the reactions occurring in the system.

A discussion of the successful electroreduction of technetium-99 from a simulated salt solution from the Savannah River Site plant did not describe the applied currents and potentials used in the process. Further, metallic contaminant species apparently were not present in the solution (Hobbs and Ebra, 1987).

4.2.3.3 Separation of Sodium Ions from the Waste Stream Solution

The major advantage of the electroreduction process is that interferences from the high concentration of sodium ions in the waste stream, which would preclude the use of other processes such as electrochemical ion exchange can be eliminated. In the electroreduction method, sodium will not deposit onto the cathode until extremely low potentials [more negative than -2.5 V (SHE)] are applied.

4.2.3.4 Selection of Electrode Materials

A number of electrode materials are available for use in an electroreduction treatment step:

- Graphite
- Steels and stainless steels
- TiO_x
- Mercury

166

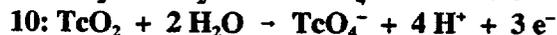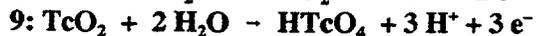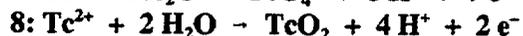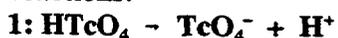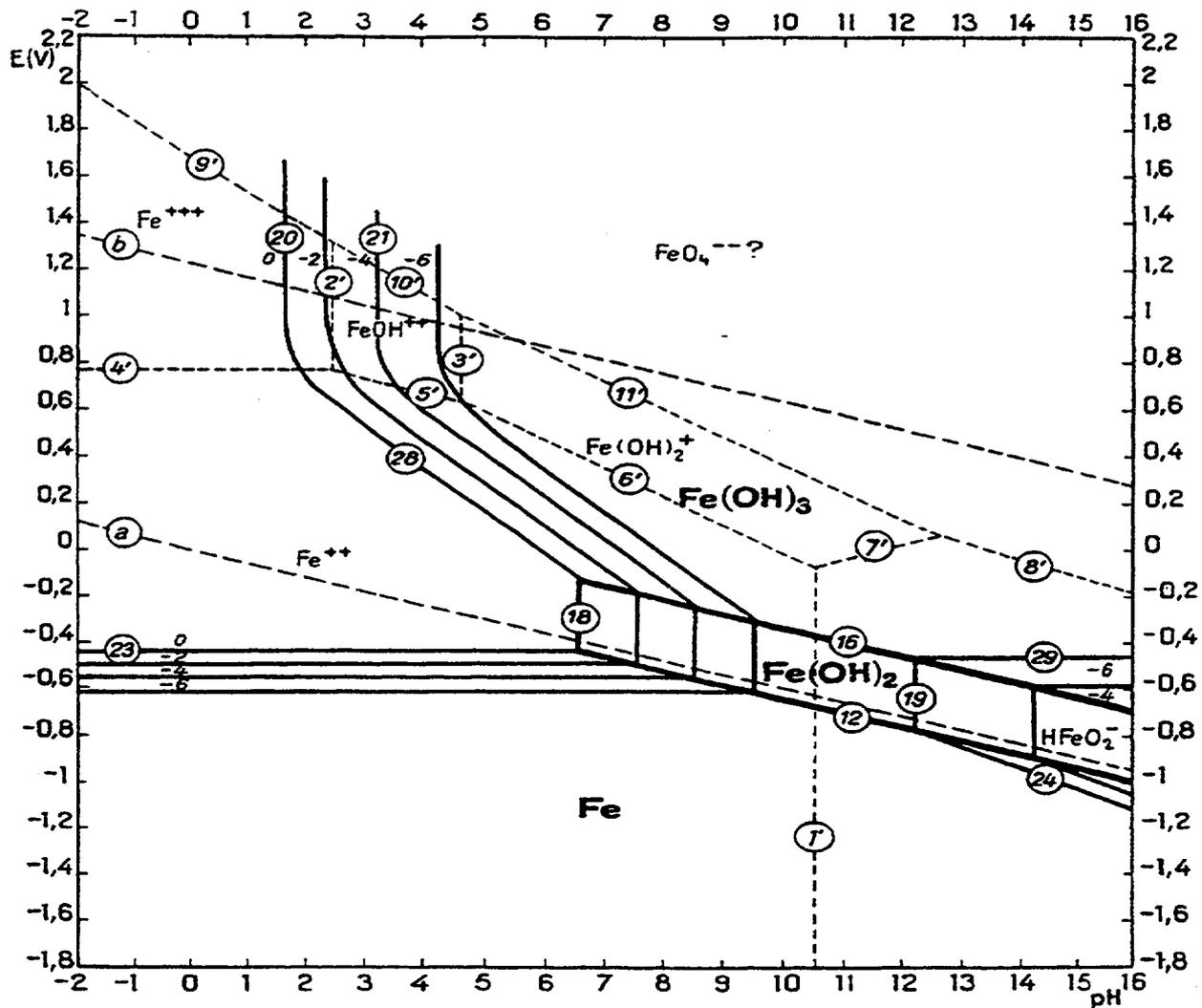**Figure 4-7. Potential–pH diagram for Fe-H₂O at ambient temperature (taken from Pourbaix, 1974, with permission from the editors: NACE and CEBELCOR). The numbers represent the following reactions:**

1: $Fe^{2+} + 2 H_2O \rightarrow HFeO_2^- + 3 H^+$

2: $Fe^{3+} + H_2O \rightarrow FeOH^{2+} + H^+$

3: $FeOH^{2+} + H_2O \rightarrow Fe(OH)_2^+ + H^+$

4: $Fe^{2+} \rightarrow Fe^{3+} + e^-$

5: $Fe^{2+} + H_2O \rightarrow FeOH^{2+} + H^+ + e^-$

6: $Fe^{2+} + 2 H_2O \rightarrow Fe(OH)_2^+ + 2 H^+ + e^-$

7: $HFeO_2^- + H^+ \rightarrow Fe(OH)_2^+ + e^-$

8: $HFeO_2^- + 2 H_2O \rightarrow FeO_4^{2-} + 5 H^+ + 4 e^-$

9: $Fe^{3+} + 4 H_2O \rightarrow FeO_4^{2-} + 8 H^+ + 3 e^-$

10: $FeOH^{2+} + 3 H_2O \rightarrow FeO_4^{2-} + 7 H^+ + 3 e^-$

11: $Fe(OH)_2^+ + 2 H_2O \rightarrow FeO_4^{2-} + 6 H^+ + 3 e^-$

12: $Fe + H_2O \rightarrow FeO + 2 H^+ + 2 e^-$

16: $2 FeO + H_2O \rightarrow Fe_2O_3 + 2 H^+ + 2 e^-$

18: $Fe^{2+} + H_2O \rightarrow FeO + 2 H^+$

19: $FeO + H_2O \rightarrow HFeO_2^- + H^+$

20: $2 Fe^{3+} + 3 H_2O \rightarrow Fe_2O_3 + 6 H^+$

21: $2 FeOH^{2+} + H_2O \rightarrow Fe_2O_3 + 4 H^+$

23: $Fe \rightarrow Fe^{2+} + 2 e^-$

24: $Fe + 2 H_2O \rightarrow HFeO_2^- + 3 H^+ + 2 e^-$

28: $2 Fe^{2+} + 3 H_2O \rightarrow Fe_2O_3 + 6 H^+ + 2 e^-$

29: $2 HFeO_2^- \rightarrow Fe_2O_3 + H_2O + 2 e^-$

167

Electrochemical Methods

- Lead
- Nickel

Graphite is one of the more commonly used electrode materials due to its low cost. However, alternative electrode materials may be required in an effort to reduce the hydrogen evolution reaction occurring on the surface of the cathode. This reaction would direct more of the applied current towards metal deposition and make the treatment process more efficient.

4.2.4 Limitations

Many studies in the public domain on the electrochemistry of technetium (IV), (V), (VI), and (VII) in aqueous solutions were directed toward the use of technetium (VI) as a diagnostic tool for nuclear medicine (e.g., Best, 1990; Hurst, 1980; Lewis, 1983; Libson, 1981; Deutsch et al., 1978). A study by Meyer et al. (1989) on the electrochemistry of the technetium (VII)/technetium (IV)-oxide couple gave a standard electrode potential of 0.747 V (SHE), which is in reasonable agreement with previously published work (Cartledge et al., 1953; Cartledge and Smith, 1955; Magee and Cardwell, 1974; Founta et al., 1987). Although the data available on the relative electrochemical potentials and reaction efficiencies for the high-valence state technetium-99 species provide valuable information, there is little data available for the thermodynamics of the reduction of technetium-99 species to metallic technetium, especially in an alkaline environment. This lack of data needs to be addressed before an accurate assessment of the efficacy of the electroreduction process for technetium-99 removal from waste streams can be obtained. In this report, the Pourbaix diagram described previously will be used to provide an initial assessment.

4.2.5 Application to Hanford High-Level Waste

4.2.5.1 Operational Considerations

The chemistry of the high-level wastes in the storage tanks at Hanford is dominated by high levels of nitrate, nitrite, hydroxide, and sodium ions, with pH in the range 10 to 14 (Pabalan et al., 1999). Other species, such as radionuclides (technetium-99, strontium-90, cesium-137) and metal contaminants (iron, aluminum, nickel, chromium, manganese) are also present in lesser quantities.

Washing and dilution processes would remove much of the nitrate and nitrite species from the waste stream prior to the proposed electroreduction pretreatment step. The solution to be treated would contain high concentrations of sodium ion and hydroxide ion, and also could have elevated concentrations of variable oxidation state elements, such as iron, aluminum, and manganese, that could interfere with the electroreduction of technetium-99. The oxidation state of the technetium-99 is unknown, but is presumed to be technetium (VII) (Peretrukhin et al., 1995).

At this time, with the limited data available, an accurate assessment of the viability of electroreduction for the treatment of Hanford waste streams cannot be made. Additional studies are required to obtain basic thermodynamic, kinetic, and transport data for technetium-99 species in aqueous solutions before this assessment can be made. As previously discussed, updated Pourbaix diagrams for all the species present in the waste solutions should be generated. Development of a single Pourbaix diagram that

incorporates all the species and considers the effect of competing reactions would be advantageous. Additional experimental work (i.e., cathodic polarization scans) should be performed to determine kinetics and current efficiencies of the competing reactions at the actual pH of the waste stream and as a function of different electrode materials. The possibility of excessive hydrogen evolution needs to be determined, particularly regarding safety considerations, and minimized, if necessary.

4.2.5.2 Safety Considerations

The electroreduction process itself will employ direct electrical current, and circulating equipment, such as pumps, will likely employ an alternating electrical current. Therefore, appropriate industrial practices for safety around electrical equipment, both alternating current and direct current, should be observed.

Electrochemical treatment of alkaline water can produce hydrogen and oxygen gases. Accumulations of these gases can be flammable or even explosive. Therefore, steps should be taken to ventilate the process and discharge such gases to the atmosphere where the hydrogen can become diluted to noncombustible concentrations.

4.2.5.3 Comparable Operations in Existence

Electrolytic removal of technetium from alkaline wastes has been demonstrated at the laboratory scale on actual decontaminated salt solution waste and on a simplified alkaline salt solution at the Savannah River Site. It has not been applied on an industrial scale.

Electroreduction is used industrially to produce a number of metals, including aluminum. To produce 1 kg of elemental aluminum from alumina, 22–26 kW-hr of direct current electrical energy are required.

$$2Al_2O_3 + 3C \rightarrow 4Al + 3CO_2 \qquad (4\text{-}38)$$

The carbon in the reaction is provided by carbon electrodes (anodes). If this was the only reaction, then the only gaseous by-product would be carbon dioxide; however, 10–50 percent of the gases evolved are carbon monoxide. Because of the toxicity of carbon monoxide, ventilation is required (Shreve, 1967).

4.3   Electrochemical Methods Proposed by BNFL Inc.

No electrochemical methods were proposed by BNFL Inc. Given the nature of the flow sheet proposed by BNFL Inc., electrochemical methods are not needed to meet the project requirements.

4.4   References

Agnew, S.F. *Hanford Tank Chemical and Radionuclide Inventories: HDW Model Rev. 4.* LA–UR–96–3860. Los Alamos, NM: Los Alamos National Laboratory. 1997.

Allen, P.M., N.J. Bridger, C.P. Jones, F.M.-T. Menapace, M.D. Neville, and A.D. Turner. Electrochemical Ion Exchange. *Proceedings of the 6th International Conference on Ion Exchange.* New York: Elsevier Publications: 272–278. 1992.

ASM International Handbook Committee. *Metals Handbook: 9th Edition, Volume 13 Corrosion.* Metals Park, OH: ASM International. 1987.

Benedict, M., T.H. Pigford, and H.W. Levi. *Nuclear Chemical Engineering.* New York. McGraw-Hill Book Company. 1981.

Best, T.A. *Studies of Some Technetium Complexes of Relevance to Nuclear Medicine.* Ph.D. thesis. University of Cincinnati. 1990.

Bontha, J.R., D.E. Kurath, and J.E. Surma. *Evaluation of Electrochemical Ion Exchange for Cesium Elution.* TWRSPP–94–093. Richland, WA: Pacific Northwest National Laboratory. 1994.

Bridger, N.J., C.P. Jones, and M.D. Neville. Electrochemical ion exchange. *Journal of Chemical Technology and Biotechnoogy* 50: 469–481. 1991.

Cartledge, G.H., and W.T. Smith, Jr. Revision of the electrode-potential diagram for technetium. *Journal of Physical Chemistry* 89: 1,111–1,112. 1955.

Cartledge, G.H., W.T Smith, Jr., and G.D. Boyd. Thermodynamic properties of technetium and rhenium compounds. II. Formation of technetium heptoxide and pertechnic acid, potential of the technetium (IV)–technetium(VII) couple, and a potential diagram for technetium. *Journal of the American Chemical Society* 75: 5,777–5,783. 1953.

Cumming I.W., H. Tai, and M. Beier. A model to predict the performance of an electrochemical ion exchange cell. *Transactions of the Institute of Chemical Engineers Part A* 75: 9–13. 1997.

Deutsch, E., W.R. Heinemann. R.W. Hurst, J.C. Sullivan, W.A. Mulac, and S. Gordon. Production, detection, and characterization of transient hexavalent technetium in aqueous alkaline media by pulse radiolysis and very fast scan cyclic voltammetry. *Journal of the Chemical Society Chemistry Communications*: 1,038–1,040. 1978.

Dini, J.W. *Electrodeposition.* Park Ridge, NJ: Noyes Publications. 1991.

Evans, S. *Electrochemically Controlled Ion-exchange.* Office of Saline Water Research and Development Report No. 126. 1965.

Evans, S. *Electrochemically Controlled Ion-exchange.* Office of Saline Water Research and Development Reports No. 598. 1970.

Founta, A., D.A. Aikens, and H.M. Clark. Mechanism and kinetics of the stepwise voltammetric reduction of pertechnetate in alkaline solution to Tc(VI), Tc(V), and Tc(IV). *Journal of Electroanalytical Chemistry* 219: 221–246. 1987.

Fletcher, P. A., C.P. Jones, A.R. Junkison, A.D. Turner, and P.R. Kavanagh. *Technetium Removal from Aqueous Wastes*. DOE–HMIP–RR–92.053. London, UK: Department of the Environment. 1992.

Hobbs, D.T. *Summary Technical Report on the Electrochemical Treatment of Alkaline Nuclear Wastes*. WSRC–TR–94–0287. Aiken, SC: Westinghouse Savannah River Company. 1994.

Hobbs, D.T., and M.A. Ebra. Electrochemical processing of alkaline nitrate and nitrite solutions. *Electrochemical Engineering Applications*. R.E. White, ed. American Institute of Chemical Engineers Symposium Series 254: 149–155. 1987.

Hurst, R.W. *Carbon and Mercury-Carbon Optically Transparent Electrodes: Investigation of Redox Properties of Technetium by Cyclic Voltammetry and Thin Layer Spectroelectrochemistry*. Ph.D. thesis. University of Cincinnati. 1980.

Jones, C.P., M.D. Neville, and A.D. Turner. Electrochemical ion exchange. D. Genders and N. Weinberg, eds. *Electrochemistry for a Cleaner Environment*. East Amherst, NY: The Electrosynthesis Company, Inc.: 207–220. 1992.

Kolarik, Z. *Separation of Actinides and Long-Lived Fission Products from High-Level Radioactive Wastes (A Review)*. KfK–4945. Karlsruhe, Germany: Kernforschungszentrum Karlsruhe G.m.b.H. 1991.

Krause, T.R., J.C. Cunnane, and J.E. Helt. *Sludge Technology Assessment*. ANL–94/95. Argonne, IL: Argonne National Laboratory. 1994.

Lewis, J.Y. *Quantitative Determination of Pertechnetate by Electrochemical Methods: Electrochemistry of Technetium Radiopharmaceutical Analogs*. Ph.D. thesis. University of Cincinnati. 1983.

Libson, K.F. *Studies in Technetium Chemistry Applied to the Practice of Nuclear Medicine*. Ph.D. thesis. University of Cincinnati. 1981.

Long, J.T. *Engineering for Nuclear Fuel Reprocessing*. LaGrange Park, IL: American Nuclear Society. 1978.

Magee, R.J., and T.J. Cardwell. Rhenium and Technetium. *Encyclopedia of the Electrochemistry of the Elements* II. Chapter 4. A.J. Bard, ed.: 125–189. 1974.

Meyer, R.E., W.D. Arnold, E.I. Case, and G.D. O'Kelley. *Thermodynamics of Technetium Related to Nuclear Waste Disposal: Solubilities of Tc(IV) Oxides and the Electrode Potential of the Tc(VIII)/Tc(IV)-Oxide Couple*. NUREG/CR–5235. Washington, DC: Nuclear Regulatory Commission. 1989.

Electrochemical Methods

Pabalan, R.T., M.S. Jarzemba, D.A. Pickett, N. Sridhar, J. Weldy, C.S. Brazel, J.T. Persyn, D.S. Moulton, J.P. Hsu, J. Erwin, T.A. Abrajano, Jr., and B. Li.. *Hanford Tank Waste Remediation System High-Level Waste Chemistry Manual*. NUREG/CR–5751. Washington, DC: Nuclear Regulatory Commission. 1999.

Peretrukhin, V.F., V.P. Shilov, and A.K. Pikaev. *Alkaline Chemistry of Transuranium Elements and Technetium and the Treatment of Alkaline Radioactive Wastes*. WHC–EP–0817. Richland, WA: Westinghouse Hanford Company. 1995.

Perry, R.H., and D.W. Green. *Perry's Chemical Engineers' Handbook*. New York: McGraw-Hill Book Company. 1984.

Pourbaix, M. *Atlas of Electrochemical Equilibria in Aqueous Solutions*. Houston, TX: NACE International. 1974.

Shreve, R.N. *Chemical Process Industries*, New York: McGraw-Hill Book Company. 1967.

Turner, A.D., N.J. Bridger, C.P. Jones, J.S. Pottinger, A.R. Junkison, P.A. Fletcher, M.D. Neville, P.M. Allen, R.I. Taylor, W.T.A. Fox, and P.G. Griffiths. *Electrochemical Ion-Exchange for Active Liquid Waste Treatment: Final Report*. AEA–D&R–0441. Oxfordshire, UK: Harwell Laboratory. 1992.

5 ORGANIC DESTRUCTION

The destruction or removal of organic compounds present in Hanford tank wastes during pretreatment could be important to process efficiency and safety. Organic destruction could improve the efficiency of radionuclide separation processes (Schmidt et al., 1994). For example, organic complexants increase the solubility of certain radioelements, primarily strontium and transuranic elements. Thus, if organic complexants are eliminated, removal of strontium-90 and transuranic elements by precipitation and filtration (discussed in chapter 6) could be improved and substantially smaller amounts of scavenging agents required.

LMAES, a former TWRS contractor, had proposed to destroy organic materials in Hanford waste envelope C by oxidation with ozone. Envelope C contains organic complexes that could make precipitation of strontium-90 and transuranics inefficient. The other low-activity waste streams, envelopes A and B, are assumed to contain little or no organic complexed radionuclides and were not considered to require organic destruction. The ozone-treated waste subsequently was to be processed to remove strontium-90 and transuranics by precipitation and filtration. LMAES had also suggested that organic materials may be destroyed by electrochemical methods. BNFL Inc. has not proposed an organic destruction step.

During waste processing, organic destruction also will eliminate safety concerns related to exothermic organic oxidation reactions and flammable gas generation resulting from organic degradation processes. Removal of organics prior to waste vitrification may also be necessary to prevent metal reduction reactions in Joule-heated glass melters (Schulz et al., 1995). The presence of organic compounds in the high-level waste adversely affects the reduction-oxidation potential of the molten glass, which could cause reducible materials (especially transition metals) to be converted to the metallic state and electrically short circuit the glass melter.

Over the past two decades, various technologies have been investigated for destruction of organic compounds in Hanford tank wastes (Schulz et al., 1995), including

- Calcination (rapid heating of solid waste below its melting temperature causing loss of moisture and reduction or oxidation)

- Plasma arc destruction

- Electro-oxidation (use of electrochemical cells to induce oxidation)

- Photolysis with ultraviolet light (rapid photodegradation of organics)

- Wet-air oxidation (controlled vapor phase reaction)

- Hydrogen peroxide oxidation (in acid) (introduction of a strong aqueous oxidizer to waste)

- Ozonation (introduction of a strong gaseous oxidizer to waste)

- Thermal treatment [low temperature, no greater than 100 °C (212 °F), or hydrothermal]

173

Organic Destruction

In this chapter, ozonation is discussed in some detail because it is the organic destruction process proposed by LMAES. Published studies suggest ozonation has the potential to achieve complete oxidation of organic chemicals, yielding carbon dioxide gas that can be removed easily, or highly oxidized organic chemicals, which will have a much lower oxidation reaction potential when exposed to high temperatures. Ozone, however, preferentially oxidizes nitrite to nitrate prior to effective oxidation of high-level waste organics. Consequently, a large quantity of ozone may be required to reach the desired results in Hanford tank waste treatments.

5.1 Ozonation

5.1.1 Background

Ozone (O_3) is a highly reactive allotrope (a structurally differentiated form) of atmospheric oxygen (O_2) present in trace quantities in the lower atmosphere. In the upper atmosphere (stratosphere), ozone is generated by the reaction of diatomic oxygen with oxygen atoms formed by ultraviolet photodissociation: ozone is believed to protect life on Earth by acting as a shield against ultraviolet radiation. In the chemical industry, ozone has proven a highly useful and powerful oxidizing agent; its production cost is the only deterrent to wider use. Ozone has been used in water purification, sewage and industrial waste treatment, bleaching waxes and paper, and in odor, color, and taste control (Bailey, 1978).

Hazards associated with ozone include being a strong irritant and a dangerous fire and explosion risk when allowed to come in contact with organic materials because of its oxidizing nature. Ozone is a toxic gas, with a threshold limit value of 0.1 ppm. Its pungent odor, however, is detectable by the nose at 0.01 ppm (Delegard et al., 1993). Because ozone is a powerful oxidizer of all kinds of organic compounds, it can react with proteins and other biomolecules of plant and animal tissues (Bailey, 1978). Ozone also contributes to the formation of photochemical smog. An important side effect of air pollution is the degradation of rubber and elastomers by ozone in the air. As a concentrated gas or liquid, ozone can decompose explosively to oxygen through the reaction shown in Eq. (5-1):

$$2O_3 (g) \rightarrow 3O_2 (g) \tag{5-1}$$

Oxygen radicals—species having unpaired electrons—are intermediates in this exothermic reaction and act as strong oxidizing agents.

Ozone is an unstable, pale blue gas at room temperature, typically produced in industry by corona (electrical) discharge in pure diatomic oxygen or in air. Ozone concentrations up to 4 percent by weight in air or 10 percent in pure oxygen may be achieved if the gases are dry, because water vapor catalyzes the decomposition of ozone to oxygen (Delegard et al., 1993). Typical gas concentrations from generators are around 2 percent for air and 4 percent for oxygen feed at the most efficient generation points. Dry gases are used primarily to avoid nitric acid formation and corrosion of the ozone generator's electrodes—ozone decomposition by water vapor is less of a concern. Because ozone is relatively dilute in the gas mixture, large quantities of carrier gas are needed for treating wastes that contain high organic concentrations.

174

In aqueous systems, the solubility of ozone is low, typically 8–12 ppm and varies with temperature and ozone concentration in the gas phase. In acid solution, ozone is exceeded in oxidizing power only by fluorine, the perxenate (XeO_6^{4-}) ion, atomic oxygen, hydroxyl radical $(OH\cdot)$,[1] and a few other such species (Cotton and Wilkinson, 1976). In alkaline solutions, ozone is also a powerful oxidant $(E° = +1.24\ V)$.[2] Ozone, however, decomposes in alkaline solutions to form a variety of highly reactive intermediates, including $OH\cdot$, $HO_2\cdot$, $O\cdot^-$, O_3, and O_2 (Phig, 1976). Of these reactive intermediate species, the hydroxyl radical $(OH\cdot)$ is the most important and accounts for the high oxidation potential of ozone solutions at high pH. The decomposition of ozone in alkaline solutions to highly reactive intermediates is fairly rapid. For example, the half-life of ozone in slightly acidic aqueous solution is about 30 min, whereas under alkaline conditions its half-life decreases to about 30 sec.

5.1.2 Structure of Ozone

To understand the reactions of ozone with organic materials, a knowledge of the ozone structure is helpful. The ozone molecule (O_3), in its ground state, is angular (117°), diamagnetic, with a low dipole moment (approximately 0.53 debye). Both oxygen-oxygen bonds are identical, exhibiting a length of 1.28 Å $(4.20 \times 10^{-10}\ ft)$, intermediate between typical single- and double-bond lengths (Bailey, 1978).

5.1.3 Types of Ozone Attack

Based on the resonance formulas of the ozone molecule illustrated in figure 5-1, it is apparent that ozone can attack compounds in a variety of ways. Ozone can function as a 1,3 dipole (ozonation of olefins), an electrophile (ozonation of nucleophiles such as amines, phosphite, or sulfur), or a nucleophile (ozonation of carbocations) (Bailey, 1978). Bailey (1978) also reports that ozone can react as a diradical (ozonation of carbon-hydrogen bonds).

The ability of ozone to behave as a 1,3-dipole, an electrophile, a nucleophile, or, under certain conditions, a diradical, enables ozone to react with a variety of organic compound types. The rates of reaction of ozone with various groups are compared in figure 5-2 (Bailey, 1978).

5.1.4 Ozonation of Specific Organic Groups

Ozone likely oxidizes organic materials into carbonates (CO_3^-) and small carbon-chain organic compounds (Colby, 1993).

The decomposition kinetics of ozone in an alkaline medium is in seconds. Because of the fast ozone decomposition kinetics, the ozone/organic reaction rate is limited by mass transport of ozone into the solution (Colby, 1993).

---

[1] The oxidation potentials are 2.07 V for ozone and 2.8 V for a hydroxyl radical in a 1-M H$^+$solution (Lutton et al., 1980).

[2] For the half-cell reaction (Cotton and Wilkinson, 1976): $O_3 + H_2O + 2e^- = O_2 + 2OH^-$.

175

Organic Destruction
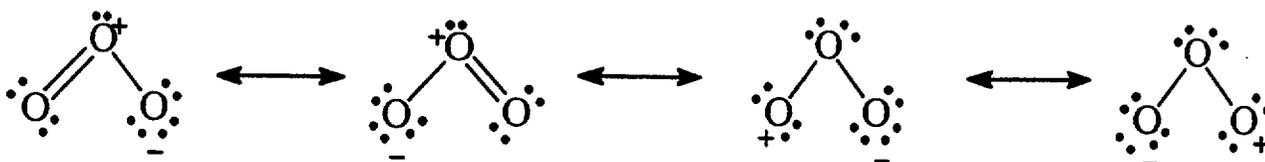
Figure 5-1. Lewis structures of ozone
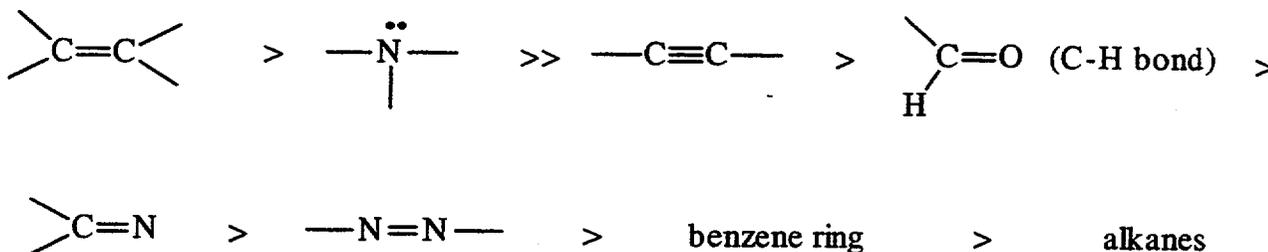
Figure 5-2. Comparison of reaction rates of various compounds with ozone

An in-depth review of ozonation in organic chemistry is available from the published literature (Bailey, 1978). The discussion that follows concentrates on compound types important to Hanford wastes.

5.1.4.1 Alkenes

Due to the highly reactive chemical environment of the Hanford tank waste, the probability of alkenes in the tank waste is low. Therefore, ozonation of alkenes is not covered in this report.

5.1.4.2 Alkanes

Alkanes react with ozone much more slowly than alkenes, and considerably more slowly than alcohols. Ozone reacts with methane to form formaldehyde, formic acid, carbon dioxide, carbon monoxide, water, and a trace of methanol. At higher temperatures, methyl hydroperoxide and formaldehyde are the major products. The other products formed include carbon dioxide, carbon monoxide, carboxylic acids, alcohols, ketones, and aldehydes (Bailey, 1978).

Products obtained from the ozonation of higher molecular weight alkanes include alcohols, ketones, carboxylic acids, esters, and peroxides. For example, the reaction of decane with ozone yields all possible alcohols and ketones of 10 carbon atoms, plus ethanol, pentanol, hexanol, and traces of heptanol, nonanol, C_1-C_9 monocarboxylic, and ketocarboxylic acids, esters, and γ-alkylbutyrolacetones. The ozonation of n-octadecane produced a variety of alcohols and ketones from the oxidation of each of the methylene groups. The ozone-initiated oxidation of commercial paraffin to a mixture of carboxylic acids has also been reported (Bailey, 1978).

5.1.4.3 Alcohols

Many open-chain (acyclic) and cyclic alcohols have been oxidized by ozone (Bailey, 1978). Primary alcohols have been ozonized to the corresponding aldehydes and carboxylic acids; secondary alcohols have been ozonized to ketones. Ozonation of 21 different acyclic and cyclic secondary alcohols in methylene chloride yields ketones (57–83 percent yield) as the major products and carboxylic acids as minor products (Waters et al., 1976).

Ozonation of primary and secondary alcohols also have been performed in water solutions. The primary alcohols (methanol, ethanol, 1-butanol, and 1-octanol) were converted to the corresponding aldehydes and carboxylic acids with some production of carbon dioxide (Bailey, 1978). The secondary alcohol, 2-propanol, was oxidized to acetone, which in turn was oxidized to acetic and oxalic acids. Trace amounts of formaldehyde and formic acid were also detected.

In various sugar alcohols and polysaccharides, the primary alcohol group was reported oxidized by ozone to aldehydes. Ozone has also been shown to degrade water soluble polymers, such as polyvinyl alcohol, to lower molecular weight polymers.

5.1.4.4 Ethers

Ozonation of the following ethers, disoamyl, dibutyl, dimethyl, diethyl, and dibenzyl, produces the corresponding aldehydes, esters, and hydrogen peroxide. In addition, the ozonation of dibutyl and diisoamyl ethers produced butyl and isoamyl formates (Bailey, 1978).

Ozonation of the following ethers, disopropyl, dibutyl, di-tert-butyl, methyl isopropyl, ethyl isopropyl, propyl isopropyl, methyl benzyl, tert-butyl benzyl, tert-butyl p-brombenzyl, ethyl 2-chloroethyl, 4-oxa-2-heptanone, ethyl ethoxyacetate, tetrahydrofuran, 2-methyltetrahydrofuran, and tetrahydropyran produces the corresponding alcohols, aldehydes, ketones, and esters (Baily, 1978).

5.1.4.5 Aldehydes

Ozonation of isobutyraldehyde, isovaleraldehyde, heptaldehyde, and benzaldehyde produces the corresponding carboxylic acids and peracids. Aldehydes react readily with ozone, or ozone can be simply an initiator of autoxidation. In both cases, the initial reaction appears to be a 1,3 dipolar insertion of ozone at the aldehydic carbon-hydrogen bond (Bailey, 1978).

5.1.4.6 Ketones

Ketones are oxidized by ozone to give the corresponding acid as the major product. The ozonation of methyl ethyl ketone in carbon tetrachloride produces acetic acid, biacetyl, organic peroxides, and hydrogen peroxide (Bailey, 1978).

5.1.4.7 Carboxylic Acids

Various studies conducted ozonation of acetic and oxalic acid in an attempt to remove them from wastewater. The oxidation of acetic acid was successful in the presence of ultraviolet light or an alkali

solution. The oxidation of oxalic acid was slow under basic conditions, but was converted to carbon dioxide under acidic conditions and in the presence of ultraviolet light (Bailey, 1978).

5.1.4.8 Polymers

Considerable attention has been given to the oxidation of polymers, such as polyethylene, polypropylene, polyvinylcyclohexane, and polystyrene. The ozone attack can occur at a methylene or methyne group resulting in the formation of hydroperoxides that decompose to alcohols, ketones, and lower molecular weight moieties (parts or portions) (Bailey, 1978).

Ozonation of the water-soluble polymers (i.e., polyethylene glycol, polyvinyl alcohol, polyvinyl pyrrolidone, polyacrylamide, and sodium polyacrylate) was studied to determine degradation efficiencies (Suzuki et al., 1979). The ozonation of these polymers was successful in lowering molecular weight and, consequently, in improving biodegradability. Ozonation in water is a complicated reaction because the self-decomposition of ozone is catalyzed by hydroxyl ions and is not the same as in organic solvents. The absorption rate of ozone into the polymer solution was affected by the reaction rate, the foaming property of the solution, and the self-decomposition of ozone (Suzuki et al., 1979).

5.1.4.9 Organometallic Compounds

In addition to the organic compounds previously mentioned, the versatility of ozone as an oxidizing agent is demonstrated by its ability to react with a variety of organometallics containing such metals as silicon, germanium, tin, lead, and mercury. In organosilicon compounds, cleavage due to ozonation is observed at silicon-hydrogen, silicon-carbon, and silicon-silicon bonds, with similar reactions for the other Group IVA organometallics. The ease of ozonation of the tetraethyl derivatives of the Group IVA elements is as follows: tetraethyl lead > tetraethyl tin > tetraethyl germanium > tetraethyl silicon. The products for the ozonation of tetraethyl tin in solvents include acetaldehyde, diethyl tin oxide, hydrogen peroxide, and triethylstannyl hydroxide. The same ozonation conducted in water produced acetaldehyde, hydrogen peroxide, and triethylstannyl hydroxide in near equal amounts (Bailey, 1978).

Other organometallic compounds oxidized by ozone include organomercurials. The major products obtained from the ozonation of organomercurials containing primary, secondary, or tertiary alkyl groups are the corresponding carboxylic acids, ketones, and alcohols (Bailey, 1978).

5.1.5 Ozonation in Aqueous Solution

Ozone oxidation of organic materials in water can occur by direct reaction of the organic material with ozone or by reaction of the organic material with hydroxyl radicals (OH·) formed by the decomposition of ozone (Hoigne and Bader, 1978). The decomposition of ozone is a hydroxide-ion catalyzed reaction that leads to the formation of more reactive species (Hoigne and Bader, 1975). At pH values less than 9, ozone reacts with organic materials directly. At pH values greater than 10, however, ozone is rapidly converted to hydroxyl radicals, which are less selective but more reactive with organic materials than ozone. In aqueous systems, ozone appears more efficient in organic destruction at an alkaline pH (pH > 9) due to the formation of these hydroxyl radicals, which are powerful oxidants.

5.2   Electrochemical Oxidation

In electrochemical oxidation, an electric potential is applied through a waste solution across two electrodes, to provide the driving force for oxidation of organic species. At the anode, electroactive species, such as organics, release electrons and are oxidized. For example, the net oxidation reaction of EDTA to carbon dioxide is as shown below.

$$C_{10}H_{16}N_2O_8 + 12H_2O \rightarrow 10CO_2 + N_2 + 40H^+ + 40e^- \qquad (5\text{-}2)$$

In alkaline wastes, carbon dioxide will react to form carbonates (Lawrence et al., 1994).

5.3   Thermal Destruction

In a wet air oxidation process, an oxidizing agent, such as oxygen or hydrogen peroxide, is applied in a pressurized water system operating at a temperature between 150 and 350 °C (300 and 660 °F). Most organic compounds are converted to carbon dioxide and water with destruction efficiencies greater than 99 percent (Krause et al., 1994).

In a supercritical water oxidation process, an oxidizing agent, such as oxygen or hydrogen peroxide, is applied in a pressurized water system operating at a temperature above 374 °C (> 705 °F), the critical temperature of water. Above the critical temperature only one phase is present, which minimizes mass transfer problems associated with wet air oxidation. Generally, the reaction is conducted at 400–650 °C (750–1,200 °F) and pressures of 250–300 atm. A residence time of only 1 to 5 min is required for destruction efficiencies greater than 99 percent. Deposition of salt is a problem that must be resolved (Krause et al., 1994), however.

In a high-temperature catalytic destruction process, a catalyst such as nickel is used to promote hydrolysis reactions to destroy organic compounds. Because hydrolysis is the primary reaction, an oxidizing agent is not required. Generally, the reactions can be conducted at, or near, ambient pressures (Krause et al., 1994).

5.4   Application to Hanford High-Level Waste

The chemistry of Hanford tank wastes is complex, with large uncertainties in the organic chemical inventory of individual tanks. Estimates of the organic inventory of the high-level waste tanks are based on a review of the available processing histories, direct analytical measurements, or a combination thereof. The total organic carbon inventory for all high-level waste tanks has been estimated between 1,500 and 1,800 t (1,700 to 2,000 tons), or less than 1 wt % of the 357,000 t (393,000 tons) of waste. Organic concentrations, however, vary widely among tanks. Based on processing histories, the Hanford Defined Waste (HDW) model was developed to predict the concentrations of a limited number of organics on a per tank-basis (Agnew, 1997). A detailed description of the model, together with the

estimated constituent inventories for each of the 177 Hanford tanks, is given in the report by Agnew (1997).[3] The total inventory for some organic materials estimated from the model is listed in table 5-1.

Five double shell tanks containing complexed concentrate waste have been determined to contain high concentrations of total organic carbon: AN–102, AN–107, AY–101, SY–101, and SY–103 (Schulz et al., 1995). To provide examples of organic constituents found in complex concentrate wastes, the results of organic speciation on samples from tanks SY–101, SY–103, and AN–107 are listed in tables 5-2, 5-3, and 5-4. Two other tanks, AN–104 and AN–105, containing double shell slurry feed also have high total organic carbon concentrations. One of the requirements for NRC Class C low-level waste designation is that the concentration of alpha-emitting transuranic isotopes, with half-lives greater than 20 yr, be less than 100 nCi/g (4.54×10^{-5} Ci/lb). This would require removal (e.g., by precipitation or ion exchange) of transuranic elements from tanks AN–102, AN–107, AY–101, and possibly from tanks AZ–101 and AZ–102, prior to vitrification. If strontium-90 or transuranic elements removal is required to meet the guidelines, organic destruction could be required to eliminate organic complexants and improve the efficiency of the pretreatment process (Schulz et al., 1995). Destruction of organic species present in tank wastes could also alleviate potential problems with gas generation and temperature rise, which could lead to explosions due to organic reactions (Colby, 1993). In-tank organic destruction is preferable to an out-of-tank destruction process, due to costs (Schulz et al., 1995). Both methods, however, need to be evaluated for optimization of cost, safety, and effectiveness.

It should be noted there is a high degree of uncertainty about the concentrations of the various organic species in Hanford tank wastes (Pabalan et al., 1999). The values listed in tables 5-2 to 5-4 may not be representative of organic concentrations in the Hanford waste streams. No detailed measurements of organic speciation, particularly for envelope C wastes, are available. However, Serne et al. (1996) concluded that proportionately more chelators and chelator fragments are found in the supernate solutions than in the solids of tanks SY–101 and SY–103, with EDTA the predominant chelator present. Because the waste stream to be treated in the organic destruction reactor is the aqueous effluent from the ion-exchange membrane process, the conclusion of Serne et al. (1996) would suggest the organics to be destroyed by ozonation would have consisted predominantly of organic complexants or degradation products.

5.4.1 Operational Considerations

5.4.1.1 pH

Solution pH can affect the kinetics and equilibrium of many of the reactions during ozonation. These include organic oxidation, decomposition of ozone to form free radicals, and metal/organic complexation.

Ozone decomposition kinetics are favorable when the solution pH is above 12. Below that value, significant amounts of ozone can pass through the solution without oxidizing other substances. In highly alkaline solutions, ozone possibly is not the primary oxidizing agent (Colby, 1993). Various reactions

---

[3] A brief description of the HDW model is given in Pabalan et al. (1999).

Table 5-1. Total inventory of organic chemicals in Hanford single-shell and double-shell tanks estimated from the Hanford Defined Waste model (Agnew, 1997)

Organic Chemical Compound	Total Mass (metric tons)
Dibutyl Phosphate	562
Butanol	198
Ethylenediaminetetraacetic Acid	619
Hydroxyethylenediaminetriacetate	1,030
Oxalate	114
Citrate	678
Glycolate	1,100
Acetate	99

Table 5-2. Average organic content of Hanford tank SY–101 core samples in milligrams of carbon, C, per gram of sample (from Serne et al., 1996)

Constituent	Drainable Liquid (mg C/g)	Solids (mg C/g)
TOC (total organic carbon)	10.9	11.1
NIDA (nitroimidazole)	1.04	0.82
NTA (nitrilotriacetic acid)	0.33	0.22
Citric acid	0.32	0.31
ED3A (ethylenediaminetriacetate)	0.30	0.28
EDTA (ethylenediaminetetraacetic acid)	2.23	0.80
HEDTA (hydroxyethylenediaminetriacetate)	—	—
Other fragments	0.61	0.42
Succinic acid	0.07	0.05
Oxalic acid	1.8	5.7
Acetic acid	—	—
Formic acid	1.4	0.62
Glycolic acid	0.54	—
NPH (normal paraffinic hydrocarbons)	0.80	0.02
Mass balance on C	79%	83%

Table 5-3. Organic carbon analyses for Hanford tank SY–103 (from Serne et al., 1996)

Constituent	Drainable Liquid (mg C/g)	Solids (mg C/g)
TOC (total organic carbon)	6.4	10.5
NIDA (nitroimidazole)	0.2	0.16
NTA (nitrilotriacetic acid)	0.14	0.16
Citric acid	0.42	0.56
ED3A (ethylenediaminetriacetate)	0.25	0.16
EDTA (ethylenediaminetetraacetic acid)	0.55	0.65
HEDTA (hydroxyethylenediaminetriacetate)	0.03	<0.01
Other fragments	<0.01	0.14
Succinic acid	0.02	0.02
Oxalic acid	—	6.0
Acetic acid	0.6	0.7
Formic acid	1.2	0.9
Glycolic acid	—	tbd
NPH	tbd*	tbd
Mass balance on C	53%	90%
*Listed as to be determined in original reference.		

were identified that yield hydroxide and ozonide radicals, which cause the oxidation of organic species (Tomiyasu et al.,1985).

For many organic chemicals, including oxalates, alkaline conditions favor oxidation. Oxidation of oxalate is maximized at a hydroxide to oxalate ratio of 6:1. Above this ratio, there is little improvement in oxidation. In solutions with no hydroxide added, little oxidation occurs. The same ratio of 6:1 also has been determined optimum for ozonation of acetate (Galutkina et al., 1977).

EDTA is the strongest complexant introduced into the Hanford tank waste in significant quantities. Experiments were conducted on EDTA in simulated Hanford tank waste over the pH range of 1–14 to determine the optimum pH for EDTA destruction. Reaction rates and stoichiometry were used to evaluate the pH effects on the ozone-EDTA reaction. At all pH levels, ozonation kinetics were characterized by pseudo-first-order reactions. When the steady-state ozone concentration was reached, the reaction rate became solely a function of EDTA concentration (Winters, 1981).

Table 5-4. Organic species identified in Hanford tank AN-107 supernate solution (from Serne et al., 1996)

Compound	mM	mg C/mL
Chelates/Complexants		
Citric acid	64.39	4.61
HEDTA	37.53	4.53
EDTA	31.41	3.77
Methane tricarboxylic acid*	17.32	1.45
NTA	7.33	0.53
Chelator Fragments		
ED3A	17.91	1.72
HEDDA	2.39	0.26
E2DTA	2.28	0.23
HEIDA	2.14	0.18
MeEDDA	1.02	0.08
others	—	0.14
Carboxylic Acids		
Docos-13en-oic	2.50	0.67
Hexanedioic	2.04	0.15
Hexadecanoic	2.04	0.39
Phthalic	1.10	0.10
Nonanedioic	0.83	0.07
Tetradecanoic	0.68	0.12
Pentanedioic	0.60	0.04
Octadecanoic	0.54	0.11
Hydroxybutanedioic	0.33	0.01
Butanedioic	0.10	0.01
Alkanes		
C_{23} to C_{35}	7.77	2.50
Phthalate esters	—	—
Dibutylphthalate	1.24	0.23
Dioctylphthalate	0.05	0.01
Total organic carbon	—	44.0

*Identification of this species is now considered erroneous (Serne et al., 1996).

Organic Destruction

At high pH, 10–14, a two-stage reaction was observed—EDTA oxidation began rapidly and increased after a period of 3 hr. A similar result was noted for intermediate pH values of 4.5–10, with significantly lower oxidation rates in the near-neutral pH region. The change in EDTA oxidation rates after about 3 hr was attributed to rapid oxidation of nitrite to nitrate after which more ozone was available for oxidation of the organic species. In the high pH region, the reaction rate increased from approximately 0.56/hr to approximately 1.2/hr, and the ozone consumption increased from 30 to 60 moles ozone per mole of EDTA. The optimum reaction rate occurred at pH values 11–12, with the lowest ozone consumption at a pH of 14. The controlling factor of the reaction appears to be the decomposition of ozone to form a hydroxyl free radical that reacts nonselectively with EDTA, tartrate, nitrite, and carbonate in the waste. Ozonation in the high pH range of 10–14 provides the highest reaction rate and lowest ozone consumption. A significant improvement in the ozonation of the waste at high pH levels could be realized if the nitrite concentration can first be reduced by some cheaper, simpler method.

In the intermediate pH region of 3–10, a similar two-stage reaction was observed in which the reaction rate increased from about 0.12/hr to about 0.70/hr; however, the ozone consumption decreased from 120 to 10 moles ozone per mole of EDTA. This change in reaction characteristics is believed caused by a change in the ozone oxidation mechanism (i.e., from one based on the formation of hydroxyl free radical to one in which the ozone molecule directly attacks the organic material) (Winters, 1981). The ozone attack is selective compared to the hydroxyl free radical attack. The initial slow EDTA reaction rate and large ozone consumption are possibly due to ozone initially attacking only nitrite; after the nitrite is oxidized, ozone rapidly and efficiently attacks EDTA. However, an undesirable consequence observed in ozonation of simulated waste in the intermediate pH region of 3–10 is the large amount of aluminum solids formed (Winters, 1981).

At low pH values, those less than three, EDTA destruction rates were low, and no increase was noted after any period of time. At these low pH values, the consumption of ozone was minimal, with 95 percent of the ozone fed detected in the offgas. At high pH values, the offgas contained only 10–20-percent ozone. The reaction rate in this pH region was about 0.047/hr and the ozone consumption was about 12 moles of ozone per mole of EDTA. The absence of a step change in EDTA destruction in low pH solutions was attributed to the lack of ozonation of nitrite, which is unstable to disproportionation in acidic conditions and not available to consume ozone. A 50-fold increase in oxidation rates for EDTA has been noticed as the pH increases from two to eight (Morooka et al., 1986). Increasing the temperature of the low pH reaction to 85 °C (185 °F) produced destruction rates comparable to those achieved by the low temperature, 60 °C (140 °F), high pH reactions. An advantage of ozonation in the low pH region is that no solids processing would be required. However, acidification of the waste would require large quantities of acid.

Ozonation at high pH levels provides the highest reaction rate and lowest ozone requirement without the need for a large solids separation process (Winters, 1981).

Although basic solutions seem to provide the best condition for organic oxidation using ozone, increasing the sodium hydroxide content of a simulated waste from 0.01 to 2.0 M caused an increase in production of stable, diatomic, oxygen and, therefore, was less reactive in oxidizing organic compounds (Winters, 1981).

184

Conversely, pH is affected by the ozonation process. The solution pH decreases as hydroxide ions are consumed. In destruction of hydroxyethylenediaminetriacetate (HEDTA)/EDTA in simulated tank SY–101 waste, the pH was observed to decrease from 13.2 to 11.8 during nearly complete ozonation of the organic components.

Ozone decomposes in alkaline solutions to form a variety of highly reactive intermediates, including OH·, HO_2·, O·⁻, O_3, and O_2 (Phig, 1976). Of these reactive intermediate species, the most important is the hydroxyl radical (OH·), which is mainly responsible for the high oxidation potential of ozone solutions at high pH. Because the hydroxyl radical is such a powerful oxidant, it can even oxidize carbonate ions. Carbonate ions scavenge hydroxyl radicals and reduce the interaction of hydroxyl radicals with other species in solution (Lutton et al., 1980). This effect is significant because the Hanford tank waste solutions contain large quantities of carbonate.

Within the concentration range studied, 0.01–2 M hydroxide, the ozone reactant decomposes faster at the higher hydroxide concentrations (Colby, 1993). When the hydroxide concentration drops below roughly 0.01 N, aluminum compounds precipitate. Therefore, when treating the wastes at Hanford, the hydroxide concentration should be maintained slightly above 0.01 M. This suggests that the pH should be at 12 or slightly higher.

5.4.1.2 Temperature

In general, higher temperatures lead to somewhat greater oxidizing potentials for ozonation of organic compounds. In experiments with oxalate, temperature had only a slight effect on the oxidation, but as noted previously, oxalate was not effectively oxidized in any of the experiments conducted (Galutkina et al., 1977). Increasing the temperature from 25 to 60 °C (77 to 140 °F) in simulated high-level waste shifted the reaction equilibria to favor oxidation of EDTA over oxidation of nitrite (Lutton et al., 1980). This shift is significant because much less ozone would be required if the organic chemicals were oxidized more favorably than nitrite. Also, tank corrosion could be prevented by keeping nitrite in solution, as opposed to converting it to nitrate.

Conversely, with respect to the effect of ozonation on temperature, studies indicate that the oxidation reactions, especially of higher molecular weight organic materials, are exothermic, leading to increasing temperatures as ozone is added to the reactor. Many thermal events occur simultaneously during ozonation of tank wastes. The addition of ozone causes some degree of cooling, and convective and evaporative losses also causes some cooling. During experiments with simulated SY–101 tank waste, the temperature rose from 25 °C (77 °F) to a maximum of 33 °C (91 °F) during nearly complete oxidation of the organic materials. When considering higher ozone flow rates, or mass ozonation processes, the thermal behavior of the system must be carefully estimated so that no thermal runaway reactions occur.

Within the temperature range studied, 30–75 °C (86–170 °F), the ozone reactant decomposes faster at higher temperatures. Therefore, cooling should be supplied to the organic destruction reactor (Colby, 1993).

185

Organic Destruction

5.4.1.3 Ozone Flowrate

Available data indicate that ozone will preferentially oxidize nitrite (NO_2^-) to nitrate (NO_3^-) before oxidizing organic materials in the waste. Ozone will also oxidize the multivalent metal ions present (Colby, 1993). Therefore, when treating Hanford wastes, sufficient ozone must be provided to oxidize the nitrites and the multivalent metal ions in the waste, in addition to the organic materials.

Ozone mass transfer and retention time are of utmost importance in maximizing the effectiveness of organic oxidation, even more than throughput. Using an enclosed reactor, the influence of the ratio of ozone flow rate to organic liquid flow rate on the conversion/oxidation of the organic species was determined (Delegard et al., 1993). With a 1:1 ratio, ozone use was about 85 percent effective. The effectiveness of ozone dropped to 60 percent when the gas-to-liquid ratio was changed to 2:1.

5.4.1.4 Reactor Design

One of the major problems associated with remediation of organic chemicals in high-level waste tanks is lack of effective mass transfer between the ozone and the waste solution. Reactors must be carefully designed to increase the contact surfaces between these phases.

Experiments have been conducted to determine the effect of reactor design on ozonation, using high shear mixers either enclosed or left open to the atmosphere (Delegard et al., 1993). Some experiments were conducted without any nitrite originally present so that ozonation products would all be derived from organic species. Tests were conducted using diluted genuine or simulated tank SY–101 wastes. Diluted wastes were used in the experiments to simulate the dilution caused by water sluicing of the wastes from the tanks (Delegard et al., 1993).

The following settings were used for both closed and open reactors: (i) ozone concentration of approximately 7.4 wt %, (ii) temperature of approximately 24 °C (75 °F), (iii) waste to diluent water ratio of 1:3, and (iv) duration of test approximately 16 hr. For the enclosed reactor tests, a diluted waste solution stream and a separate ozone gas stream, both with flow rates of 1 mL/min, were pumped into the reactor and blended using a high-shear mixer. For open reactor tests, the ozone was pumped at about 6.6 L/min into the bottom portion of a graduated cylinder containing 440 mL of dilute waste solution. The open reactor design supplied ozone to the solution at about 15 times the volumetric flow rate of the enclosed reactor system (15 versus 1 solution vol/min). The calculated gas-solution contact times for the two reactor designs were 12 sec for the closed reactor, and only 0.8 sec for the open reactor. The test results indicated that for the configurations tested, contact time was not the limiting factor in ozone oxidation of the wastes and that the rate of waste oxidation was limited by equipment design (i.e., gas-to-solution mass transfer), not by ozone/organic reaction kinetics. The study suggests that the open design provides the most rapid and efficient introduction of ozone reactant to the wastes.

Ozone is typically introduced as a minor constituent in a carrier gas of oxygen in air. The reactor must be ventilated to collect, treat, and discharge the carrier gas, along with any contaminants and reaction products swept from the reactor with the carrier gas.

Offgas analyses were also conducted to determine the by-products of ozonation as a function of time during oxidation (Delegard et al., 1993). Trace concentrations of carbon monoxide, hydrogen, nitrogen,

and carbon dioxide were observed, but most notably, no nitrogen oxides, ammonia, or volatile organic compounds were detected in the gas samples. Of these offgases, hydrogen concentrations reached a maximum of 0.011 percent, which is well below the flammability limit of hydrogen in oxygen. The presence of nitrogen in the offgas confirmed theories that amine-containing organic compounds, such as HEDTA and EDTA, are oxidized to produce nitrogen. In the experiments, integrated nitrogen gas concentration corresponded to 12 percent of the nitrogen present in HEDTA and EDTA. The remaining organic nitrogen was found oxidized to form nitrate (Delegard et al., 1993).

5.4.1.5 Application to Hanford Tank Waste Remediation System

Because nitrites and nitrates are present in large quantities in most Hanford tank wastes, ozonation to remove organic compounds is inherently difficult. Ozone has such a high oxidizing potential that it oxidizes all reduced species, including metals. In Hanford tank wastes, ozone would preferentially oxidize nitrites to nitrates prior to any significant oxidation of carbon compounds. However, some studies show that ozonation has a good potential to successfully treat organic-bearing tank wastes. One of the important parameters for successful oxidation of organic chemicals using ozone is intimate contact between the ozone and the chemical constituents. This intimate contact requires the use of a high shear mixer in laboratory scale tests, or some other method of maximizing gas/waste contact in the process tanks.

Predicting the effectiveness of ozonation in treating Hanford tank wastes is difficult because (i) numerous organic species are present; and (ii) depending on mass transfer conditions, the organic species can be oxidized to any intermediate between the original compound and carbon dioxide (Horvath et al., 1985).

The rate of decomposition of ozone in alkaline solutions is in seconds, which means that the rate limiting step in the oxidation of organic species would be the mass transfer of ozone into solution (Colby, 1993). Mass transfer can be improved by increasing the contact area, by improving the mixing in the ozonation reactor, or by increasing the residence (contact) time of the ozone in the reactor.

5.4.1.6 Ozonation Experiments on High-Level and Simulated Wastes

Over the past two decades, a number of ozonation studies have been conducted using simulated and genuine Hanford tank wastes. Some of the experiments that evaluated the effectiveness of ozonation in oxidizing organic species present in Hanford wastes are summarized in the next sections.

In general, ozone is used to oxidize organic compounds. It acts by attacking organic carbon to form carbonates, carboxylic acids, and other oxidized compounds. Ozone also reacts with amines to break nitrogen-carbon bonds, forming carboxylic acids, and carbonate and nitrate species, along with stable oxidized organic chemicals, such as oxalate. EDTA and acetate can be degraded to carbonate and nitrate with sufficient ozone. Oxalate reacts slowly with ozone, however, and remains in solution after other organic carbon compounds have been degraded to carbonate. Many of the ozonation reactions approach equilibrium, and an excess of ozone allows nearly 100 percent oxidation of organic species. Kinetic rate constants were published, and the waste/ozone contact was optimized to improve mass transfer. Some studies indicate, however, that the equilibrium position of some oxidation reactions, especially those involving oxalate, may be influenced by the presence of high-carbonate concentrations produced by the

187

break-down of organic compounds. The efficiency of organic oxidation by ozonation may be enhanced if oxidation products are removed from the process tanks to drive the equilibrium reactions to completion. Basically, the maximum conversion achievable is a question of kinetic rate versus thermodynamic equilibrium.

Various investigators conducted ozonation studies with specific organic compounds, simulated high-level waste, and actual high-level waste from double-shell tank SY–101. The chemicals present in tank SY–101 are listed in table 5-5 (Delegard et al., 1993; Herting et al., 1992). Notes and observations from ozonation experiments using several of the organic and inorganic compounds present in SY–101 tank waste are detailed in the following paragraphs.

Oxalate

Available data indicate that oxalates in waste are not easily oxidized by ozone (Colby, 1993). Ozonation of oxalate to carbonate was optimum at 60 °C (140 °F) in water with a pH of 8–10, with 2–4 moles ozone required per mole oxalate (Aloy et al., 1989), which is four times the stoichiometric requirement. The stoichiometry for the oxidation of oxalate by ozone is shown in Eq. (5-3).

$$C_2O_4^{2-} + O_3 + 2OH^- \rightarrow 2CO_3^{2-} + O_2 + H_2O \qquad (5\text{-}3)$$
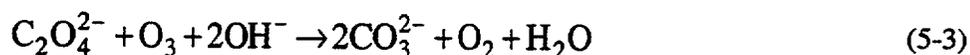
Although the stoichiometry indicates that 1 mole ozone will oxidize 1 mole oxalate, much less oxalate is actually oxidized and converted to carbonate. In fact, in a study of oxalate oxidation in aqueous medium, only 27 percent of oxalate was oxidized in the presence of a 60-fold excess of ozone (Galutkina et al., 1977). In other experiments (Colby, 1993), a well-stirred tank reactor was used for ozonation of oxalate in the presence of EDTA, acetate, and citrate (species present in the high-level waste tanks). Oxalate concentrations were reduced by about 10 percent using about 25 g of ozone/g of oxalate. Therefore, oxalate is considered relatively resistant to ozonation under the conditions tested (Colby, 1993).

The previous results were confirmed by Delegard et al. (1993) in experiments on ozonation of EDTA. In these experiments, oxalate comprised greater than two-thirds of the residual organic content after ozonation. Oxalate, due to its highly oxidized state, is relatively unreactive to gas generation and exothermic oxidation processes (Pabalan et al., 1999), especially as compared to HEDTA and glycolate. Thus, ozone-treated wastes, with residual organics mostly in the form of oxalate, will be much safer for further remediation, such as strontium and transuranic precipitation or other technology.

Oxidation of oxalic acid to carbon dioxide occurs in acidic aqueous solutions in the presence of ultraviolet light (Bailey, 1978). Therefore, if additional oxidation is required after removal of other organic chemicals that oxidize in basic conditions, near complete oxidation of oxalate may be achieved by acidifying the solution and operating under ultraviolet light.

Acetate

Four moles of ozone are theoretically required per mole of acetate for complete oxidation, based on the stoichiometry in Eq. (5-4):

Table 5-5. Organic chemical constituents of high-level waste in Hanford double-shell tank SY–101 (Delegard et al., 1993)

Chemical Name	Formula	Concentration (μg carbon/g sample)
NIDA (N-nitrosoiminodiacetate)	$ON-N-(CH_2CO_2)_2^{2-}$	168–2,210
NTA (Nitrilotriacetate)	$N-(CH_2CO_2)_3^{3-}$	54–337
CA (Citrate)	$^-O_2CCH_2-COH(CO_2^-)-CH_2CO_2^-$	10–84
ED3A (Ethylenediamine triacetate)	$^{-2}(O_2CCH_2)_2-N-CH_2CH_2-NH-CH_2CO_2^-$	20–260
EDTA (Ethylenediamine tetraacetate)	$^{-2}(O_2CCH_2)_2-N-CH_2CH_2-N-(CH_2CO_2)_2^{2-}$	51–480
HEDTA (2-Hydroxyethyl ethylenediamine triacetate)	$^{-2}(O_2CCH_2)_2-N-CH_2CH_2-N-(CH_2CH_2OH)CH_2CO_2^-$	10–20
Formate	HCO_2^-	1,700–1,790
Acetate	$CH_3CO_2^-$	1,640–1,840
Oxalate	$^-O_2CCO_2^-$	850–950

$$CH_3CO_2^- + 4O_3 + 3OH^- \rightarrow 2CO_3^{2-} + 4O_2 + 3H_2O \qquad (5\text{-}4)$$
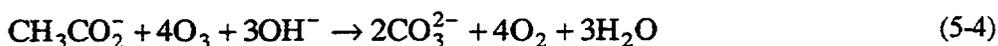
Acetate in aqueous solutions has been completely oxidized by a three-fold excess (four times the stoichiometric requirement) of ozone (Galutkina et al., 1977). A 50-percent decrease in acetate concentration was observed using an ozone-to-organic carbon ratio of about 20:1 (Colby, 1993). Acetate was also observed to readily oxidize during the ozonation of EDTA/HEDTA, while acetate was formed as an intermediate product prior to break-down to carbonates and carbon dioxide gas (Delegard et al., 1993). Temperature affected acetate oxidation. A temperature increase from 20–70 °C (68–158 °F) led to a 50-percent increase in acetate oxidation.

Organic Destruction

Citrate

Ozonation results on citrate are similar to those for acetate, with a 50-percent reduction in citrate concentration occurring when ozone was used at about 20:1 ratio of ozone-to-total organic carbon (Colby, 1993). Citrate oxidation is less effective below this ratio, but no increase in citrate destruction rates occur at higher ozone ratios.

Assuming that ozonation of citrate in alkaline solution produces carbonate, oxygen, and water, the theoretical chemical reaction is as follows:

$$C_6H_5O_7^{3-} + 9O_3 + 9OH^- \rightarrow 6CO_3^{2-} + 6O_2 + 7H_2O \tag{5-5}$$
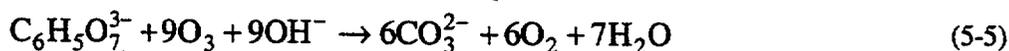
Formate

Ozonation tests have been conducted using formate as the source organic compound in simulated tank SY–101 waste (Delegard et al., 1993). About 80 percent of the organic carbon was destroyed readily by ozonation using a closed tank reactor. Ozonation of formate required greater than 10 moles ozone per mole formate, or about 10 times the stoichiometric requirement.

Assuming that ozonation of formate ($HCOO^-$) in alkaline solution produces carbonate, oxygen and water, the theoretical chemical reaction is

$$HCO_2^- + O_3 + OH^- \rightarrow CO_3^{2-} + O_2 + H_2O \tag{5-6}$$
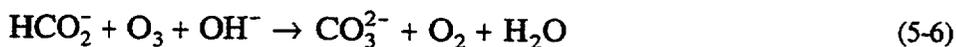
Triethylamine

Although not a chemical specifically known to exist in Hanford waste tanks, triethylamine can be a degradation product of EDTA. The inferred ozonation stoichiometry of the reaction in aqueous solutions (Elmghari-Tabib et al., 1982) is shown in Eq. (5-7).

$$(CH_3CH_2)_3N + 22O_3 + 13OH^- \rightarrow 6CO_3^{2-} + 22O_2 + NO_3^- + 14H_2O \tag{5-7}$$
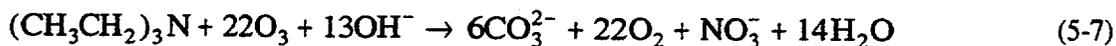
Ethylenediaminetetraacetic Acid and Chelating Agents

The Hanford tank wastes contain large quantities of organic complexants such as EDTA, HEDTA, citrate, and tartrate introduced during Hanford B Plant processing. Ozone is believed the most suitable reagent for oxidation of EDTA and HEDTA for several reasons: (i) ozone is a powerful oxidant in alkaline solutions, (ii) ozone easily can be made wherever and whenever desired using air (or oxygen) and electricity, and (iii) its use does not introduce any undesirable metal ions into the waste solution (Schulz, 1980).

Ozone will oxidize EDTA and HEDTA in both synthetic and actual waste solutions (Lutton et al., 1980). Available data indicate that about 90 percent of EDTA in the waste can be oxidized by ozone (Colby, 1993).

Essentially complete oxidation of EDTA was shown in experiments at 60 °C (140 °F) and a pH range 8–10 (Aloy et al., 1989). Ten moles ozone were required to destroy one mole of EDTA after correcting for ozone used in forming nitrate from nitrite present in the reactant stream (Winters, 1981). EDTA breaks down during oxidation to form intermediate species, such as formate, acetate, oxalate, and other organic compounds. Acetate and formate groups were shown metastable intermediates, which were subsequently oxidized to form inorganic carbons (e.g., carbonates and carbon dioxide). Oxalate, as discussed previously, was found not effectively oxidized by ozonation. Thus, the concentration of oxalate was observed to increase and eventually become the dominant organic species during ozonation of EDTA/HEDTA.

Tests were conducted to determine if organic nitrogen, present as amine forms in HEDTA and EDTA, could be oxidized by ozone. In a simulated waste solution without any initial concentration of nitrates or nitrites, 90 percent of the organic amine group nitrogen was converted to nitrate (Delegard et al., 1993).

Researchers observed no effect on the ozonation of EDTA due to solids removal, ozone concentration, or addition of manganese dioxide as a potential ozonation catalyst (Delegard et al., 1993).

A derived overall reaction equation for the ozonation of EDTA and HEDTA (Delegard et al., 1993) is shown as Eq. (5-8):

$$524\,OH^- + 760\,O_3 + 20\,C_{10}\,H_{15}\,N_2\,O_7^{3-} + 10C_{10}\,H_{12}\,N_2\,O_8^{4-} \rightarrow$$
$$760\,O_2 + 270\,CO_3^{2-} + 15C_2\,O_4^{2-} + 54NO_3^- + 3N_2 + 472\,H_2O$$

(5-8)
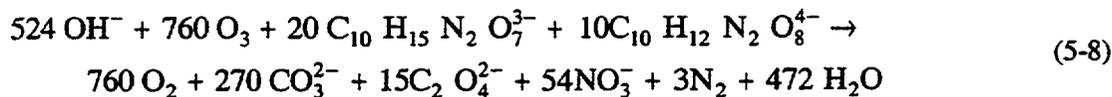
Both EDTA and HEDTA were nearly completely destroyed during ozonation experiments with simulated and actual SY–101 tank waste (Delegard et al., 1993).

Several inorganic elements can form complexes with EDTA and HEDTA, and more ozone is needed to break the bonds in these complexes. Two moles ozone were required to break one mole ligand coordination sites for organic complexes in high-level waste tanks. Iminodiacetate, nitrilotriacetate, and glycine were observed as the initial products of ozonation of complexed EDTA. Solution pH was found an important factor in ozonation. An increase in the pH from 2 to 8 produced a 50-fold increase in the oxidation rates for EDTA in an aqueous solution (Morooka et al., 1986).

Calcium and nickel have been observed to precipitate out of solution during ozonation (Delegard et al., 1993). This precipitation was attributed to the oxidation of organic complexing agents, such as EDTA, which previously kept the calcium and nickel in solution.

Organic Destruction

Nitrite

Nitrite, which resulted from radiolysis of nitrate or was added intentionally to several tanks to inhibit tank corrosion, is a significant component of Hanford tank wastes. Nitrite is readily oxidized by ozone, with only stoichiometric quantities of ozone needed to completely convert nitrite to nitrate.

$$NO_2^- + O_3 \rightarrow NO_3^- + O_2 \tag{5-9}$$

This reaction is important because nitrite is more readily oxidized than the organic species present in the waste (Delegard et al., 1993). Additionally, in experiments monitoring concentrations of various compounds in solution, the rate of organic chemical oxidation increased markedly at the point where nitrite had been fully oxidized to nitrate because ozone was then available for oxidation of other reduced species.

Because nitrite is the favored reactant for ozonation, some studies attempted to oxidize the nitrite prior to ozonation to reduce the total ozone needed to oxidize the organic chemicals. Attempts to preoxidize the nitrites by adding hydrogen peroxide to simulated high-level waste produced no observable effect on the organic material destruction rate or on the extent of organic destruction (Delegard et al., 1993).

Hydroxides

Hydroxide ions are present in high concentration in Hanford tank wastes. Observations of the concentration of hydroxide during ozonation of EDTA/HEDTA revealed hydroxide concentrations decreased by a factor of about seven, from 11 g/L (0.092 lb/gal.) to approximately 1.5 g/L (0.013 lb/gal.), after 14 hr of exposure to ozone (Delegard et al., 1993). The consumption of hydroxide ions was interpreted caused by three simultaneous reactions, shown in Eq. (5-10) to (5-12).

$$H_2O + O_3 + 2e^- \rightarrow 2OH^- + O_2 \tag{5-10}$$

$$68OH^- + C_{10}H_{12}N_2O_8^{4-} \rightarrow 10CO_2 + 2NO_3^- + 40H_2O + 5O_2 + 70e^- \tag{5-11}$$

$$CO_2 + 2OH^- \rightarrow H_2O + CO_3^{2-} \tag{5-12}$$
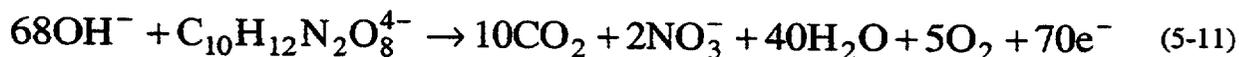
Eq. (5-10) represents the formation of hydroxide ions by reduction of ozone, Eq. (5-11) the consumption by oxidation of organic carbon and nitrogen in EDTA, and Eq. (5-12) the neutralization of carbon dioxide. Combining and chemically balancing these three reactions yield the net reaction:

$$18OH^- + 25O_3 + C_{10}H_{12}N_2O_8^{4-} \rightarrow 25O_2 + 10CO_3^{2-} + 2NO_3^- + 15H_2O \tag{5-13}$$
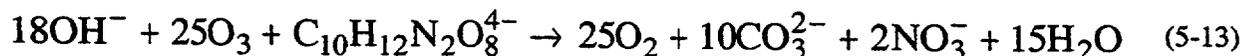
Additional hydroxide ions come from metal hydroxides (e.g., aluminum hydroxide and chromium hydroxide), which precipitate out of solution during ozonation and release OH⁻ ions that participate in reactions shown in Eqs. (5-11) and (5-12).

Aluminum hydroxide, which is present in the aqueous phase of tank wastes as aluminate ion, serves as a donor of hydroxide ions during ozonation (Delegard et al., 1993). The aluminum precipitates out of solution as the reaction shown in Eq. (5-14) is pushed to the right by the depletion of hydroxide ions:

$$Al(OH)_4^- \rightarrow \alpha - Al(OH)_3(s) + OH^- \tag{5-14}$$

X-ray diffraction analysis was used to establish that the aluminum hydroxide precipitate in Eq. (5-14) was bayerite (Delegard et al., 1993). If aluminate ions are present in the aqueous phase in sufficient quantities, the reaction shown in Eq. (5-14) could keep the waste liquid alkaline, which is favorable toward ozonation of the organics.

Chromium (III) is an important component in some Hanford tank wastes. For example, chromium (III) represents about 0.4 wt % of tank SY–101 waste (Herting et al., 1992). Thus, the oxidative dissolution of chromium also may occur during ozonation. Chromic hydroxide [Cr(OH)₃] is a green solid precipitate that is stable in tank wastes. During ozonation, however, chromic hydroxide is oxidized to form chromate ions (CrO₄⁻), which are soluble in the liquid layer and give the solution a yellow color. A color change from green to yellow was correlated with completion of organic oxidation in ozonation experiments using simulated SY–101 tank waste (Delegard et al., 1993). Although oxidation of chromium was found slower than oxidation of nitrite and organic complexants (HEDTA and EDTA), it was possible to fully oxidize the chromium (Delegard et al., 1993). Chromium oxidation is accomplished via the following reaction:

$$2\,Cr(OH)_3(ppt) + 3O_3(g) + 4OH^- \rightarrow 2CrO_4^{2-} + 3O_2(g) + 5H_2O \tag{5-15}$$

Other Inorganic Components

Many inorganic components that likely complex with organic chemicals in the liquid state precipitated during experimental ozonation (Delegard et al., 1993). These components include calcium, nickel, phosphate, barium, chromium, manganese, and iron. Other components that have also been noted to fall out of solution include the radionuclides promethium-147, strontium-90, europium-155, cobalt-60, americium-241, and plutonium. The concentration of cesium-137 was not affected by ozonation.

5.4.1.7 Overall Effectiveness of Ozonation on Simulated and Actual Waste

One of the main objectives of ozonation oxidation of organic chemicals present in high-level waste is to reduce the risk of exothermic reactions that could lead to high temperatures, and possible explosions, inside the high-level waste or process tanks. Simulated tank SY–101 waste, both before and after ozonation, was tested by differential scanning calorimetry for exotherms resulting from high temperature oxidation. The differential scanning calorimetry was run from 200 to 450 °C (390 to 840 °F), and an exotherm of 77 cal/g (140 Btu/lb) was detected on the sample prior to ozonation. After ozonation, the

total organic content on a dry basis was reduced from 2.3 wt % to 0.23 wt %, and no exotherm was observed. This suggests that ozonation could be an effective way to treat high-level waste containing organic species.

In the study by Delegard et al. (1993) on ozone oxidation of simulated tank SY–101 waste, complete oxidation of nitrite to nitrate occurred in 6–8 hr. The rate of oxidation of the organics (EDTA and HEDTA) was observed to increase to its maximum rate between 6–8 hr, corresponding to the time when nitrite had been fully oxidized to nitrate. Subsequently, the organic oxidation rate was observed to decrease and was essentially zero at 12 hr.

Delegard et al. (1993) conducted experiments using actual and simulated high-level wastes. One major difference between the two wastes was the initial oxidation state of the organic compounds. Only HEDTA and EDTA were used in the simulated high-level waste, but much of the organic carbon in the actual high-level waste existed as semioxidized species, including acetate, formate, and oxalate before ozone was added to the reactor. The relative amount of organic materials oxidized by ozonation in the two waste samples was 90 percent in simulated high-level waste but only 80 percent in the actual tank SY–101 waste. The lower ozonation efficiency in the actual waste was attributed to the larger concentration of oxalate, which is not oxidized effectively by ozone (Delegard et al., 1993). Because the residual organic carbon content after ozonation was 0.90 g/L (7.5×10^{-3} lb/gal.), of which only 0.44 g/L (3.7×10^{-3} lb/gal.) were oxalate, one can theorize another organic species, which is refractory and not susceptible to oxidation by ozone, was present. This species was not identified (Delegard et al., 1993).

Most other indicators of oxidation followed the same trends for both genuine and simulated high-level waste, including hydroxide concentration, aluminum concentration in solution, chromium dissolution, temperature, and pH. Additionally, plutonium was likely dissolved due to oxidation to plutonium (V) or plutonium (VI), which complex with hydroxide more readily than plutonium (III) or plutonium (IV). The elements calcium, strontium, and nickel all precipitated from solution as the actual waste was treated with ozone. The organic species that complexed these metals were oxidized, which made the metals insoluble in the liquid phase. The metal concentrations in solution were below detection limits after 8 hr of ozonation. Likewise, americium precipitated from solution to below its detection limit after 8 hr of ozonation.

5.4.1.8 Costs

The power requirement to ozonate 20,000 m³/yr (5.3×10^6 gal./yr) of Hanford tank waste has been estimated to be 70,000 kW-hr/yr, at a cost of about $2,000/day. An additional 90,000 kg/day (99 tons) of oxygen would be needed as carrier gas, at a cost of about $5,000/day. These estimates assumed three-to-one dilution of the waste and were based on use of an out-of-tank processing method, where waste feed would be pumped into stainless steel reservoirs for mixing, then sent to an ozone reactor kept in a small vault and, finally, sent to a product reservoir (Colby, 1993).

5.4.1.9 Electrochemical Oxidation

In electrochemical oxidation, an electric potential is applied through a waste solution across two electrodes to provide the driving force for oxidation of organic species. At the anode, electroactive

species, such as organics, release electrons and are oxidized. For example, the net oxidation reaction of EDTA to carbon dioxide is shown in the following equation:

$$C_{10}H_{16}N_2O_8 + 12H_2O \rightarrow 10CO_2 + N_2 + 40H^+ + 40e^- \qquad (5\text{-}16)$$
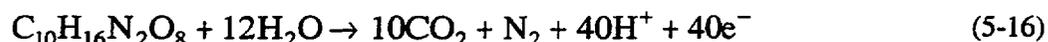
In alkaline wastes, the carbon dioxide will react to form carbonates (Lawrence et al., 1994).

Bench-scale testing on simulated Hanford waste suggests that electrodes of platinized titanium are preferable to others tested (Lawrence et al., 1994).

The maximum destruction rate of organic material (EDTA) in simulated Hanford wastes was observed at approximately 50 °C (122 °F). At lower temperatures, the decreased organic destruction rate is attributable to theoretical chemical reaction kinetics as a function of temperature. At higher temperatures, the decrease in destruction rate is attributable to increased competition from other reactions (Lawrence et al., 1994).

Higher flow rates of simulated Hanford waste through the electrochemical cell produced increased turbulence. Turbulence produced an increase in the organic destruction rate of the organic material (EDTA) (Lawrence et al., 1994).

If the hydroxide concentration in simulated Hanford tank SY–101 waste was allowed to drop below approximately 0.01 N, aluminum compounds precipitated. A build-up of precipitated solids could impact electrochemical cell efficiency. Because the inorganic carbon produced during organic oxidation consumes free hydroxide, additions of hydroxide may be needed to prevent excessive solids generation (Colby, 1993).

5.4.1.10 Thermal Oxidation

Operational considerations vary depending on which thermal oxidation method is selected. Neither BNFL Inc. nor LMAES proposed thermal oxidation. Therefore, no specific set of operational considerations were identified as applicable.

5.4.2 Safety Considerations

5.4.2.1 Ozone Oxidation

Appropriate ventilation is necessary for the ozonation process, so that oxygen, carbon dioxide and other gaseous products can be removed from the tanks. If ozonation is conducted in-tank, then the capacity of double-shell tank ventilation systems must be carefully checked. Major modifications may be necessary to treat the waste in-tank. Corrosion of the double-shell tank steel liner, which has been maintained by using high nitrite concentrations, must be avoided during oxidation. Corrosion could lead to stress cracking in the tanks; therefore, nitrite and free hydroxide ion concentrations must be carefully monitored. Also, gas generation rates may lead to entrapment of flammable gases in the double-shell

tanks containing high-solids concentrations (Schulz et al., 1995). Agitation using a high-shear mix may be needed, both to disperse ozone throughout the waste and to prevent entrapment of gas bubbles.

Pressurization of the tanks, as well as the hazards of working with ozone, a ground-level pollutant, must be carefully considered when designing an ozonation process to oxidize high-level waste at Hanford.

Ozone is created by passing oxygen through an electric corona (Colby, 1993). If the ozone generator is located onsite, industrial practices for safety around electric equipment must be observed.

Ozone is a human poison by inhalation. Systemic effects include secretion of tears, headache, dermatitis, cough, and difficulty in breathing. It is an irritant to skin, eyes, upper respiratory system, and mucous membranes. A concentration of 1 ppm produces a disagreeable sulfur-like odor and may cause headache and irritation of the eyes and upper respiratory tract. These symptoms discontinue after leaving the 1 ppm exposure. Mutation data have been reported (Lewis, 1997).

The OSHA PEL and the ACGIH TLV are both 0.1 ppm. These are time-weighted averages (Lewis, 1997) representing the amount to which workers can be exposed for a normal 8-hr day, 40-hr work week, without ill effects. The 0.1 ppm limit is for light work; moderate and heavy work have lower limits of 0.08 and 0.05 ppm, respectively. The ACGIH Short-Term Exposure Limit (STEL) is 0.3 ppm. Ozone is considered immediately dangerous to life and health at a concentration of only 5 ppm. Therefore, the area where ozone is generated should either be isolated, well ventilated, or both.

Because ozone is on the list of Extremely Hazardous Substances established under the Superfund Amendments and Reauthorization Act, certain emergency planning activities may be required. Ozone is reported in the EPA TSCA Inventory (Lewis, 1997).

Ozone is a powerful oxidizing agent that reacts dangerously with a large number of substances (Lewis, 1997). Therefore, it should not be combined with other chemicals unless the possible reactions have been adequately investigated and appropriate precautions taken.

Incomplete oxidation can form stable intermediate compounds that can be hazardous (Krause et al., 1994). Offgases created from destruction of organic materials in the waste could be flammable. Combination of oxygen and flammable organic offgases could produce an explosive mixture in the organic destruction reactor (Colby, 1993).

5.4.2.2 Electrochemical Oxidation

Appropriate industrial practices for safety around electrical equipment must be observed.

5.4.2.3 Thermal Destruction

For a wet-air oxidation operation or for supercritical water oxidation, industrial practices for safety around high-temperature equipment and around pressurized equipment must be observed.

For a high-temperature catalytic destruction process, industrial practices for safety around high-temperature equipment must be observed.

5.4.3 Comparable Operations in Existence

5.4.3.1 Ozone Oxidation

Ozone has been used for the past 100 yr in the municipal waste industry to oxidize trace amounts of organic materials (Colby, 1993). Ozone has not been used on an industrial scale for pretreatment of radioactive waste, however.

5.4.3.2 Electrochemical Oxidation

No industrial scale electrochemical oxidation of organic complexants in radioactive wastes was identified. Study of electrochemical oxidation of Hanford wastes is presently developmental. Only bench-scale work has been performed and published, and that was performed using simulated wastes.

5.4.3.3 Thermal Destruction

No industrial scale wet-air oxidation operation, or supercritical water oxidation operation, or high-temperature catalytic destruction operation, for destruction of organic materials in high-level waste was identified.

5.5 Organic Destruction Methods Proposed by BNFL Inc.

BNFL Inc. proposed no organic material destruction operations. Should an organic destruction step be needed for envelope C wastes, ozonation would be a logical process to evaluate because it is better developed for this application than electrochemical and thermal destruction technologies. It should be recognized, however, that studies on destruction by ozonation of organic complexants in radioactive wastes that were published are developmental studies. Most experiments used solutions of relatively simple chemistry compared to actual tank wastes. Because of the high degree of uncertainty in the speciation and concentration of organic materials in Hanford tank wastes, even those experiments that used actual wastes may not reflect accurately the organic species that would be present in Hanford waste streams. Thus, additional testing would be required to verify the applicability of ozonation on actual Hanford waste feeds. Furthermore, larger scale tests would be needed to obtain data for scaling up to an industrial size reactor (Colby, 1993).

5.6 References

Agnew, S.F. *Hanford Tank Chemical and Radionuclide Inventories: HDW Model Rev. 4.*
    LA–UR–96–3860. Los Alamos, NM: Los Alamos National Laboratory. 1997.

Aloy, A.S., V.E. Vyatkin, and D.M. Gurevitch. Cleaning of liquid radioactive waste by the methods of
    ozonization and magnetic separation. *Waste Management '89*. R.G. Post and M.E. Wacks, eds.
    University of Arizona, Tucson, AZ: 391–395. 1989.

Bailey, P.S. *Ozonation in Organic Chemistry.* Volume I and II. New York: Academic Press. 1978.

197

Organic Destruction

Colby, S.A. *Ozone Destruction of Hanford Site Tank Waste Organics.* WHC–SP–1004. Richland, WA: Westinghouse Hanford Company. 1993.

Cotton, F.A., and G. Wilkinson. *Advanced Inorganic Chemistry.* 4th edition. New York: John Wiley and Sons. 1976.

Delegard, C.H., A.M. Stubbs, and S.D. Bolling. *Laboratory Testing of Ozone Oxidation of Hanford from Tank 241–SY–101.* WHC–EP–0701. Richland, WA: Westinghouse Hanford Company. 1993.

Elmghari-Tabib, M., A. Laplanche, F. Venien, and G. Martin. Ozonation of amines in aqueous solutions. *Water Research* 16: 223–229. 1982.

Galutkina, K.A., E.V. Rubinskaya, and A.G. Nemchenko. Reactions of oxalic and acetic acids with ozone in an aqueous medium. *Journal of Applied Chemistry (USSR)* 50: 2,498–2,500. 1977.

Herting, D.L., D.B. Bechtold, B.E. Hey, B.D. Keele, L. Jensen, and T.L. Welsh. *Laboratory Characterization of Samples Taken in December 1991 (Window E) from Hanford Waste Tank 241–SY–101.* WHC–SD–DTR–026. Revision 0. Richland, WA: Westinghouse Hanford Company. 1992.

Hoigne, J., and H. Bader. The role of hydroxyl radical reactions in ozonation process in aqueous solutions. *Water Research* 10: 377–386. 1975.

Hoigne, J., and H. Bader. Ozonation of water: kinetics of oxidation of ammonia by ozone and hydroxyl radicals. *Environmental Science and Technology* 12: 79–84. 1978.

Horvath, M., L. Bilitzky, and J. Huttner. *Ozone.* Amsterdam, Netherlands: Elsevier. 1985.

Krause, T.R., J.C. Cunnane, and J.E. Helt. *Sludge Technology Assessment.* ANL–94/95. Argonne, IL: Argonne National Laboratory. 1994.

Lawrence, W.E., J.E. Surma, K.L. Gervis, M.F. Buehler, G. Pillay, and A.J. Schmidt. *Electrochemical Organic Destruction in Support of Hanford Tank Waste Pretreatment.* PNNL–10131. Richland, WA: Pacific Northwest National Laboratory. 1994.

Lewis, R.J. *Hazardous Chemicals Desk Reference.* New York: Van Nostrand Reinhold Publisher. 1997.

Lutton, T.W., W.W. Schulz, D.M. Strachan, and L.J. Bollyky. *Ozonation of Hanford Nuclear Defense Waste.* RHO–SA–98. Richland, WA: Rockwell Hanford Operations. 1980.

Morooka, S., K. Ikemizu, H. Kamano, and Y. Kato. Ozonation rate of water-soluble chelates and related compounds. *Journal of Chemical Engineering of Japan* 19: 294–299. 1986.

Pabalan, R.T., M.S. Jarzemba, D.A. Pickett, N. Sridhar, J. Weldy, C.S. Brazel, J.T. Persyn, D.S. Moulton, J.P. Hsu, J. Erwin, T.A. Abrajano, Jr., and B. Li. *Hanford Tank Waste Remediation System High-Level Waste Chemistry Manual.* NUREG/CR–5751. Washington, DC: Nuclear Regulatory Commission. 1999.

Phig, M. The chemistry of ozone in the treatment of water. *Water Resources* 10: 361–365. 1976.

Schmidt, A.J., M.R. Elmore, R.J. Orth, E.O. Jones, A.H. Zacher, T.R. Hart, G.G. Neuenschwander, and J.C. Poshusta. *Organic Destruction to Enhance the Separation of Strontium in Radioactive Wastes.* PNNL–SA–24698. Richland, WA: Pacific Northwest Laboratory. 1994.

Schulz, W.W. *Removal of Radionuclides from Hanford Defense Waste Solutions.* RHO–SA–51. Richland, WA: Rockwell Hanford Operations. 1980.

Schulz, W.W., M.J. Kupfer, and M.M. McKeon. *In-Tank Processes for Destruction of Organic Complexants and Removal of Selected Radionuclides.* WHC–SD–WM–ES–321. Richland, WA: Westinghouse Hanford Company. 1995.

Serne, R.J., G.A. Whyatt, S.V. Mattigod, Y. Onishi, P.G. Doctor, B.N. Bjornstad, M.R. Powell, L.M. Liljegren, J.H. Westsik, Jr., N.J. Aimo, K.P. Recknagle, G.R. Golcar, T.B. Miley, G.R. Holdren, D.W. Jeppson, R.K. Biyani, and G.S. Barney. *Fluid Dynamic Particulate Segregation, Chemical Processes, and Natural Ore Analog Discussions that Relate to the Potential for Criticality in Hanford Tanks.* WHC–SD–WM–TI–757. Richland, WA: Westinghouse Hanford Company. 1996.

Suzuki, J., N. Taumi, and S. Suzuki. Ozone treatment of water-soluble polymers. IV. Ozone degradability of water-soluble polymers. *Journal of Applied Polymer Science* 23: 3,281–3,288. 1979.

Tomiyasu, H., H. Fukutomi, and G. Gordon. Kinetics and mechanism of ozone decomposition in basic aqueous solution. *Inorganic Chemistry* 24: 2,962–2,966. 1985.

Waters, W.L., A.J. Rollin, C.M. Bardwell, J.A. Schneider, and T.W. Aanerud. Oxidation of secondary alcohols with ozone. *Journal of Organic Chemistry* 41: 889–891. 1976.

Winters, W.I. *Effect of pH on the Destruction of Complexants with Ozone in Hanford Nuclear Waste.* RHO–SA–203. Richland, WA: Rockwell Hanford Operations. 1981.

6 PRECIPITATION AND FILTRATION

Envelope C low-activity waste feeds are characterized by high amounts of organic complexants, resulting in aqueous complexes of strontium and transuranic elements that inhibit removal by ion exchange. In the proposed BNFL Inc. pretreatment flowsheet, plans are to subject these particular wastes to an additional treatment step involving coprecipitation of strontium-90 and transuranic elements with a ferric floc precipitate.

6.1 Theory of Ferric Floc Precipitation and Coprecipitation

Coprecipitation, or carrier precipitation, is the removal of a target element in this case, strontium and transuranic elements from solution and incorporation into solids as a result of forced precipitation of another solid phase. From a thermodynamic perspective, coprecipitation is the lowering of the concentration of a dissolved target element below the solubility limit of its pure solid phase. The equilibrium aqueous concentration of an element in the presence of a solid may be expressed by a reaction such as the following, with plutonium (Pu) as an example target element:

$$Pu(OH)_4(s) = Pu(OH)_4^0$$
$$K = 10^{-10.1} \text{ at } 25\,°C \qquad \text{(Ewart et al., 1980)} \qquad (6\text{-}1)$$

In this example for plutonium, the reaction is written in a form that shows (i) what is believed the solubility-limiting plutonium solid phase and (ii) a key dissolved plutonium species under typical Hanford tank waste conditions (Serne et al., 1996). If the solid plutonium hydroxide [(Pu(OH)$_4$(s)] is present, its activity may be assumed to be one, and the activity—and approximate molarity—of dissolved plutonium hydroxide [Pu(OH)$_4^0$] will be $10^{-10.1}$. Note that reactions may be written using other dissolved plutonium species, such as

$$Pu(OH)_4(s) = Pu^{4+} + 4OH^-$$
$$K = 10^{-55.2} \text{ at } 25\,°C \qquad \text{(Lemire and Tremaine, 1980)} \qquad (6\text{-}2)$$

A simple calculation shows the presence of the solid with free hydroxide ion concentration equal to 1 M, as will be imposed during processing, limits the plutonium (Pu^{4+}) concentration to approximately 10^{-55} M. This low value does not represent the total plutonium concentration. The total is better expressed by Eq. (6-1), which involves the dominant dissolved plutonium species under tank conditions. The situation is more complex in wastes with high concentrations of ligands, both organic and inorganic, that may form stable aqueous complexes of the target elements and result in dissolved concentrations above those imposed by the relatively simple hydrolysis reactions discussed previously.

The goal, then, of coprecipitation treatment is to lower dissolved concentrations to well below stoichiometric solubility limits, which may exceed operational, regulatory, or safety limits, and then remove the excess to filterable solid phases. In the following section, a conceptual discussion of the various coprecipitation phenomena is presented, with specific reference to the proposed BNFL Inc. pretreatment. From a thermodynamic approach, the key process for achieving coprecipitation is through

solid solution in a carrier solid. Another, less quantifiable, chemical process that removes dissolved elements is adsorption onto the carrier solid. Removal may also be a physical process, as coagulating carrier solids, such as ferric hydroxide, trap precipitates or colloids of target radionuclides and allow them to settle more readily (Orth and Kurath, 1994). Also discussed later are two processes (displacement and dilution) that are not coprecipitation but may be at work in the proposed treatment. Two general reviews that discuss coprecipitation methods in a larger context of radionuclide separation may be found in Krause et al. (1994) and Kolarik (1991).

6.1.1 Solid Solution

If a trace metal precipitates along with a major metal and substitutes for it at trace levels in the crystal lattice of the major solid phase, the metals are said to form a solid solution. The key thermodynamic attribute of a solid solution is that it allows the presence of a solubility-limiting solid at a chemical activity substantially below unity (e.g., Stumm and Morgan, 1996; Bruno et al., 1995). Consider, for example, the solid solution of americium in ferric hydroxide. Solubility reactions for hydroxides of both elements, using the dominant aqueous species at 1 M hydroxide ion, can be written as in the following equation [using log K values from the data0.com.R2 database for EQ3/6 (Wolery, 1992)]:

$$Am(OH)_3(s) = Am(OH)_3^0(aq)$$
$$K = 10^{-10.5} \text{ at } 25\,^{\circ}C$$

(6-3)

$$Fe(OH)_3(s) + H_2O = Fe(OH)_4^- + H^+$$
$$K = 10^{-17.5} \text{ at } 25\,^{\circ}C$$

(6-4)

The activities of the hydroxide solids are no longer unity; rather, they are approximated by the molar fraction of the corresponding solid component in the mixed solid hydroxide. If americium composes a small molar fraction of the ferric hydroxide, the activity of the dissolved americium hydroxide [$Am(OH)_3^0$] species is lower than if pure solid americium hydroxide [$Am(OH)_3(s)$] were present. Combining these reactions and writing a simplified equilibrium constant relationship that, for the sake of brevity, neglects activity coefficients (which can be substantially lower than unity at the high ionic strengths of Hanford wastes) yields

$$\left(\frac{Am}{Fe} \right)_{aq} \cdot \left(\frac{Fe}{Am} \right)_s \cdot \left(\frac{1}{H^+} \right) \cong 10^7$$

(6-5)

where aq denotes the molar ratio of dissolved concentrations, and s denotes the molar ratio in the solid hydroxide.

At 1 M hydroxide, the pH equals 14 and the expression becomes

$$\left(\frac{Am}{Fe} \right)_{aq} \cong 10^{-7} \left(\frac{Am}{Fe} \right)_s$$

(6-6)

In other words, the ratio of the moles of americium to the moles of iron in the liquid is many orders of magnitude lower than the ratio in the solid. Another way of expressing the lowering of dissolved americium in this case is to note that, by Eq. (6-3), the activity of dissolved americium hydroxide [Am(OH)$_3$^{0}] is reduced by the same factor as solid americium hydroxide [Am(OH)$_3$(s)] {i.e., the mole fraction of americium in solid ferric hydroxide [Fe(OH)$_3$(s)]}. It can be seen that solid solution can be effective at removing trace metals from solution.

Caution is appropriate in applying the coprecipitation model to the removal of strontium and transuranic elements from Hanford tank wastes for a number of reasons. First, reactions such as the preceding apply only to the specific aqueous and solid species modeled, and only if true solid solution is a viable process. For example, ionic plutonium (Pu^{4+}) should not form a solid solution with ferric hydroxide (Serne et al., 1996), though plutonium removal is noted in ferric hydroxide precipitation experiments (e.g., Hobbs et al., 1993; Hobbs, 1995). Neither is strontium removal under these circumstances believed to be true solid solution (Orth and Kurath, 1994). Furthermore, the distribution of dissolved metals may be strongly influenced by the presence of a variety of anions, so that coprecipitation could be highly waste-specific. Second, experimentally based thermodynamic data are typically sparse in the high-pH range under consideration. Third, kinetic effects may prevent the achievement of equilibrium relationships. Fourth, and finally, accurate information on solid-phase activity coefficients, which may differ substantially from a value of one, may be lacking.

6.1.2 Coagulation

Coagulation (or flocculation) is a physical phenomenon, but is generally included under the category of coprecipitation (Pabalan et al., 1999). While ferric hydroxide precipitates and settles, colloids and other precipitates may adhere to surfaces, be enveloped by the growing hydroxide, and settle out with it. Coagulation is conceptually distinguished from adsorption (below) in that it does not act on truly dissolved species. Coagulation is dependent on electrostatic effects that vary with chemical parameters such as solution pH and ionic strength. Coagulation is thought to be an important process for plutonium coprecipitation with ferric floc, because plutonium may be partly present in waste liquids as a polymer that may otherwise remain suspended (Slater et al., 1994; Serne et al., 1996). In addition, experiments suggest that coagulation is an effective mechanism for strontium removal from waste simulants (Orth et al., 1995). However, coagulation is a difficult process to quantify without experimental data on plutonium and strontium decontamination factors from ferric hydroxide precipitation in actual waste solutions.

6.1.3 Adsorption

While adsorption of dissolved metals onto solid surfaces is a chemical process (see discussion in Pabalan et al., 1999), like coagulation, it is difficult to model and quantify without waste-specific experiments. Even in such experiments, isolating adsorption effects may be difficult. Adsorption is highly dependent on the aqueous speciation of a metal and, thus, on pH (e.g., Turner, 1995). If, under a given set of circumstances, a metal forms highly stable dissolved species (e.g., uranium at high pH and aqueous carbonate concentration), adsorption may be less important in limiting dissolved metal. Again, specific adsorption data applicable to Hanford waste treatment conditions are lacking. For example, a review of plutonium precipitation phenomena was unable to conclude whether plutonium adsorption onto

hydroxides would be dominant or negligible at high-pH and high-dissolved carbonate concentration (Serne et al., 1996). Understanding adsorption effects would be advanced by experiments designed to determine distribution coefficients for plutonium and strontium at chemical conditions analogous to those of actual wastes. Such tests could be designed to isolate the effects of adsorption from the effects of other decontamination processes.

6.1.4 Displacement

Displacement is not a coprecipitation phenomenon, but it may contribute to radionuclide removal from solution during treatment. Displacement takes place when an added metal cation forms complexes with ligands (e.g., organic complexants) that may be contributing to elevated concentrations of target metals. The added metal may successfully compete with the target metal for the complexants and, thus, lead to precipitation of the target metal. The affinity of the metal ion for complexation with an organic ligand such as EDTA may be represented by a complexation constant (K) such as (Orth et al., 1995)

$$Fe^{3+} + EDTA^{4-} = FeEDTA^-$$
$$K = 10^{24.2}$$

(6-7)

Displacement is most readily achieved when the added metal has a complexation constant significantly higher than the target radioelement (Orth et al., 1995). The complexation constant for plutonium (Pu^{3+}, Pu^{4+}, and Pu^{6+}) is approximately 10^{18} and for strontium (Sr^{2+}) it is $10^{8.8}$, suggesting that ferric ion (Fe^{3+}) may be useful for displacement. For the case of strontium, however, Orth et al. (1995) concluded that removal via ferric nitrate addition was controlled by coagulation, rather than by displacement.

6.1.5 Isotope Dilution

The addition of strontium nitrate in the pretreatment stage of the BNFL Inc. process has the effect of mixing a large amount of nonradioactive strontium with the radioactive strontium-90 in the waste liquid and raising the total dissolved strontium content above the solubility limit. The combination of isotopically diluting the strontium-90 and precipitating strontium salts results in a lowering of the liquid strontium-90 content. This removal process is therefore largely dependent on pure phase precipitation. Several studies (Orth and Kurath, 1994; Schulz et al., 1995; Herting, 1995) concluded that strontium precipitation is an efficient process for strontium-90 removal and is likely aided by coagulation of strontium precipitates onto precipitating hydroxides, such as the ferric floc produced in the BNFL Inc. process.

6.2 Application to Hanford High-Level Waste

6.2.1 Operational Considerations

This section presents test results on strontium and transuranic elements removal from Hanford wastes or similar wastes using methods applied in the BNFL Inc. treatment plan. This discussion is not intended as an exhaustive review. Recent tests by BNFL Inc. were not available for review. Data are often presented using the decontaminaiton factor, which is the factor by which the liquid concentration of the target

204

radionuclide is diminished (e.g., a decontamination factor of 20 means that 95 percent of the radionuclide was removed). Table 6-1 shows test results on Hanford complexant concentrate wastes or simulants, representative of the type of wastes to be subjected to coprecipitation.

6.2.1.1 Strontium

Studies involving ferric hydroxide precipitation, without strontium addition, in European liquid wastes that apparently did not contain organic complexants, resulted in decontamination factors of greater than 100 (Orth and Kurath, 1994). In those studies, the pH of the originally acidic wastes was raised to greater than 13 by addition of sodium hydroxide, causing iron, originally present in the waste, to precipitate as ferric hydroxide. It is unclear from the studies whether the pH adjustment to alkaline values caused the strontium to precipitate. It is likely the precipitated ferric hydroxide acted to carry the coprecipitated strontium out of solution. The ferric hydroxide removal process takes place rapidly, and increasing the amount of contact time from 30 min to 2 hr had no measurable impact on strontium removal (Orth and Kurath, 1994). For those tests in which the strontium-iron-precipitate remained in contact with the solution for 13 days, the amount of strontium that redissolved was insignificant. This result on the stability of the precipitate suggests that, for pretreatment of Hanford wastes, there would be sufficient time for the planned filtration step and subsequent transfer to the high-level waste melter feed.

In contrast to the results on European wastes, which gave decontamination factors greater than 100, tests on Hanford wastes or simulants (Herting, 1995; Schulz et al., 1995; Orth et al., 1995) at high hydroxide ion concentrations show decontamination factors of only 2–5 from ferric precipitation through addition of ferric nitrate alone. Strontium-90 decontamination factors of 15–170 were achieved in studies that used strontium nitrate addition, although decontamination factors were lower in tests on organic complexed wastes compared to those on noncomplexed wastes. Results for the complexed wastes are shown in table 6-1. Strontium-90 removal by strontium nitrate addition would be sufficient to meet Class C limits even if organic complexants were not removed (Schulz et al., 1995). These results show that strontium-90 precipitation by isotope dilution is important in treating these wastes. Additional data from Orth et al. (1995) indicate that temperature had minimal effect on strontium removal.

6.2.1.2 Transuranics

Ferric hydroxide removal of transuranics from noncomplexed waste takes place rapidly, and increasing the contact time from 30 min to 2 hr has no measurable impact on plutonium removal (Orth and Kurath, 1994). Therefore, the plan to allow 4 hr of contact time for precipitation of transuranic isotopes from the wastes at Hanford should be adequate to meet Class C limits in the absence of organic complexants.

Precipitation testing has been successfully performed for concentrations of 540 mg/L of iron together with 5 mg/L of strontium. In these tests, decontamination factors of greater than 100 were reported for strontium precipitation. The precipitation (separation) of plutonium was described as adequate to reach goals (Orth and Kurath, 1994). These results suggest that, for the wastes at Hanford, the desired removal of transuranic elements from noncomplexed wastes is probably achievable.

A survey of hydroxide coprecipitation methods for transuranic elements in a variety of wastes using a variety of precipitant metals found a decontamination factor range of 5–5,000 (Brooks and Kurath, 1993). None of these tests appeared to involve solutions bearing significant amounts of organic

Table 6-1. Decontamination factors for strontium and transuranics from Hanford complexant concentrate wastes (i.e., wastes containing organic complexants)[*]

Study	Conditions	Precipitant Concentration	Sr	Pu	Am
Herting (1995)	1.5 M OH⁻ 22–25 °C	0.1 M Fe^{3+}	2	2	6
		0.1 M Fe^{3+} twice	4	3	22
		0.3 M Fe^{3+}	4	4	10
		0.1 M Sr^{2+}	19	1.1	2
	3.0 M OH⁻ 22–25 °C	0.1 M Fe^{3+}	2	—	24
		0.1 M Fe^{3+} twice	5	2	32
		0.3 M Fe^{3+}	5	5	22
		0.1 M Sr^{2+}	15	1.2	2
Orth et al. (1995)	~1 M OH⁻ 65 °C	0.11 M Fe^{3+}	3–4	—	—

[*] Iron or strontium was added to the waste as nitrate. The tests by Orth et al. (1995) were performed on a waste simulant.

complexants. In a similarly broad survey (Slater et al., 1994), decontamination factors of up to 19,000 for transuranic elements were reported. Tests on organic complexed Hanford wastes using single-stage ferric nitrate additions at high-hydroxide concentrations (table 6-1), however, show significantly lower decontamination factors overall for plutonium (2–5) and americium (6–24; somewhat higher values are obtained when the supernatant is treated a second time). It is apparent that organic complexants have a detrimental effect on the efficiency of transuranic element coprecipitation. However, Schulz et al. (1995) concluded that the level of transuranic element reduction achieved in the tests is sufficient to allow the immobilized low-activity waste to meet NRC Class C and incidental waste concentration criteria.

6.2.1.3 Summary

The process of strontium-90 and transuranic element removal adopted by BNFL Inc.—strontium precipitation and ferric floc coprecipitation—likely encompasses a number of chemical and physical processes. While solid solution in the precipitate may be important for some elements (e.g., americium), coagulation (plutonium) and isotope dilution (strontium) may also be at work. Furthermore, because the envelope C wastes are organically complexed, displacement of complexants by added iron (Fe^{3+}) may contribute to radionuclide removal. Variability due to the effects of pH on these processes will be alleviated by taking all wastes to 1 M hydroxide ion concentration. However, these processes are also strongly affected by the nature and amount of anionic ligands; all else being equal, metal solution speciation controls solid-aqueous chemical interaction. This observation, combined with (i) the often wide range in experimental results illustrated previously, (ii) the paucity of reliable thermodynamic data for many of the elements of interest, and (iii) the lack of knowledge of kinetic effects, emphasizes the

importance of confirmatory tests on the complete range of affected wastes. These tests, preferably designed to isolate the various removal mechanisms and to cover the expected range of chemical parameters, such as pH and ionic strength, should be performed on actual waste samples.

6.2.2 Safety Considerations

6.2.2.1 Sodium Hydroxide

Sodium hydroxide, also known as caustic soda and lye, is soluble in water. It is a corrosive irritant to skin, eyes, and mucous membranes, with a significantly corrosive action on all body tissue, causing burns and frequently deep ulceration. Mists, vapors, and dusts cause small burns, and contact with the eyes rapidly causes severe damage to the delicate tissue. Ingestion causes serious damage to the mucous membranes or other tissues with which contact is made. Inhalation of the dust or concentrated mist can cause damage to the upper respiratory tract and to lung tissue. Mutation data have been reported (Lewis, 1997). Therefore, appropriate protective clothing should be worn whenever sodium hydroxide is handled.

For sodium hydroxide, the OSHA PEL, the ACGIH TLV, and NIOSH REL ceiling values are all 2 mg/m^3. This is the amount to which workers can be exposed for a normal 8-hr day, 40-hr work week, without ill effects (Lewis, 1997).

Sodium hydroxide is a strong base that can react violently with many substances (Lewis, 1997). Therefore, it should not be combined with other chemicals unless the possible reactions have been adequately investigated and appropriate precautions taken.

Sodium hydroxide is reported in the EPA TSCA Inventory and is subject to controls under the CERCLA. A release of 450 kg (1,000 lb) or more must be reported to the National Response Center and also state and local government officials.

Sodium hydroxide should be handled only in well-ventilated areas. When handling sodium hydroxide solution, workers should wear a mist respirator, impervious gloves, chemical goggles, full-face shield, apron, boots, and gauntlets.

6.2.2.2 Ferric Nitrate

For ferric nitrate, mutation data have been reported (Lewis, 1997). The ACGIH TLV is 1 mg of iron per m^3. This is the amount to which workers can be exposed for a normal 8-hr day, 40-hr work week, without ill effects (Lewis, 1997). Therefore, ferric nitrate should be handled only in well-ventilated areas.

Ferric nitrate is a reactive oxidizer (Lewis, 1997). It can cause a fire when brought into contact with combustible materials, and in a fire it produces toxic oxides of nitrogen. Therefore, it should not be combined with other chemicals unless the possible reactions have been investigated adequately and appropriate precautions taken, and it must not be stored with combustible materials.

Precipitation and Filtration

Ferric nitrate is reported in the EPA TSCA Inventory (Lewis, 1997) and is subject to controls under CERCLA. A release of 450 kg (1,000 lb) or more must be reported to the National Response Center and also state and local government officials.

When handling ferric nitrate, workers should wear impervious gloves and chemical splash goggles.

6.2.2.3 Strontium Nitrate

Strontium nitrate is soluble in water. It is moderately toxic by ingestion. When heated to decomposition, strontium nitrate emits toxic NO_x fumes (Lewis, 1997).

Strontium nitrate is a powerful oxidizer that can ignite combustible materials, and when heated to decomposition, emits toxic NO_x fumes (Lewis, 1997). Therefore, it should not be combined with other chemicals unless the possible reactions have been adequately investigated and appropriate precautions taken, and it must not be stored with combustible materials.

Strontium nitrate is reported in the EPA TSCA Inventory (Lewis, 1997), but is not subject to CERCLA controls.

When handling strontium nitrate, workers should wear rubber gloves and goggles.

6.2.3 Comparable Operations in Existence

The use of flocculating agents to remove suspended solids from waste water is common to many industries (Shreve, 1967). No industrial scale plant for precipitation and filtration of strontium was identified. A precipitation and filtration process to remove actinides is used in the British Nuclear Fuels Limited Enhanced Actinide Removal Plant in Sellafield, United Kingdom.[1] The plant started operating in 1994 and was designed to treat concentrated liquids from the evaporators, bulk liquids from the solvent treatment plant, and low-activity effluents from the reprocessing plant. The process involves adding sodium hydroxide to the iron-bearing acidic streams, resulting in formation of ferric hydroxide floc and coprecipitation of the actinides. The ferric floc, containing the majority of the actinides, is separated from the aqueous liquor using porous graphite tube cross flow ultrafilters. The resulting solid waste is suitable for encapsulation in cement, and the aqueous permeate is discharged to sea. About 250 m^3/day of bulk liquids and 2,400 m^3/yr of concentrates are treated by the plant.

6.3 Precipitation and Filtration Methods Proposed by BNFL Inc.

BNFL Inc. proposed to remove strontium-90 and transuranic elements from envelope C wastes by evaporating the wastes to a certain concentration of sodium, adding sodium hydroxide solution to increase the free hydroxide concentration, followed by adding ferric nitrate to generate a ferric floc solution. BNFL Inc. also plans to add strontium nitrate to cause coprecipitation of strontium and

---

[1]Pasciak, W. and R. Wescott. 1999. *Visit to Sellafield Facilities, BNFL Engineering Limited (BEL) in Risely and the Nuclear Installations Inspectorate (NII) in Liverpool, United Kingdom.* Trip Report July 7, 1999. Washington, DC: Nuclear Regulatory Commission.

transuranic elements. The precipitate would be ultrafiltered from the solution, washed, and sent to the high-level waste melter feed.

Coprecipitation can be effective for removing trace metals from solution (with possible contributions from displacement and dilution). However, coprecipitation could be highly waste-specific, and applicable experimentally-based thermodynamic data are sparse in the high pH range under consideration. Therefore, to assure the process will meet contract and regulatory requirements, experimental testing using samples of the actual wastes to be processed by the TWRS vitrification system should precede finalization of the system design.

6.4   References

Brooks, K.P., and D.E. Kurath. *Preliminary Survey and Assessment of Non-Solvent Extraction Technologies for Removal of TRU Contamination from Radioactive Tank Waste.* TWRSPP–93–067. Richland, WA: Pacific Northwest Laboratory. 1993.

Bruno, J., J. de Pablo, L. Duro, and E. Figuerola. Experimental study and modeling of the U(VI)-Fe(OH)$_3$ surface precipitation/coprecipitation equilibria. *Geochimica et Cosmochimica Acta* 59: 4,113–4,123. 1995.

Ewart, F.T., R.M. Howse, H.P. Thomason, S.J. Williams, and J.E. Cross. The solubility of actinides in the near-field. *Scientific Basis for Nuclear Waste Management IX.* L.O. Werme, ed. Pittsburgh, PA: Materials Research Society: 701. 1985.

Herting, D.L. *Report of Scouting Study on Precipitation of Strontium, Plutonium, and Americium from Hanford Complexant Concentrate Waste.* WHC–SD–WM–DTR–040. Revision 0. Richland, WA: Westinghouse Hanford Company. 1995.

Hobbs, D.T. *Effects of Coprecipitation on the Concentrations of Uranium and Plutonium in Alkaline Salt Solutions.* WSRC–TR–95–0462. Aiken, SC: Westinghouse Savannah River Company. 1995.

Hobbs, D.T., T.B. Edwards, and S.D. Fleischman. *Solubility of Plutonium and Uranium in Alkaline Salt Solutions.* WSRC–TR–93–056. Aiken, SC: Westinghouse Savannah River Company. 1993.

Kolarik, Z. *Separation of Actinides and Long-Lived Fission Products from High-Level Radioactive Wastes (A Review).* KfK 4945. Karlsruhe, Germany: Kernforschungszentrum Karlsruhe. 1991.

Krause, T.R., J.C. Cunnane, and J.E. Helt. *Sludge Technology Assessment.* ANL–94/45. Argonne, IL: Argonne National Laboratory. 1994.

Lemire, R.J., and P.R. Tremaine. Uranium and plutonium equilibria in aqueous solutions to 200 °C. *Journal of Chemical Engineering Data* 25: 361–370. 1980.

Lewis, R.J. *Hazardous Chemicals Desk Reference.* New York: Van Nostrand Reinhold Publisher. 1997.

Precipitation and Filtration

Orth, R.J., and D.E. Kurath. *Review and Assessment of Technologies for the Separation of Strontium from Alkaline and Acidic Media.* PNNL–9053/UC–721. Richland, WA: Pacific Northwest Laboratory. 1994.

Orth, R.J., A.H. Zacher, A.J. Schmidt, M.R. Elmore, K.R. Elliott, G.G. Neuenschwander, and S.R. Gano. *Removal of Strontium and Transuranics from Hanford Tank Waste via Addition of Metal Cations and Chemical Oxidant—FY 1995 Test Results.* PNNL–10766/UC–721. Richland, WA: Pacific Northwest Laboratory. 1995.

Pabalan, R.T., M.S. Jarzemba, D.A. Pickett, N. Sridhar, J. Weldy, C.S. Brazel, J.T. Persyn, D.S. Moulton, J.P. Hsu, J. Erwin, T.A. Abrajano, Jr., and B. Li. *Hanford Tank Waste Remediation System High-Level Waste Chemistry Manual.* NUREG/CR–5751. Washington, DC: Nuclear Regulatory Commission. 1999.

Schulz, W.W., M.J. Kupfer, and M.M. McKeon. *In-Tank Processes for Destruction of Organic Complexants and Removal of Selected Radionuclides.* WHC–SD–WM–ES–321. Revision 0. Richland, WA: Westinghouse Hanford Company. 1995.

Serne, R.J., G.A. Whyatt, S.V. Mattigod, Y. Onishi, P.G. Doctor, B.N. Bjornstad, M.R. Powell, L.M. Liljegren, J. Westsik, J.H., N.J. Aimo, K.P. Recknagle, G.R. Golcar, T.B. Miley, G.R. Holdren, D.W. Jeppson, R.K. Biyani, and G.S. Barney. *Fluid Dynamic Particulate Segregation, Chemical Processes, and Natural Ore Analog Discussions that Relate to the Potential for Criticality in Hanford Tanks.* WHC–SD–WM–TI–757. Richland, WA: Westinghouse Hanford Company. 1996.

Shreve, R.N. *Chemical Process Industries.* New York: McGraw-Hill Book Company. 1967.

Slater, S.A., D.B. Chamberlain, C. Conner, J. Sedlet, B. Srinivasan, and G.F. Vandegrift. *Methods for Removing Transuranic Elements from Waste Solutions.* ANL–94/43. Argonne, IL: Argonne National Laboratory. 1994.

Stumm, W., and J.J. Morgan. *Aquatic Chemistry: Chemical Equilibria and Rates in Natural Waters.* 3rd Edition. New York: John Wiley & Sons, Inc. 1996.

Turner, D.R. *A Uniform Approach to Surface Complexation Modeling of Radionuclide Sorption.* CNWRA 95-001. San Antonio, TX: Center for Nuclear Waste Regulatory Analyses. 1995.

Wolery, T.J. *EQ3/6, A Software Package for Geochemical Modeling of Aqueous Systems: Package Overview and Installation Guide.* UCRL–MA–110662 PT1. Livermore, CA: Lawrence Livermore National Laboratory. 1992.

7 GLOSSARY

ACGIH—American Conference of Governmental Industrial Hygienists

ALARA—A requirement and approach to control of radiological or hazardous material whereby individual and collective exposures to the work force and to the general public are managed and controlled to be at levels As Low As Reasonably Achievable. This is not a dose limit but a process that has the objective of attaining doses as far below the applicable controlling limits as is reasonably achievable. It takes into account the social, technical, economic, practical, and public policy factors.

Bu-am ZrP—Butyl-ammonium zirconium phosphate

CERCLA—Comprehensive Environmental Response, Compensation and Liability Act of 1986

CNWRA—Center for Nuclear Waste Regulatory Analyses, San Antonio, Texas

Complexant Concentrate—Liquid and solid alkaline waste containing high concentrations of organic complexants that retain strontium and transuranic elements in solution

DBP—Dibutyl phosphate

DOE—U.S. Department of Energy

Double-Shell Slurry Feed—Suspension-rich, high-salt solution formed from evaporation of single-shell tank and reprocessing plant wastes

Double-Shell Tank—A reinforced concrete underground vessel with two inner steel liners to provide containment and backup containment of liquid wastes; annulus is instrumented to permit detection of leaks from the inner liner. The Hanford site has 28 double-shell tanks.

ED3A—Ethylenediaminetriacetate

EDTA—Ethylenediaminetetraacetic acid; an organic complexant used for retaining transuranic elements in solution

EPA—U.S. Environmental Protection Agency

HEDTA—Hydroxyethylenediaminetriacetate; an organic complexant used for retaining transuranic elements in solution

Hex-am ZrP—Hexyl-ammonium zirconium phosphate

High-Level Waste—Means (i) irradiated reactor fuel; (ii) liquid wastes resulting from the operation of the first cycle solvent extraction system, or equivalent, and the concentrated wastes from subsequent extraction cycles, or equivalent, in a facility for reprocessing irradiated fuel; and (iii) solids into which such liquid wastes have been converted

HTiO—Hydrous titanium oxide

Low-Activity Waste—Low-level tank waste that has not yet received the Nuclear Regulatory Commission concurrence as incidental

Low-Level Waste—Waste that contains radioactivity and is not classified as high-level radioactive waste, transuranic waste, spent nuclear fuel, or byproduct material (as defined in Section IIc(2) of the Atomic Energy Act of 1954, [42 USC 2014(e)(2)])

LMAES—Lockheed Martin Advanced Environmental Systems

Neutralized Current Acid Waste—Mostly liquid waste generated since 1983 by reprocessing irradiated fuel from N Reactor at the Hanford PUREX Plant

NIDA—Nitroimidazole

NIOSH—National Institute for Occupational Safety and Health

NPH—Normal paraffinic hydrocarbons; diluent used in uranium recovery and PUREX processes

NRC—Nuclear Regulatory Commission

NTA—Nitrilotriacetic acid

OSHA—Occupational Safety and Health Administration

PEL—Permissible Exposure Level

PUREX—Plutonium Uranium Extraction Plant process that used a mixture of tributyl phosphate and kerosene as the solvent phase for extraction of uranium and plutonium

REL—Recommended Exposure Level

Single-Shell Tank—An older-style underground vessel with a single steel wall liner surrounded by reinforced concrete. The Hanford site has 149 single-shell tanks.

TLV—Threshold Limit Value

Transuranic—(i) Transuranic elements are elements with atomic numbers above 92 all are radioactive and are products of artificial nuclear changes; and (ii) transuranic wastes are those wastes containing more than 100 nanocuries of alpha-emitting transuranic isotopes, with half-lives greater than twenty years, per gram, except for high-level waste

TSCA—Toxic Substance Control Act

TWRS—Tank Waste Remediation System

APPENDIX A

CHAPTER 1 SUPPLEMENTARY TABLES

Table A-1. Concentration limits for the A, B, and C low-activity waste feed envelopes to be transferred by the U.S. Department of Energy to the contractor for low-activity waste services (U.S. Department of Energy, 1996a)[*]

Chemical Analyte	Maximum Ratio, Analyte (mole) to Sodium (mole)		
	Envelope A Waste	Envelope B Waste	Envelope C Waste
Al	2.50E-01	2.50E-01	2.50E-01
Ba	1.00E-04	1.00E-04	1.00E-04
Ca	4.00E-02	4.00E-02	4.00E-02
Cd	4.00E-03	4.00E-03	4.00E-03
Cl	3.70E-02	8.90E-02	3.70E-02
Cr	6.90E-03	2.00E-02	6.90E-03
F	9.10E-02	2.00E-01	9.10E-02
Fe	1.00E-02	1.00E-02	1.00E-02
Hg	1.40E-05	1.40E-05	1.40E-05
K	1.80E-01	1.80E-01	1.80E-01
La	8.30E-05	8.30E-05	8.30E-05
Ni	3.00E-03	3.00E-03	3.00E-03
NO_2	3.80E-01	3.80E-01	3.80E-01
NO_3	8.00E-01	8.00E-01	8.00E-01
Pb	6.80E-04	6.80E-04	6.80E-04
PO_4	3.80E-02	1.30E-01	3.80E-02
SO_4	1.00E-02	7.00E-02	2.00E-02
Total Inorganic Carbon[#]	3.00E-01	3.00E-01	3.00E-01
Total Organic Carbon[@]	5.00E-01	5.00E-01	5.00E-01
U	1.20E-03	1.20E-03	1.20E-03

[*]The waste feed will be delivered with a sodium concentration between 3 and 10 M and up to 2 weight percent solids (dry basis). Trace quantities of radionuclides, chemicals, and other impurities may be present in the waste feed.
[#]Mole of inorganic carbon atoms per mole of sodium
[@]Mole of organic carbon atoms per mole of sodium

Table A-2. Low-activity waste radionuclide content limits for the soluble fraction of envelope A, B, and C wastes (U.S. Department of Energy, 1996b)[*]

Radionuclide	Maximum Ratio, Radionuclide (Bq) to Sodium (mole)		
	Envelope A Waste	Envelope B Waste	Envelope C Waste
Transuranics	4.8E+05	4.8E+05	1.0E+06
Cs-137	4.3E+09	2.0E+10	4.3E+09
Sr-90	4.4E+07	4.4E+07	8.0E+08
Tc-99	7.1E+06	7.1E+06	7.1E+06
Co-60	6.1E+04	6.1E+04	3.0E+05
Eu-154 + Eu-155	1.2E+06	1.2E+06	4.5E+06

[*]Shading indicates differences among the three low-activity waste envelopes. Some radionuclides, such as strontium-90 and cesium-137, have daughters with relatively short half-lives. These daughters are not listed in this table, but are present in concentrations associated with the normal decay chains of the radionuclides.

Table A-3. High-level waste feed composition limits for nonvolatile components (U.S. Department of Energy, 1996a)

Nonvolatile Element	Maximum (grams per 100 grams nonvolatile waste oxides)
As	0.16
B	1.3
Be	0.065
Ce	0.81
Co	0.45
Cs	0.58
Cu	0.48
Hg	0.1
La	2.6
Li	0.14
Mn	6.5
Mo	0.65
Nd	1.7
Pr	0.35
Pu	0.054
Rb	0.19
Sb	0.84
Se	0.52
Sr	0.52
Ta	0.03
Tc	0.26
Te	0.13
Th	0.52
Tl	0.45
V	0.032
W	0.24
Y	0.16
Zn	0.42

Appendix A

Table A-4. High-level waste feed composition limits for volatile components (U.S. Department of Energy, 1996a)

Volatile Components	Maximum (grams per 100 grams nonvolatile waste oxides)
Cl	0.33
CO_3	30
NO_2 NO_3	36 (total NO_2/NO_3) as NO_3
Total organic carbon	11
CN	1.6
NH_3	1.6

Table A-5. Maximum radionuclide composition of high-level waste feed unwashed solids (U.S. Department of Energy, 1996a)

Isotope	Curies per 100 grams waste oxides	Isotope	Curies per 100 grams waste oxides
H-3	6.50E–05	Eu-154	5.20E–02
C-14	6.50E–06	Eu-155	2.90E–02
Co-60	1.00E–02	U-233	9.00E–07
Sr-90	1.00E+01	U-235	2.50E–07
Tc-99	1.50E–02	Np-237	7.40E–05
Sb-125	3.20E–02	Pu-238	3.50E–04
Sn-126	1.50E–04	Pu-239	3.10E–03
I-129	2.90E–07	Pu-241	2.20E–02
Cs-137	1.00E+01	Am-241	9.00E–02
Eu-152	4.80E–04	Cm-243 + Cm-244	3.00E–03

Appendix A

Table A-6. Chemical content of Tank Waste Remediation System envelope B waste and West Valley tank 8D-2 supernate[*]

Chemical Species	Units	Tank Waste Remediation System Envelope B Waste	West Valley Tank 8D-2
Al	mol/mol Na	5.76×10^{-2}	6.4×10^{-5}
As	mol/mol Na	2.80×10^{-6}	no data
Ba	mol/mol Na	8.04×10^{-8}	no data
Ca	mol/mol Na	9.98×10^{-6}	no data
Cd	mol/mol Na	4.27×10^{-6}	no data
Cl	mol/mol Na	8.37×10^{-4}	5.6×10^{-3}
Cr	mol/mol Na	4.52×10^{-3}	1.8×10^{-3}
Cs	mol/mol Na	7.02×10^{-5}	1.9×10^{-4}
F	mol/mol Na	2.09×10^{-2}	1.0×10^{-3}
Fe	mol/mol Na	4.60×10^{-7}	1.2×10^{-5}
Hg	mol/mol Na	1.08×10^{-7}	no data
K	mol/mol Na	1.71×10^{-2}	3.7×10^{-3}
La	mol/mol Na	8.48×10^{-7}	no data
Na	mol/liter	3 to 14	6.95
NH$_4$	mol/mol Na	1.45×10^{-2}	no data
Ni	mol/mol Na	2.05×10^{-6}	no data
NO$_2$	mol/mol Na	2.85×10^{-1}	3.2×10^{-1}
NO$_3$	mol/mol Na	2.30×10^{-1}	5.2×10^{-1}
OH	mol/mol Na	1.26×10^{-1}	3.1×10^{-2}
Pb	mol/mol Na	0.0	no data
PO$_4$	mol/mol Na	2.30×10^{-3}	1.6×10^{-3}
SO$_4$	mol/mol Na	5.07×10^{-2}	3.8×10^{-2}
Sr	mol/mol Na	7.57×10^{-8}	1.3×10^{-6}
TIC	mol/mol Na	1.45×10^{-1}	5.2×10^{-2}
TOC	mol/mol Na	3.26×10^{-2}	no data
U	mol/mol Na	8.76×10^{-4}	5.1×10^{-5}

[*]West Valley Demonstration Project information developed from data in Rykken (1986).

Table A-7. Radionuclide content of Tank Waste Remediation System envelope B waste and West Valley tank 8D–2 supernate[*]

Radionuclide	Units	Tank Waste Remediation System Envelope B Waste	West Valley Tank 8D–2
C-14	Bq/mol Na	1.51×10^4	3.5×10^5
Sr-90	Bq/mol Na	1.70×10^7	7.6×10^6
Y-90	Bq/mol Na	1.70×10^7	7.6×10^6
Tc-99	Bq/mol Na	2.98×10^6	4.1×10^6
Cs-137	Bq/mol Na	8.81×10^9	1.9×10^{10}
Ba-137	Bq/mol Na	8.24×10^9	1.8×10^{10}
U-238	Bq/mol Na	2.59×10^3	1.3×10^2
Np-237	Bq/mol Na	6.35×10^2	no data
Pu-239	Bq/mol Na	1.09×10^5	no data
Pu-240	Bq/mol Na	2.70×10^4	4.9×10^4
Pu-241	Bq/mol Na	5.77×10^4	4.1×10^6
Am-241	Bq/mol Na	1.65×10^5	no data

[*]West Valley Demonstration Project information was developed from data in Rykken (1986).

Appendix A

Table A-8. Chemical content of composite sludge from Hanford tanks AZ–101 and AZ–102 and sludge from West Valley tank 8D–2*

Chemical Species	Units	Hanford Tanks AZ–101 and AZ–102[†]	West Valley Tank 8D–2
Ag	g/g of sludge	4.83×10^{-4}	6×10^{-6}
Al	g/g of sludge	6.85×10^{-2}	2.26×10^{-2}
B	g/g of sludge	9.29×10^{-5}	no data
Ba	g/g of sludge	5.69×10^{-4}	1.83×10^{-3}
Ca	g/g of sludge	5.15×10^{-3}	1.32×10^{-2}
Cd	g/g of sludge	1.34×10^{-2}	1.34×10^{-5}
Ce	g/g of sludge	1.28×10^{-3}	2.67×10^{-3}
Co	g/g of sludge	8.18×10^{-5}	no data
Cr	g/g of sludge	3.00×10^{-3}	3.38×10^{-4}
Cu	g/g of sludge	2.46×10^{-4}	2.52×10^{-3}
Fe	g/g of sludge	1.38×10^{-1}	3.97×10^{-1}
K	g/g of sludge	5.96×10^{-3}	no data
La	g/g of sludge	3.60×10^{-3}	1.39×10^{-3}
Mn	g/g of sludge	3.37×10^{-3}	2.98×10^{-2}
Na	g/g of sludge	meaningless data[‡]	no data
Nd	g/g of sludge	2.72×10^{-3}	4.72×10^{-3}
Ni	g/g of sludge	8.76×10^{-3}	7.09×10^{-3}
Pb	g/g of sludge	1.73×10^{-3}	no data
Ru	g/g of sludge	5.47×10^{-4}	2.82×10^{-3}
Si	g/g of sludge	6.42×10^{-3}	6.08×10^{-3}
Sr	g/g of sludge	3.37×10^{-4}	1.07×10^{-3}
Ti	g/g of sludge	1.40×10^{-4}	no data
U	g/g of sludge	1.23×10^{-2}	2.49×10^{-2}
Zn	g/g of sludge	3.96×10^{-4}	8.67×10^{-4}
Zr	g/g of sludge	8.50×10^{-3}	5.68×10^{-3}

[*]Hanford data from Rapko and Wagner (1997). West Valley Demonstration Project information developed from data in Rykken (1986).
[†]Only those species for which reported values supported by direct analysis are included.
[‡]The reported value was 1.97 gram of sodium per gram of sludge. A large amount of sodium was added during leaching.

Table A-9. Radionuclide content of composite sludge from Hanford tanks AZ–101 and AZ–102 and sludge from West Valley tank 8D–2*

Radionuclide[†]	Units	Hanford Tanks AZ–101 and AZ–102	West Valley Tank 8D–2
Co-60	μCi/dry gram	8.85×10^0	4.2×10^{-2}
Sr-90	μCi/dry gram	1.14×10^4	7.1×10^4
Tc-99	μCi/dry gram	5.30×10^{-1}	no data
Ru-106, Rh-106	μCi/dry gram	4.64×10^1	2.7×10^0
Sb-125	μCi/dry gram	9.70×10^1	4.6×10^1
Cs-134	μCi/dry gram	5.50×10^0	no data
Cs-137	μCi/dry gram	2.20×10^3	no data
Ce-144	μCi/dry gram	6.13×10^1	no data
Eu-154	μCi/dry gram	6.42×10^1	1.3×10^3
Eu-155	μCi/dry gram	1.55×10^2	2.4×10^2
Pu-238	μCi/dry gram	1.27×10^0	6.1×10^1
Pu-239, -240	μCi/dry gram	5.99×10^0	3.09×10^1
Am-241	μCi/dry gram	2.17×10^2 [‡]	7.1×10^2
Cm-242	μCi/dry gram	8.06×10^{-2}	7.4×10^0
Cm-243, -244	μCi/dry gram	2.50×10^{-1}	2.1×10^2

*Hanford data from Rapko and Wagner (1997). West Valley Demonstration Project information developed from data in Rykken (1986).
[†]Rearranged by atomic weight.
[‡]Two decay modes combined here for comparability.

Appendix A

References

Rapko, B.M., and M.J. Wagner. 1997. *Caustic Leaching of Composite AZ–101/AZ–102 Hanford Tank Sludge*. PNNL–11580. Richland, WA: Pacific Northwest National Laboratory.

Rykken, L.E. *High-Level Waste Characterization at West Valley*. DOE/NE/44139–14. West Valley, NY: West Valley Nuclear Services Company, Inc. 1986.

U.S. Department of Energy. *Tank Waste Remediation System Privatization Request for Proposals*. DE–RP06–96RL13308. Richland, WA: U.S. Department of Energy. 1996a.

U.S. Department of Energy. *TWRS Privatization Contract with BNFL Inc*. DE–AC–06–96RL13308. Richland, WA: U.S. Department of Energy. 1996b.

APPENDIX B

CHAPTER 3 SUPPLEMENTARY TABLE

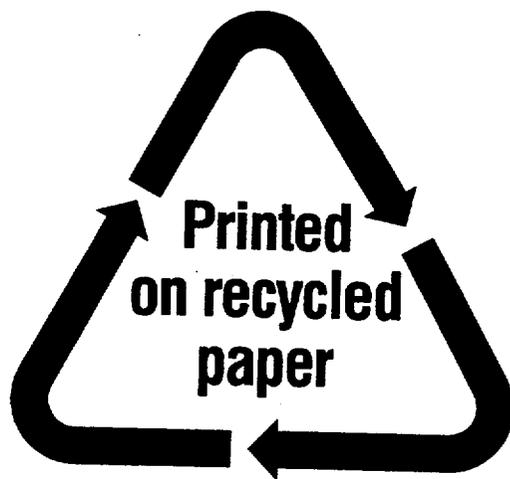**Table B-1. Source companies for selected ion-exchange materials**

Material	Company	Description
Crystalline silicotitanate (CST) ion exchangers	UOP Molecular Sieves Mt. Laurel, NJ	IONSIV® IE-910, powder form IONSIV® IE-911-08, spherical form IONSIV® IE-911-38B, granular form
Carbon, activated	Nucon International, Inc. Columbus, OH	Nusorb LP-70-S
Char	Stauffer Chemical Co. Westport, CT	Calcined cattle bones
Inorganic oxides with acidic functional groups	GTS Duratek Columbia, MD	Durasil 230-210-190
Macroporous anion resin with tributyl amine groups	Sybron Chemicals, Inc. Birmingham, NJ	Ionac™ SR-6
Macroporous anion resin with triethyl amine groups	Purolite Company Bala Cynwyd, PA	Purolite™ A-520-E
Macroporous anion resin with trimethyl amine groups	Sybron Chemicals, Inc. Birmingham, NJ	Ionac™ SR-3
Macroporous anion resin with tripropyl amine groups	Sybron Chemicals, Inc. Birmingham, NJ	Sybron $(Pr)_3N$
Macroporous cation resin with aminodiacetate functional groups	Miles Pittsburgh, PA	Lewatit TP-207
Macroporous cation resin with phosphorous functional groups	Resin Tech Cherry Hill, NY	RT-3972
Macroporous resins with sulfonic acid groups	Rohm-Haas Philadelphia, PA	Amberlyst® 15 Amberlyst® XN-1010
Phenol-formaldehyde resin	Rohm-Haas Philadelphia, PA	Duolite® CS-3 Duolite® CS-100
Polyfunctional resin with diphosphonic, carboxylic, and sulfonic groups	ElChrom Industries Darien, IL	Diphonix™

Appendix B

Table B-1. Source companies for selected ion-exchange materials (cont'd)

Material	Company	Description
Polystyrene anion resin with tertiary amine groups	Dow Chemicals Midland, MI	Chelex™ 1-X8 Chelex™ 2-X8 Dowex™ 1-X8 Dowex™ 2-X8
Polystyrene/divinylbenzene copolymer with aminophosphonic acid groups	Rohm-Haas Philadelphia, PA	Duolite® C-467
Polyvinylpyridine anion resin	Reilly Industries, Inc. Indianapolis, IN	Reillex™ HPQ
Potassium cobalt hexacyanoferrate, granular form	ElChrom Industries Darien, IL	KCoFeC
Resorcinol-formaldehyde resins	Boulder Scientific Mead, CO	BIB-DJ SLR-DJ SRR RF (BSC-210)
Superligands (Macrocyclic polymer resins)	IBC Advanced Technologies American Fork, UT	SuperLig® 639 SuperLig® 644
	3M St. Paul, MN	SLIG 644 WWL WEB
Tannin	Mitsubishi Nuclear Fuels Japan	—
Zeolites (Alkali metal aluminosilicates)	UOP Molecular Sieves Mt. Laurel, NJ	IONSIV® IE-96 IONSIV® TIE-96, titanium coated
	Steelhead Spokane, WA	Chabazite, natural occurring zeolite

2. TITLE AND SUBTITLE

Hanford Tank Waste Remediation System Pretreatment Chemistry and Technology

5. AUTHOR(S)

Roberto T. Pabalan, Vijay Jain, Rich F. Vance, Socrates Ioannidis, David A. Pickett, Christopher S. Brazel, Joseph T. Persyn, E. Jennings Taylor, and Maria E. Inman

8. PERFORMING ORGANIZATION–NAME AND ADDRESS (If NRC, provide Division, Office or Region, U.S. Nuclear Regulatory Commission, and mailing address; if contractor, provide name and mailing address)

Center for Nuclear Waste Regulatory Analyses
6220 Culebra Road
P.O. Drawer 28510
San Antonio, TX 78228-0510

10. SUPPLEMENTARY NOTES

A. Murray, NRC Project Manager

11. ABSTRACT (200 words or less)

The U.S. Department of Energy (DOE) will remediate the high-level radioactive wastes (HLWs) stored in 177 aging underground storage tanks at the Hanford, Washington site. The retrieved wastes will be separated into a HLW stream containing most of the radionuclides and a low-activity waste (LAW) stream containing the bulk of the nonradioactive chemicals and the soluble components of the tank waste. Both waste streams will be vitrified. Pretreatment of the LAW stream is required to remove cesium-137, strontium-90, technetium-99, and transuranic elements.

This report provides information useful to Nuclear Regulatory Commission staff for understanding the technical bases of the pretreatment technologies proposed by DOE privatization contractors and for identifying potential hazards associated with those technologies. A review of publicly available information on the chemistry and technology of unit operations proposed by BNFL Inc. and by Lockheed Martin Advanced Environmental Systems is presented. These unit operations are sludge washing, ion exchange, electrochemical methods, organic destruction, and precipitation/filtration. The physicochemical bases of the unit operations and published experimental studies involving alkaline tank wastes are discussed. The proposed pretreatment technology is discussed in the context of its application to Hanford wastes, including operational and safety considerations.

12. KEY WORD/DESCRIPTORS (List words or phrases that will assist researchers in locating the report)

Hanford
Tank Waste Remediation System
Tank Waste
Low-activity Waste
Pretreatment
Sludge Washing
Ion Exchange
Ozonation
Precipitation
Ultrafiltration
Electroreduction

13. AVAILABILITY STATEMENT

Unlimited

14. SECURITY CLASSIFICATION

(This Report)

Unclassified

15. NUMBER OF PAGES

16. PRICE

Printed
on recycled
paper

Federal Recycling Program

UNITED STATES
NUCLEAR REGULATORY COMMISSION
WASHINGTON, DC 20555-0001